Sustainability Assessment of Utilizing Recycled Plastic Waste as an Alternative to Fine Aggregates in Cement Mortars and Concretes

A THESIS SUBMITTED IN PARTIAL FULFILMENT FOR THE DEGREE OF

DOCTOR OF PHILOSOPHY

FACULTY OF ENGINEERING

GOA UNIVERSITY

By

Govind Vishnoo Bhagat

Goa University

Goa

MAY 2024

Sustainability Assessment of Utilizing Recycled Plastic Waste as an Alternative to Fine Aggregates in Cement Mortars and Concretes

A THESIS SUBMITTED IN PARTIAL FULFILMENT FOR THE DEGREE OF

DOCTOR OF PHILOSOPHY

FACULTY OF ENGINEERING

GOA UNIVERSITY

By

Govind Vishnoo Bhagat

Under the Supervision of

Prof. Purnanand P. Savoikar

MAY 2024

DECLARATION

I, Govind Vishnoo Bhagat hereby declare that this thesis represents work that has been carried out by me and that it has not been submitted, either in part or full, to any other University or Institution for the award of any research degree.

Place: Taleigao Plateau. Govind Vishnoo Bhagat

Date:

CERTIFICATE

I hereby certify that the above Declaration of the candidate, Govind Vishnoo Bhagat is true and the work was carried out under my supervision.

Dr. Purnanand P. Savoikar
Professor in Civil Engineering
Goa College of Engineering, Farmagudi – Goa
Goa University, Goa

Acknowledgment

I am deeply indebted to my supervisor, Prof. Purnanand P. Savoikar, for his invaluable help, guidance, and support during this research. I fall short of words to thank him for his motivation in selecting this very topic, constant encouragement, guidance and reassurance that pushed me to accomplish something that I never could have on my own.

I am also indebted to the Departmental Research Committee (DRC) members, Prof. Sunil Y. Kute and Prof. Govind R. Kunkolienkar for their critical suggestions and encouragement during the six-monthly and annual progress seminars, presynopsis, and overall preparation of this thesis. I would also like to thank the Principal of Goa College of Engineering, Farmagudi for his constant encouragement. I thank the Head of the Civil Engineering Department, Prof. K. G. Guptha for his constant support and encouragement.

The blessings of my parents and strong support from my wife and all family members require a special mention in my words of acknowledgment. Along with them, I thank my both sons who never complained about my busy schedules and marathon academic engagements during this dedicated journey.

Let me fold both my hands and bow my head to express my deep sense of gratitude to a visionary industrialist Shri. Anil Counto, Founder of Alcon - Anil Counto Enterprises for providing testing material and laboratory facilities at ALCON Labs, Kundaim, Goa. I am grateful to Shri. Siddhesh Kamat, Shri. Janki Prasad Sahu, Shri. Gaurish Kerkar, Miss. Tanushree, Mr. Janu, Mr. Ratan, Mr. Manoj, Mr. Pradeep, Mr. Javed, and other technical and non-technical staff of ALCON Labs for extending their kind help during the laboratory investigation.

I wholeheartedly thank Shri. Kadakia, Managing Director, Ubhayodaya Plastic Recycling Industry, Navi Mumbai for providing an adequate volume of shredded PET particles as per our requirements. I also thank M/s. Hindustan Zinc Limited, Chanderiya plant, Rajasthan, India, Vedanta group for the supply of smelting furnace slag. Special thanks to Miss. Leena Verenkar, CSIR Head, Sesa Goa for her efforts.

I am thankful to the National Centre for Polar and Ocean Research, Vasco, Goa for providing a facility for microstructural testing at their laboratory. I would like to thank Dr. Rahul Mohan and Ms. Sahina for their technical support during the SEM-EDS analysis.

I acknowledge with gratitude the support from my workplace Government Polytechnic Panaji. With a thanking note, I offer my respect and tribute to Ex-Principal late Shri. Luis R. Fernandes for constant support and motivation. I also thank my colleague and friend Smt. Nancy Dias, Shri. J.M.R. Noronha, Shri. Rajendra G. Hegde and all other colleagues for their help and co-operation during the project.

I also thank Dr. Vivek B. Kamat, Director of Technical Education for sanctioning me the study leave and for his kind support and encouragement.

Finally, a big thanks to all the teachers and well-wishers in my life.

Date: **Govind Vishnoo Bhagat**

Place: Goa University, Taleigao

Dedicated to

my parents and my family

THESIS APPROVAL SHEET

Thesis entitled: **Sustainability assessment of utilizing recycled plastic waste as an alternative to fine aggregates in cement mortars and concretes** by **Shri. Govind Vishnoo Bhagat** is approved for the degree of **DOCTOR OF PHILOSOPHY.**

Examiners

Supervisor

Chairman

Date:

Place: Goa University, Taleigao

Table of Contents

List of Figures

List of Tables

List of Annexures

List of Abbreviations

ADP	Abiotic Depletion Potential
AP	Acidification Potential
CDW	Construction and Demolition Waste
CED	Cumulative Energy Demand
CPCB	Central Pollution Control Board
CPS	Copper Slag
EAFS	Electric Arc Furnace Slag
EDS	Energy Dispersive X-Ray Spectroscopy
EP	Eutrophication Potential
EPD	Environmental Product Declaration
EPS	Expanded Polystyrene
EU	European Union
f_b	Flexural Strength
FCS	Ferrochrome Slag
FLA	Fly Ash
FM	Fineness modulus
FRC	Fiber-Reinforced Concrete
f_t	Splitting Tensile Strength
FU	Functional Unit
GBFS	Granulated Blast Furnace Slag
GHG	Green House Gas
Gi	Global Warming Potential Intensity
GWP	Global Warming Potential
HDPE	High Density Polyethylene
HH	Human Health
HIPS	High Impact Polystyrene
HPC	High Performance Concrete
HSC	High Strength Concrete
HVFA	High Volume Fly Ash
IFS	Induction Furnace Slag

ITZ	Interfacial Transition Zone
LC3	Limestone Calcined Clay Cement
LCA	Life Cycle Assessment
LCI	Life Cycle Inventory
LCIA	Life Cycle Impact Assessment
LDPE	Low Density Polyethylene
LLDPE	Linear Low-Density Polyethylene
LSF	Lime Stone Flour
LWA	Lightweight Aggregates
LWC	Lightweight Concrete
MEPS	Modified Expanded Polystyrene
MLWA	Manufactured Lightweight Aggregates
MRF	Material Recovery Facility
NCA	Natural Coarse Aggregate
NFA	Natural Fine Aggregate
NS	Nano Silica
N-Sand	Natural Sand
NWC	Normal Weight Concrete
ODP	Ozone Depletion Potential
OPC	Ordinary Portland Cement
PA	Polyamide
PC	Polycarbonate
P_C	Coarse flakes of PET
PCE	Poly Carboxylic Ether
PE	Polyethylene
PE (NRe)	Primary Energy (Non-Renewable)
PET	Polyethylene Terephthalate
PET-Sand	Polyethylene Terephthalate Sand
PF	Fine flakes of PET
PFA	Pulverized Fuel Ash
PMMA	Poly Methyl Methacrylate
POCP	Photochemical Oxidation Creation Potential

PP	Polypropylene
Pp	Pallets of PET
PPA	Polyester Polyamide Acrylic Fibres
PPVC	Plasticized Polyvinyl Chloride
PS	Polystyrene
PSL	Polyaryl Sulphone
PUR	Polyurethane
PVC	Polyvinyl Chloride
PWA	Plastic Waste Aggregates
PWCC	Plastic Waste Cement Composites
RAC	Recycled Aggregate Concrete
RCA	Recycled Concrete Aggregate
RHA	Rice Husk Ash
RMC	Ready Mixed Concrete
SCC	Self-Compacting Concrete
SCM	Supplementary Cementitious Materials
SEM	Scanning Electron Microscope
SF	Silica Fume
SFS	Smelting Furnace Slag
SFS-Sand	Smelting Furnace Slag Sand
SPS	Stabilized Polystyrene
SSS	Stainless Steel Slag
TP	Toxicity Potential
UEPS	Unexpanded Polystyrene
UNEP	United Nations Environmental Program
UPV	Ultrasonic Pulse Velocity
UPVC	Unplasticized Polyvinyl Chloride
w/b	Water to Binder
w/c	Water to Cement

ABSTRACT

The growing consumption of plastics in the packaging industry and use and throw away culture of the consumers have brought plastics to the global agenda due to the deposition of gigantic volumes of plastic waste in terrestrial and aquatic environments. The management of plastic waste is taken up as a global challenge and the alternative of recycling of plastics has been considered at the focal point of research in the waste management sector. Recycling of plastics to obtain new products of same genre in the secondary chain could not be certified as the favorable option in dealing with plastic waste. This was mainly due to the increased economic commitments, degradation of quality of the secondary products and marginal benefit on useful life of new products before it appears as waste in the environment. Considering the versatility of plastics and ability to mould to any requirements, the utilization of plastic species as aggregate fillers inside concrete are considered a novel and favorable way of plastic waste management. Extensive research works in the past on the utilization of plastic waste as aggregate fillers in cementitious mixes have shown a negative effect on most of the performance indicators. Several attempts were made to improve the performance characteristics of plastic-seeded mixes. This included the treatment of plastic particles with surfactant solutions and use of mineral admixtures like fly ash, granulated blast furnace slag, silica fume, and nano materials like Nano Silica as supplementary cementitious materials to compensate for the deterioration in the quality of composites after plastic incorporation. The current work proposes the use of high-density slag as an aggregate filler inside the concrete in which plastic waste in the form of Polyethylene Terephthalate sand (PET-Sand) is used as a substitute for natural sand. The high-density slag in the form of smelting furnace slag sand (SFS-Sand) is used as a blend with natural sand with the hypothesis that the degradation of the strength of concrete due to the incorporation of PET-Sand is partially controlled by the presence of SFS-Sand in the mix. This is an attempt of making 'green concrete' through the utilization of plastic waste and metal industry waste. The quantification of the environmental advantage of making such green concrete is also the primary aim of the current exercise. Thus, a holistic approach to Life cycle assessment to estimate the environmental impacts caused by the production of novel concrete is adopted in the current study. A comparative analysis of the functional characteristics and the

environmental performance of the proposed green concrete mixes with that of the conventional mix forms a major contribution of the current research.
Keywords: Concrete, plastic waste, fine aggregate, mortar, properties, strength, sustainability, life cyle assessment

Chapter 1

Introduction

1.1 Background and Introduction

Plastic is a major technical breakthrough of the 20th century. It has become an inseparable and integral part of human life. It is a resource-efficient material characterized by its versatility, durability, low density, cost-effectiveness, user-friendly designs, and ability to mold to the requirements of the consumer (Da Silva et al., 2014; Hossain et al., 2016a). It has been considered a revolutionary material with uncountable applications in every phase and aspect of human life (Saxena et al., 2018). The myriad uses of plastics in fields as diverse as the packaging industry, building and construction, household appliances, electrical and electronics industry, medicine, food industry, and aerospace sector have made it difficult to imagine the world without plastics (Wicaksono et al., 2018). The exponential surge in the production of plastics provides enough evidence of the popularity of this material. World virgin plastic production reached 367 million metric tons in the year 2020 with an average annual increase of 4.6% over the past decade. The production share of China was 32%, while the European countries produced 17% of the global plastic (Plastics Europe, 2021). Plastic production and consumption in India also showed a five-fold increase from 3 million metric tons in the year 2000 to a sporadic value of 17.8 million metric tons in 2017 (Parikh et al., 2018). Even the dreadful pandemic COVID-19 could not decelerate the plastic production rate throughout the world (Benson et al., 2021; Bhagat and Savoikar, 2022). When the severity of the COVID-19 pandemic led to a shrinking global Foreign Direct Investment by 5-15%, populous countries like China reported a surge of 1% in plastic production (Newswire, 2021). Sudden and skyrocketing demand for plastic-based equipment like plastic-based ventilators, surgical masks, and hand sanitizer bottles compelled industrial managers and policymakers to shift their manufacturing focus from their primary products to plastic-based products. The change in the manufacturing priority of leading global manufacturers in aircraft and motor industries like Tesla, Airbus, and Ford to plastic-based medical

equipment is a classic example showing that no pandemic can ever stop plastic production (Kumar et al. 2020). Moreover, such pandemics have ultimately evolved into a scenario of a 'pandemic of plastic pollution' (Lamba et al. 2022).

Plastic is not just one material. The terms 'plastics' or 'plastic materials' are used to describe an extremely large family of vastly different materials with different characteristics, properties, and uses (Plastics Europe, 2018). Plastics can be categorized into two basic types: Thermoplastics and Thermosets. Thermoplastics are a family of plastics that can potentially be melted on the application of heat and reshaped into the same or different form for the same or different applications. These are reversible forms of plastic and 80% of the plastics produced fall under this category (Ogundairo et al. 2021). Thermoplastics include Polyethylene (PE) (High-Density Polyethylene (HDPE)/Low-Density Polyethylene (LDPE)/Linear Low-Density Polyethylene (LLDPE)), Polypropylene (PP), Polyvinyl Chloride (PVC), Polyethylene Terephthalate (PET), Polystyrene (PS), Expanded Polystyrene (EPS), Polyamides (PA), Polycarbonate (PC), Poly Methyl Methacrylate (PMMA), Polyarylsulphone (PSL), Polyester-Polyamide and Acrylic fibers (PPA), etc. Thermoplastics are recyclable and can be used in the secondary product life cycle. Thermosets are a family of plastics that cannot be remolded or reformed after heating. They are irreversible forms of plastics that undergo a chemical change when heated and cannot return to their original shapes after subjecting to a heating and cooling cycle. Thermosets include Polyurethane (PUR), Unsaturated polyester, Epoxy resins, Melamine resin, Vinyl ester, Silicone, Phenol formaldehyde, Urea formaldehyde, acrylic resins, etc. (Plastics Europe, 2019). Although thermosets are tougher, stronger, and more resilient than thermoplastics, they are almost non-recyclable (Ogundairo et al. 2021). Table 1.1 summarizes the properties of some common thermoplastics and their applications in the primary life cycle and secondary life cycle post-recycling.

The packaging industry represents the largest end market for the plastics produced. It includes plastics from water bottles to plastic layers in tea bags to plastic straws, glasses, plates, and just about anything and everything that we package for our consumption (CSE, 2020). Fig. 1.1 shows the global plastic demand in various industrial sectors for the year 2015. In 2020, the European Union (EU27+3) packaging industry recorded a plastic demand of 40.5%. The building and construction industry and

automotive industry ranked second and third on the list with a plastic demand of 20.4% and 8.8% respectively (Plastics Europe, 2021). Considering the useful life span of plastics in the packaging industry, the statistical value of consumption of around 40% of produced plastics as a packaging material is very alarming due to the use and throw-away culture of the consumers. Such plastics are thrown away just a few minutes after their debut application. The issue is more severe in the case of single-use plastics (UNEP, 2018). Consequently, plastic is a perennial contribution to the global solid waste stream (Albano et al. 2009). The plastics from other consumer sectors also add to these perennial deposits as and when their useful service life is exhausted. Therefore, the sporadic unstoppable growth in the production and consumption of plastics has contributed to unstoppable plastic waste pollution bringing plastics to the global agenda.

Table 1.1 Common thermoplastics- Properties and applications
(Almeshal et al., 2020b; Bahij et al., 2020; Bhagat and Savoikar, 2022; Siddique et al., 2008)

Thermoplastic type	Properties	Applications in virgin form	Applications after recycling
PET: Polyethylene Terephthalate	Clarity, transparency, stiffness, toughness, chemical resistance, usable in fiber form	Mineral water and soft drink bottles, textile fibers, sleeping bags, and pillow filler	Transparent film for packaging and wrapping, soft drink and detergent bottles, rain wears, carpet fibers
LDPE: Low-Density Polyethylene	Softness and flexibility, easy processing, low density, low moisture barrier	Ice cream and food container lids, garbage bags, and bins	Transparent soft films for wrapping nurseries, plant take-away bags, film for builders
HDPE: High-Density Polyethylene	colored or white, rigidity and high impact strength, chemical resistance	Crinkly shopping bags, milk, and cream storage bottles, storage bags for frozen items	Compost bins, crates, mobile rubbish bins, agricultural pipes, detergent bottles, recycling crates
UPVC: Unplasticized Polyvinyl Chloride	Hardness, rigidity, and may have clarity	Plumbing and sanitary pipes and fittings, juice bottles, blister packs	Plumbing pipe fittings, detergent bottles, tiles
PPVC: Plasticised Polyvinyl Chloride	Clarity, flexibility, elasticity, transparency	Shoe soles, blood bags and tubing, garden hose, and pipes	The inner core of the hose, factory flooring
PP: Polypropylene	Hard, but flexible, low density, creep resistance, chemical barrier	Ice cream bowls, potato crisp bags, chairs, drinking straws, hinged lunch boxes	Manure bins, recycling crates, and worm production units
PS: Polystyrene	Glassy, transparent, rigid, hard, high clarity	Kitchen cutlery, light fixtures, toys, bottles, food packaging, imitation crystal glassware	Laundry pegs, coat hangers, VCD/CD boxes, spools, rulers, office items
EPS: Expanded Polystyrene	Lightweight, Energy absorption, thermal insulation	Tea coffee cups, disposable food containers, meat trays, and packaging	Non-recyclable
HIPS: High Impact Polystyrene	High impact strength, hardness, rigidity, translucent	Refrigerator lining, vending cups, bathroom cabinets, toilet seats, tanks	Purchase display countertops, indoor signs
PC: Polycarbonate	Thermal stability, stiffness, hardness, toughness, rigidity, transparency	Electronic, business machine, optical media, medical, lighting, automotive	CD/DVD data storage devices, dome lights, and sound walls in the construction sector

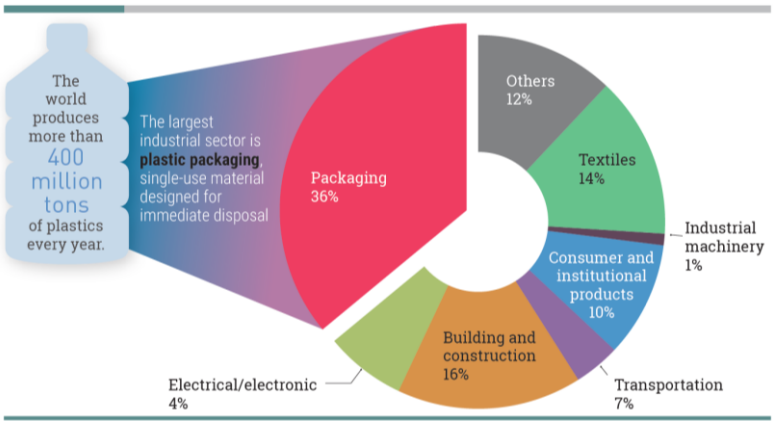

Fig. 1.1 Global plastic production by the industrial sector (Geyer et al., 2017)

1.1.1 Plastic Waste Generation- Global and Regional Context

The statistical data on the global consumption of plastic is based on the amount of plastic waste generated (UNEP, 2018). This indicates the magnitude and significance of plastic waste generation in the plastic industry. The first global analysis of all mass-produced plastics ever manufactured, and the waste generated was presented by Geyer et al. (2017). This data on global plastic waste generation is presented in Fig. 1.2.

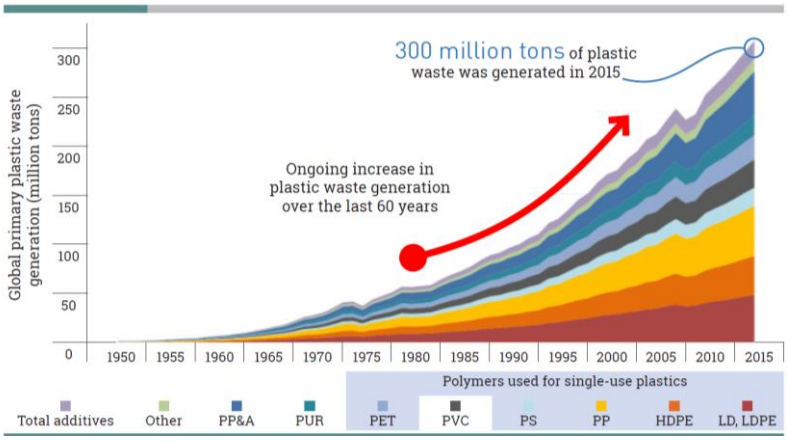

Fig. 1.2 Global plastic waste generation- 1950 to 2015 (Geyer et al. 2017)

Almost 47% of the plastic waste produced on a global scale was comprised of plastic packaging waste in 2015. Asian countries contributed to half of this waste. Fig. 1.3 presents the data about waste generation from plastic packaging. China remained the giant worldwide contributor to this waste amounting to 42.5 million metric tons. The USA ranked as the largest producer of this waste per capita, recording 47.5 kg per capita waste, followed by Japan and the European Union (UNEP, 2018). As per the Plastic Waste

Rules, 2016, the Central Pollution Control Board (CPCB) provides the only source of national data on the regular estimation of plastic waste generated in India. It is stated that plastic waste contributes to 5-6 percent of the total solid waste generated in India. In 2018-19, the annual plastic waste generated was 3.36 million metric tons, i.e., roughly 0.092 million metric tons per day (CPCB Report, 2019). Almost 66 percent of this waste comprised mixed waste, like polybags, and multilayer pouches used in the food packaging industry. Fig. 1.4 illustrates the contribution of seven major Indian states to plastic waste generation in India in 2018-19. Although Maharashtra and Tamil Nadu were the largest contributors to the total plastic waste generation, the state of Goa was ranked the highest in the per capita waste generation. It was estimated that Goa generates about 60 grams per capita per day, almost double what Delhi generates (37 grams per capita per day) and way above the national average of 8 grams per capita per day (CSE, 2020).

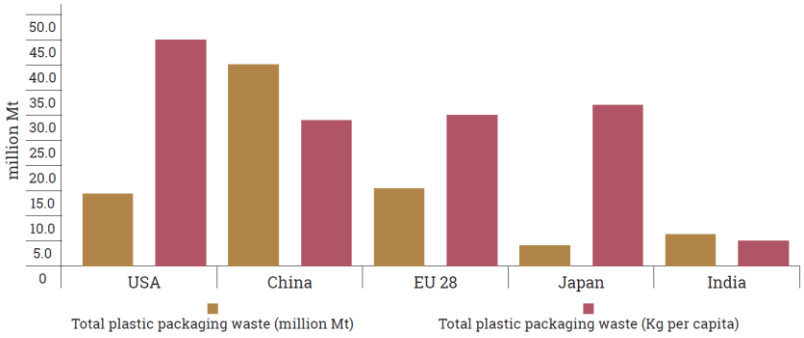

Fig. 1.3 Total and per capita plastic packaging waste generation of leading waste generators

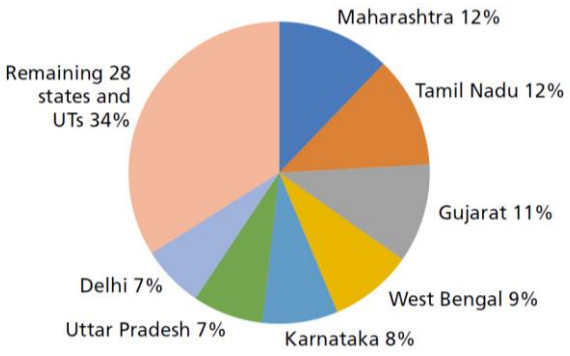

Fig. 1.4 State-wise contribution to plastic waste generation in India as of 2018-19 (CPCB Report, 2019)

1.1.2 Plastic Waste Management Scenarios

According to the waste hierarchy principle, plastic waste essentially follows three fates: landfilling, incineration, and recycling. In landfilling, discarded plastic can be contained in a managed system, left uncontained in the open environment, or dumped in the natural surroundings. Incineration is the method of thermal destruction of plastic waste. Plastic has a high calorific value, so the incineration activity is taken up with an option of energy recovery. Although oil extraction from plastic waste by pyrolysis is an emerging technology, it still lacks preference over incineration (Geyer et al. 2017). In recycling, plastic waste is reprocessed into secondary material. Recycling can avoid the use of virgin plastics to some extent, and more importantly, delay or avoid the final disposal of waste. With the follow-up of the circular economy concept, recycling should have been the most popular plastic waste management option. However, the statistical data over the last decade urges the need for a boost for the plastic recycling sector.

The estimates state that only 30% of the plastics ever produced are currently in use. The remaining 70% of the produced plastics emerged as waste. Geyer et al. (2017) revealed the findings that approximately 6300 million metric tons of plastic waste had been generated between 1950 to 2015 (See Fig. 1.5). Of this, 4900 million metric tons (79%) of waste have been discarded and dumped in landfills or natural surroundings. Nearly 800 million metric tons (12%) of this waste have been incinerated for energy recovery, and only 600 million metric tons (9%) have been recycled. The historical data about plastic waste generation and the three scenarios of plastic waste management projected that at the end of the year 2050, primary plastic waste generation will strike the 26000 mark. By then, 9000 million metric tons will have been recycled and 12000 million metric tons each will have been incinerated or dumped in landfills, oceans, and the surrounding environment (Geyer et al. 2017).

Most modern-day plastic is made up of non-biodegradable sources. It takes 400-500 years to decompose under natural conditions. Their degradation occurs due to the disintegration of plastic materials into smaller pieces over hundreds of years (Almeshal, et al., 2020b; Kamaruddin et al., 2017; Lamba et al., 2022). Therefore, landfilling of plastic waste would mean burying a non-biodegradable material that would remain in the natural soil for hundreds of years. These deposits may hinder the groundwater movement and movement of roots of the plants inside the soil. The presence of several toxic

chemicals like cadmium, lead, etc. in plastics may contaminate rainwater leading to pollution of natural water sources (Rama and Jagadeesh, 2017). It can also impede the rate of percolation and eventually interfere with soil fertility if mixed with the soil (Saikia and De Brito, 2012). The unmanaged disposal of these plastic wastes in public drains, rivers, seawater, or oceans has a direct and deadly effect on terrestrial and marine life. Many foraging cows have died in India due to the ingestion of plastic waste (Lokeshwari et al. 2019). The disposal of plastics in water bodies has damaged the health of aquatic animals. Marine life has been noticed with plastic components in their stomachs and polymeric molecules in their muscles. In 2006, The UN Environment program found that every square mile of ocean contains 46000 pieces of floating plastics. Moreover, ingestion and entanglement with plastic waste have cost the lives of more than a million sea birds and approximately 100,000 sea mammals (Saikia and De Brito, 2012). Due to these persistent pollution problems and ecological impacts, the disposal of plastic waste in landfills and natural surroundings is the least preferred, so much so that EU-28 member countries have resolved to adopt the 'zero plastic to landfill concept' (Záleská et al. 2018).

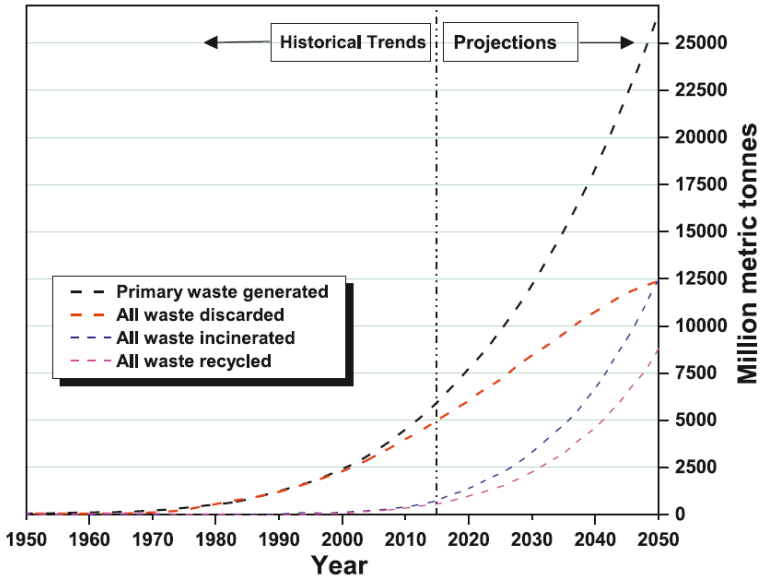

Fig. 1.5 Plastic waste management – Historical trends and future projections (Geyer et al. 2017)

Plastic waste is derived from organic hydrocarbon-based raw materials. Thus, it has a high calorific value. Furthermore, its low moisture-holding capacity makes it suitable for combustion in incinerators or boilers. However, it has been reported that

burning plastics at a lower temperature is responsible for releasing toxic and poisonous chemical gases into the air, causing air pollution. Moreover, the emissions also include dioxins, one of the most toxic substances extremely harmful to human health (Almeshal et al., 2020b; Gu and Ozbakkaloglu, 2016). The incineration of plastic waste is an attractive source of alternative energy. It can contribute to the preservation of natural resources with the additional advantage of a reduction in waste volume by 90 to 95%. However, emissions of harmful toxic fumes have resulted in growing public resistance to the incineration technique of plastic waste management (Almeshal et al., 2020b).

Under these circumstances, recycling, and utilization of plastic waste in a sustainable and environmentally friendly manner remains the only alternative to tackle the environmental menace caused otherwise due to landfilling and incineration of plastic waste (Verdolotti et al.,2014).

1.1.3 Recycling of plastic waste- the conventional approach

Plastic recycling is considered the most beneficial method in plastic waste management for its environmental and climatic benefit over landfilling and incineration. Plastic recycling reduces raw material extraction and production of virgin plastics (EEA Report, 2021). Additionally, recycling offers the advantage of a significant reduction in greenhouse gas (GHG) emissions. This is because of the avoided emissions caused during the equivalent production of raw plastics. The life cycle analysis of the most common types of plastics has demonstrated that avoiding the production of virgin plastic and using recycled plastics provide substantial environmental benefits. It may reduce GHG emissions by 20-50% in comparison to landfill and incineration scenarios (Al-Maaded et al. 2012; Bataineh 2020; Gandhi et al. 2021). Plastics are a family of a large number of individual polymers. These polymers are characterized by varying chemical and technical properties. Plastic waste emerges as a complex mixture of different polymers posing lots of difficulties in the recycling process. Therefore, the knowledge of plastic waste composition is of great importance in modeling plastic recycling methods, as different polymers have diverse product applications and may have varying recycling potential. Thus, sorting and separation of wastes are considered the primary stage of waste recycling (Faraca and Astrup, 2019).

Sorting is carried out by typical material recovery facilities (Hopewell et al., 2009). Manual and automatic methods are adopted for sorting co-mingled polymer wastes. The latter is preferred by most recycling facilities, considering the quantum of waste generated in recent times. Automated systems like FT-NIR spectroscopy and optical color recognition camera systems have been used to separate different polymer types. Also, other sorting technologies like X-ray technology have been useful in segregating polymer products like PVC containers (Hopewell et al. 2009). Trommels, density-based air classification systems, ballistic separators, sophisticated hydrocyclones, air classifiers, etc. have been used to segregate flexible packaging. To separate polyolefins like PP, HDPE, and LDPE from PET, PE, and PS, the method of density sorting is generally adopted (as in Asian recycling systems). However, this method is not beneficial for materials with overlapping density ranges, as in the case of PET and PVC (Al-Salem et al., 2009). In such cases, sometimes the air elutriation method is used. Endless configurations and combinations of sorting processes are provided by the recent technological innovations for the effective sorting of complex plastic waste. Sorting and source segregation of plastic waste is an essential step in deciding about the method of recycling and the manufacture of products in the secondary line (Faraca and Astrup, 2019). There are three methods of recycling plastic waste: mechanical recycling, chemical recycling, and thermal recycling.

Mechanical recycling or secondary recycling is the popular recycling solution for post-consumer plastic waste. It involves the physical degradation of the waste, where the plastic waste is melted, shredded, or granulated to obtain new secondary plastic materials without any modification in their chemical properties (Faraca and Astrup, 2019). Mechanical recycling is effective on single polymer plastic, e.g., PE, PP, PS, etc. After sorting, plastics are either melted directly and cast into new shapes or melted after being shredded into flakes and then processed to obtain granulates (Siddique et al. 2008). Heterogeneity in waste composition and degradation in properties post-recycling are the main issues in mechanical recycling (Al-Salem et al. 2009). However, it is still the most used technique for plastic recycling due to its effectiveness and rapid execution (Awoyera and Adesina, 2020).

In chemical recycling, the chemical structure of the polymer is modified. Polymeric wastes are converted into smaller molecules, usually in liquid and gaseous

form. The modified product is subsequently used as feedstock to produce new petrochemicals and plastic products. Thus, it is also called feedstock recycling (Almeshal et al., 2020b; Awoyera and Adesina, 2020; Siddique et al., 2008). This method can be used for treating heterogeneous and contaminated waste with minimum pre-treatment. Although it is a capital-intensive technology, high product yield, and minimal waste generation classify it as a profitable and sustainable alternative to recycling, subject to the treatment of large volumes of waste (Almeshal et al., 2020b; Al-Salem et al., 2009). Depolymerization, which forms the basis of chemical recycling can be achieved by hydrolysis or chemical decomposition and pyrolysis or thermal decomposition. Single condensation polymers such as urethanes, PET, nylon, and PMMA can be depolymerized with relative ease to produce useful and economic feedstocks, unlike mixed plastics (Siddique et al. 2008).

Thermal recycling involves heating thermoplastics at remarkably high temperatures such that the plastic flows. While the molten mass cools, it is molded into a novel product. It does not involve any modifications in the chemical composition of plastics. There is a limitation on the number of cycles for which plastics can be recycled by thermal reprocessing, as there is degradation in the properties of plastics after each cycle. This method can be advantageously used for pure thermoplastics. However, it cannot be used for thermosets which degrade at high temperatures without softening. Thermal recycling of heterogenous thermoplastics is a much more involved process. In such cases, special equipment that is responsive to the thermal properties of plastics or has few demands on the melting behavior of different plastics is used. Furthermore, commingled wastes are also thermally recycled by systems/mechanisms in which plastics with lower melting points act as a matrix that envelops other plastics and contaminants (Siddique et al. 2008).

Even with the best collection and sorting systems in place, the recycling rate of plastic waste is still not encouraging (Alqahtani et al. 2018). Table 1.2 shows polymer-wise waste generation and the recycling rate in the year 2018 in the USA. In a country like the USA where technological advances and social awareness are at their best, the overall recycling percentage could just touch 8.7%. The data also illustrates that the recycling rate is also affected by the type of the collected polymer. Faraca and Astrup (2019) conducted a study in a Danish recycling center to understand the effect of

characteristics of collected plastic waste on recycling potential. The authors concluded that the recyclability of collected waste depends on the sorting and reprocessing ability of the polymer type. The comparative sorting, reprocessing, and recycling potentials of the most used hard plastic products like HDPE, PET, PP, PS, and PVC are presented in Fig. 1.6. The sorting and reprocessing potential of all plastics is above 50%. However, polymers like PET exhibited low recycling potential.

Table 1.2 Waste recycling rate in the USA in 2018 (USEPA Fact Sheet, 2020)

Polymer type	Waste generation (Million tonnes)	Waste recycled	
		Quantity (Million tonnes)	Percent of generated waste
PET	5.29	0.98	18.5
HDPE	6.30	0.56	8.9
PVC	0.84	Neg.	-
LDPE/LLDPE	8.59	0.370	4.3
PP	8.15	0.050	0.6
PS	2.26	0.020	0.9
Other resins	4.16	1.110	26.7
Total polymer waste	35.68	3.090	8.7

Neg. = Negligible (< 0.005 million tonnes)

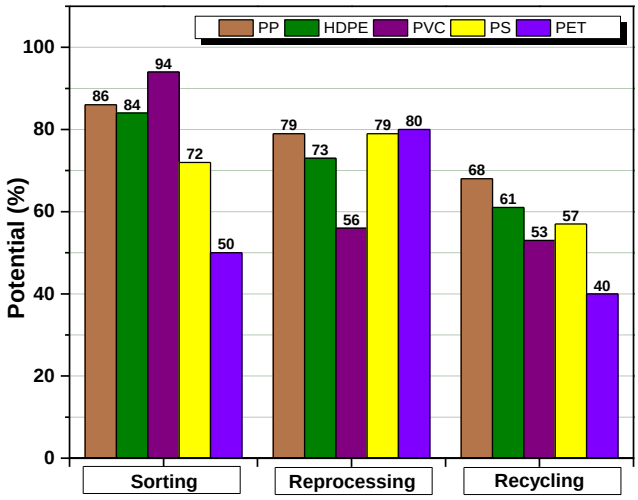

Fig. 1.6 Sorting, reprocessing, and recycling potential of plastic wastes (Faraca and Astrup, 2019)

The recycling of plastic waste is undoubtedly a step toward the circular economy in the plastic industry. However, the practical implementation and efficiency of the recycling process are subject to a few technological and economic constraints. These are (i) the commingled nature of plastic waste with different types of plastics with different

grades and properties; (ii) the insoluble nature of plastics and their tendency to form a discrete phase within a continuous phase; (iii) the presence of non-plastic entities like dirt and metals that can interfere with the efficient functioning of reprocessing equipment; (iv) relatively low density of plastic waste; and (v) non-uniform feed stock levels of plastic wastes over time (Almeshal et al., 2020b; Bhagat and Savoikar, 2022; Siddique et al., 2008). Due to these constraints, recycling plastics to obtain new plastic-based products is questioned on the residual quality and economic viability of the obtained products (Ferdous et al., 2021; Singh and Ruj, 2015). It is estimated that only one-tenth of the recyclate is recycled multiple times (Bhagat and Savoikar, 2022). It is worth noting that most of the secondary products obtained from recycled plastics are known to have short-span usage. The degradation in the quality of processed plastics after every cycle exhausts the serviceability of the recyclate and eventually, it ends up as waste in landfills. Almost 75% of the plastic produced is used for short-term applications and the rest 25% is used for comparatively long-term applications like pipelines (Awoyera and Adesina, 2020). Therefore, it can be said that recycling plastics to produce secondary plastic products may marginally extend their useful life. It may not take those plastics far from the time at which they are dumped into the environment to cause ecological and environmental problems (Bhagat and Savoikar, 2022). Although lower biodegradability is the most beneficial property of plastics, the same property defames plastics when dumped into the natural surroundings. This property can be advantageously utilized by incorporating waste plastics into a material that satisfies the following important criteria: (i) the material should have a sufficiently long useful life. (ii) plastic incorporation should not cause any effect on the physical, functional, and environmental performance of the material, and (iii) material should accommodate the plastic wastes without much processing effort. In the construction industry, concrete is considered a material that satisfies the aforesaid specified criteria for housing plastic waste, subject to evaluation of the effect of plastic on its physical, functional, and environmental performances. Considering the use and waste life span of plastic in comparison to that of concrete, the advantage of utilizing plastic waste in concrete is depicted in Fig. 1.7.

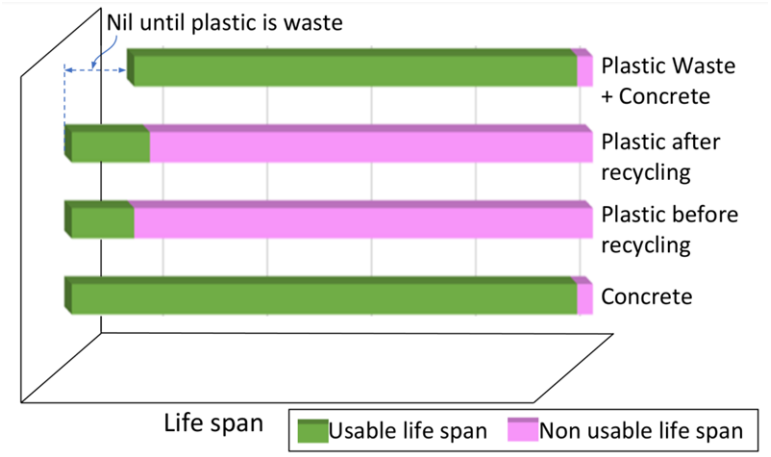

Fig. 1.7 Utilization of plastics in concrete (Sharma and Bansal, 2016)

1.1.4 Utilization of Plastic Waste in Concrete

Rapid industrialization and widespread urbanization have seen a booming increase in construction activities around the world. The construction industry is the main pillar of social and economic development on a global scale. It consumes almost 40% of the raw materials of the world, ranking next to the food industry (García-Segura et al, 2014). The huge burden of resource depletion by the construction industry and its effect on the environmental system cannot be neglected. It is reported that 15-45% of the total environmental deterioration in eight major environmental impact categories, including resource depletion, energy use, freshwater use, and atmospheric emissions are caused by construction materials (Fares et al., 2021). Concrete is the prime material in the construction industry which is known to be the most consumed material on earth next to the water. The production of cement volumes is a direct indicator of volumes of concrete production. In 2015, 4.1 billion tons of cement were produced worldwide which corresponds to 25-30 billion tons of concrete (Miller, 2018). With a global increase of 5% per year, cement consumption is expected to reach 6 billion tons in the year 2025 hinting at a mammoth concrete volume of around 40 billion tons (Kurad et al., 2017).

Concrete is a mixture of aggregates (sand, gravel, or crushed stone) agglomerated by a binding material like cement. Both these materials have a major direct impact on the environment. Each ton of cement consumed in concrete is responsible for an equivalent amount of greenhouse gas emission in the atmosphere. Aggregates occupy nearly 60 to 75% volume inside the concrete. The global consumption of aggregates was estimated to

exceed 28 billion tons in the year 2017 (Fares et al., 2021). With the current trend of concrete production, the demand for aggregates has been forecasted to double in the next two to three decades (Wang et al., 2021a). Conventional concrete utilizes the aggregates obtained from the natural womb, may it be the stone quarries or the natural riverbed. The exploitation of these huge volumes of natural strata to meet the demands of the concrete aggregates posed a great threat to environmental sustainability. In an era of follow-up of the goal of sustainable development, the concrete manufacturing industry is exploring ways to mitigate the environmental problems of greenhouse gas emissions caused by cement and resource depletion caused by the exploitation of aggregates. Recently, concrete research has concentrated on finding alternatives to these conventional materials. The adaption of by-products and waste material as alternative concrete constituents is looked upon as a beam of hope in the achievement of the goal of sustainability in concrete. The by-products from coal-fired power plants and the steel manufacturing industry viz. fly ash (FLA) and granulated blast furnace slag (GBFS) as supplementary cementitious materials (SCM) have been successfully used as alternatives for cement in conventional concrete (Aïtcin, 2016; Bhagat and Savoikar, 2021; Juenger et al., 2012). The use of waste materials and byproducts to replace the natural aggregates inside concrete has been perceived to mitigate the problem of resource depletion of natural strata. The utilization of different industrial wastes, including waste slag from the steel industry, copper industry, glass waste, ceramic waste, rubber waste, construction and demolition waste (CDW), etc. has excessively been explored in enormous research efforts (Fares et al., 2021). Plastic wastes have also exhibited the potential to be used as an aggregate component inside the concrete, providing a dual advantage through the conservation of natural resources and a concrete solution for plastic waste management.

Extensive research on using plastic waste in concrete has been reported in the literature. The plastic waste was mostly subjected to mechanical shredding to obtain the discrete plastic particles in fiber form or aggregate form to make it suitable for use in concrete. The use of plastic in the fiber form to produce fiber-reinforced concrete was experimented with by many researchers (Akça et al., 2015; Borg et al., 2016; Pereira De Oliveira and Castro-Gomes, 2011; Silva et al., 2005). The fiber content volume in such concretes was limited from 0.5% to 3% by volume. Although there was a noticeable improvement in the mechanical performance of concrete due to the fiber effect of plastics,

the amount of plastic recycled in fiber-reinforced concrete is not significant (Rahmani et al., 2013). The use of plastic waste to substitute as aggregates in cement composites is the most economical way of plastic recycling that presents noticeable volumes of conservation of natural resources, waste consumption, prevention of environmental pollution, and decrease in energy demand (Batayneh et al., 2007; Sadrmomtazi et al., 2016). In addition to these sustainability-related advantages, plastic waste aggregates (PWA) being a low-density constituent can reduce the density of concrete. Plastic can be an excellent substitute for conventional lightweight aggregates (LWA) like pumice, tuff, diatomite, volcanic cinders, pulverized fuel ash, etc., to obtain lightweight concrete (LWC) with a lower specific mass that can withstand dynamic loads in earthquake-prone areas (Ersan et al., 2020). Additionally, it may provide enhanced thermal properties, impact resistance, sound insulation, and improvement in some durability-related characteristics (Coppola et al. 2018). However, one of the major disadvantages of using PWA in cement mixes is the deterioration of the mechanical strength of the mixes (Almeshal et al., 2020b; Bahij et al., 2020; Gu and Ozbakkaloglu, 2016; Saikia and De Brito, 2012; Siddique et al., 2008). It is a major drawback that restricts the use of PWA inside cementitious composites, especially in higher volumes to derive the benefits of waste consumption and resource conservation.

The research findings on the mechanical properties of plastic waste cement composites (PWCC) revealed that the weak adhesion between the plastic particles and the cement matrix and the resulting increase in porosity of concrete is the main reason responsible for the loss of strength in PWCC (Babafemi et al., 2018; Bhagat and Savoikar, 2022; Mohammed et al., 2020a; Pacheco-Torgal et al., 2012; Sharma and Bansal, 2016). Various attempts have been made to improve the bond characteristics of PWA with cement matrix to improve the mechanical performance of PWCC. The effect of the treatment of PWA with various surfactants like hypochlorite solution, sodium hydroxide solution, etc. has been studied by a few researchers (Lee et al. 2019; Correa et al. 2020; Naik et al. 1996). Novel LWA obtained by thermal fusion of PWA with other ingredients such as sand, SCM like FLA, GBFS, or any concrete-compatible materials has been experimented with to understand the possibility of achieving an enhanced mechanical performance of PWCC (Alqahtani et al. 2018; Choi et al. 2005, 2009; Gouasmi et al. 2017). These techniques could minimize the loss of strength to some extent by improving

the bond characteristics of PWA with cement paste. However, the economic and environmental costs involved in the additional treatment and/or processing of the waste may be too heavy in comparison to the magnitude of strength replenishment and quantity of PWA consumed inside the PWCC. Therefore, other alternatives that favor the use of PWA with minimum processing costs and a better outcome in terms of the mechanical performance of concrete were explored. This included the use of SCM like FLA, GBFS, silica fume (SF), and nano materials like Nano Silica (NS) as a partial substitute to cement in the conventional concrete mix. These materials were responsible for the improvement in microstructural characteristics of the interfacial transition zone between PWA and cement matrix, thereby contributing to the mitigation of strength reduction due to PWA (Chen et al., 2019; Faraj et al., 2019; Sadrmomtazi et al., 2016).

Concrete made with PWA exhibits a resemblance to recycled aggregate concrete (RAC) obtained from CDW in terms of its physical and mechanical performance. RAC is characterized by a porous microstructure due to a weak interfacial transition zone (ITZ) identical to PWCC and exhibits lower mechanical strength and lower modulus of elasticity (McNeil and Kang 2013). The use of SCM and NS has shown a replenishment in the strength values of RAC due to the improvement in rheology and pozzolanic action of the additives (Darji et al., 2014; Hosseini et al., 2011; Kurda et al., 2018b; Li et al., 2017; Marinković et al., 2017; Mukharjee and Barai, 2014; Turk et al., 2015). Other than using pozzolanic materials to replace cement inside RAC, a novel and sustainable approach to using high-density aggregate from industrial waste in tandem with recycled aggregate has been attempted with anticipation of better mechanical behavior of RAC (Qasrawi et al., 2009). The hypothesis of this innovative approach was sourced from the investigations that revealed the positive influence of partial replacement of natural aggregates in conventional mixes with high-density industrial wastes. These wastes included copper slag (CPS) (Al-Jabri et al., 2009, 2011; Gupta and Siddique, 2019; Wu et al., 2010), electric arc furnace slag (EAFS) (Alizadeh et al. 2003; L. Coppola et al. 2016; Faleschini et al. 2015), ferrochrome slag (FCS) (Al-Jabri et al., 2018; Dash and Patro, 2018; Gencel et al., 2012), induction furnace slag (IFS) (Miah et al. 2020; Uddin Mohammed et al. 2017), stainless steel slag (SSS) (Bodor et al., 2016; Guo et al., 2018; Singh and Siddique, 2016a), smelting furnace slag (SFS) (Maslehuddin et al., 2003; Saikia et al., 2012; Tripathi and Chaudhary, 2016), etc. The use of these high-density

slags (HDS) in PWCC may improve the overall performance of composites, which otherwise is affected due to the incorporation of plastic particles. This innovative approach may present the following benefits:

1) Additional savings in natural aggregates due to the use of industrial slag along with plastic waste.
2) Possibility of obtaining normal-weight and normal-strength concrete even after using low-density plastic aggregates which otherwise degrades the mechanical strength of concrete.
3) Possible improvements in durability characteristics of concrete through symbiotic contribution by plastic waste and high-density industrial slag.
4) Environmental benefit achieved due to avoided landfill of waste slag and plastic waste.

1.1.5 Sustainability Assessment of Novel Concrete

The issue of sustainable development has been at the focal point of implementation in all emerging economies across the globe. The Brundtland Report of the World Commission on Environment and Development and the Oslo Round Table on Sustainable Production and Consumption defined sustainable development and consumption as "the use of goods and services that respond to basic needs and bring a better quality of life while minimizing the use of natural resources, toxic materials and emissions of waste and pollutants over the life cycle, so as not to jeopardize the needs of future generations" (Jernolov and Jernolov, 1994). Concrete is the second most consumed material after water throughout the world, and no development can be imagined without this material. Therefore, producing sustainable concrete may be a giant step in fulfilling the global sustainability goal.

The ideology of developing sustainable concrete is not restricted to resource conservation only. It includes other aspects viz. reduction in carbon footprint including a reduction in the emission of pollutants, reduction in waste generation, recycling of industrial and agricultural by-product materials and post-consumer materials, and use of environmentally friendly manufacturing process in the production of concrete (R. Kumar and Naik, 2016). This approach is popularly known as 'Green Concrete' technology. This 'greenness' of such concrete is questionable unless its environmental assessment is carried out throughout its life cycle and compared with ordinary concrete (Van Den Heede

and De Belie, 2012). Thus, sustainability assessment of these novel green concretes is a must before their practical onsite application.

The sustainability assessment is conducted to support policy and decision-making in a broad environmental, economic, and social context, and transcends a purely technical/scientific evaluation (Salas et al., 2016a). The evaluation of the sustainability potential of concrete is an extraordinarily complex exercise. It involves the quantification of the following interacting and interdependent parameters: technical performance, environmental impact, economic implications, and lifetime (Müller et al., 2014). The technical and economic benefits of utilizing industrial byproducts in concrete have been explored in various research studies over the past several decades. However, the study of the environmental implications of using these industrial byproducts in concrete is mandatory to assess the sustainability of concrete (Kumar and Naik, 2016).

Each activity in the concrete manufacturing process contributes to the environmental impact. The environmental assessment cannot be restricted only to the impact created by the ingredients inside the concrete. All the activities that demand energy consumption right from the extraction of raw materials, the transportation, concrete manufacturing phase, the repairs and maintenance during the use phase, demolition activity after the useful life, and disposal/recycling activity should be considered to assess and compare the environmental impact of novel concrete with the conventional mix (Collins, 2010; Flower and Sanjayan, 2017; Kim et al., 2017). A holistic approach is recommended for the analysis and quantification of the overall impact of the production of concrete. The life cycle assessment (LCA) approach is considered a suitable approach for a diverse audience to give comparable results for different types of concretes (Petek Gursel et al. 2014).

1.2 Aim of research

The present research aims to determine the suitability of plastic waste as a partial replacement of natural fine aggregate (NFA) in cementitious composites. In addition to the investigation of the technical performance of the PWCC, the current research also aims at the assessment and comparison of the environmental impact caused by the novel composites with that of the composites in the conventional form, using LCA methodology.

1.3 Objectives of the research

The motivation of this thesis is the use of PWA in cement mortar and concrete in combination with other industrial waste like HDS. It is proposed to analyze and give technical specifications on the rheological, mechanical, and durability characteristics of the PWCC containing these recycled aggregates and compare the results with the performance of the composites containing conventional aggregates. Furthermore, the environmental impact assessment of the novel composites is also proposed in the current research. The objectives of the proposed research are listed below:

1) To identify the plastic waste and industrial waste to be incorporated as fine aggregate fractions inside mortar and concrete through a comprehensive literature review.
2) To determine the material characteristics of the plastic waste and industrial waste high-density slag and to arrive at volumetric substitution levels of the individual and combined alternative aggregates inside concrete and mortar.
3) To determine the physical, mechanical, and durability characteristics of mortar and concrete with plastic and industrial waste fine aggregates.
4) To study the effects of the addition of plastic waste on various properties of modified mortar and concrete with optimum levels of industrial waste incorporation in mortar and concrete.
5) To determine the effect of adding SCM inside mortar and concrete containing plastic waste and industrial waste fine aggregates.
6) To carry out a sustainability assessment of the usage of plastic waste in concrete using an LCA methodology.

1.4 Scope of Study

In this research, PET particles obtained after mechanical shredding of PET bottles obtained from the collected waste stream are used as fine aggregates inside cementitious mixes by replacing increasing volume contents of NFA. The PET particles of size fractions confirming NFA size are used in the mixes. These particles are obtained after mechanical shredding of PET bottles which are washed after sorting from the collected municipal solid waste. The used volume does not include any plastic-type other than PET. The upper limit of replacement volume is decided based on the ease of making a workable

mix with the use of plasticizer within permissible dosage. To gain a comprehensive perspective on increasing volumes of research on PWCC and to complement the current study, fundamental and empirical laboratory tests are conducted on mortar and concrete. These tests include tests to determine rheological characteristics, and mechanical strength tests such as compressive strength, flexural strength, splitting tensile strength, and modulus of elasticity. The durability characteristics such as water absorption, permeability, and chloride migration are performed on concrete specimens. Furthermore, the effect of exposure to elevated temperatures is also investigated. The amount of usage of HDS is determined based on experimental evaluation of the optimum amount of substitution from consideration of the mechanical strength of the conventional concrete. To study the effect of the use of SCM in this novel aggregate concrete, FLA is blended with cement at a 30% replacement ratio based on the most favorite trend reflected in the comprehensive literature study. While conducting LCA studies of the novel concrete, cradle to cradle-to-gate approach was used for the analysis. The assessment was based on the databases applicable on a global scale due to the unavailability of a local database for environmental emission details. Most of the emission-related data for environmental impact assessment was sourced from the literature fetching a domain of limitation in the analysis. This research is not intended to investigate and compare theories in plastic-modified cement composites but to embrace the application of this novel technology with due regard to future research developments and emerging general critique.

1.5 Outline of research

To achieve the aim and the objectives of the current research study as listed in sections 1.2 and 1.3, the following step-by-step procedure is adopted:

1) Perform a comprehensive literature review to understand the effect of the addition of PWA on the physical, mechanical, and durability characteristics of cement composites and overview the methods adopted to enhance the functional performance of the PWCC.
2) Perform a comprehensive literature review to understand the effect of high-density industrial waste slag on the physical, mechanical, and durability characteristics of conventional concrete.

3) Conduct the preliminary tests to understand the material characterization of all the ingredients used in the cement composites of the current research including the substituting materials, i.e., PWA, HDS, and FLA.
4) Design the mix proportions for cement mortar and cement concrete in three tiers: 1) Composite containing PWA as substitutes for NFA; 2) Composites containing PWA as substitutes for the blend of NFA and HDS; 3) Composites containing FLA as SCM blended with cement in a mix containing NFA, PWA, and HDS.
5) Perform laboratory tests to determine the physical, mechanical, and durability characteristics of the control/reference mix as well as the modified mixes in the three tiers of mix design.
6) Perform the sustainability assessment of the cement composites in all three tiers of mix design as well as reference mix using the holistic approach of LCA for a selected system boundary and appropriate functional unit.

1.6 Novelty of Research

The use of plastic waste in concrete to replace the aggregates can no longer be considered an innovative approach, thanks to the voluminous research studies conducted in this sector over the past two decades. However, most studies were conducted to understand the effect of increasing volumes of plastic inclusions on the physical and mechanical performance of concrete. Very few studies focused on durability-related investigations. Considering the conclusions of degradation in strength-related properties of concrete, the application of plastic waste containment in concrete looked far away from its practical implementation. Few research initiatives could attempt mitigation of the decline in the strength of the composites through surface treatment of plastic aggregates by improvement of bond characteristics between polymer surface and cement paste. Although these attempts could not raise the concrete mixes to the standards of conventional concrete, the mixes with volumetric replacement of aggregates up to 10-15% could satisfy the requirements of the LWC category. Obtaining normal-strength concrete with PWA has always been a challenge for the concrete research field. The current research aims at obtaining normal strength and normal density concrete with substantial volumes of PWA, although plastic is known for its low density. A novel and

unprecedented approach to seeding conventional concrete with a high-density industrial waste slag is adopted in the present study. This approach envisages the ability of HDS to improve the mechanical performance of conventional concrete through its better bonding characteristics. The research is based on the hypothesis that the HDS shall compensate for the loss in density as well as mechanical strength in concrete containing PWA. Furthermore, the current study uses the LCA methodology to present the environmental assessment of this novel concrete. Although, sufficient literature is available on the LCA of green concretes utilizing SCM, recycled aggregates, and other non-conventional aggregates, concrete with plastic waste aggregates is yet to be thoroughly scanned under the LCA spectrum. This study is a unique attempt toward the LCA of concrete containing PWA. The study of concrete containing HDS and PWA in a single concrete mix may be the breaking new ground in the concrete research area. The LCA of this concrete in comparison to conventional concrete is another contemporary facet of the current study.

1.7 Structure of Thesis

The current research study of sustainability assessment of utilizing recycled plastic waste in cement composites has been presented with the following structure of thesis:

Chapter 1: Introduction

This chapter covers the introduction to plastic production on a global and regional scale, plastic waste generation, and plastic waste management scenarios. It also covers brief information about the use of plastic waste and high-density industrial slag waste in concrete. A brief introduction to the need for LCA to ascertain the sustainability of novel concrete is also presented. The aim, objectives, scope and limitations, and novelty of current research are focused on in this chapter.

Chapter 2: State of the Art

A comprehensive review of the use of different types of plastics as aggregates in cement composites and their effect on the physical, mechanical, and durability characteristics of composites is presented in this chapter. It also covers the literature regarding the attempts undertaken to improve the performance of plastic-incorporated concretes. Historical research findings on the use of industrial waste slags as aggregates in cementitious mixes are also covered in this chapter. The environmental impact assessment of green concrete

is also reviewed from the literature to understand the methodology of LCA and to apply it to the current study. The research gaps are identified and a critical appraisal of the review of the literature is also presented.

Chapter 3: Materials and Mix Proportions

This chapter presents the details of the materials used for experimentation and their characterization. The details about the scheme of experimentation, the variables involved, the array of mixes, and the mix design are included in this chapter.

Chapter 4: Methodology

The experimental details regarding the methodology of testing the mixes with due consideration of relevant standards are presented in this section. A brief introduction to LCA methodology and the step-by-step procedure of assessment is also presented in this chapter.

Chapter 5: Test Results and Discussions

This chapter presents the results of the physical, mechanical, and durability tests conducted on cement mortar and concrete containing plastic waste. Elaborative discussions are presented explaining the attributes of the behavior of the test mixes for each performance indicator.

Chapter 6: Mathematical Modeling and Validation

This chapter is devoted to the validation of the results with the previous findings in the literature. The results are also analyzed for possible mathematical relationships between the properties. These relationships are validated with the models suggested by other research studies and codal provisions.

Chapter 7: Sustainability Assessment of Concrete

Using the methodology of assessment and step-by-step procedure presented in Chapter 3, the environmental impact and energy demand for concrete samples containing plastic waste are determined in this chapter. The results are compared with the impacts associated with the making of conventional concrete.

Chapter 8: Conclusion

This chapter presents the major conclusions derived from the current research, the major contribution of the work, and the future scope of research as a continuation of this work. The **References** and **Appendices** follow in succession.

Chapter 2

State of the art

2.1 General

The use of plastic inside concrete can be traced back to research studies from over the last three decades from the 1990s. Initially, plastic was used as a fiber to strengthen the concrete. It was followed by studies on the use of polymeric resins and more recently, extensive research has been reported on the utilization of plastic as aggregates in cementitious mixes (Ahmad et al. 2022). The environmental advantages of recycling plastic waste as concrete or mortar aggregates have been discussed in Chapter 1. Extreme versatility and ability of plastic materials to be tailored to meet specific technical needs, their lighter weight compared to other ingredients in concrete easing transportation efforts, their durability and longevity characteristics, resistance to chemicals and water, better impact resistance, lower thermal conductivity, and excellent electrical insulation properties postulates optimistic opinion about the use of plastic as aggregate inside the concrete (Yadav, 2008). However, the other intrinsic properties of plastics, such as low modulus of elasticity, lower temperature resistance, shape, and surface texture can significantly affect the performance of PWCC relative to the control mix. This is attributed to the essential difference between the engineering properties of plastics and the replaced natural aggregates in the mix (Bhagat and Savoikar, 2022). The material properties of some common types of plastics and natural aggregates presented in Table 2.1 depict the extent of variation in these properties.

From the values of the bulk density of plastics relative to natural aggregates, it is quite predictable that the overall density of the composites would decline after the incorporation of PWA in PWCC. An elastic modulus value of plastics, 70 times lower than the natural aggregates signifies a drastic reduction in the overall Young's modulus of concrete. A similar trend may be anticipated for the thermal conductivity of composites due to the lower thermal conductivity of plastics. Although these hypotheses are supported by the research findings in the literature, the results of some of the physical and

mechanical properties revealed the mysterious behavior of PWA in PWCC. A comprehensive review of the effect of PWA on various physical, mechanical, and durability characteristics of PWCC is presented in § 2.2. The findings are presented for the most common thermoplastics utilized as fine and coarse aggregates in cementitious mixes.

Table 2.1 Material properties of some common plastics and natural aggregates

Material	Bulk density (kg/m^3)	Water absorption (%)	Specific gravity	Elastic modulus (GPa)	Tensile strength (MPa)	Thermal conductivity (W/mK)	Dielectric constant
PET	326-547	0.09	1.34	2.1-3.1	55-80	0.15	3.00-4.00
PE	24	0.10	0.80-1.10	0.6-1.4	18-30	0.33-0.52	2.30-2.70
PVC	575-750	0	1.44	2.7-3.0	50-60	0.17-0.21	3.00
PP	900-910	0.02	0.9-1.00	1.3-1.8	25-40	0.12	2.20
PS	8.5-52	0	0.34	3.1-3.3	30-55	0.105	2.50-2.60
Sand	1650	1.80	2.65	70	-	4.45	3-5
Gravel	1620	1.32	2.79	70	-	2.29-2.78	4-8

Source: (Bhagat and Savoikar, 2022; Jacob-Vaillancourt and Sorelli, 2018; Li et al., 2020; Mohammed, 2018; Mohammed et al., 2020a; Pavlík et al., 2018; Saikia and De Brito, 2012)

This study also proposes to use high-density industrial waste slag as supplementary fine aggregate to enhance the mechanical performance of conventional concrete as well as plastic-modified concrete. To pursue this innovative approach, it is imperative to review the research items dedicated toward the use of such slags as aggregate fillers in concrete. Table 2.2 illustrates the physical properties of some industrial waste slags which have already been experimented with as aggregate fillers in cement-related mixes. Considering the difference in the material properties, shape, and surface texture of the slags in comparison to natural aggregates, it is evident that the use of these aggregates in cementitious mixes would significantly affect the properties of the modified mixes. Section 2.3 presents an overview of the use of such industrial slags and their influence on the physical, mechanical, and durability properties of concrete.

The environmental impact assessment of the proposed novel concrete using the LCA approach is one of the salient objectives of the current research study. To produce a detailed diagnosis of this assessment, thorough knowledge of the methodology of the LCA is desired. The green concrete concept is gaining momentum over the past two decades and the LCA of green concrete has been considered a trustworthy tool to evaluate

and certify the eco-efficiency of such concrete. Sufficient literature is available providing insight into the LCA of conventional concrete as well as concrete containing alternative binders and alternative aggregate fractions. Section 2.4 presents a review of these LCA studies having relevance and/or similarity with the current research.

The discussions presented in each section, the critical appraisal, and the identification of research gaps form the basis of the research objectives of the current study.

Table 2.2 Material properties of industrial waste slag used as aggregates in concrete

Material	Bulk density (kg/m^3)	Water absorption (%)	Specific gravity	Crushing value (%)	Impact Value (%)
CPS	1900-2200	0.20-0.40	3.30-3.75	10-21	8-16
EAFS	1800-2000	1.70-2.50	3.30-3.80	<20	<15
FCS	1700-1800	0.4-0.6	2.70-3.05	25	23
IFS	1650	2.60	2.65	30	-
SSS	1870	1.75	2.95	20	-
SFS	2150	0.45	3.65	-	-
Sand	1650	1.80	2.65	-	-
Gravel	1620	1.32	2.79	14-25	10-18

Source: (Alizadeh et al., 2003; Dash and Patro, 2018; Khanzadi and Behnood, 2009; Ouda and Abdel-Gawwad, 2017; Qasrawi et al., 2009; Tripathi et al., 2013; Uddin Mohammed et al., 2017)

2.2 Cement composites containing plastic waste aggregates

Numerous works on the utilization of plastic as an aggregate in cement mortar and concrete have been performed to investigate the engineering properties. Different forms of thermoplastics, viz. PET, PVC, PP, LDPE, HDPE, EPS, HIPS, etc. were used as fine aggregates and coarse aggregates in cement mixes in numerous studies in the past. These studies have been reviewed in many review articles to arrive at a conclusive finding about the behavior of plastic particles inside cement mixes as a substitute for natural aggregates (Ahmad et al., 2022; Alfahdawi et al., 2016; Almeshal et al., 2020b; Babafemi et al., 2018; Bahij et al., 2020; Bhagat and Savoikar, 2022; Gu and Ozbakkaloglu, 2016; Kamaruddin et al., 2017; Li et al., 2020; Mahmood and Kockal, 2020; Mercante et al., 2018; Pacheco-Torgal et al., 2012; Park and Kim, 2020; Saikia and De Brito, 2012; Sharma and Bansal, 2016; Siddique et al., 2008). The majority of the studies conducted over the last two decades have been reviewed in the current study. Fig. 2.1 summarizes

the details of year-wise and resin-wise publications of research studies conducted with plastic waste as aggregates over the past two decades.

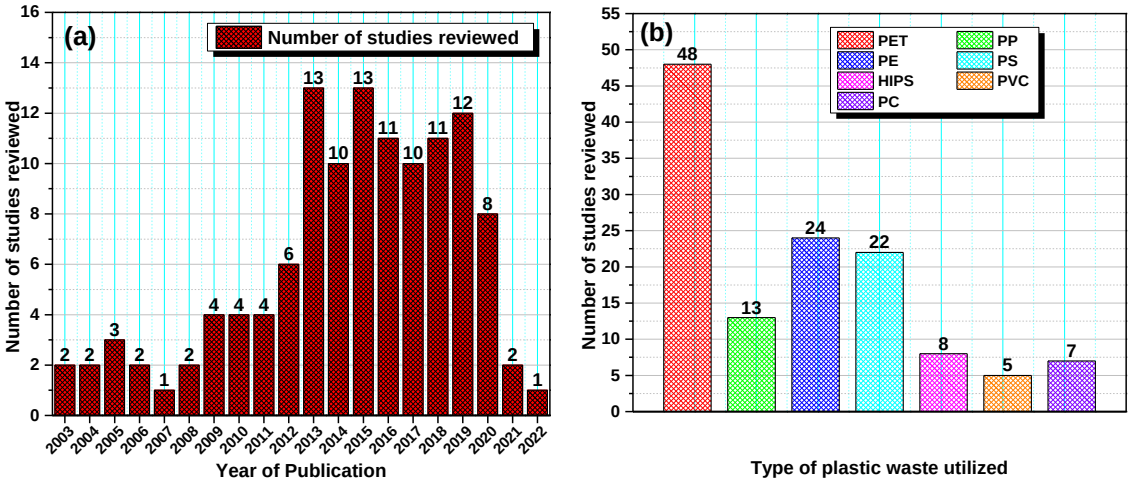

Fig. 2.1 Statistical data showing the details of research articles reviewed (a) Year wise publications (b) Type of plastic waste utilized

To understand the effect of using PWA on the physical, mechanical, and durability characteristics of cement composites, 119 research studies published in peer-reviewed publications were selected. Table 2.3 lists the research articles selected for the literature review with salient details regarding the type of polymer used, type of composite, shape, and size of polymer particles, type of aggregate replaced, and the ratio of replacement.

Table 2.3 Previous studies selected for review with plastic replacement details

Author index	References	Plastic-type	Composite	Plastic form: size	Aggregate replaced: replacement ratio
P1	Sri Ravindrarajah and Tuck (1994)	EPS	Concrete	Beads: 2.36-4.75mm	CA: 40% (Volume)
P2	Babu and Babu (2003)	(U)EPS	Concrete	Beads: 6.3mm/4.75mm	CA: 21-36.4% (Total volume)
P3	Babu and Babu (2004)	EPS	Concrete	Beads: 2.36-4.75mm/ 4.75-8mm	CA: 16.3-66.5% (Total volume)
P4	Gavela et al. (2004)	PP/PET	Concrete	Shredded particles: 0.6-6.3mm	FA, CA: 20,30% (Volume)
P5	Babu et al. (2005)	EPS	Mortar/ Concrete	Beads: 4.75, 6.3mm	FA, CA: 0-66.5% (Volume)
P6	Choi et al. (2005)	PET	Concrete	MLWA: 1.2-2.5mm	FA: 25,50,75% (Volume)
P7	Marzouk et al. (2005)	PET/HDPE	Mortar	Shredded particles: 2.5mm	FA: 5,10,15,30,50,100 % (Volume)
P8	Babu et al. (2006)	EPS	Concrete	Beads: 2.36-8mm/6.3-8mm	CA: EPS- 20-50% / UEPS- 30% (Total volume)
P9	Ahmed and Mohammed (2006)	PET	Mortar	Crushed particles:4.75mm, 6.35mm, 9.5mm	FA: 25,27,30% (NM)
P10	Marzouk et al. (2007)	PET	Mortar	Shredded particles:1-5mm	Sand: 2,5,10,15,20,30,50, 70,100% (Volume)
P11	Tang et al. (2008)	PS	Concrete	Beads: 4mm	CA: 20,40,60,80% (Volume)

P12	Ismail and AL-Hashmi (2008)	PE+PS	Concrete	Crushed particles: 0.15-12mm long 0.15-4mm thick	FA: 10,15,20% (Mass)
P13	Kou et al. (2009)	PVC	Concrete	Ground granules: <5mm	Sand: 5,15,30,45% (Volume)
P14	Albano et al. (2009)	PET	Concrete	Crushed granules: 2.6mm/11.4mm	Sand: 10,20% (Volume)
P15	Kan and Demirboğa (2009b)	(M)EPS	Concrete	Heat-treated EPS foams: 0-4mm/4-16mm	FA, CA:25,50,75,100% (Volume)
P16	Choi et al. (2009)	PET	Mortar/ Concrete	MLWA: FM 4.11	Sand: Mortar- 25,50,75,100% Concrete- 25,50,75% (Volume)
P17	Frigione (2010)	PET	Concrete	Ground particles: 0.1-5mm	Sand: 5% (weight)
P18	Akçaözoğlu et al. (2010)	PET	Concrete	Crushed granules: 0-4mm	Sand: 50 and100% of the binder (Volume)
P19	Hannawi et al. (2010a)	PET/PC	Mortar	Shredded particles: PET- <10mm; PC<5mm	Sand: 3,10,20,50% (Volume)
P20	Hannawi et al. (2010b)	PET	Mortar	Shredded particles: 1-9mm (0.1/1mm thick)	Sand: 3,10,20,50% (Volume)
P21	Galvão et al. (2011)	PET/LDPE	Concrete	PET-Agglutinated: 6-12.5 mm; LDPE-Crushed:0.15-2.4mm	Sand: 0.5,1,2.5,5,7.5% (Weight)
P22	Chidiac and Mihaljevic (2011)	HDPE/LDPE	Concrete	Pellets: FM- 3.6-4.1	Sand: 3,6,9,15% (Volume)
P23	Madandoust et al. (2011)	EPS	Concrete	Beads: 4.75mm, 9.5mm	FA, CA: 15,22.5,30% (Volume)
P24	Lakshmi and Nagan (2011)	HIPS	Concrete	Ground particles:1.18-2.36mm	CA: 4,8,12,16,20,24 % (Weight)
P25	Guilherme et al. (2012)	PET	Concrete	Ground particles P_F: 2-4mm; P_C: 4-8mm; Pallets-P_p: 2-4mm	FA, CA: 7.5,15 % (Volume)
P26	Mbadike and Osadebe (2012)	EPS	Concrete	Granules: 3.5mm dia	CA: 10,20,30,40 % (Volume)
P27	Rahman et al. (2012)	EPS/HDPE	Concrete	Shredded particles EPS: 4-8.5mm HDPE: 4-12mm	Total aggregtae: 10,20,30,40% (Volume)
P28	Wang and Meyer (2012)	HIPS	Mortar	Granules: <4mm	Sand: 10,20,50% (Volume)
P29	Demirboga and Kan (2012)	(M)EPS	Concrete	Heat-treated EPS foams: 0-4mm/4-16mm	FA, CA: 25,50,75,100% (Volume)
P30	Ferreira et al. (2012)	PET	Concrete	Flakes-P_F: 1-4mm; P_C: 2-11.2mm; Pallets-P_p: 1-4mm	FA, CA: 7.5,15% (Volume)
P31	Safi et al. (2013)	PET	Mortar	Shredded particles: 0.08-4mm	Sand: 10,20,30,50% (Weight)
P32	Ge et al. (2013)	PET	Mortar	Shredded particles: 1.18-2.36mm	Sand: 25,50,75,100% (Volume)
P33	Herki et al. (2013)	SPS	Mortar	MLWA: 0.125-8mm	FA: 20,40% (Volume)
P34	Rahmani et al. (2013)	PET	Concrete	Ground particles:< 7mm	FA: 5,10,15 % (Volume)
P35	Suganthy et al. (2013)	HDPE	Concrete	Pulverized pellets: 4-5mm	Sand: 25,50,75,100 % (Volume)
P36	Saikia and De Brito (2013)	PET	Concrete	Flakes-P_F: 1-4mm; P_C: 2-11.2mm; Pallets-P_p: 1-4mm	FA: 5,10,15% (Volume)
P37	Silva et al. (2013)	PET	Concrete	Flakes-P_F: 1-4mm; P_C: 2-11.2mm; Pallets-P_p: 1-4mm	FA: 7.5,15% (Volume)
P38	Iucolano et al. (2013)	PET+PE+PP	Mortar	MLWA: <8mm	Sand: 10-50% (Weight)
P39	Hannawi et al. (2013)	PET/PC	Mortar	Shredded particles:1-9mm (PET-0.1/1mm thick)	Sand: 3,10,20,50% (Volume)
P40	Ferrándiz-Mas and García-Alcocel (2013)	EPS	Mortar	Beads: 1-3mm	Sand: 10,30,50,70 (Volume)
P41	Shalaby et al. (2013)	PET	Mortar	Shredded particles: 1-4mm	Sand: 10,20,30,50% (Weight)
P42	Juki et al. (2013)	PET	Concrete	Granules: 0-5mm	FA: 25,50,75% (Volume)
P43	Akçaözoğlu et al. (2013)	PET	Concrete	Crushed granules: 0-4mm	FA: 30,40,50,60% (Volume)
P44	Akçaözoğlu and Ulu (2014)	PET	Concrete	Crushed granules: 0-4mm	FA: 20,40,60,80,100% (Volume)
P45	Da Silva et al. (2014)	PET	Mortar	Flakes- P_F: 1-4mm/ Pallets- P_P: 1-4mm	Sand: 5,10,15% (Volume)
P46	Ababio Ohemeng et al. (2014)	LDPE	Concrete	Ground particles: FM-3.51	Sand: 10,20,30,40,50,60% (Volume)
P47	Ghernouti et al. (2014)	LDPE	Concrete	Melted, crushed granules: 0.08-1.5mm	FA: 10,20,30,40% (Volume)
P48	Irwan et al. (2014)	PET	Concrete	Ground particles:<5mm	FA: 25,50,75% (Volume)

P49	Malkapur et al. (2014)	HDPE	Concrete	Crushed particles: F.M. 6.76	CA: 10,20,30 % (Volume)
P50	Saikia and De Brito (2014)	PET	Concrete	Flakes-P_F: 1-4mm; P_C: 2-11.2mm; Pallets-P_p: 1-4mm	FA, CA: 5,10,15% (Volume)
P51	Correia et al. (2014)	PET	Concrete	Flakes-P_F: 1-4mm; P_C: 2-11.2mm; Pallets-P_p: 1-4mm	FA, CA: 7.5,15% (Volume)
P52	Sojobi and Owamah (2014)	LDPE	Concrete	Granules: 2-4.75mm	Sand: 5,10,15% (Weight)
P53	Ranjbar and Mousavi (2015)	EPS	Concrete	Beads: 4.75mm/9.5mm	FA/CA: 10,15,22.5,30% (Volume)
P54	Hannawi and Prince-Agbodjan (2015)	PC	Mortar	Shredded particles: 5mm	Sand: 3,10,20,50% (Volume)
P55	Lo Monte et al. (2015)	EPS	Concrete	Beads: NM	Total Aggregates: 13.5,14% (Volume)
P56	Senthil Kumar and Baskar (2015)	HIPS	Concrete	Shredded particles: 6-12mm	CA: 10,20,30,40,50% (Volume)
P57	Senhadji et al. (2015)	PVC	Concrete	Grinded granules: 0-3mm/3-8mm	FA, CA: 30,50,70% (Volume)
P58	Janfeshan Araghi et al. (2015)	PET	Concrete	Flakes: 0.15-4.75mm	Sand: 5,10,15% (Volume)
P59	Akinyele et al. (2015)	PP	Concrete	Ground particles: <4mm	FA: 4,8,12,16 % (Weight)
P60	Chen et al. (2015)	HDPE	Concrete	Pulverized particles:0.3-4mm	FA: 10,20,30,50,100 % (Volume)
P61	Harini and Ramana (2015)	PET	Concrete	NM: <4.75mm	FA: 5,6,8,10,20 % (Volume)
P62	Liu et al. (2015)	PC	Concrete	Shredded particles: 1-3mm	FA: 5,10,15,20 % (Volume)
P63	Yang et al. (2015)	PP	Concrete	Ground particles: 1.5-4mm	Sand: 10,15,20,30 % (Volume)
P64	Ramesan et al. (2015)	HDPE	Concrete	Processed particles: 20mm	CA: 5,10,15,20,25,30,35,40 % (Volume)
P65	Hossain et al. (2016a)	PET	Concrete	Crushed granules: 4.75-9.5mm	CA: 5,10,20% (Volume)
P66	Guendouz et al. (2016)	LDPE	Sandcrete	NM- 1.5mm	FA: 10,20,30,40 % (Volume)
P67	Islam et al. (2016)	PET	Concrete	Shredded particles: 5-20mm	CA:20,30,40,50 % (Volume)
P68	Sadrmomtazi et al. (2016)	PET	Concrete	Shredded granules: <4.75mm	Sand: 5,10,15% (Weight)
P69	Haghighatnejad et al. (2016)	PVC	Concrete	Ground particles: <5mm	Sand: 20,30,40,50% (Weight)
P70	Nikbin et al. (2016b)	PET	Concrete	Flakes: 0.15-4.75mm	Sand: 5,10,15% (Volume)
P71	Ruiz-Herrero et al. (2016)	PVC/PE	Mortar/ Concrete	NM/ 4-32mm	FA, CA: 2.5,5,10,20% (NM)
P72	Azhdarpour et al. (2016)	PET	Concrete	Flakes-P_F: 0.05-2mm; P_C: 2-4.9mm	FA: 5,10,15,20,25,30 % (Weight)
P73	Coppola et al. (2016)	PP+PE	Mortar	Foamed particles:0.18-2mm	FA: 10,25 % (Volume)
P74	Habib et al. (2017)	HDPE	Concrete	Shredded particles:12-19mm	CA: 5,10,15,20 % (Volume)
P75	Herki and Khatib (2017)	SPS	Mortar	MLWA: 0.125-8mm	FA: 30,60,100 % (Volume)
P76	Gouasmi et al. (2017)	PET	Mortar	MLWA: 0-3mm	Sand: 25,50,75,100% (Weight)
P77	Herki (2017b)	SPS	Concrete	MLWA: 0.125-12.5mm	Total aggregates: 30,60,100% (Volume)
P78	Herki (2017a)	SPS	Mortar	MLWA: 0.125-8mm	FA: 60,100 % (Volume)
P79	Shanmugapriya and Santhi (2017)	HDPE	Concrete	Shredded particles: FM-2.98	Sand: 5,10,15% (Weight) CA: 10,15,20% (Weight)
P80	Ozbakkaloglu et al. (2017)	PP	Concrete	Granules: <9.5mm	CA: 10,20,30% (Volume)
P81	Alqahtani et al. (2017)	LLDPE	Concrete	MLWA: 10mm	CA: 25,50,75,100 % (Volume)
P82	Ismail Josa and Jumaa Khalaf (2017)	PET	Concrete	Shredded particles: 0.15-1mm thick 12mm long	CA: 10,20,30,40,50 % (Volume)
P83	Singh and Pandey (2017)	E-Plastic	Concrete	Crushed particles 4.75-20mm	CA: 5,10,15% (NM)
P84	Cadere et al. (2018)	PS	Concrete	Granules: 4-8mm	FA: 20,40,60,80,100 % (Volume)
P85	Skominas et al. (2018)	PP/PE	Concrete	NM	CA: 5,10,15,20,25% (Volume)

P86	Aciu et al. (2018)	PVC	Mortar	Crushed Granules: 8mm	Sand: 25,50,100% (Weight)
P87	Wicaksono et al. (2018)	PET	Sandcrete	Molded Granules: 10mm	Sand: 10,20,30,40,50,100% (Volume)
P88	Akinyele and Toriola (2018)	PP	Sandcrete	Crushed Granules: NM	FA: 5,10,15,20,100% (Weight)
P89	Záleská et al. (2018)	PP	Concrete	Granules: <8mm	Sand: 10,20,30,40,50% (Weight)
P90	Alqahtani et al. (2018)	LDPE	Concrete	MLWA: 10mm	CA: 25,50,75,100% (Volume)
P91	Coppola et al. (2018)	PP+PE	Mortar	MLWA: 0.18-2mm	Sand: 10,25% (Volume)
P92	Saxena et al. (2018a)	PET	Concrete	NM: 0-4.75mm/4.75-20mm	FA, CA: 5,10,15% (Weight)
P93	Badache et al. (2018)	HDPE	Mortar	Ground particles: 3.15mm	FA: 15,30,45,60% (Volume)
P94	Sabău and Vargas (2018)	HIPS	Concrete	Ground particles: 0.6-9.5mm	CA: 40,50,60% (Volume)
P95	Aslani and Ma (2018)	EPS	Concrete	Beads: NM	FA: 20,30% (Volume)
P96	Majeed et al. (2019)	HDPE	Concrete	Shredded and granulated: NM	CA: 0,12,14,16,18 (Volume)
P97	Gouasmi et al. (2019)	PET	Mortar	MLWA: 0-2.7mm	Sand: 25,50,75,100% (Weight)
P98	Chen et al. (2019)	PP	Mortar	Shredded Granules: 2.5-3mm	Sand: 20,40,60% (Volume)
P99	Faraj et al. (2019)	PP	Concrete	Columnar particles: 4-8mm	CA: 10,20,30,40% (Volume)
P100	Hernández and Etxeberria (2019)	HDPE	Concrete	Pallets: 4-10mm	CA: 25,50,75% (Volume)
P101	Ohemeng and Ekolu (2019)	LDPE	Mortar	Ground particles: FM-2.52	Sand: 10,20,30,40,50,60% (Volume)
P102	Chunchu and Putta (2019a)	HIPS	Concrete	NM: 1.8-3mm	FA: 10,20,30,40 % (Volume)
P103	Chunchu and Putta (2019b)	HIPS	Concrete	Granules: 1-4mm	Sand: 10,20,30,40% (Volume)
P104	Mohammed et al. (2019)	PVC	Concrete	Crushed Granules: 1-9mm	FA, CA: 5,15,30,45,65,85% (Volume)
P105	Lee et al. (2019)	PET	Concrete	Crushed particles: 2-12mm	CA: 10,20,30% (Volume)
P106	Farooq (2019)	E-Plastic	Concrete	Crushed particles:<4mm	FA: 5,10,15,20 % (Volume)
P107	Lokeshwari et al. (2019)	PP	Concrete	Ground particles: 0.1-3mm/8-10mm	FA: 5,10,15,20 % (Weight)
P108	Mustafa et al. (2019)	PC	Concrete	Shredded particles: 2.36-5mm	FA: 5,10,20 % (Volume)
P109	Jain et al. (2020)	LDPE	Concrete	Shredded particles: 3-5mm width;15-30mm length	FA: 5,10,15,20% (Weight)
P110	Gayatri and Popat (2020)	LDPE	Concrete	Granules: 1.18-2.30mm/ 2.40-3.80mm	FA: 7.5,10,12.5% (Volume)
P111	Saxena et al. (2020)	PET	Concrete	Shredded particles: 0-4.75mm/4.75-20mm	FA, CA: 5, 10,15,20% (Weight)
P112	Almeshal et al. (2020a)	PET	Concrete	Ground particles: 0.075-4mm	FA: 10,20,30,40,50% (Weight)
P113	Petrella et al. (2020)	EPS	Mortar	Ground beads: 1-6mm	Sand: 25,50,100 % (Volume)
P114	Mohammed et al. (2020b)	LDPE	Mortar/ Concrete	Granules: <4.5mm	FA: 5,10,15,25,30 % (Volume)
P115	Al-Tayeb et al. (2021)	PC	Concrete	Shredded particles: 4-5mm	CA: 5,10,20% (Volume)
P116	Górak et al. (2021)	PET	Mortar	Flakes:< 12mm	FA: 10,25 % (Volume)
P117	Abed et al. (2021)	PET	Mortar	Shredded particles: <4.75mm	Sand: 5,15,25,50 % (Weight)
P118	Dawood et al. (2021)	PET	Concrete	Shredded particles: <4mm	Sand: 5,7.5,10,12.5,15,20 % (Weight)
P119	Babafemi et al. (2022)	PET	Concrete	Shredded particles: <2.5mm	Sand: 5,10,15 % (Volume)
P120	Jaskowska-Lemańska et al. (2022)	PET	Concrete	Shredded particles: 0.5-4mm	FA: 5,10,15,20 % (Weight)

Plastic-type-UEPS: Unexpanded Polystyrene; SPS: Stabilized Polystyrene; MEPS: Modified EPS
Plastic form- P_F- Fine flakes, P_c- Coarse flakes, P_p- Pallets
MLWA- Manufactured lightweight aggregate
NM- Not mentioned; FM- Fineness modulus

The form in which the plastic is used as aggregate can be better understood from the photographic images in Fig. 2.2 and Fig. 2.3. Most of these forms of aggregates are obtained by the mechanical shredding or grinding of plastics.

In the case of PET, the waste is mostly converted into flakes having coarser fractions (P_C) (Fig. 2.2 (a)) or finer fractions (P_F) (Fig. 2.2 (b)). These plastic flakes may further be processed to form plastic pellets (P_P) which are pre-defined and even-sized PET grains free of contamination (Fig. 2.2 (c)). To obtain such pellets, the PET flakes obtained after shredding are introduced into a reactor having a vacuum maintained at less than 10 bar. The reactor is provided with an agitation system that promotes the heating of the material to the drying temperature due to the friction effect. The heated material is extruded through an extruder spindle which is provided with a polymer filter and a spinneret with holes. The melt is collected in a cooling bath that solidifies the material. Then the material is granulated in a rotary cutter in water using a vibratory separation, centrifuging action, and crystallization to obtain plastic pellets (Ferreira et al., 2012; Saikia and De Brito, 2013). PET was also used in the form of an LWA obtained from coating PET particles with sand to improve the bond characteristics of PET with cement paste (Fig. 2.2 (e)). For this, the river sand powder was put in a circular air-tight mixer rotating at a speed of 30-50 rpm and was heated to 250ºC. PET particles of size 5-15mm were then added into the mixer and rotated at 30-50 rpm for more than 5 minutes. The aggregates are air-cooled to get an innovative LWA with PET (Choi et al. 2009). A similar LWA with an agglomeration of PET with GBFS instead of sand was also experimented with in the past (Fig. 2.2 (d)) (Choi et al. 2005). In another innovative approach, siliceous sand and PET were subjected to heat treatment and accompanied by thorough mixing. This mixture was allowed to undergo a long stepwise cooling process to obtain hardened slabs which are then subjected to semi-industrial grinding and sieving process to give sand-sized composite LWA as shown in Fig. 2.2 (f) (Gouasmi et al. 2019).

Other types of polymer wastes are also processed into aggregate form using a shredding and grinding process (Fig. 2.3 (i)- (v)). Other novel approaches to obtain synthetic aggregates were also adopted as in the case of PET. A mixture of LLDPE and red dune sand at 30% and 70% proportion respectively was compressed, heated, and then cooled to get solid sheets or slabs. These slabs were ultimately crushed to get novel synthetic aggregates (Fig. 2.3 (vi)). In the case of LDPE, the shredded pieces were heated

to their melting point and the melt was poured on sheets to allow them to solidify. These solidified plastics were then ground into small sand-sized fractions as shown in Fig. 2.3 (xviii) (Ababio Ohemeng et al., 2014). Some polymers like EPS are commercially manufactured as foams and classified as virgin plastics in concrete (Fig. 2.3(xi)). Sometimes these EPS foams were modified by thermal treatment in a hot air oven at 130ºC (Kan and Demirboğa, 2009a). To prevent the segregation tendency of EPS particles, the waste polystyrene was stabilized with 10% clay powder and 10% Portland cement to get a novel LWA called stabilized polystyrene (SPS) as shown in Fig. 2.3 (xii) (Herki, 2017b).

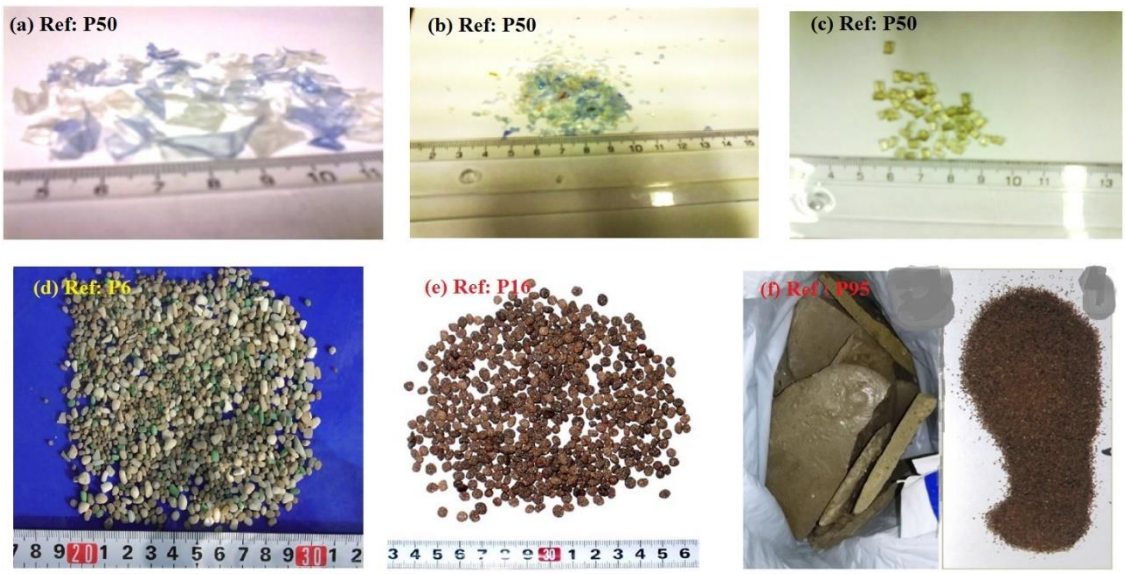

Fig. 2.2 PET aggregates experimented in literature (Ref: Author index in Table 2.3)

2.2.1 Properties of cement composites containing plastic waste

The effect of the use of PWA in cement mortar and concrete mixes is influenced by several factors viz. type of resin, the type and replacement ratio of natural aggregates, the shape and size of PWA, and the substitution strategy i.e., whether the aggregates are replaced by volume or weight proportions. The following sections discuss the effect of all these factors on the fresh and hardened properties of cement composites.

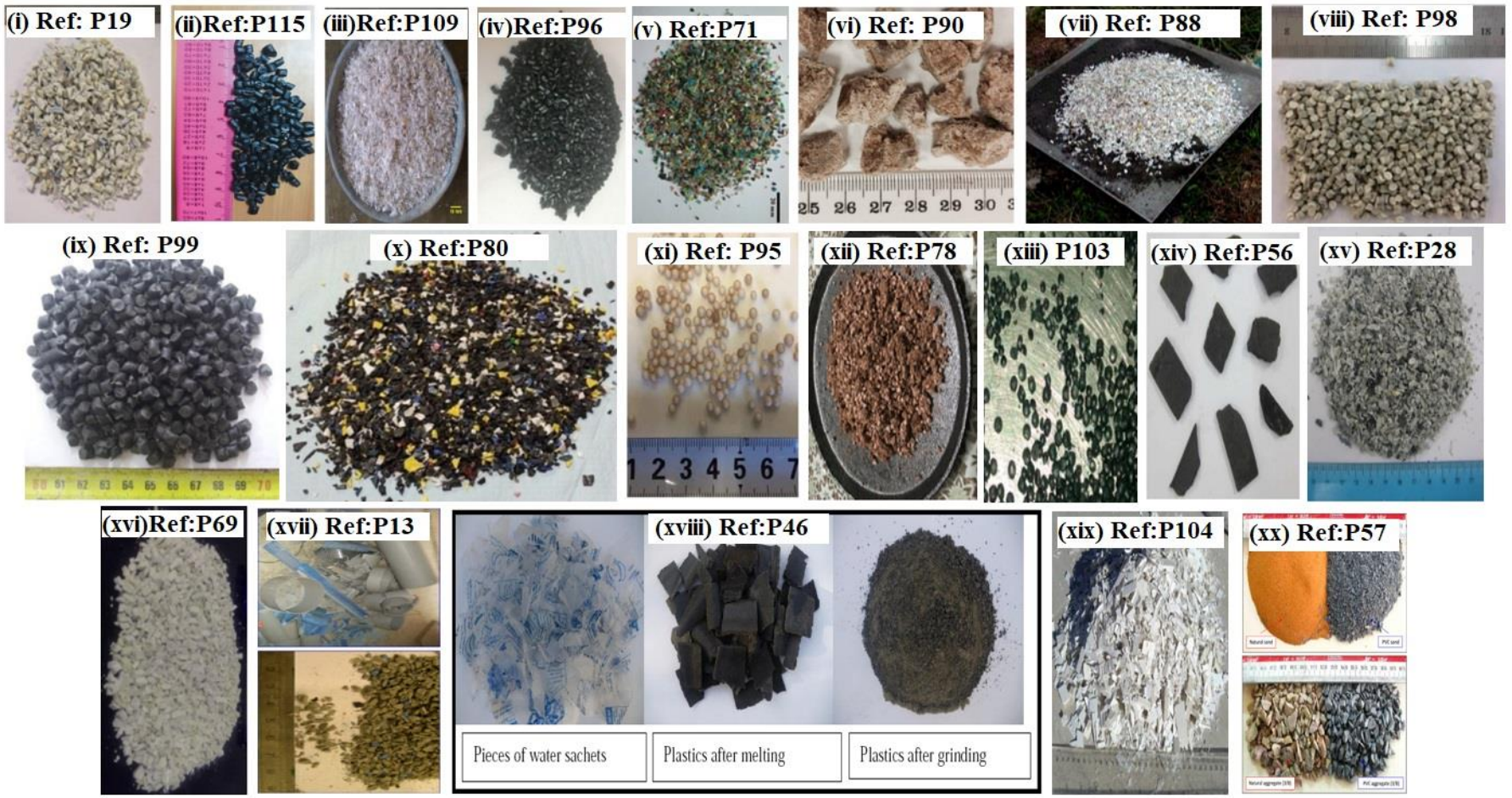

Fig. 2.3 Other polymer aggregates experimented with in literature (Ref: Author index in Table 2.3)

2.2.1.1 Workability

Workability is the relative ease or the difficulty with which the concrete can be placed or consolidated into the forms. It is an indicative parameter of stiffness, homogeneity, and void content of any mix. The workability or consistency of a cement mortar and cement concrete is mostly measured in terms of flow value and slump value respectively.

The relative change in workability of the mixes containing PET waste as aggregates for increasing replacement ratios is presented in Fig. 2.4. The results present two different schools of thought on the effect of the inclusion of PET waste on workability. Few researchers advocated the finding that workability is enhanced with the increase in PET substitution ratios (Abed et al. 2021; Babafemi et al. 2022; Harini et al. 2015; Islam et al. 2016; Safi et al. 2013; Da Silva et al. 2014). This was attributed to the reduced interparticle frictional resistance due to the smooth and slippery exterior surfaces of plastic particles and their low absorption capacity (Abed et al. 2021; Choi et al. 2005; Islam et al. 2016; Lee et al. 2019). A few researchers also presented a contradicting finding that workability is prone to decrease with the increase in PET particles in the mix due to their angular and non-uniform mercenary shape compared to the natural aggregates (Ismail and AL-Hashmi, 2008). This shape has a more specific surface area compared to natural sand and results in more friction between particles leading to less workability in the mixtures (Rahmani et al. 2013; Saxena et al. 2020).

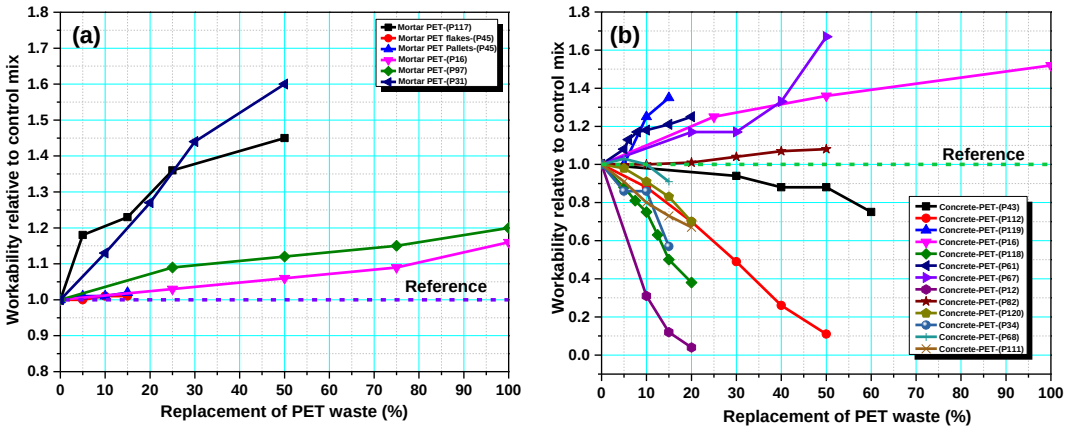

Fig. 2.4 Workability of cement composites containing PET aggregates (a) Mortar (b) Concrete

Da Silva et al. (2014) showed that pallet-shaped PET aggregates deliver higher workability compared to flaky aggregate particles due to their lower specific surface in addition to lower absorption characteristics (Silva et al. 2013; Da Silva et al. 2014). Also, a more continuous particle size distribution of plastic particles leads to higher consistency due to a more compact mix (Albano et al. 2009).

The effect of the water-cement ratio (w/c) of the mixes on the workability of PET-modified composites showed that an increase in the w/c adversely affects the flowability. It was assumed that due to low absorption by PET aggregates, the water content of the mix is not reduced and water that does not take part in cement hydration increases the porosity of the mix. This leads to a reduction in workability (Albano et al. 2009; Rahmani et al. 2013).

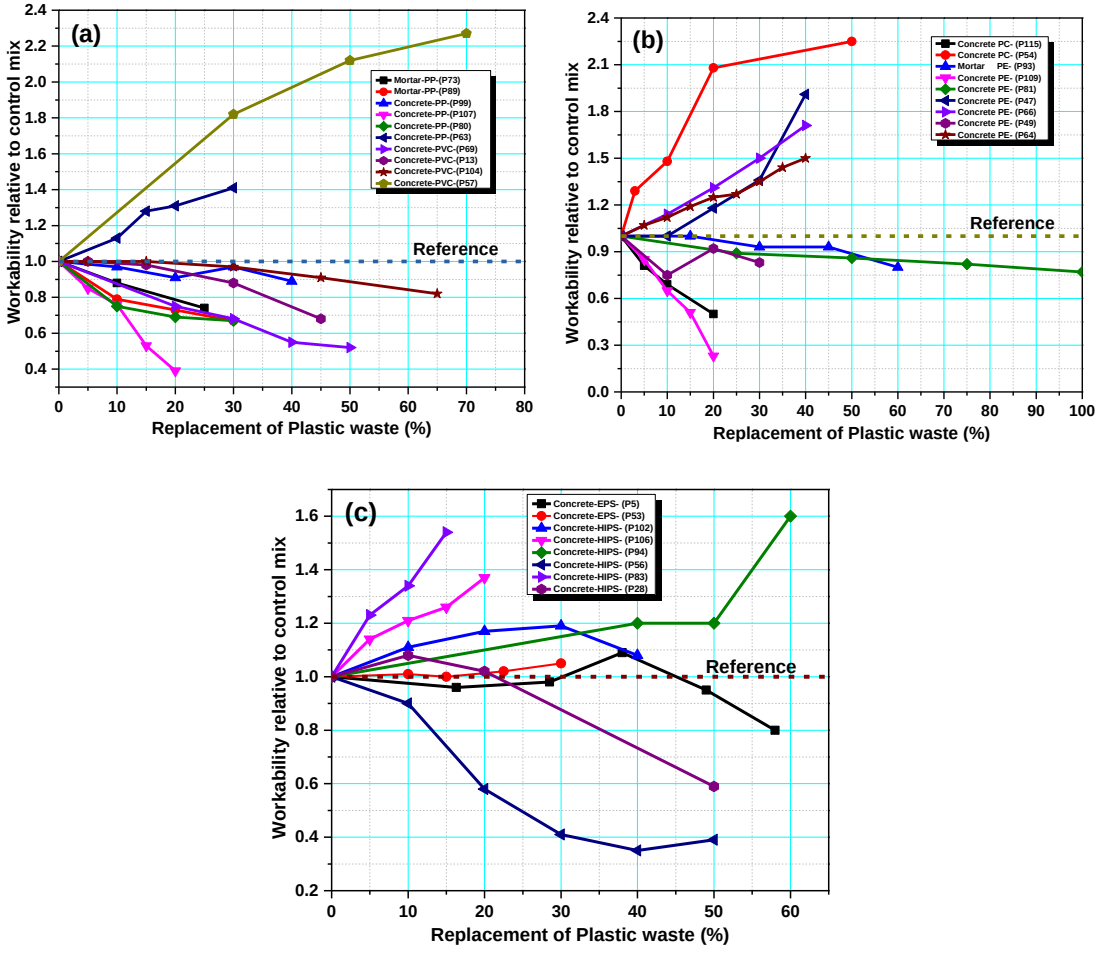

Fig. 2.5 Workability of cement composites containing non-PET plastic aggregates (a) PP and PVC (b) PE and PC (c) EPS and HIPS

The effect of PWA other than PET was also investigated by several research studies. Fig. 2.5 exhibits the results of the research findings for other polymer aggregates like EPS, PE, PVC, PP, HIPS, etc.

Like PET aggregates, the results visible from the available literature do not allow a generalized statement on the effect of PWA on the workability of cement composites. As evident in Fig. 2.5, some researchers have shown a decrease in the workability of the composites with the increase in plastic content. Jain et al. (2020) stated that the decrease in workability is due to the balling effect of waste plastics and ingredients of concrete. The authors also postulated that the long and non-uniform shapes of plastics may result in higher void content in concrete, segregation, and improper cohesiveness, ultimately decreasing workability (Haghighatnejad et al., 2016; Jain et al., 2020; Kou et al., 2009; Ozbakkaloglu et al., 2017; Saikia and De Brito, 2014; Záleská et al., 2018).

The increase in the workability of the composites was attributed to the smooth surface of the polymer aggregates and the availability of excess free water in the mixes due to ignorable absorption by plastics (Chunchu and Putta, 2019b; Ghernouti et al., 2014; Guendouz et al., 2016; Hannawi and Prince-Agbodjan, 2015; Madandoust et al., 2011; Ranjbar and Mousavi, 2015; Senhadji et al., 2015; Yang et al., 2015).

2.2.1.2 Density

As already discussed in section 2.1 and the material properties presented in Table 2.1, it is evident that the specific weight of all the forms of plastic materials is considerably lower compared to the natural aggregates that it replaces in the cement composites. This fact hints at an obvious conclusion that the density of the cement mixes continues to decrease with the increase in plastic content in the mix. This is an undisputed and established conclusion confirmed by the research works conducted with all plastics irrespective of the type of plastic and the size or shape of its particles. Fig. 2.6 presents the dry density values of cement composites at 28 days for different types of plastics. In addition to the low specific weight of the PWA, the increase in void content in the mixes due to the angular shape of plastic particles and the excess water availability on account of lower absorption by plastics, also adds to the reduction in density of the mixes (Akinyele et al., 2015; Badache et al., 2018; Ismail Khalil and Jumaa Khalaf, 2017). The studies have also shown that loss in density is higher for coarser and flaky plastic

aggregates and also for a higher w/c of the mix (Coppola et al. 2016; Silva et al. 2013). The higher resistance to compaction and lower workability of the mixes also resulted in lower density values for the concrete (Chen et al., 2015; Jain et al., 2020).

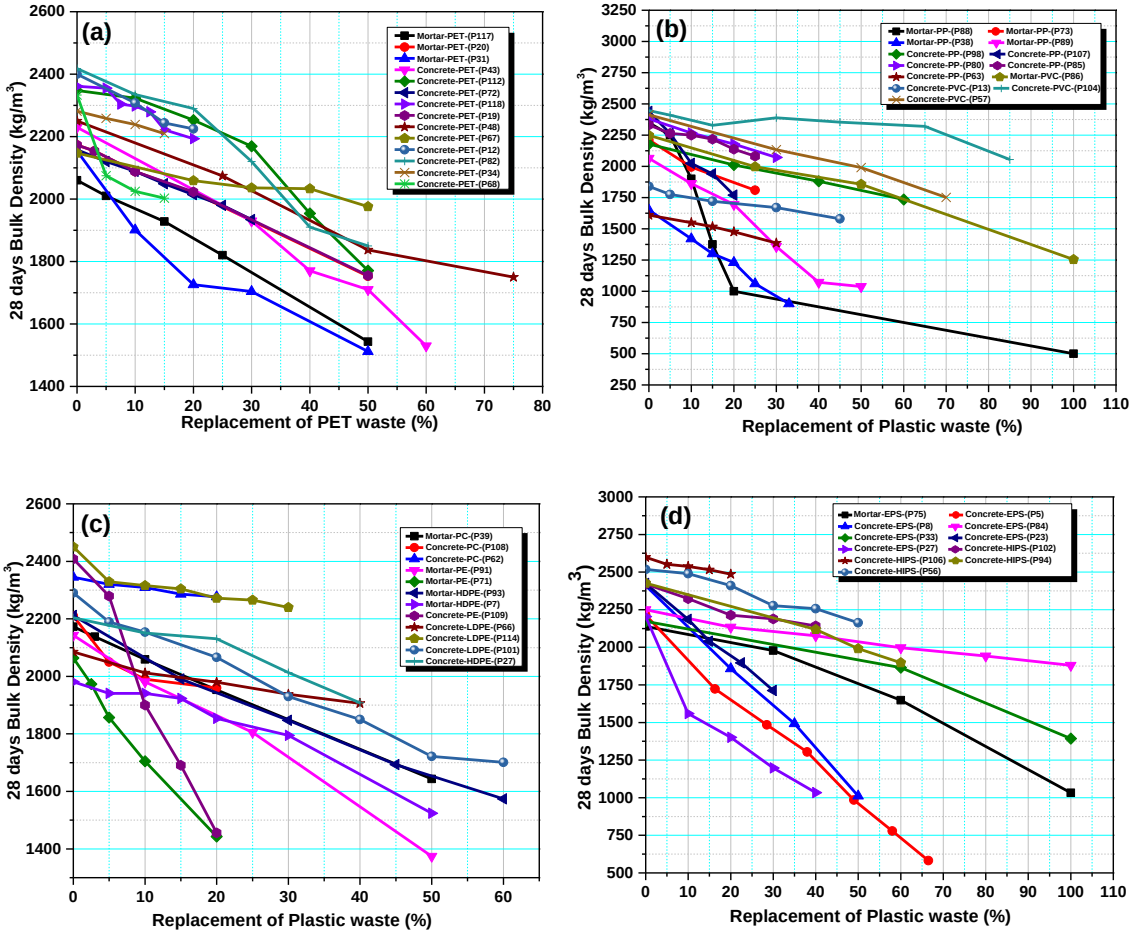

Fig. 2.6 Dry density of cement composites containing plastic aggregates at 28 days (a) PET (b) PP and PVC (c) PE and PC (d) EPS and HIPS

2.2.1.3 Compressive Strength

Compressive strength is a property of paramount importance to assess the overall performance of concrete. It is considered a direct indicator of the quality of concrete. Most of the other mechanical and durability properties of concrete are related to compressive strength. Considering the characteristics of PWA in comparison to natural aggregates, the effect of the inclusion of plastic on the compressive strength of the modified mixes may give an overall picture of the confidence in using plastic waste in cement mixes.

Extensive research on the compressive strength of cement mortar and concrete containing various proportions of PET aggregates as a substitute for fine and coarse natural aggregates is available in the literature. The compressive strength values of mixes with incremental proportions of PET aggregates relative to the mix without PET waste are displayed in Fig. 2.7.

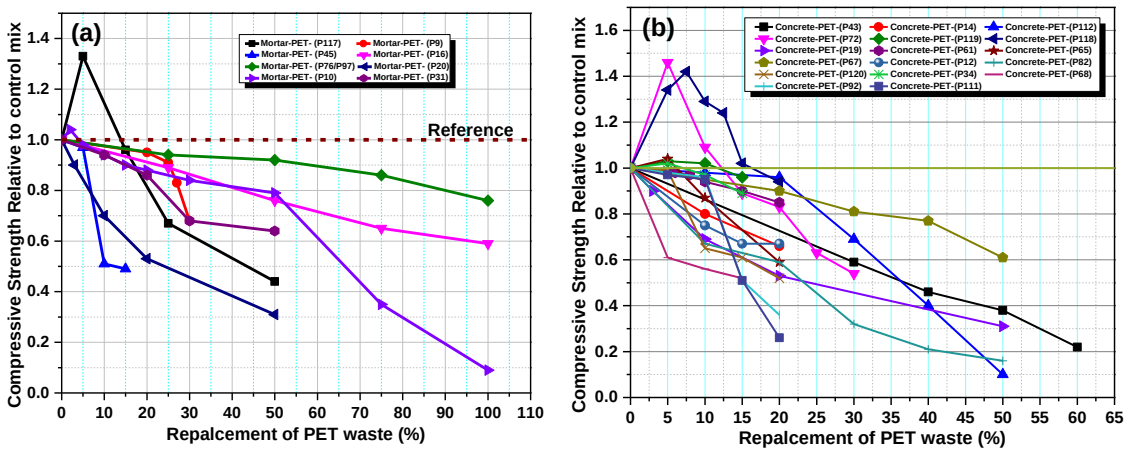

Fig. 2.7 Compressive strength of cement composites containing PET aggregates at 28 days (a) Mortar (b) Concrete

The results available in the literature show that the addition of PET decreases the resistance of concrete to compressive failure compared to conventional aggregate material. It indicates that, unlike natural aggregates, recycled PET does not contribute to the strength of the concrete, especially at higher replacement levels (Hossain et al. 2016a; Juki et al. 2013). Few researchers stated that there is an increase in the strength of cement mixes for replacement levels up to 15% volume of aggregates and compressive strength decreases thereafter for additional substitution levels (Abed et al. 2021; Azhdarpour et al. 2016; Dawood et al. 2021).

The degradation in the strength of concrete after PET addition is attributed to the weak adhesion between the surface of PET particles and the cement matrix (Frigione, 2010; Hannawi et al., 2010b; Irwan et al., 2014; Ismail and AL-Hashmi, 2008). This is because of the smooth surface of plastic aggregates which jeopardizes the connection between the matrix and aggregates (Da Silva et al. 2014). Secondly, the higher porosity introduced inside the mix due to the inefficiency in mixing between two heterogeneous aggregate phases i.e., plastic and natural aggregates also contribute to the strength

reduction (Ismail Khalil and Jumaa Khalaf, 2017; Jaskowska-Lemańska et al., 2022). Thirdly, limited cement hydration at the surface of plastic waste due to its hydrophobic nature creates a weak interfacial transition zone (ITZ) between PET and cementitious material (Abed et al., 2021; Akçaözoğlu et al., 2013; Hannawi et al., 2010b; Ismail and AL-Hashmi, 2008; Sadrmomtazi et al., 2016). Studies on different shapes and sizes of PET particles have concluded that the coarser and lamellar particles cause higher strength degradation than the finer and spherical-shaped particles (de Brito and Saikia, 2013; Ferreira et al., 2012; Guilherme et al., 2012; Ismail and AL-Hashmi, 2008; Silva et al., 2013). The lower stiffness of plastics also decreases the mechanical strength of the composites (Correia et al. 2014; Guilherme et al. 2012).

Few researchers postulated that at a lower percentage substitution of natural aggregates by PET, there is an increase in the strength of concrete relative to the conventional mix (Azhdarpour et al. 2016; Babafemi et al. 2022). Azhdarpour et al., (2016) showed that at 5% and 10% replacement of NFA, the increase in compressive strength was 39% and 7.6% higher than the control mix respectively. Authors advocated that the shear stress on the failure planes gets converted to tensile stress while dealing with the flexible PET fragments. So, the part of the applied stress is tolerated by the elongated and sheet-shaped structure of PET particles before their detachment from other materials. However, such an effect vanishes with an increase in replacement volumes due to the loss of cohesion between mixed materials (Azhdarpour et al. 2016; Dawood et al. 2021; Rahmani et al. 2013). It was also stated that the use of PET aggregates with the same grading as the substituted aggregates may give a relatively better packing density at lower replacement ratios leading to enhanced strength characteristics (Babafemi et al. 2022; Ge et al. 2013; Thorneycroft et al. 2018).

A similar trend of results on compressive strength was observed for other types of PWA. Fig. 2.8 presents the results for the relative values of compressive strength for different types of PWA when substituted for natural aggregates in PWCC. The declining trend of compressive strength for the increased replacement ratios was attributed to the lower strength of PWA, and the lack of bond between aggregates and cement paste (Alqahtani et al., 2017; Chidiac and Mihaljevic, 2011; Faraj et al., 2019; Iucolano et al., 2013; Jain et al., 2020; Mohammed et al., 2020b; Rahman et al., 2012; Senhadji et al.,

2015). Like PET, the increased void content of the mixes due to the hydrophobic nature of plastics and the lower modulus of elasticity of the particles was another prominent reason cited for the strength loss (Akinyele et al. 2015; Chen et al. 2019; Haghighatnejad et al. 2016; Kou et al. 2009; Liu et al. 2015; Ozbakkaloglu et al. 2017). The failure of the specimens with PWA under compression showed a well-defined variation when compared to the brittle failure in the case of the conventional mix specimens. The plastic-incorporated samples exhibited a ductile failure by sustaining the load for a few minutes after failure without full disintegration which shows the energy absorption capacity of such concrete (Babu et al., 2006; K. G. Babu and Babu, 2003; Hannawi et al., 2010a; Petrella et al., 2020; Wang and Meyer, 2012). Senthil Kumar and Baskar (2015) also cited that low-density plastic particles like HIPS move toward the top surface of the cast cubes leading to a higher concentration of weaker material at the top layer of the specimen (Senthil Kumar and Baskar, 2015).

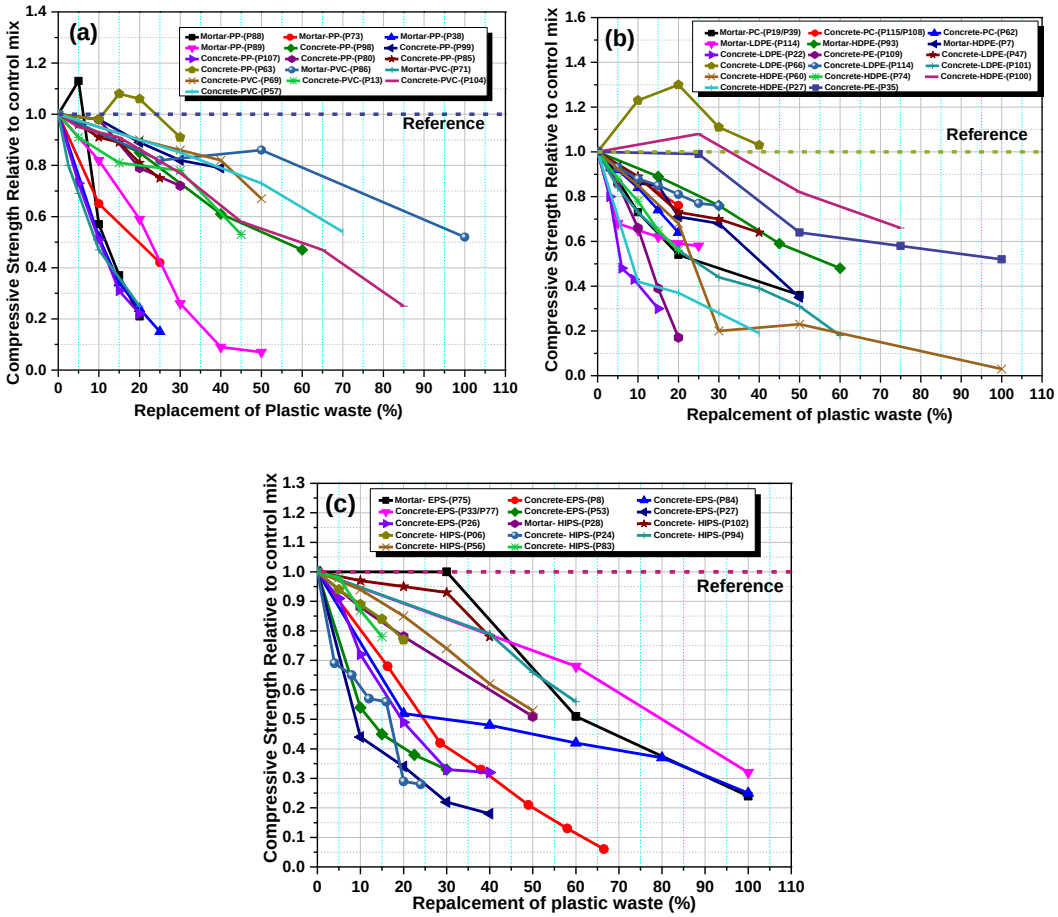

Fig. 2.8 Compressive strength of cement composites containing non-PET aggregates at 28 days (a) PP and PVC (b) PC and PE (c) EPS and HIPS

2.2.1.4 Splitting Tensile Strength

The tensile strength behavior of the PWCC followed a similar trend to the behavior under compressive stresses. With few exceptions as cited in the studies on compressive strength, the majority of studies confirmed a decline in the tensile strength of cement mixes when the amount of plastics in the mix increased, especially at higher levels of incorporation. The analyzed tensile behavior was attributed to the same reasons as stated for the behavior under compressive loading in § 2.2.1.3.

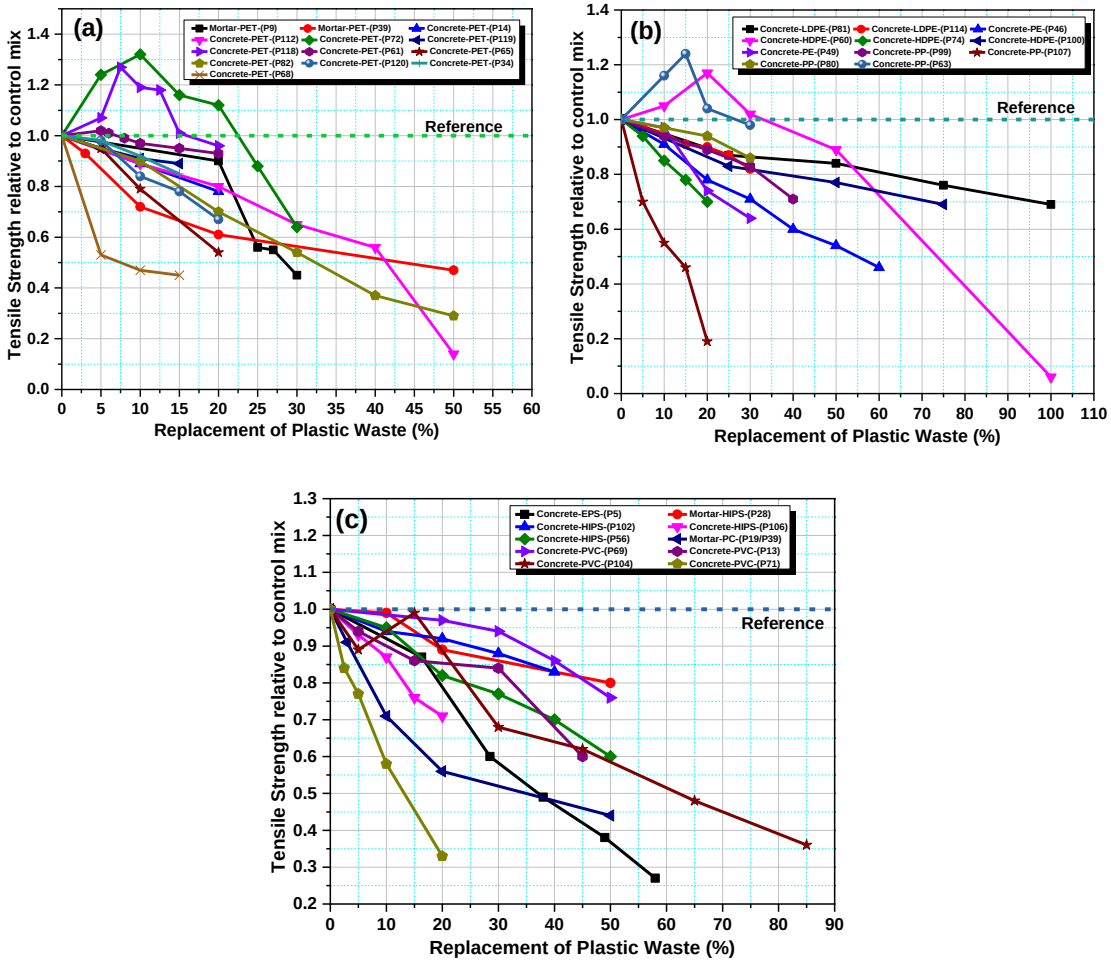

Fig. 2.9 Splitting Tensile strength of cement composites containing plastic aggregates at 28 days (a) PET (b) PP and PE (c) EPS, HIPS, PC, and PVC

The effect of varying proportions of PWA on the splitting tensile strength of the PWCC can be well understood from the literature data presented in Fig. 2.9. The difference in stiffness, shape, and poor bonding characteristics of PWA was the popular attributes of the early tensile failure of PWCC in comparison to conventional mixes

(Albano et al., 2009; Almeshal et al., 2020b; Babafemi et al., 2022; Hannawi et al., 2013; Rahmani et al., 2013). Few research studies stated that at lower replacement ratios up to 10-15%, tensile strength may be enhanced. This behavior may be due to the increased ductility and sharp edges of plastic particles that may reduce slipping between aggregate and matrix in comparison to natural aggregates (Azhdarpour et al. 2016; Dawood et al. 2021).

The ratio of tensile strength and compressive strength is an indicator of the toughness behavior of concrete. Higher the ratio, the more the toughness of the material. Studies have shown that the toughness behavior of concrete improves with an increase in plastic content and the effect is more pronounced in the case of large flaky plastic particles (Saikia and De Brito, 2013; Senthil Kumar and Baskar, 2015; Wang and Meyer, 2012). This is attributed to the fact that synthetic sand has a different morphology with a shape similar to short fibers that offer a bridging action at cracks and impart an improved post-cracking toughening (Iucolano et al. 2013; Yang et al. 2015).

2.2.1.5 Flexural Strength

Studies on the flexural behavior of cement mixtures containing synthetic aggregates have shown that the flexural strength values decrease with the increase in plastic content in the mix. The declining trends of flexural strengths are evident from the relative values presented for different types of plastics in Fig. 2.10. The effect is due to the same factors which interfere with the compressive and tensile performance of concrete as discussed in § 2.2.1.3 and § 2.2.1.4. Although the behavioral pattern under flexural loading resembles the pattern observed for compressive and tensile loadings, the decrease in flexural strength is comparatively smaller. This is attributed to the nature of the shape of the synthetic material which behaves as a reinforcement in the mix (Abed et al. 2021; Azhdarpour et al. 2016; Górak et al. 2021). Such an effect was particularly observed by some researchers in the case of PET blended cementitious mixes, especially at low PET ratios. The plastic fragments were found to exist at starting points of failure creating a locking arrangement at these failure points, thus improving the strength. On the contrary, this effect diminishes at higher PET levels due to the accumulation of these fragments in close vicinity to each other sacrificing the cohesion with the cement matrix (Azhdarpour et al. 2016; Dawood et al. 2021; Gouasmi et al. 2017; Hannawi et al. 2010a). A similar

effect was also observed in the case of HDPE fragments in cement mortar and HIPS fragments in concrete (Badache et al., 2018; Senthil Kumar and Baskar, 2015).

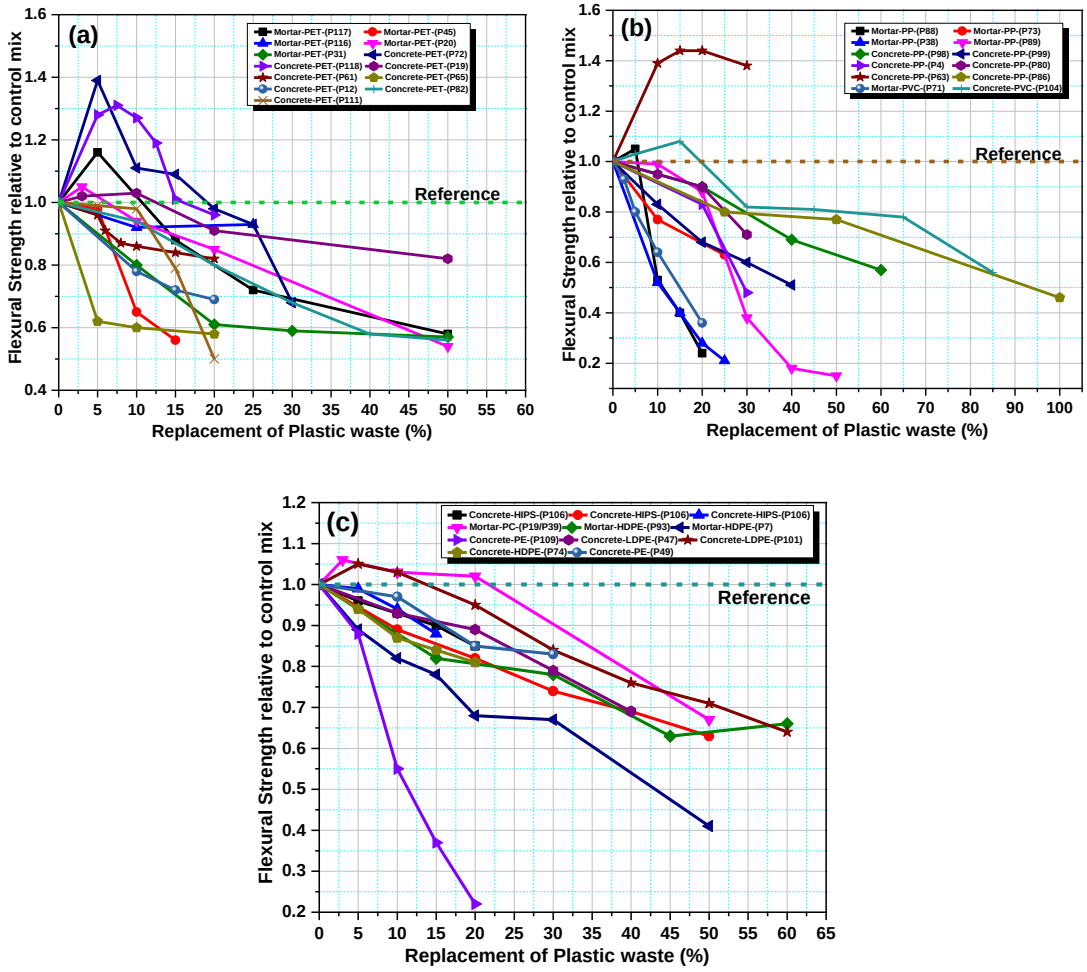

Fig. 2.10 Flexural strength of cement composites containing plastic aggregates at 28 days (a) PET (b) PP and PVC (c) EPS, HIPS, PC, and PE

2.2.1.6 Modulus of Elasticity

It is a well-known fact that the type of aggregates has a major influence on the modulus of elasticity of the concrete. The deformation produced in concrete is partially related to the elastic deformation of aggregates (Jones and Facarao, 1971). The material characteristics of different types of plastic in Table 2.1 reveal that all the plastic types have a significantly low modulus of elasticity than the natural aggregates. Plastic is less resistant and more flexible than natural aggregates and hence it exhibits higher deformability when equivalent stress is applied (Albano et al. 2009; Azhdarpour et al. 2016; Faraj et al. 2019; Rahmani et al. 2013; Da Silva et al. 2014). Thus, cement

composites with all types of plastics showed a gradual decrease in modulus of elasticity with the increase in plastic content as evident in Fig. 2.11. The effect on the modulus of elasticity may not be attributed to the lower elastic modulus of plastic aggregates alone. The poor bond characteristics between plastic fragments and the cement matrix and the associated internal defects or cracks around polymer particles also contribute to the decrease in the elastic modulus of the mix as a whole (Badache et al., 2018; Jain et al., 2020; Ozbakkaloglu et al., 2017; Senthil Kumar and Baskar, 2015).

2.2.1.7 Ultrasonic Pulse Velocity

The ultrasonic pulse velocity (UPV) of the concrete is an indicator of the quality of the concrete. It assists in the investigation of the uniformity of concrete, the presence of cracks or voids, and changes in the property of concrete with time (Herki and Khatib, 2017). The wave propagation speed in the material is dependent on the porosity of the material. PWCC are prone to an increase in porosity with an increase in synthetic content. The available data presented in Fig. 2.12 shows that the UPV decreases with the increase in plastic content in the mix. This is attributed to the decrease in unit weight and increase in the porosity of the mix (Akçaözoğlu et al. 2013). The void spaces formed by the plastic inclusions attenuate the ultrasonic wave due to acoustic impedance (Hannawi et al., 2010b; Ismail Khalil and Jumaa Khalaf, 2017; Jaskowska-Lemańska et al., 2022). The heterogeneity of the medium through which the incident wave passes i.e., concrete, plastic fragments, and cavities, causes partial reflection and transmission of waves. This leads to a decrease in UPV (Albano et al., 2009; Almeshal, et al., 2020a; Badache et al., 2018; Dawood et al., 2021; Mohammed et al., 2019). A few studies also stated that the decrease in UPV is due to the ability of plastic to absorb the ultrasonic waves (Gouasmi et al., 2017; Hannawi, Prince, et al., 2010b; Senthil Kumar and Baskar, 2015). As per IS 13311(Part 1) (1992) concrete with pulse velocity values higher than 4500 m/sec is rated as excellent, between 3500-4000 m/sec are rated as generally good and those below 3500 m/sec are considered to be questionable or of poor quality (IS 13311, 1992). The values of pulse velocity as presented in Fig. 2.12 indicate that when the plastic content is limited up to 20%, it is possible to obtain good quality concrete and any further addition of plastic may drastically affect the quality of concrete.

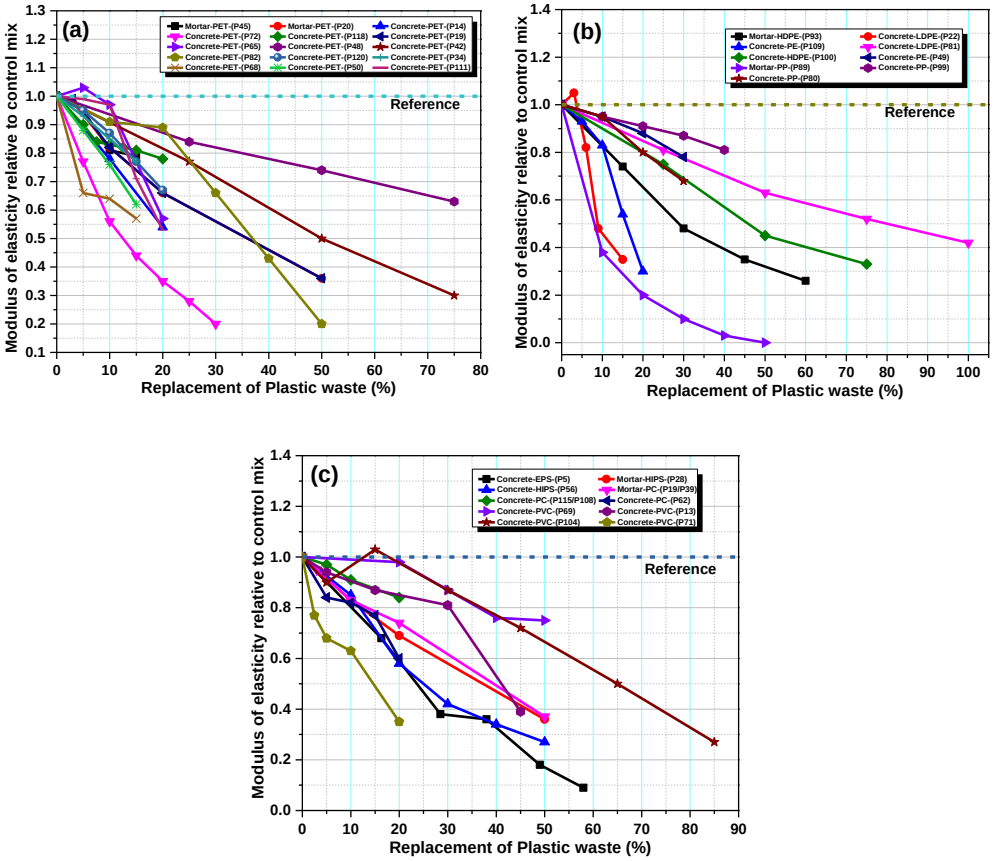

Fig. 2.11 Modulus of Elasticity of cement composites containing plastic aggregates at 28 days (a) PET (b) PP and PE (c) EPS, HIPS, PC, and PVC

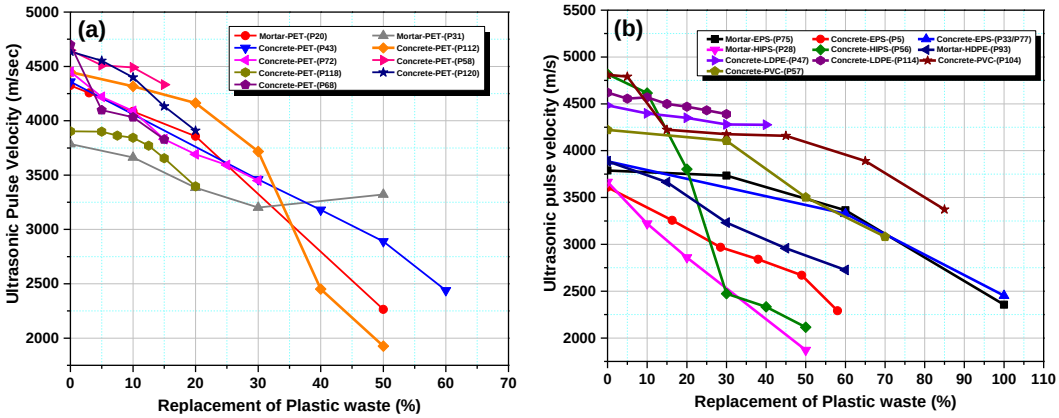

Fig. 2.12 Ultrasonic pulse velocity of cement composites containing plastic aggregates at 28 days (a) PET (b) EPS, HIPS, PE, and PVC

2.2.1.8 Thermal Conductivity

The coefficient of thermal conductivity of plastic materials is very low compared to the conventional aggregates involved in concrete making. The coefficient of around

0.15 W/mk of PET against 2 W/mk of natural aggregate gives a clear indication of the thermal conductivity of the concrete when plastic is used as a substitute for natural aggregates. PWA tends to slow down heat propagation and thus decrease the global conductivity of the composite (Akçaözoğlu et al. 2013; Hannawi et al. 2010b). In addition to the intrinsic property of plastics, the porosity induced by the plastic inclusion in the concrete also adds to the reduction in thermal conductivity. This is attributed to the thermal conductivity of air present in the pores being much lesser than all other components of concrete (Iucolano et al. 2013). These findings in the literature are evident from the data presented in Fig. 2.13. The PWCC are considered to be more heat-insulating due to this behavior (Badache et al. 2018).

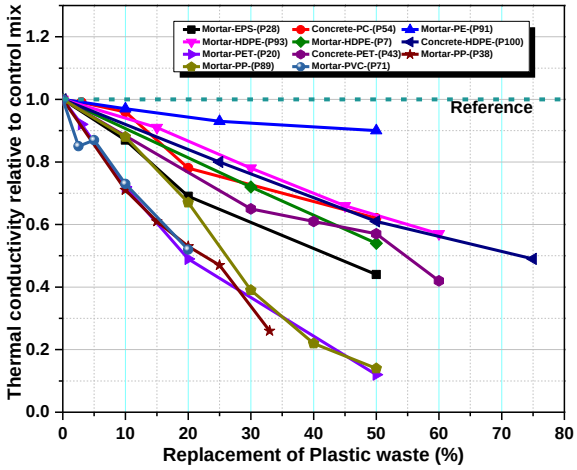

Fig. 2.13 Thermal conductivity of cement composites containing plastic aggregates

2.2.1.9 Water absorption

Water absorption of cement mixture is another parameter that is directly associated with the porosity of the mix. An increase in water absorption is an indicator of higher porosity and the greater vulnerability of concrete to the ingress of aggressive agents. This ingress is detrimental to the long-haul performance of concrete. So, the determination of water absorption characteristics is essential to ascertain the long-term durability of concrete.

By the majority, the water absorption studies conducted on PWCC presented an increasing trend of water absorption with the increase in plastic content inside the mix (Ababio Ohemeng et al., 2014; Akçaözoğlu et al., 2010; Albano et al., 2009; Correia et al., 2014; Da Silva et al., 2014; Hannawi et al., 2010a; Hossain et al., 2016a; Sadrmomtazi

et al., 2016; Saikia and De Brito, 2013; Silva et al., 2013). This trend can be confirmed by the data presented in Fig. 2.14. Various factors influencing the increase in porosity of the mix also affected the water absorption. The planar and elongated shape of plastic particles in comparison to spherical granules of natural aggregates, as in the case of PET and PVC increased the absorption of the mix (Saikia and De Brito, 2013; Silva et al., 2013). Studies also showed that the coarser the plastic fragments higher the absorption (Saikia and De Brito, 2013; Silva et al., 2013). Through morphological studies of cement mortar, Záleská et al. (2018) confirmed that there exist cavities in the ITZ between three heterogeneous material phases, i.e., cement paste, sand, and PP particles. Such cavities open a preferred path for water transport (Záleská et al. 2018). Not to neglect the contradictory findings, few studies stated that plastic inclusions lower the water absorption of the mixes (Akinyele and Toriola, 2018; Alqahtani et al., 2018; Gouasmi et al., 2017; Haghighatnejad et al., 2016; Marzouk et al., 2007). Authors attributed the exceptional behavior to the water-repellent effect of the hydrophobic plastic aggregates and a stronger adhesion between plastic and matrix, the latter being denied by the majority (Gouasmi et al. 2017). Marzouk et al. (2007) focused on the resistance offered by non-sorptive PET particles to the propagation of the imbibition front. They advocated an increase in tortuosity as the liquid flow bypasses the plastics and decreases the rate of transfer of water (Marzouk et al. 2007).

The studies on water absorption of concrete with EPS beads reported an important finding that the mix having lower density and lower strength exhibits higher absorption than the higher density and high strength concrete (Babu et al., 2006; Babu and Babu, 2004). EPS-embedded concrete showed an increase in absorption with a volumetric increase in EPS content. However, the values of initial (30 min) and final (72 h) absorption were reported well below 7% compared to most other LWC which reported an absorption ranging from 8-25% (Babu and Babu, 2004; Ranjbar and Mousavi, 2015). Investigations of concrete containing PVC aggregates by Mohammed et al. (2019) presented results in agreement with this finding (Fig. 2.15). As per CEB-FIP guidelines such concretes could be classified as concrete of "good" quality having initial and final absorption of less than 3%, particularly for replacement levels up to 30-45% (Babu and Babu, 2004; Mohammed et al., 2019; Ranjbar and Mousavi, 2015). Chunchu and Putta (2019a) and Senthil Kumar and Baskar (2015) reported "average" quality concrete with

absorption values between 4.5-5% when HIPS were substituted in concrete mixes for 40-50% aggregate volumes (Chunchu and Putta, 2019a; Senthil Kumar and Baskar, 2015).

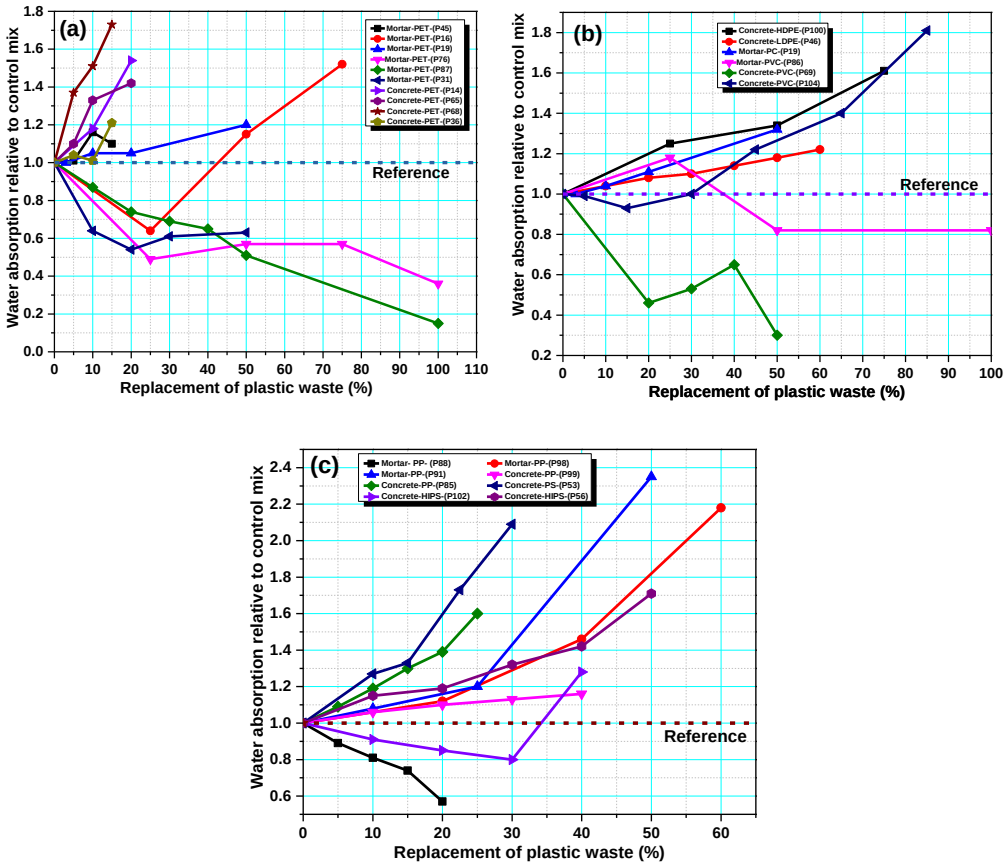

Fig. 2.14 Water absorption of cement composites containing plastic aggregates (a) PET (b) PE and PVC (c) PP, PS, and HIPS

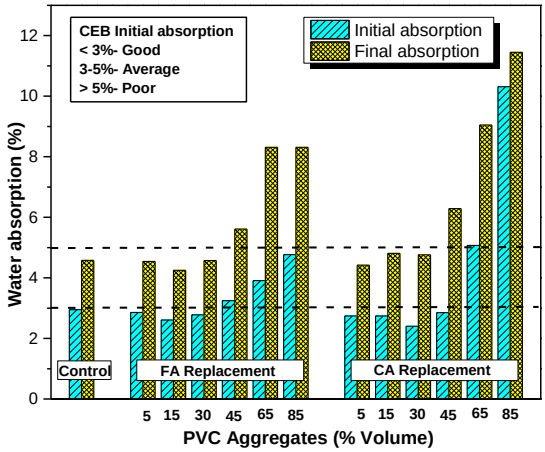

Fig. 2.15 Water absorption of concrete containing PVC fine and coarse aggregates (Source: Mohammed et al. (2019))

2.2.1.10 Liquid or Gas Permeability

The vulnerability of concrete to the ingress of aggressive forms of liquid chemical species, permeating gases like carbon dioxide and other suspended ions is a key factor in determining the durability of concrete. This property is highly related to the porosity and water absorption characteristics of composites. Fig. 2.16 summarizes the variation in water/gas permeability of PWCC when natural aggregates are replaced by PWA.

The studies on permeability characteristics reported an increase in permeability with an increase in plastic content in the mix. This increase was attributed to the increase in percolated porosity of the mix due to various factors already discussed in the previous sections (Faraj et al. 2019; Hannawi et al. 2010a; Iucolano et al. 2013; Saxena et al. 2020; Da Silva et al. 2014). The majority of the studies envisaged that the weak ITZ between synthetic aggregates and cement paste is the favorite access for permeating medium (Gayatri and Popat, 2020; Jain et al., 2020). The studies on EPS blended concrete reported significant moisture migration with an increase in the volume and size of beads. The effect was attributed to the shrinkage of EPS beads during the drying of concrete for the performance of the test (Babu et al. 2006). Contrary to the popular finding, a study on the permeability characteristics of mortar with HIPS particles by Wang and Meyer (2012) exhibited that the permeability and permeance are reduced by 14% for 50% volume replacement of sand by HIPS.

2.2.1.11 Drying shrinkage

Concrete having excessive shrinkage cannot be considered a durable mass. Such shrinkage can fissure the concrete even before it is exposed to superimposed loads. It is the aggregate component in concrete that can be relied upon to offer internal restraint against this shrinkage. The use of plastic waste having lower stiffness value as aggregates are expected to reduce this internal restraint and increase the strain on concrete causing shrinkage cracking. Fig. 2.17 conveys that this hypothesis has been accepted by most research studies.

The increase in drying shrinkage was attributed to the fact that the modulus of elasticity of plastics is much lower than the conventional aggregate which is replaced (Demirboga and Kan, 2012; Frigione, 2010; Hannawi et al., 2013; Marzouk et al., 2007; Tang et al., 2008). Chen et al. (2019) assumed that the increased internal porosity and

evaporation of free/capillary water from the pores is the main reason for the increased shrinkage (Chen et al. 2019).

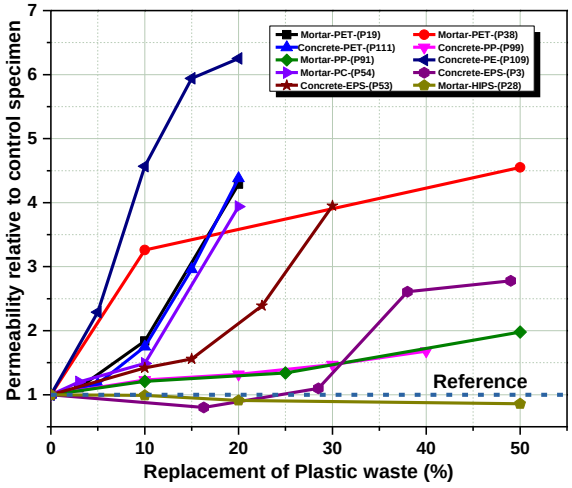

Fig. 2.16 Relative permeability of cement mixes with plastic aggregates

Few researchers disagreed with the attribute that the shrinkage behavior of concrete is influenced by the elasticity of plastic. However, they seconded the postulation that the drying shrinkage is the outcome of the capillary tensile force induced due to the evaporation of water from the capillaries and stated that the slower the evaporation, the slower and lower the shrinkage. Da Silva et al. (2014) and Silva et al. (2013) in the case of PET and Kou et al. (2009) in the case of PVC aggregates confirmed such behavior in their studies (Kou et al. 2009; Silva et al. 2013; Da Silva et al. 2014).

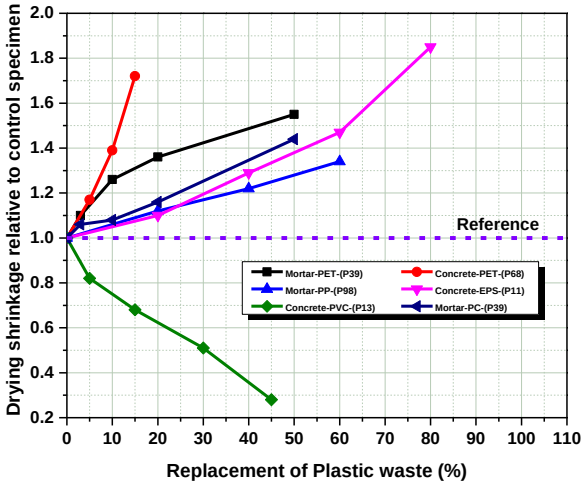

Fig. 2.17 Relative drying shrinkage of composites with plastic aggregates

2.2.1.12 Chloride Permeability

Chloride migration in the concrete mass is a detrimental phenomenon that causes the de-passivation of steel reinforcement in reinforced sections and initiates corrosion in reinforcement. Therefore, it is one of the major durability indicators of concrete. The chloride migration in concrete is influenced by the porosity and permeability of concrete. Enough discussions on the increased porosity, water absorption, and permeability of composites containing plastic aggregates in the previous sections reveal that polymer blended concrete should be highly susceptible to the chloride migration process. However, conflicting outcomes have been reported on chloride ion penetration in PWCC (Bhagat and Savoikar, 2022). The data extracted from the literature are summarized in Fig. 2.18.

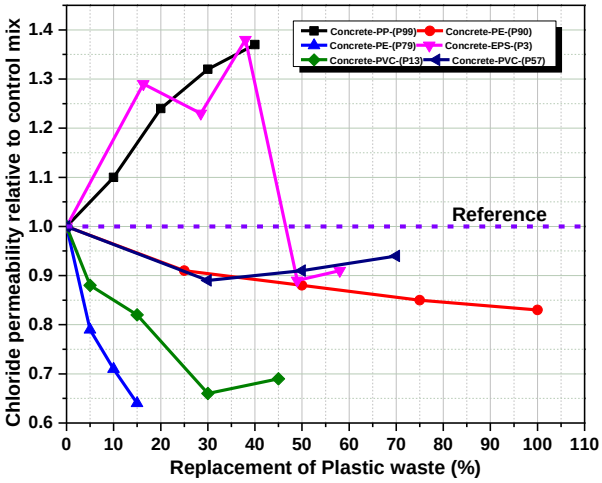

Fig. 2.18 Relative chloride permeability of concrete containing plastic aggregates

Silva et al. (2013) and other studies reported that the chloride ion penetration in concrete with PWA increases with the increase in plastic content. Furthermore, it was shown that concrete with flaky aggregates is more susceptible to chloride migration than the palleted forms. This was attributed to the increase in the porosity of concrete (Faraj et al., 2019; Ranjbar and Mousavi, 2015; Silva et al., 2013).

By contrast, few other studies exhibited that the plastic aggregates block or distract the transfer of chloride ions in the matrix due to the impermeable nature of plastics and thus, provide better resistance against chloride migration (Alqahtani et al., 2018; Gouasmi et al., 2019; Kou et al., 2009; Shanmugapriya and Santhi, 2017; Senhadji et al., 2015).

In the case of EPS blended concrete, Babu and Babu (2003) showed that the chloride permeability was classified as "low" as per ASTM C 1202 as the values of charge passed were in the range of 1000-1500 coulombs (ASTM C 1202; Babu and Babu, 2003). Furthermore, Ranjbar and Mousavi (2015) stated that although EPS inclusion aggravates the chloride penetration in concrete, the threshold chloride content necessary to initiate chloride-induced corrosion is not surpassed for EPS content up to 15% volume of aggregates (Ranjbar and Mousavi, 2015).

2.2.1.13 Freeze and thaw resistance

This is an important property to ascertain the durability of concrete, especially in colder regions with freezing temperatures. At such temperatures, water occupied in the void spaces of concrete may expand in volume imposing tensile stresses within the mass. This may cause the dilation of cavity spaces and eventually rupture in concrete. The phenomenon is extremely severe in the case of successive freeze and thaw conditions inviting irreversible damage in concrete through expansion cracking, scaling, and crumbling (Bhagat and Savoikar, 2022). Considering the lower stiffness values and poor adhesion characteristics of plastic particles, this phenomenon is proved to be more severe in PWCC (Da Silva et al. 2014).

A study by Hannawi and Prince-Agbodjan (2015) investigated the effect of 60 freezing (-20º C) and thawing (+20º C) cycles on the mechanical properties of mortar samples containing PC aggregates. The authors reported a loss in compressive strength, flexural strength, and UPV beyond 20% of replacement volumes of sand and explained that the degradation in the properties was caused by cracking due to thermal contraction/expansion of the material (Hannawi and Prince-Agbodjan, 2015).

In a classical study with heat-modified EPS, Kan and Demirboğa (2009b) highlighted the effect of freeze-thaw cycles on the relative dynamic modulus of elasticity, weight loss, and compressive strength loss of different mixes (Fig. 2.19). The findings showed that the relative dynamic modulus of elasticity decreased after 240 cycles approaching nil value at 300 cycles. The maximum loss in weight and compressive strength was 6.25% and 48% respectively (Kan and Demirboğa, 2009b). On the other hand, Ferrándiz-Mas and García-Alcocel (2013) demonstrated that the addition of EPS up to 50% of aggregate volume could minimize the loss in compressive strength of mortar

due to the ability of EPS to absorb the ice crystallization pressure (Ferrándiz-Mas and García-Alcocel, 2013).

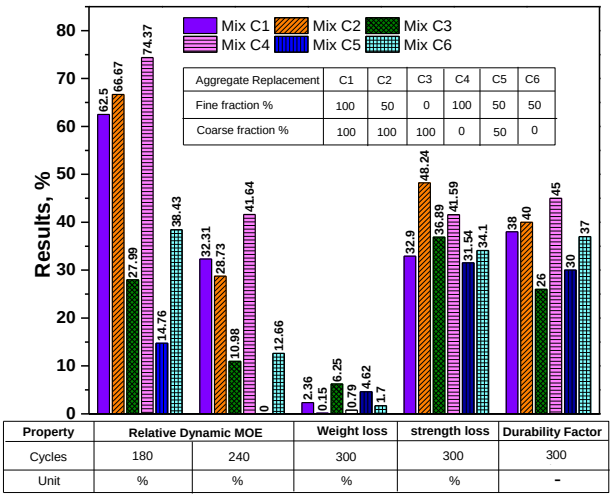

Aggregate Replacement	C1	C2	C3	C4	C5	C6
Fine fraction %	100	50	0	100	50	50
Coarse fraction %	100	100	100	0	50	0

Property	Relative Dynamic MOE		Weight loss	strength loss	Durability Factor
Cycles	180	240	300	300	300
Unit	%	%	%	%	-

Fig. 2.19 Effect of freeze and thaw cycles on properties of EPS concrete (Source: Kan and Demirboğa, 2009b)

2.2.1.14 Resistance to acid and sulphate attack

The after-effects of acid and sulphate attack on the quality of concrete is an important parameter to assess the long-term performance of concrete under an aggressive environment. The acid attack may lead to an increase in porosity, loss of coherence, loss of bonding capacity, and ultimately loss of strength in concrete. The sulphate attack leads to the generation of new reaction products in the pore solution of concrete which possesses an expansive characteristic. These products may induce stresses leading to the cracking of concrete (Nijland and Larbi, 2010).

Janfeshan Araghi et al. (2015a) and Nikbin et al. (2016b) investigated the effect of an acid attack by immersion of concrete samples with varying proportions of PET in a 5% sulphuric acid solution for 60 days. The authors found that samples with PET showed a lower deterioration ratio. There was a minimization of the weight loss, reduction in compressive strength, and reduction in UPV (see Fig. 2.20). This positive effect was attributed to the ability of PET particles to absorb the internal pressure caused by expansive movements in the matrix due to acid attack (Janfeshan Araghi et al. 2015; Nikbin et al. 2016b).

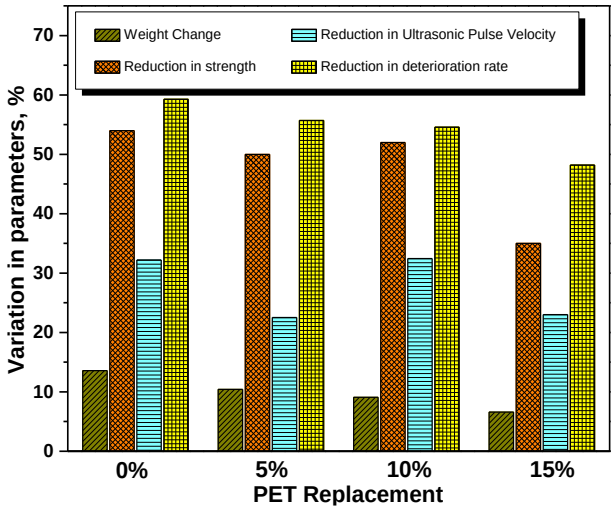

Fig. 2.20 Effect of acid attack on properties of concrete containing PET aggregates (Data source:(Janfeshan Araghi et al. 2015))

Coppola et al. (2018) performed an experimental investigation to analyze the effect of sulphate attack on mortar containing porous foamed PP and PE aggregates. The authors highlighted that the porosity induced in the global mass of the composite due to synthetic particles was beneficial against the expansive phenomenon caused by the sulphate reaction. However, this benefit vanished at higher substitution levels due to a loss in cohesive bonding with the matrix(Coppola et al. 2018). The studies on concrete containing EPS agreed with the hypothesis that acidic solutions adversely affect concrete properties. However, there was an insignificant effect of sulphate solution on the quality of concrete (Sri Ravindrarajah and Tuck, 1994).

2.2.1.15 Resistance to elevated temperature

When concrete is exposed to elevated temperatures, its mechanical properties are severely degraded. This is attributed to a series of physical transformations and chemical reactions inside the concrete mass after the exposure. In the case of PWCC, the worrying fact is that the decomposition temperature of plastic is significantly lower than the natural aggregates that are substituted. Therefore, examining the performance of PWCC at elevated temperatures is of great significance.

Albano et al. (2009) investigated the thermo-degradative behavior of concrete containing PET particles of two different sizes. The loss in flexural strength of concrete observed in the study is presented in Fig. 2.21 (a). It can be seen that there was no

noticeable loss in flexural strength at 200º C. However, a considerable decrease in flexural strength was observed for exposure at 400º C and 600º C. This was attributed to the fact that the decomposition temperature of PET lies between 350º C and 450º C. After the decomposition of PET, the production of volatile products led to an increase in porosity and thermal stresses. Additionally, the reaction of involatile products resulted in the formation of holes inside the concrete mass, which aggravated the effect of strength loss (Albano et al. 2009). Similar results were also presented by other researchers (Saxena et al. 2018; Shalaby et al. 2013). Correia et al. (2014) and Guilherme et al. (2012) subjected concrete containing flakes and pellets of PET to temperatures at 600º C and 800º C. The authors reported an overall reduction in strength properties and a substantial increase in water absorption with the increase in volumes of substitution of PET. It was also claimed that at 600º C, the decomposition of plastic was partial and mostly concentrated at the surface layer creating a water-tight film of melted plastic at the surface reducing absorption (Correia et al. 2014; Guilherme et al. 2012).

Fig. 2.21 (b) presents the results of an investigation on normal-strength and high-strength concrete containing PP coarse aggregates (Ozbakkaloglu et al. 2017). At a higher temperature of 200º C the build-up of pore pressure, increase in porosity of concrete due to dehydration of C-S-H crystal structure, and a parallel decrease in elastic modulus of PP particles were considered as the main causes of strength degradation at higher temperatures (Ozbakkaloglu et al. 2017).

With LDPE plastics as aggregates, Sojobi and Owamah (2014) presented an exceptional finding that richer mixes exhibit strength gains at higher temperatures. This was attributed to the intermingling of cement hydrate with a polymeric film formed due to the action of heat on LDPE (Sojobi and Owamah, 2014). Lo Monte et al. (2015) proved that EPS-based concrete is highly sensitive to elevated temperatures and reported a mass loss of about 50% higher than ordinary concrete when exposed to temperature of 700º C (Lo Monte et al. 2015).

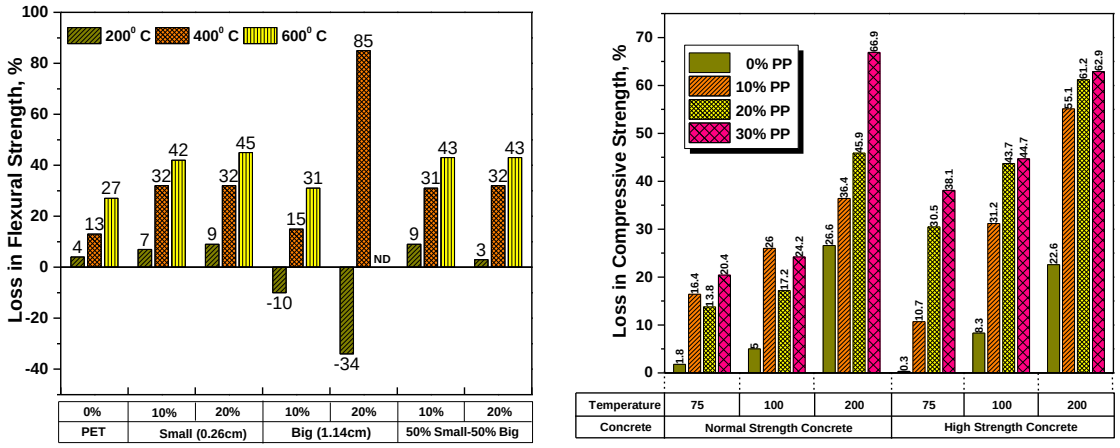

Fig. 2.21 Effect of elevated temperature on mechanical properties of concrete containing plastic aggregates (a) PET (Albano et al. 2009) (b) PP (Ozbakkaloglu et al. 2017) ND- Not Determined

2.2.1.16 Abrasion resistance

The abrasion resistance is the indicator of the quality of the surface of the concrete. The properties of the aggregates inside the concrete and their bonding with the cement paste have a significant influence on abrasion resistance (Saikia and De Brito, 2014). Abrasion resistance is determined in terms of abrasion value which is measured as a mass loss of the concrete or depth of wear after subjecting it to abrasive action. Fig. 2.22 summarizes the relative abrasion values of PWCC with different plastic contents.

Most of the research studies reported that concrete with PET aggregates showed lower abrasion value compared to the conventional mix. This finding was attributed to the fact that PET has enhanced toughness and higher abrasion resistance (Ferreira et al., 2012; Galvão et al., 2011; Saxena et al., 2020). Saikia and De Brito (2014) revealed that the coarser the plastic particles, the better the abrasion resistance. The authors advocated that the flaky coarse particles arrest, bypass, and bridge the cracks produced in concrete during abrasion, and fine particles get plucked off the matrix allowing substantial wear (Saikia and De Brito, 2014).

A similar result was obtained for concretes with LDPE/HDPE aggregates (Alqahtani et al., 2018; Galvão et al., 2011; Jain et al., 2020) and PVC aggregates (Mohammed et al. 2019).

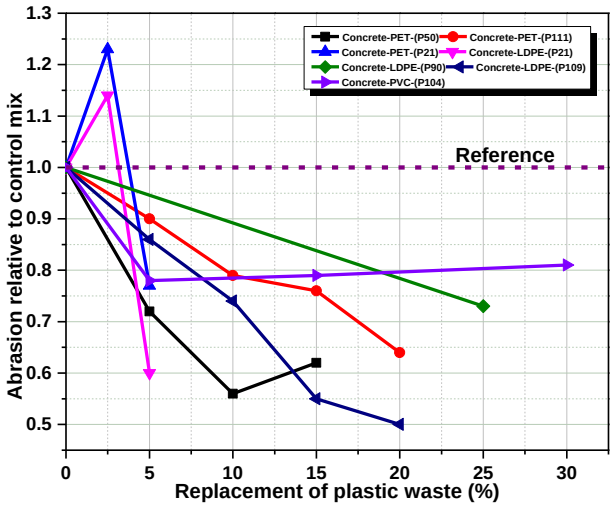

Fig. 2.22 Relative abrasion values for concrete containing plastic aggregates

2.2.1.17 Impact resistance

Several research works on cement composites with PET have shown that the lower modulus of elasticity and higher energy absorption capacity of PET are beneficial properties from the point of view of impact resistance of concrete (Jain et al. 2020; Saxena et al. 2018; Da Silva et al. 2014). Saxena et al. (2018a) have presented results for energy absorption capacity and impact energy required for cracking when concrete mixes are prepared with increasing PET contents. These results are summarized in Fig. 2.23. It can be appreciated that the more PET content, the higher the resistance to impact and the higher the absorption capacity of concrete (Saxena et al. 2018). This behavior was attributed to the flexible nature of plastics and their bridging action between the cracked sections averting the possible separation (Jain et al. 2020). A similar observation was presented by Al-Tayeb et al. (2021) for concrete containing PC waste as coarse aggregates (Al-Tayeb et al. 2021).

2.3 Cement composites containing high-density industrial slag aggregates

The significant expansion of the industrial sector has resulted in a vast number of by-products. Considering the impact of these by-products on the ecosystem, their disposal has come to be a serious problem(Ahmad et al. 2022). HDS from the metal industry such as CPS, EAFS, FCS, IFS, SFS, SSS, etc. are a few such by-products that demand an environment-friendly disposal alternative. For many years industrial waste and by-products have been explored as green construction materials (Fares et al. 2021). The

physical, chemical and mechanical properties of HDS have indicated a high potential to be used as aggregates in concrete making. Several studies have reported the use of HDS as fine and coarse aggregates inside concrete. These studies have been reviewed in various review articles to arrive at consensual finding about the physical and mechanical performance of cement composites manufactured by using such slags (Ahmad et al., 2022; Brand and Fanijo, 2020; Dash et al., 2016; Fares et al., 2021; Jiang et al., 2018; Lye et al., 2015; Wang et al., 2021b).

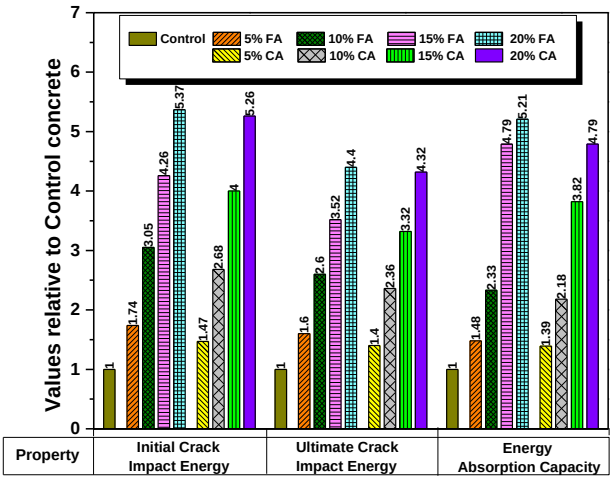

Fig. 2.23 Impact resistance of concrete containing PET aggregates (Data source: (Saxena et al. 2018))

In the current review, 77 studies on different types of slags as aggregates are selected. The details about year-wise publications and types of HDS reviewed are presented in Fig. 2.24. Table 2.4 summarizes the details about the type of slag used, type of composite, and replacement ratio of aggregates for each study selected for review.

2.3.1 Properties of cement composites containing HDS aggregates

The HDS waste from industry was used in cement composites to replace fine and coarse aggregate fractions either partially or fully. These slags were used after minimal processing efforts like crushing to obtain the desired gradation to meet the requirements of the aggregates that are replaced. The findings from the literature on the physical and mechanical properties of the cementitious mixes containing these HDS as aggregates are discussed in the following sections.

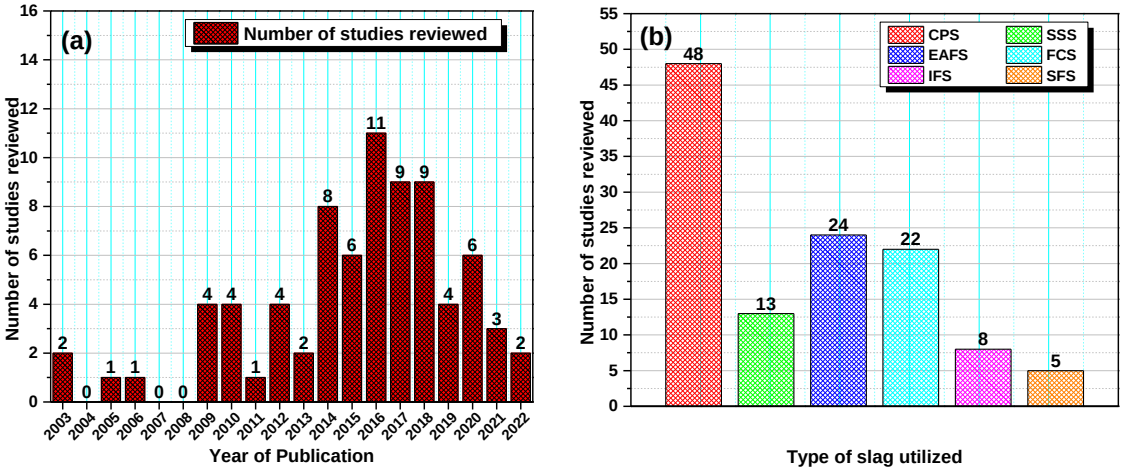

Fig. 2.24 Statistical data showing the details of research articles reviewed (a) Year wise publications (b) Type of slag utilized

Table 2.4 Previous studies selected for the review on cement mixes with HDS

Author index	Author/s, Publication year	HDS-type	Composite	Aggregate replaced	Replacement percentage	weight/ volume
S1	Alizadeh et al. (2003)	EAFS	Concrete	NCA	100	NM
S2	Maslehuddin et al. (2003)	EAFS	Concrete	Total aggregates	45,50,55,60,65	weight
S3	Penpolcharoen (2005)	SFS	Concrete	Total aggregates	20,40,60,80,100	weight
S4	Al Jabri (2006)	CPS	HPC	NFA	0,10,20,3040,50,70,100	weight
S5	Al-Jabri, et al. (2009a)	CPS	HPC	Sand	10,20,40,50,60,80,100	weight
S6	Al-Jabri et al. (2009b)	CPS	HPC	Sand	0-100 at a 10% increase	weight
S7	Qasrawi et al. (2009)	SSS	Concrete	NFA	15,30,50,100	weight
S8	Khanzadi and Behnood (2009)	CPS	HSC	NCA	100	volume
S9	Pellegrino and Gaddo (2009)	EAFS	Concrete	Total aggregates	100	volume
S10	Wu et al. (2010)	CPS	HSC	Sand	20,40,60,80,100	weight
S11	Brindha et al. (2010)	CPS	Concrete	Sand	20,40,60	weight
S12	Coppola et al. (2010)	EAFS	Concrete	Total aggregate	10,15,20,25	volume
S13	Etxeberria et al. (2010)	EAFS	Concrete	NCA	25,50,100	volume
S14	Al-Jabri et al. (2011)	CPS	Mortar/ Concrete	NFA	Mortar-20,40,50,60,80,100 Concrete-10,20,40,50,60,80,100	weight
S15	Alnuaimi (2012)	CPS	Concrete	NFA	20,40,60,80,100	weight
S16	Gencel et al. (2012)	FCS	Concrete	NCA	25,50,75	weight
S17	Nadeem and Pofale (2012)	SSS	Mortar	Sand	25,50,75,100	volume
S18	Saikia et al. (2012)	SFS	Mortar	NFA	25,30	weight
S19	Tripathi et al. (2013)	SFS	Concrete	Sand	0-70 at 10% increase	volume
S20	Chavan and Kulkarni (2013)	CPS	Concrete	Sand	10,20,30,40,50,60,75,100	weight
S21	Velumani and Nirmalkumar (2014)	CPS	Concrete	NFA	10,20,30,40,50,60,80,100	NM
S22	Naganur and Chethan (2014)	CPS	Concrete	Sand	10,20,30,40,50,60	NM
S23	Kothai and Malathy (2014)	SSS	Concrete	NFA	10,20,30,40,50	NM
S24	Prasanna and Kiranmayi (2014)	SSS	HSC	NFA	5,10,15,20,25,30,35	NM

S25	Madheswaran et al. (2014)	CPS	Mortar	NFA	25,50,75	weight
S26	Subathra Devi and Gnanavel (2014)	SSS	Concrete	NFA, NCA	10,20,30,40,50	weight
S27	Qasrawi (2014)	SSS	Concrete	NCA	25,50,75,100	volume
S28	Sheen et al. (2014)	SSS	Mortar/ Concrete	NFA	25,50,75,100	weight
S29	Sekaran et al. (2015)	EAFS	Concrete	NCA	50	weight
S30	Sezer and Gulderen (2015)	SSS	Concrete	NFA, NCA	50,100	volume
S31	Adegoloye et al. (2015)	EAFS	Concrete	NCA	50,100	volume
S32	Brand and Roesler (2015)	SSS	Concrete	NCA	100	volume
S33	Susheel et al. (2015)	FCS	Concrete	NCA	25,50,75,100	weight
S34	Faleschini et al. (2015)	EAFS	HPC	NCA	100	volume
S35	Tripathi and Chaudhary (2016)	SFS	Concrete	Sand	0-70 at 10% increase	volume
S36	Al Qurishee et al. (2016)	SSS	Concrete	NCA	0-100 at 10% increase	NM
S37	Autade and Saluja (2016)	SSS	Concrete	NFA	20,40,60,80,100	weight
S38	Coppola et al. (2016)	EAFS	Concrete	Total Aggregate	10,15,20,25	volume
S39	Borole et al. (2016)	SSS	Concrete	NFA	25,50	volume
S40/ S41	G. Singh and Siddique (2016a, 2016b)	SSS	SCC	NFA	10,25,40	weight
S42	Deepika and Asha (2016)	CPS	Concrete	NFA	40,80,100	weight
S43	Sathwik et al. (2016)	FCS	HSC	NCA	25,50,75,100	NM
S44	Kiran Sambhaji and Autade (2016)	CPS	Concrete	Sand	0-100 at 10% increase	NM
S45	Dharan and Lal (2016)	SSS	FRC	NFA	25,30,35	NM
S46	Saha and Sarker (2017)	FCS	Mortar	Sand	25,50,75,100	weight
S47	dos Anjos et al. (2017)	CPS	Concrete	NFA	20,40,60,80,100	weight
S48	Arockia Allwin et al. (2017)	SSS	Concrete	Sand	20,40,60	NM
S49	Biskri et al. (2017)	SSS	HPC	Sand	50	weight
S50	Mavroulidou (2017)	CPS	Concrete	Sand	20,40,60,80,100	weight
S51	Uddin Mohammed et al. (2017)	IFS	Concrete	NCA	25,50,75,100	volume
S52	Ouda and Abdel-Gawwad (2017)	SSS	Mortar	Sand	40,80,100	weight
S53	Rezaul et al. (2017)	IFS/EAFS	Concrete	NCA	25,50,75,100	volume
S54	Sharma and Khan (2017)	CPS	SCC	Sand	20,40,60,80,100	volume
S55	Ahmad and Rahman (2018)	IFS	RAC	NCA	25,50,75,100	weight
S56	Al-Jabri et al. (2018)	FCS	Mortar	Sand	5,10,15,20	weight
S57	Saxena and Tembhurkar (2018)	SSS	Concrete	NCA	15,25,50,75,100	weight
S58	Babu and Reddy (2018)	CPS	HSC	NFA	20,40,60,80,100	weight
S59	Dash and Patro (2018)	FCS	Concrete	NFA	10,20,30,40,50	weight
S60	Desai et al. (2018)	SSS	Concrete	NFA	10,20,30	NM
S61	Guo et al. (2018)	SSS	Concrete	NFA	10,20,30,40	volume
S62	Mishra and Bharosh (2018)	SSS	Concrete	NFA	10,20,30,40,50	weight
S63	Prince and Tiwary (2018)	CPS	Concrete	NFA	15,30,45,60	weight
S64	Rooholamini et al. (2019)	EAFS	Mortar/ Concrete	NFA, NCA	NFA: 25,50 NCA: 50,100	volume
S65	Baalamurugan et al. (2019)	IFS	Concrete	NCA	25,50	NM
S66	Gupta and Siddique (2019)	CPS	SCC	Sand	10,20,30,40,50,60	weight
S67	Singh et al. (2019)	SSS	SCC	NFA	20,30,40	NM
S68	Gupta and Siddique (2020)	CPS	SCC	Sand	10,20,30,40,50,60	weight

S69	Miah et al. (2020)	IFS	Concrete	NCA	10,20,30,40,50,60,80,100	volume
S70	Maharishi et al. (2020)	CPS	Concrete	NFA	20,40,60,80,100	volume
S71	Pan et al. (2020)	SSS	SCC	NFA	20,40,60,80,100	volume
S72	Sharifi et al. (2020)	CPS	SCC	NCA	0-100 at 10% increase	weight
S73	Tangadagi et al. (2020)	SSS	Concrete	NFA	10,20,30,40,50	weight
S74	Alwaeli (2021)	SFS	Concrete	NFA	25,50,75,100	weight
S75	Islam et al. (2021)	FCS	Concrete	Sand	25,50,75,100	weight
S76	Manjunatha et al. (2021)	CPS	Concrete	Sand	20,40,60,80,100	weight
S77	Sivamani (2022)	CPS	HSC	Sand	10,30,50,70,100	NM
S78	Prithiviraj et al. (2022)	CPS	SCC	Sand	10,20,30,40,50	weight

Type of HDS: CPS- Copper slag; SSS- Stainless Steel Slag; EAFS- Electric Arc Furnace Slag; SFS- Smelting Furnace Slag; IFS- Induction Furnace Slag
Type of Composite: HPC- High-Performance Concrete; HSC- High Strength Concrete; SCC- Self Compacting Concrete; RAC- Recycled Aggregate Concrete; FRC- Fibre Reinforced Concrete
Type of aggregate: NFA- Natural Fine Aggregate; NCA- Natural Coarse Aggregate
NM- Not Mentioned

2.3.1.1 Workability

The studies on the flowability of cement mixtures containing different types of HDS have shown varying outcomes depending on the surface texture and other material properties of the slag. The workability parameters of slag-seeded mixes relative to the conventional mix with natural aggregates are presented in Fig. 2.25.

The studies on CPS composites showed that there is a gradual increase in the workability of the mix with the increase in CPS (Fig. 2.25a). This was due to low surface porosity, low water absorption, and the glassy surface of CPS compared to NFA. The availability of increased free water content was responsible for the enhancement of flowability. The studies assumed that the additional free water act as a lubricant between solid particles and reduces interparticle friction, improving workability (Al-Jabri et al. 2009a; Gupta and Siddique, 2019; Madheswaran et al., 2014; Prithiviraj et al., 2022; Sharifi et al., 2020; Sivamani, 2022; Wu et al., 2010). In addition to these factors increased workability was attributed to the elevated specific mass of the composite (dos Anjos et al. 2017). By contrast, Mavroulidou (2017) found that there is a decrease in the slump of concrete, possibly due to the angular shape of copper slag aggregates (Mavroulidou 2017).

The studies on concrete with SSS aggregates showed extremely opposite trends of workability in comparison with CPS (Fig. 2.25b). Mixes with SSS were seen to lack mobility. This was attributed to the increased angularity and roughness of SSS causing a higher void ratio in the mix than the sand grains (Qasrawi, 2014; Qasrawi et al., 2009;

Sheen et al., 2014; Singh and Siddique, 2016a). Saxena and Tembhurkar (2018) stated that the slump value of SSS-modified mixes is lowered due to the highly porous nature of slag aggregate. The authors assumed that these porous aggregates consume more cement paste and entrap a significant amount of mixing water from the fresh composite and resulting in reduced workability (Saxena and Tembhurkar, 2018).

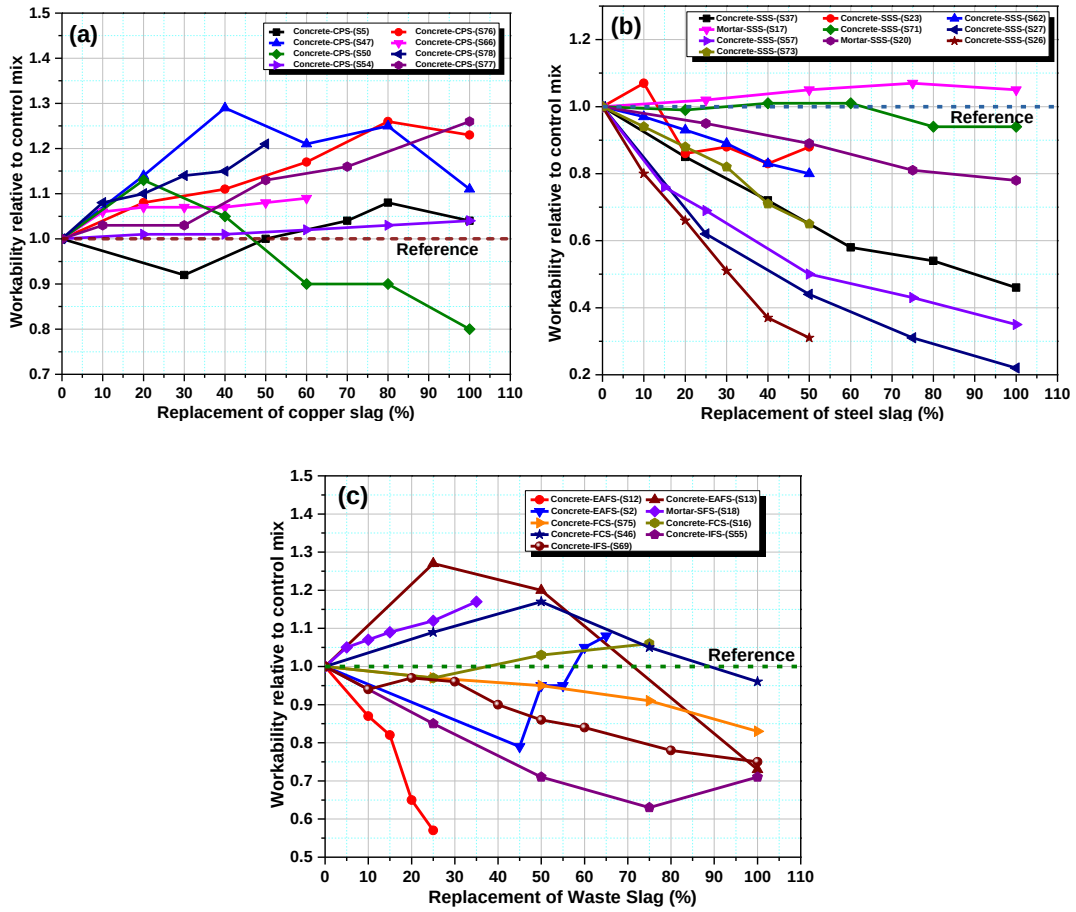

Fig. 2.25 Relative workability of cement composites containing HDS (a) Copper slag (b) Steel slag (c) EAFS, FCS, IFS and SFS

EAFS, FCS, and IFS aggregates exhibited behavior similar to SSS aggregates. The crushed nature and rough texture of aggregates increased the loss of workability (Fig. 2.25(c)). Excessive water absorption from the mix by the slag aggregates also caused a loss of flowability (L. Coppola et al. 2016; Faleschini et al. 2015; Miah et al. 2020). Additionally, an increase in surface area due to the fineness of FCS also reduced the slump flow of the mix (K. Al-Jabri et al., 2018; Dash and Patro, 2018; M. Z. Islam et al., 2021). Saha and Sarker (2017) showed that well-graded FCS can improve workability (Saha and

Sarker, 2017). In a study with SFS aggregates, Saikia et al. (2012) also showed that improvement in the grading curve of slag aggregate in addition to the use of relatively large-sized cubical particles can improve workability (Saikia et al. 2012).

2.3.1.2 Dry density

The use of slag aggregates with higher density values compared to conventional fillers in concrete presents an obvious finding that the density of composite increases with an increase in the HDS addition ratio in the cementitious mixes. The literature data on the dry density of composites is presented in Fig. 2.26. All the types of HDS showed an increasing trend of density with an increase in HDS aggregates.

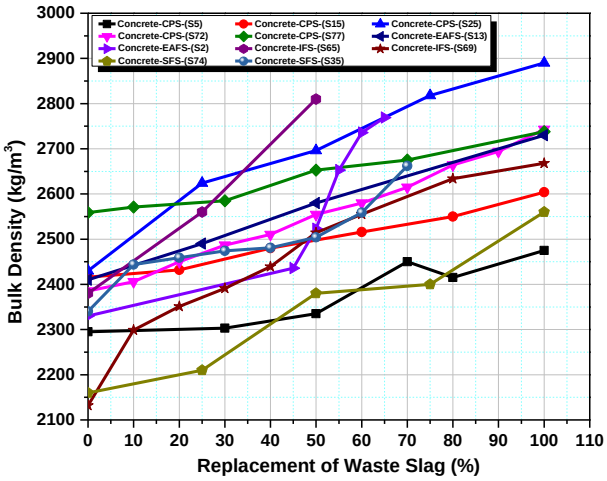

Fig. 2.26 Dry density of cement composites with HDS aggregates

2.3.1.3 Compressive Strength

The results of the compressive strength of cement composites with HDS aggregates have shown an optimistic picture of the use of such aggregates in the construction sector. Fig. 2.27 summarizes the compressive strength values of cementitious mixes with varying percentages of HDS aggregates relative to the mixes with no HDS aggregates.

In the case of CPS aggregates, most of the studies revealed that the compressive strength goes on increasing with an increase in the substitution level of slag waste (Fig 2.27a). This increase is observed for 40-60% optimum substitution levels of natural aggregates (Al-Jabri et al., 2011; K. S. Al-Jabri et al., 2009b; Sharma and Khan, 2017a). This positive effect on compressive strength was attributed to the following factors: 1)

strength of slag aggregates which improved the stress concentration of concrete mix and b) angular sharp edges and surface texture of slag which improves the bond characteristics between cement paste and aggregates (Al-Jabri et al., 2011; Khanzadi and Behnood, 2009). CPS exhibited better bonding with cement paste than natural aggregates (Maharishi et al. 2020; Manjunatha et al. 2021). Beyond optimum substitution levels of 40-50%, it was noticed that there was excess free water in the mix due to lower absorption values of slag aggregates. This excess water beyond the quantity required for hydration of cement paste causes constituent particles of concrete to remain apart and induce porosity in the mix, consequently causing a reduction in concrete strength (Al-Jabri et al., 2009b; Gupta and Siddique, 2019; Prithiviraj et al., 2022; Sivamani, 2022; Wu et al., 2010). Another reason for the decrease in strength was the settlement of CPS due to its heavy weight and the rising of water to the surface. This rising water creates a porous web of capillaries, cavities, and cracks in the concrete mass assisting its failure (Maharishi et al., 2020; Sharifi et al., 2020; Sharma and Khan, 2017b).

A trend similar to that of CPS aggregates for variation in compressive strength was observed in the case of SSS aggregates (Fig. 2.27b). The crushed shape, rough surface texture, and higher intrinsic porosity of SSS aggregates were assumed to provide a better mechanical bite with cement paste and improve compressive strength (Biskri et al., 2017; Brand and Roesler, 2015; Guo et al., 2018; Saxena and Tembhurkar, 2018; Sheen et al., 2014). Guo et al. (2018) also stated that beyond the optimum replacement of 20% volume of conventional aggregates, the strength declines. The authors claimed that the roughness of SSS slag increases its absorption and when the slag content is high the hydration process of cementitious content may be hampered leading to a lesser and weaker binding paste (Guo et al. 2018; Qasrawi 2014). Sezer et al. (2015) also highlighted the positive effect of the fineness of slag on compressive strength. The authors mentioned that due to the fineness of slag, more water was required to wet the aggregates. This led to a decrease in the effective w/c and eventually an increase in the strength of the mix (Sezer et al., 2015). A similar attribute was claimed by other studies for an increase in the compressive strength of concrete with FCS and SFS aggregates (Islam et al. 2021; Saikia et al. 2012; Tripathi et al. 2013).

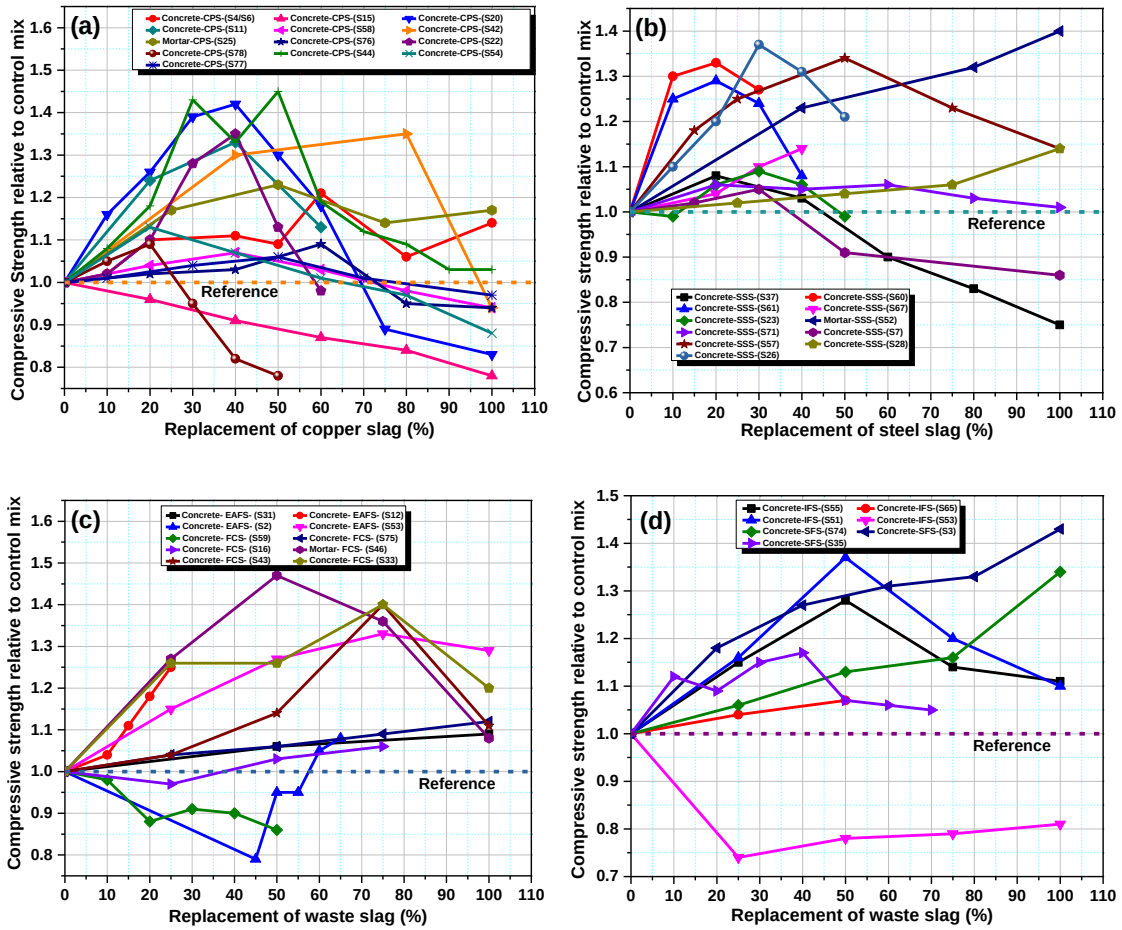

Fig. 2.27 Compressive strength of cement composites at 28 days with HDS aggregates (a) Copper slag (b) Steel Slag (c) EAFS and FCS (d) IFS and SFS

The cement composites containing other HDS aggregates also exhibited compressive strength variations identical to those with CPS and SSS aggregates (Fig. 2.27 (c), (d)). The enhancement in compressive strength was due to the interlocking between the porous texture of slag and cement paste and the improvement of the ITZ between slag and the paste (Adegoloye et al. 2015; Alizadeh et al. 2003; Al-Jabri et al. 2018; Coppola et al. 2010; Rooholamini et al. 2019; Uddin Mohammed et al. 2017). Through microstructural studies, Faleschini et al. (2015) showed that failure in conventional concrete occurs both in natural aggregates and through the interface between aggregate and cement matrix. On the other hand, concrete with EAFS failed only at the interface, with no failure in EAFS. The authors thus proved that slag has better mechanical strength than natural aggregates (Faleschini et al. 2015).

2.3.1.4 Splitting tensile strength

The variation in splitting tensile strength with the HDS content in the cementitious mix follows the similar trends observed in the case of compressive strength (see Fig. 2.28). With few exceptions, the majority of the studies reviewed exhibited an increase in the tensile strength of the composites with the increase in HDS content till an optimum substitution level. It was seen that tensile strength is more sensitive to the addition of slag and the rate of development of tensile strength is more than that of compressive strength (Khanzadi and Behnood, 2009; Sharifi et al., 2020). The behavior was majorly attributed to the better interlocking between the slag aggregates and cement matrix and the other factors responsible for enhanced compressive strength already discussed in § 2.3.1.3 (Sharma and Khan, 2017b).

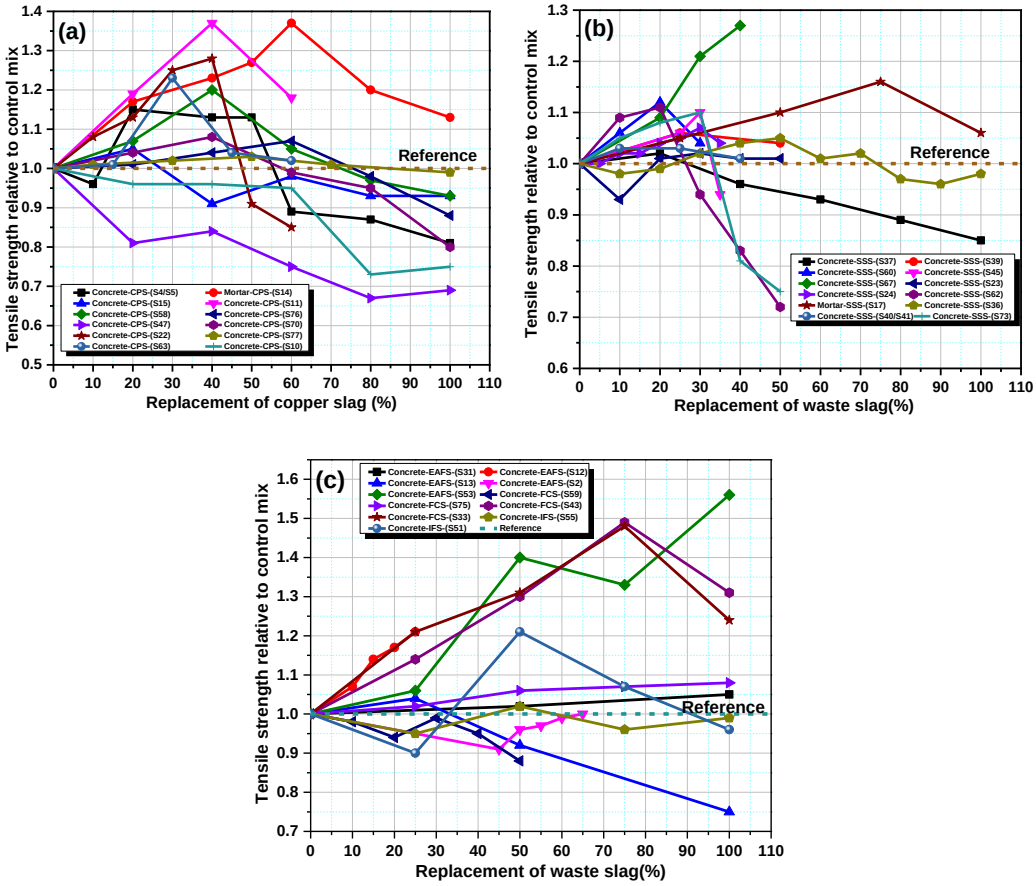

Fig. 2.28 Splitting tensile strength of cement composites at 28 days with HDS aggregates (a) Copper slag (b) Steel Slag (c) EAFS and FCS and IFS

2.3.1.5 Flexural Strength

The data available in the literature on the flexural strength studies of cement mixes with HDS aggregates presented trends similar to the behavioral trends observed in the case of compressive and tensile strength. With few exceptions, the majority of the studies claimed enhanced flexural strength of cement mixes with the increase in slag content in the mix (Fig. 2.29). This increase was attributed to the same factors that are responsible for the increase in compressive strength of the mix as discussed in § 2.3.1.3.

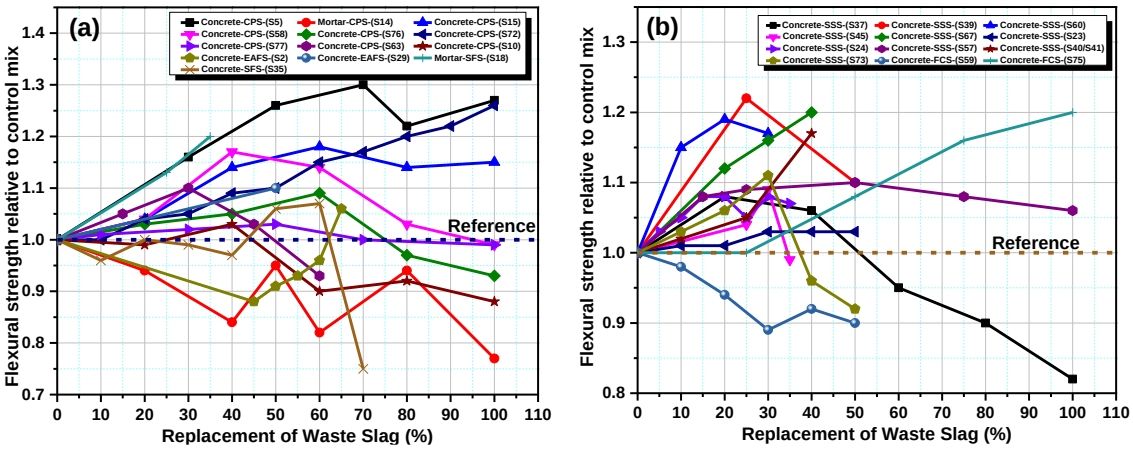

Fig. 2.29 Flexural strength of cement composites at 28 days with HDS aggregates (a) Copper slag, EAFS, and SFS (b) Steel Slag and FCS

2.3.1.6 Modulus of elasticity

As already discussed in the earlier sections, the modulus of elasticity of the concrete depends on the elasticity of the aggregate fillers in the concrete. Concrete containing soft aggregates having lower elasticity exhibits a lower modulus of elasticity. The results from the literature on the modulus of elasticity of HDS aggregate-based concrete are summarized in Fig. 2.30. It is evident that the modulus of elasticity of concretes containing all types of HDS aggregates shows increasing trends with an increase in utilization ratios in the majority of studies. This increase is attributed to the better strength of HDS aggregates compared to natural aggregates replaced by it. Pellegrino and Gaddo (2009) stated that higher cohesion between aggregate and matrix due to the higher roughness of aggregates may give higher stiffness to the mix (Pellegrino and Gaddo, 2009).

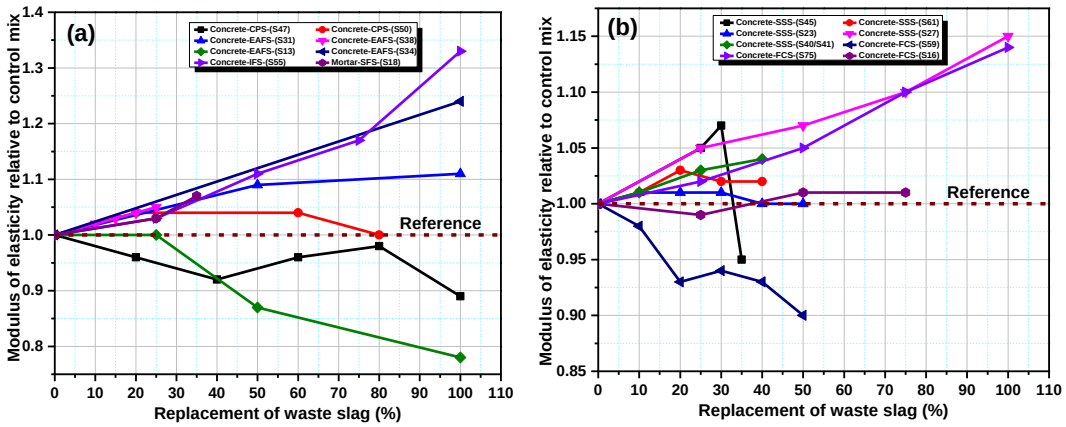

Fig. 2.30 Modulus of elasticity of cement composites with HDS aggregates (a) Copper slag, EAFS, IFS, and SFS (b) Steel Slag and FCS

2.3.1.7 Ultrasonic pulse velocity

Fig. 2.31 summarizes the UPV values for concrete mixes having an increasing substitution of natural aggregates by HDS aggregates. From the trends depicted by the majority of studies, it can be seen that the pulse velocity increases with the increase in slag content in the mix. This indicates that HDS aggregates give more compact concrete (Sheen et al. 2014). As per BIS 13311 (Part 1) – 1992, the quality of concrete is considered as medium, good, and excellent if the pulse velocity falls in the range of 3000–3500 m/s, 3500–4500 m/s and more than 4500 m/s respectively (BIS 13311,1992). The result depicts that the concretes made with HDS aggregates can be rated as “good” quality. Not much has been reported about the UPV of HDS-based concrete and it is felt that more investigations are required to have a generalized opinion about such concretes.

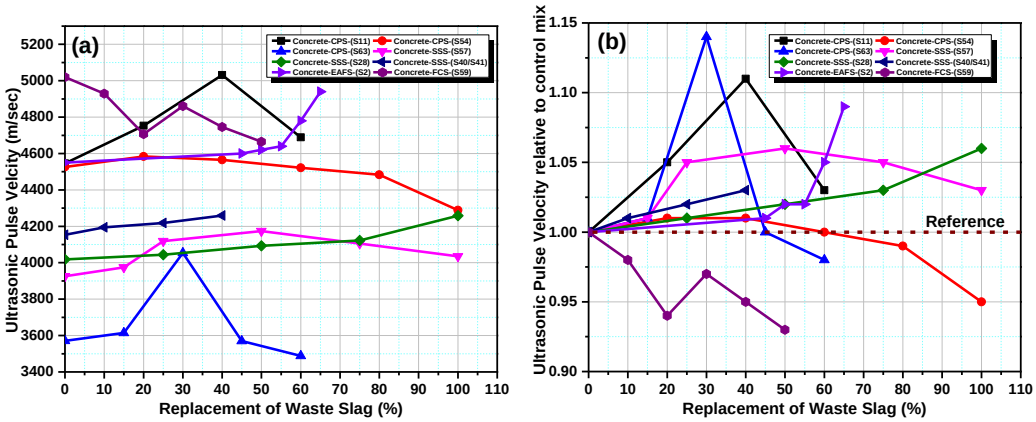

Fig. 2.31 UPV of cement composites with HDS aggregates (a) UPV value (b) UPV Relative to control mix

2.3.1.8 Water absorption

The surface water absorption showed a decreasing trend for an increase in HDS in the cementitious mix up to certain optimum levels of replacement in the mix (see Fig. 2.32). This reduction was attributed to better particle packing of aggregates (Sharma and Khan, 2017a). It was claimed that additional use of HDS beyond optimum levels would lead a to rise in free water content and the creation of voids, thereby increasing absorption (Gupta and Siddique, 2020; Sharifi et al., 2020; Sivamani, 2022). Tripathi and Chaudhary (2016) presented the transport behavior of SFS aggregate concrete and stated that the sorptivity of concrete mass decreases due to the shape of slag particles which contributes to incoherence between particle-to-particle connection and restricts the continuity of water uptake by capillary action (Tripathi and Chaudhary, 2016).

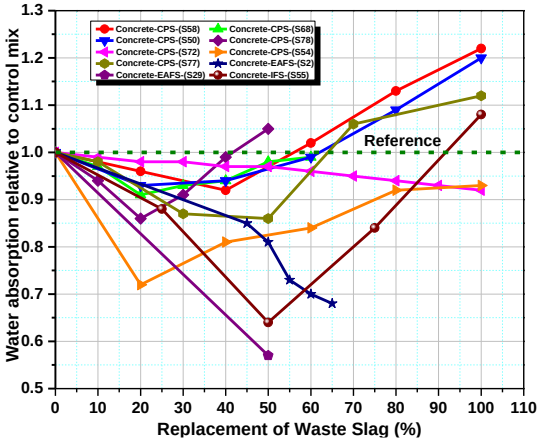

Fig. 2.32 Water absorption of cement composites at 28 days with HDS aggregates

2.3.1.9 Chloride permeability

Fig. 2.33 exhibits the relative chloride permeability values of HDS-modified concrete in comparison to conventional concrete without HDS aggregates. Although results depict that the durability of such concretes in a chloride-exposed environment is higher, it is felt that more investigations are required on this front to arrive at an undisputed conclusion.

2.3.1.10 Resistance to elevated temperature

Islam et al. (2021) conducted an experimental study on the exposure of FCS aggregate concrete to elevated temperatures of 600º C and 1000º C. The authors concluded that the mass loss in the concrete mix with FCS aggregates was lower than in

the control mix. Furthermore, it was also claimed that the strength degradation of concrete with FCS is generally lower than that of the control mix. This was attributed to the higher thermal conductivity and diffusivity of FCS aggregate which maintained uniform heat distribution in concrete unlike the control mix and minimized thermally induced cracks in cement paste. However, the loss in tensile and flexural strength was reported to be higher than in the control mix. This was due to the loss of aggregate interlocking advantage at higher temperatures and the easy propagation of micro-cracks under tensile stresses. The elasticity modulus was the most affected property with only 7-10% residual value retained after 600º C exposure. This was attributed to the deterioration of bonding strength between paste and aggregates. The studies of UPV indicated that FCS-based concrete suffered less damage than the control mix at elevated temperatures (Islam et al. 2021).

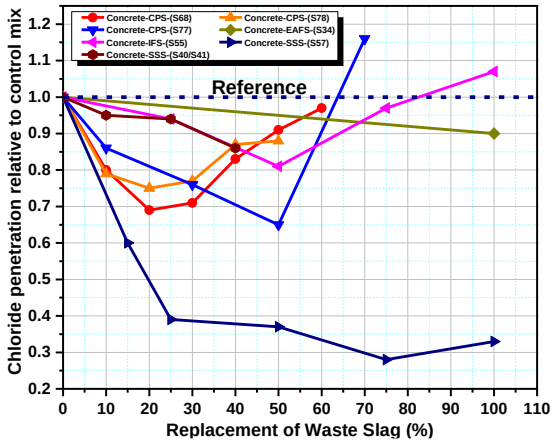

Fig. 2.33 Relative chloride penetration of cement composites at with HDS aggregates

2.4 Sustainability assessment of green concrete using LCA methodology

It has been an accepted fact that the use of wastes and industrial byproducts to replace the traditional ingredients in concrete is an appreciated step toward the global agenda of sustainable concrete manufacturing. Such concrete which is designated as ‘green concrete’ is mostly assessed for its sound technical performance comparable to conventional concrete. The benefit of resource conservation offered by such modifications is appreciated, however, overlooking the environmental impacts associated with such concrete over its entire life cycle is unjustified. The two major environmental impacts of concrete production are the emission of Green House gases (GHG) into the

atmosphere and the depletion of natural resources (Braga et al., 2017; Gursel et al., 2016; Kim et al., 2013; Kurda et al., 2018b). Each activity in the concrete-linked chain contributes to the carbon emission process. Energy-demanding activities right from extraction and processing of raw materials, transportation phase, concrete-making phase, service life phase, demolition phase after service life and reuse or disposal phase cannot exist without any emissions (Collins, 2010; Flower and Sanjayan, 2017; Kim et al., 2017). Considering the total emissions, the contribution of Ordinary Portland Cement (OPC) to the GHG emissions of concrete shadows all other ingredients and processes involved in its making (Kurad et al. 2017; Latawiec et al. 2018). Nearly 90-95% of emissions are attributed to OPC inside the concrete (Celik et al., 2015; Miller et al., 2016; Wimpenny, 2009). Various SCM that are byproducts from another industrial process such as FLA, GBFS, SF, etc., are used as an alternative for partial replacement of OPC to contribute towards the reduction in carbon emissions (Aïtcin 2016; Juenger et al. 2012). Even the total replacement of OPC with alkali-activated binders called geopolymers is a major finding in greening the concrete industry (Van Deventer et al. 2012). The substitution of natural aggregates with recycled aggregates or other suitable industrial wastes presents the second face of 'green concrete' technology reducing the environmental impact through the preservation of natural resources and minimization of waste disposal (Marinković et al., 2013). The adoption of 'Green Concrete' technology is thus rectification of mix design parameters of ordinary concrete to obtain concrete with similar workability, mechanical strength, and durability. This 'greenness' of such concretes is questionable unless its environmental assessment is carried out throughout its life cycle and compared with ordinary concrete (Van Den Heede and De Belie, 2012). LCA of concrete is a standard methodology used across the globe to quantify these impacts.

Extensive work of evaluation of impact in terms of energy and environment has been carried out for construction materials using the LCA method (Zabalza et al. 2011). Comprehensive reviews on GHG emissions and environmental impacts emerging from the production of cement (Altwair and Kabir, 2010; Andrew, 2018; Huntzinger and Eatmon, 2009; Salas et al., 2016), production of virgin and recycled aggregates (Blengini et al. 2012; Estanqueiro et al. 2018; Hossain et al. 2016b; Rosado et al. 2017) are available at a global scale. Few reviews of the environmental assessment of concrete as a composite

material in its traditional and 'green' forms have been also presented (Colangelo Forcina, et al. 2018; Petek Gursel et al. 2014; Vieira et al. 2016).

2.4.1 Review of studies on LCA of green concrete

ISO 14040 has presented a standardized methodology for LCA of any material (ISO 14040, 2006). However, the variation in the selection of parameters in each step of LCA imparts case-based uniqueness for the same kind of material. Concrete is one of the classical materials which provide enough evidence of its case-based uniqueness in LCA outcomes. The selection of system boundary and/or functional unit (FU) induces the first level of uniqueness in the analysis of concrete. It directly influences inventory data collection for the raw materials as well as processes involved in the life cycle of concrete. In the case of a particular grade of concrete, for a given system boundary and given FU, the inventory data is subjective to the mix design of concrete. Needless to mention that even for similar functional and durability requirements, each mix design delivers unique concrete composition. Even concrete in its most traditional form cannot be exempted from this consideration. The concept of "Greening the concrete industry" with environmental sustainability approach has introduced alternative binders in the form of SCM or mineral admixtures and alternative aggregates in the form of recycled aggregates from the construction and industrial sector into the concrete production flow line. The entry of such materials into the life cycle of concrete has made the LCA of concrete a challenging exercise. The concept of LCA of concrete has indeed come into the limelight a decade ago. However, substantial work has been reported in this sector which gives an overview of the environmental sustainability of green concrete. This section presents a review of studies on green concretes utilizing SCM to lower the impact of cement consumption and alternative aggregates to offer to save in natural aggregates, thus contributing toward the mitigation of resource depletion and associated environmental impacts.

2.4.1.1 Green concrete with OPC partially replaced by SCM

Considering the environmental impact of cement manufacturing on a global scale, the use of SCM to reduce the cement content in the concrete mix is considered the first phase of greening the concrete industry (Bhagat and Savoikar, 2019). Various types of SCM are used in concrete which is found to be an acceptable alternative for partial replacement of general cement inside the concrete. FLA, GBFS, SF, Limestone flour

(LSF), Rice Husk Ash (RHA), Lime Stone Calcined Clay Cement (LC3), etc. are a few examples of the most commonly used SCM in concrete in recent times. This section presents an overview of LCA studies on concretes containing SCM. Table 2.5 summarizes the details of these studies regarding the type of SCM, the selected FU, and the geographical context of the study. The salient findings of each study have been discussed subsequently.

Nisbet et al. (2002) and Prusinski (2004) presented a quantitative assessment of embodied energy and CO_2 emissions from Ready-mixed concrete (RMC), precast concrete, and masonry concrete block by replacement of OPC with FLA and GBFS. The results indicated that there is a reduction in embodied energy of the concrete to the extent of 10-14% due substitution of cement by 15-20% of FLA (Nisbet et al. 2002). Prusinski, (2004) claimed that the replacement of 50% of OPC by GBFS can lower embodied energy and CO_2 emissions by 37% and 46% respectively (Prusinski, 2004). Although GBFS has a higher emission factor than FLA, it allows a greater reduction in the environmental impact of concretes. This is because of the substitution potential of GBFS in higher quantity without affecting the mechanical behavior, unlike FLA (García-Segura et al. 2014). The findings from the studies confirmed that the cement content of the mix is the giant contributor to CO_2 emissions and it can be reduced by the use of SCM like FLA, GBFS, LSF, etc. Celik et al. (2015) inferred that the total Global Warming Potential (GWP) of concrete production sourced from OPC can be reduced from 93% to 69% by the introduction of SCM in concrete. These findings were also supported by other studies in the literature (Celik et al., 2015; Crossin, 2015; García-Segura et al., 2014; Jiménez et al., 2015; Kim et al., 2016; Kurda et al., 2018a; Mohammadi and South, 2017; Tait and Cheung, 2016; Teixeira et al., 2016). With a caution to the stated agreement, Miller (2018) proved that the factors like allocation procedure for FLA and GBFS, transportation modes, design service life, and material availability can outweigh the conventionally considered environmental benefits associated with the use of SCM and stated that higher level of SCM may not necessarily lower GHG emissions per unit strength (Miller 2018).

Table 2.5 LCA studies of concretes with OPC replaced by SCM

Author reference	Author/s	SCM used	Functional unit	Geographical context
L1	Nisbet et al. (2002)	FLA, SF	1m^3 of concrete	United States
L2	Prusinski et al. (2004)	GBFS	1 cubic yard of concrete	United States
L3	García-Segura et al. (2014)	FLA, GBFS	A reinforced concrete column	Spain
L4	Celik et al. (2015)	FLA, LSF	1m^3 of concrete	United States
L5	Crossin (2015)	GBFS	1m^3 of concrete of specific strength and service life	Australia
L6	Kim et al. (2016)	FLA	1m^3 of concrete	Korea
L7	Tait and Cheung (2016)	FA, GBFS	1m^3 of concrete of specific strength and durability	United Kingdom
L8	Teixeira et al. (2016)	FLA	1m^3 of concrete	Portugal
L9	Mohammadi and South (2017)	FLA, GBFS, SF	1m^3 of concrete	Australia
L10	Kurda et al. (2018a)	FLA	1m^3 of concrete	Europe
L11	Miller (2018)	FLA, GBFS	1m^3 of concrete of specific compressive strength	United States
L12	O'Brien et al. (2009)	FLA	1m^3 of concrete of specific compressive strength	Australia
L13	Van Den Heede and De Belie (2010)	FLA	1m^3 of concrete of 50 years' service life	Belgium
L14	Van Den Heede and De Belie (2014)	FLA	An axially loaded column with 1500KN design load for service life of 100 years	Belgium
L15	Van Den Heede et al. (2012)	FLA, GBFS	An axially loaded column with 1500KN design load for service life of 100 years	Belgium
L16	Nath et al. (2018)	FLA	1m^3 of concrete per year of service life	Australia
L17	Park et al. (2012)	FLA, GBFS	1m^3 of concrete	Korea
L18	Proske et al. (2013)	FLA, GBFS, LSF	1m^3 of concrete	Germany
L19	Gettu et al. (2019)	FLA, GBFS, LC3	1m^3 of concrete	India
L20	Pillai et al. (2019)	FLA, LC3	1m^3 of concrete of specific strength per year of service life	India
L21	Gursel et al. (2016)	FLA, LSF, RHA	1m^3 of concrete of specific compressive strength, durability, and elastic modulus	United States
L22	Marinkovic et al. (2016)	FLA	1m^3 of concrete of specific compressive strength and workability	Serbia
L23	Marinković et al. (2017)	FLA	1m^3 of concrete and 1.1m^3 of concrete for concrete with FLA and RAC for two different scenarios	Serbia
L24	Van den Heede and De Belie, (2017)	FLA, GBFS, SF	1m^3 of concrete/ concrete volume required per unit strength and service life/steel reinforced slab with design load and service life.	Belgium
L25	Flower and Sanjayan (2017)	FLA, GBFS	1m^3 of concrete	Australia
L26	Nikbin et al. (2016a)	Red mud, LSF	1m^3 of concrete	Iran
L27	Valipour et al. (2014)	Natural Zeolite	1m^3 of concrete of 15 years' service life	Persian Gulf
L28	Jiang et al. (2014)	Glass powder	1m^3 of concrete of specific compressive strength	United States
L29	Hilton et al. (2019)	Cathode ray tube and glass powder	1 metric ton of concrete	United States

In classical analysis, O'Brien et al. (2009) presented the effect of FLA content and FLA transportation distance on the GHG emissions of the concrete mix. The authors

highlighted that increasing FLA content in the mix will only reduce emissions to the degree that OPC usage is reduced without sacrificing the operational and structural features of concrete application. The study also claimed that FLA can be transported from very large distances by road, rail, or sea, and still can offer environmental benefits (O'Brien et al. 2009).

The effect of the service life of concrete on environmental impact throughout its life cycle was studied by Van Den Heede and De Belie (2010) and Van Den Heede and De Belie (2014). Both studies underlined the importance of the durability aspect in environmental impact assessment. The authors advocated that concrete with lower durability demands making an equal volume of virgin concrete for its replacement. This aspect indicates the direct environmental impact of concrete having lower durability against its declared service life (Van Den Heede and De Belie, 2010, 2014). In another study, Van Den Heede et al. (2012) quantified these volumetric requirements of SCM blended concrete for a functional unit of declared service life. After predicting the service life of FLA and GBFS blended concrete using a mathematical model, it was inferred that the blending of SCM would lower the GWP by 35-50% by their ability to impart longer service life to concrete (Van Den Heede et al. 2012). The latter finding was agreed upon by Nath et al. (2018), however, contradicted by García-Segura et al. (2014). Contradicting the findings, the authors stated that at higher substitution rates of SCM, there is a reduction in the service life of blended cement concretes leading to a hike in the CO_2 emission per year of service life (García-Segura et al. 2014).

To understand the effect of the type of SCM, strength class of concrete and seasonal effect on CO_2 emission, Park et al. (2012) conducted a rigorous analysis of 560 concrete mixes in a Korean context. It was concluded that the higher the strength class, the more CO_2 emission. The authors also claimed that for the concrete manufactured in the standard season, the use of SCM can deliver an environmental saving of 53% in terms of carbon emissions. On the other hand, concreting in winter conditions increases the emissions by 5%, courtesy of the additional cement required to meet the curing requirements (Park et al. 2012).

Environmental performance evaluation of low carbon concretes was carried out by Proske et al. (2013) in terms of GWP. Ecofriendly SCM were incorporated in concrete

with optimization techniques to satisfy functional requirements. For no allocation scenario i.e., considering GBFS as a waste in totality resulted in the highest value of 60% reduction in GWP over conventional concrete, with 35% being the average reduction for other SCM. However, consideration of the economic allocation method for SCM showed that the benefit is reduced by 10-20% (Proske et al. 2013).

In the Indian context, Gettu et al. (2019) showed that concrete with FA, GBFS, and limestone calcined clay cement (LC3) reduces GWP emissions from 6% to 26%. Pillai et al. (2019) also performed a similar analysis of concrete with LC3 and pulverized fuel ash (PFA) binders with consideration of service life as a component of the FU and reported significant environmental benefit for both the binders (Gettu et al.,2019; Pillai et al., 2019).

With a multi-criteria FU, Gursel et al. (2016) thoroughly investigated nine concrete mixes with ternary and quaternary combinations of cement, FA, RHA, and LSF using the Green concrete LCA tool. The most environment-friendly mix was selected based on normalized values of CO_2 intensity concerning the strength value. Additionally, the performance ranking of all the mixes was also rated based on durability in terms of chloride penetration and stiffness of the mix (Gursel et al. 2016).

Marinković et al. (2016) exhibited the effect of allocation approaches for FLA in the case of three RAC mixes. The study showed that no allocation and economic allocation approach to FLA led to a reduction in impact directly proportional to the substitution levels of FLA with a maximum reduction of 34% in GWP similar to the values presented by Chen et al. (2010). Contrarily, an increase in GWP value by 64% was reported under the mass allocation approach attributed to large mass production but the low economic value of FLA in Serbia (Chen et al., 2010; Marinkovic et al., 2016). In a similar study, S. Marinković et al. (2017) conducted a sensitivity analysis by improvising the basic FU having strength criteria with a special scenario FU involving durability and serviceability criteria along with the strength (Marinković et al. 2017).

Van den Heede and De Belie (2017) thoroughly investigated concretes with High Volume Fly Ash (HVFA), GBFS, and SF considering no allocation and economic allocation approach for three different FU. In case of no allocation, the environmental benefits of SCM were confirmed for a volumetric FU with superior performance by GBFS

additive. Interestingly, when strength and service life criteria were integrated into the FU, the environmental benefit of green concrete was noticed as rising from 67% to 85% compared to OPC concrete (Van den Heede and De Belie, 2017).

Flower and Sanjayan (2017) provided the most popular and systematic LCA of the concrete life cycle for cradle-to-gate system boundary. The Life Cycle Inventory (LCI) of production and transportation of raw materials, CO_2 emissions due to concrete batching, transport, and placement were highlighted in the analysis. In a comparative analysis of FLA and GBFS blended concrete with conventional concrete, it was claimed that GBFS is superior to FLA in the reduction of environmental impacts, thanks to its substitution potential. This finding was agreed upon by other studies (García-Segura et al., 2014; Van den Heede and De Belie, 2017). A reduction of CO_2 emission by 22% was reported for GBFS blending up to 40% weight of OPC (Flower and Sanjayan, 2017).

In addition to the most popular SCM like FLA and GBFS, several researchers also performed LCA of concrete containing other SCM like bauxite residue (red mud), natural zeolite, glass powder, recycled glass, etc. These studies claimed a GWP reduction of 18-30% over conventional concrete when 20% of cement was replaced by alternative products (Hilton et al. 2019; Nikbin et al. 2016a; Valipour et al. 2014).

2.4.1.2 Green Concrete with partial replacement of conventional aggregates

Aggregates inside concrete occupy almost 70% of the volume of concrete. The use of natural aggregates in concrete making is a straight invite to the natural resource depletion and the environmental impacts associated with its procurement. Therefore, the utilization of technically suitable alternative aggregates is considered the second phase of greening the concrete industry (Bhagat and Savoikar, 2019). Recycled concrete aggregates (RCA) from CDW and byproducts from the industrial sector such as EAF slag, cement kiln dust, marble sludge, foundry sand, etc. are the most commonly used alternative aggregate forms in the concrete industry. Apart from assessing the mechanical and durability performance of the concrete containing such alternative aggregates, environmental evaluation is also gaining momentum in recent times. Table 2.6 summarizes the details of LCA studies of concrete containing alternative aggregates partially replacing volumes of conventional aggregates. The salient findings of the research studies are presented subsequently.

Table 2.6 LCA studies on concrete containing alternative aggregates

Author reference	Author/s	Alternative aggregate used	Functional unit	Geographical context
L30	C. Jiménez et al. (2015)	RCA	1m^{3}of concrete of specific compressive strength for similar exposure condition	Spain
L31	H. Kim et al. (2016)	EAFS	1m^3 of concrete	Korea
L32	Kurda et al. (2018b)	RCA	1m^3 of concrete	Europe
L33	Marinkovic et al. (2016)	RCA	1m^3 of concrete of specific compressive strength and workability	Serbia
L34	S. Marinković et al. (2010)	RCA	1m^3 of concrete of specific compressive strength and workability	Serbia
L35	Mcintyre et al. (2009)	RCA	1m^3 of concrete of specific compressive strength	North America
L36	Faleschini et al. (2014)	EAFS	1m^3 of concrete	Italy
L37	Anastasiou et al. (2017)	EAFS	1m^3 concrete / 1m^2 of Concrete	Greece
L38	Liu et al. (2018)	RCA	1 ton of blocks	China
L39	Kleijer et al. (2017)	RCA	1m^3 of concrete of specific compressive strength	Switzerland
L40	Jiménez et al. (2018)	RCA	1m^3 of concrete	Mexico
L41	Serres et al. (2016)	RCA	1m^3 of concrete of specific compressive strength	France
L42	Yazdanbakhsh et al. (2018)	RCA	1m^3 of concrete with specified compressive strength	United States
L43	Knoeri et al. (2013)	RCA	1m^3 of concrete of specific compressive strength	Switzerland
L44	Turk et al. (2015)	Foundry sand/ Steel slag	1m^3 of concrete with specified compressive strength	Europe
L45	Ingrao et al. (2014)	RCA	1m^3 of concrete	Italy
L46	Tošić et al. (2015)	RCA	1m^3 of concrete of specific compressive strength	Serbia
L47	Ding et al. (2016)	RCA	1m^3 concrete of specific compressive strength	China
L48	Napolano et al. (2016)	LWA from industrial waste	1m^3 of concrete	Italy
L49	Kurad et al. (2017)	RCA	1m^3 of concrete	Europe
L50	Kurda et al. (2018a)	RCA	1m^3 of concrete	Europe
L51	Colangelo et al. (2018a)	RCA, marble dust and Cement kiln dust	1m^3 concrete of specific weight 2400Kg/m^3	Italy
L52	Colangelo et al. (2018b)	RCA and marble dust and Cement kiln dust	1m^3 concrete of specific weight 2400Kg/m^3	Italy
L53	Fraj and Idir (2017)	RCA	1m^3 of 30MPa concrete	France
L54	Gursel and Ostertag (2019)	Copper slag	1m^3 of concrete of specific compressive strength	Singapore
L55	Zulcão et al. (2016)	PET crushed aggregates	1m^3 of concrete	Brazil
L56	Javadabadi (2019)	Recycled PET aggregates	1m^3 of concrete of 30 MPa strength	Norway

Mcintyre et al. (2009) conducted an environmental evaluation of RAC for North American recycling operations. The authors showed that for a threshold substitution of 20% of virgin coarse aggregates by RCA, there was no increase in the environmental impact of RAC. However, the addition of RCA beyond 20% increased the environmental impact. This was due to the additional cement demanded by concrete to achieve the strength equivalent to the control concrete (Mcintyre et al., 2009). Similar results were

reported for concrete containing EAFS (Anastasiou et al., 2017; Faleschini et al., 2014). Liu et al. (2018) stated that the emission corresponding to the production of RCA is 57% lower than the production of natural aggregate. However, an additional 64% cement quantity is required to achieve the strength level of conventional concrete. This additional cement content hikes the emissions (Liu et al. 2018).

Marinković et al. (2010), in their specific case study, reported that the environmental impact of RAC having 100% coarse RCA is higher than that of conventional concrete. The study also highlighted the effect of the mode of transport and transportation distance of RCA and natural aggregates. The sensitivity analysis was performed to ascertain the limiting transportation distance of natural aggregates beyond which RCA substitution proves to be environmentally favorable (Marinković et al. 2010). On the other hand, Kleijer et al. (2017), Jiménez et al. (2018) and Serres et al. (2016) showed that the GWP of RAC is slightly lower than that of ordinary concrete due to the low emission factor embodied with RCA (Jiménez et al. 2018; Kleijer et al. 2017; Serres et al. 2016). In an identical study, similar results were also presented by Yazdanbakhsh et al. (2018) with another important observation that avoided impacts of landfilling of waste significantly influences the reduction of environmental impact (Yazdanbakhsh et al. 2018).

Knoeri et al. (2013) conducted a damage-oriented Life Cycle Impact Analysis (LCIA) of twelve RAC mixtures with two different types of cement for three different structural applications. With 25% and 40% RCA dosage scenarios, it was seen that RAC can provide an environmental benefit scaling to about 30% over conventional concrete. The benefit was attributed to avoided impacts of transportation and disposal of CDW from which RCA is obtained and recoveries of iron scrap. Sensitivity analysis showed that if the additional demand for cement is limited to 10% to maintain the functional requirements, the GWP values of RAC will be at par with conventional concrete (Knoeri et al. 2013).

Turk et al. (2015) investigated an ecological concrete with foundry sand, EAFS, and RCA as manufactured aggregates. Considering the avoided impacts of landfilling and recovery of metal from EAFS waste, the environmental benefit was reported to be 15-35% when foundry sand and EAFS were utilized in concrete. Whereas, the benefit

declined to 12-26% when RCA was used individually or in combination with foundry sand and FLA (Turk et al. 2015). However, specific gain in GWP was reported to be within 5% only. Kim et al. (2016) presented a significantly higher reduction of 37% in GWP for concrete containing EAFS as aggregate with GBFS and LSF as SCM (Kim et al. 2016).

Ingrao et al. (2014) compared the environmental impact of concrete containing basaltic aggregates against concrete containing limestone aggregate. In the damage-oriented approach of assessment "climate change," GWP was second-ranked environmental impact after "human health" and a total damage decrease of 67% was highlighted for limestone aggregate concrete (Ingrao et al. 2014).

Tošić et al. (2015) used a normative multi-criteria optimization (Vikor) method to find the optimal solution for concrete mixes with RCA substituted for natural aggregates from a technical, economic, and environmental viewpoint. It was concluded that RAC delivers a clear advantage in environmental load, resource depletion, and waste production (Tošić et al. 2015).

Ding et al. (2016) performed a cradle-to-cradle closed loop LCA along with aggregate transportation sensitivity to understand the potential environmental impact of RAC over conventional concrete in China. It was proved that RAC has limited environmental benefits on GWP. The effect of optimizing approaches for RCA production was also analyzed for energy demand and GWP and it was concluded that RAC with 100% RCA substitution shows a GWP increase of 6.3% with due acknowledgment to the enhanced structural and mechanical performance (Ding et al., 2016).

Napolano et al. (2016) studied the environmental performance of concrete with artificial and natural LWA sourced from industrial waste. In a damage-oriented impact analysis using the system expansion allocation rule, it was seen that artificial LWA concrete presents a significantly lower environmental burden compared to its natural counterpart. The conclusions were supported by sensitivity analysis for different allocation rules and transportation scenarios. The potential benefit of avoided impacts was noted as an influencing factor (Napolano et al. 2016).

Kurad et al. (2017) and Kurda et al. (2018a) ruled out any significant influence of admixture on GWP values except for concretes in which FLA was used as a mineral admixture (Kurad et al. 2017; Kurda et al. 2018a). The observation was in agreement with the results of a similar study by Jiménez et al. (2018).

Colangelo et al. (2018a) and Colangelo et al. (2018b) determined the damage-oriented impact of RAC with RCA from a variety of sources. Different end-life scenarios from full disposal in landfills to part disposal and part recycling at plants situated from 30 to 150km away from the place of demolition were considered. It was highlighted that even though the aspects of resource conservation and recycling potential were encouraging, the results of the increasing distance of recycling plants were discouraging (Colangelo et al. 2018a; Colangelo et al. 2018b).

A case study of RAC from the Paris region was taken up by Fraj and Idir (2017). The study evaluated the effect of grades of RCA and their delivery distances on the environmental impact of RMC. It was proved that a higher grade of RCA reduces the GWP of concrete due to lowered cement consumption (Fraj and Idir, 2017).

For Singapore's Environmental Constructs, Gursel and Ostertag (2019) recommended the replacement of 40-50% of CPS for NFA from the point of view of environmental impact normalized concerning the compressive strength (Gursel and Ostertag, 2019).

A recent review of the use of the concept of LCA in the application of plastic materials in construction by da Silva et al. (2021) could focus on overall construction applications. However, the literature on LCA of the specific use of plastic materials as aggregates in cementitious composites was too scanty to elaborate on. Also, the search of the literature in the context of the current study could not deliver much of the relevant guiding information(da Silva et al. 2021). Nonetheless, Zulcão et al. (2016) conducted LCA of the utilization of waste PET particles as a partial replacement of sand in self-compacting concrete. The study primarily agreed that the waste PET as an aggregate has a reduced environmental load when compared with natural sand. Considering the share of cement in environmental damage, it was stated that the environmental improvement due to PET incorporation is not significant when the whole supply chain is analyzed (Zulcão et al., 2016). In an extensive study, Javadabadi (2019) presented a comparative

LCA of incorporating recycled PET aggregates into concrete. The study revealed that the advantage of using recycled PET in concrete for different environmental impact categories is exhibited only when the environmental credits due to the elimination of the incineration of PET are considered. Otherwise, there was no reduction in environmental impact except in the land use category (Javadabadi 2019).

2.5 Critical appraisal

The potential of using PWA as an alternative aggregate filler in concrete to replace natural aggregates is extensively investigated by several research studies. The investigations of PWCC with different types of plastic waste in various forms, shapes, sizes, and substitution ratios have raised great concern about the degradation of the functional performance of the composites using such waste, especially in higher volumes. The inclusion of plastic fragments that are characterized by their low-density values is found to be advantageous in making concrete that is acceptable under the lightweight category. However, other characteristics such as smooth surface texture, hydrophobic nature, the mercenary or irregular shape of particles, etc. are found to be unfavorable for the preparation of composites with better rheology and strength parameters. With few exceptions, most of the studies displayed poor workability of the mixes with increasing plastic contents due to the non-uniform shapes of plastic particles and the frictional resistance offered by them in the mix. This lack of flowability in the mix was a contributory factor toward the increase in porosity in the mix. This increase in porosity was aggravated by the hydrophobic nature of plastic that allowed the accumulation of excess water around the particles. The subsequent evaporation of this excess water created void pockets in the mix converting it into a porous mass. This increased porosity and inability of plastic to have a better bond with the cement matrix was responsible for the deterioration of the strength of the mixes. The increased porosity of plastic blended mixes also increased the water absorption and permeability characteristics of the concrete. Although this property is advantageous in the case of pervious concrete which is expected to have a higher ability to expel water, the possibility of ingress of harmful chemical species is a worrying concern for the durability of normal concrete. Furthermore, the hypothesis that an increase in porosity increases the chloride ion penetration inside concrete containing plastic aggregates is accepted by most of the studies. Nonetheless,

few studies contradicted the findings stating that the impermeable nature of plastic particles blocks or disrupts the flow of chloride ions, providing better chloride resistance. The thermal conductivity of plastic is lower than the aggregates replaced by it. Concrete containing plastic aggregates, therefore, exhibits lower propagation of heat than conventional concrete, the effect being additionally favored by voids present in the concrete. However, when exposed to elevated temperatures, it was observed that there are no adverse effects on the performance of concrete until the temperatures are below the decomposition temperature of plastics. At higher temperatures, the disintegration of concrete was reported due to the development of thermal stresses inside the mass and the decomposition of plastic particles. The lower modulus of elasticity of plastic materials adversely affects the performance of PWCC. It directly leads to a decrease in the elastic modulus of concrete, the decrease being directly proportional to the amount of plastics. It is also responsible for an increase in drying shrinkage of the composites due to the poor internal restraint offered by plastic materials to the shrinkage of surrounding cementitious mass. Despite increased shrinkage, it was observed that PWA reduce the sensitivity of the composites to shrinkage cracking. Therefore, it was recommended that PWA may be used in cementitious materials for enhancing durability when resistance to cracking is a priority under imposed deformations. The studies have mentioned that PWA having higher ductility and better strain capacity like EPS may improve the resistance of concrete to the expansive cracking phenomenon, especially in cases of aggressive exposures to freeze and thaw environment as well as acid and sulfate attack. Plastics are characterized by their inherent toughness, flexible nature, better energy absorption capacity, and excellent wear resistance. These characteristics were found to be decisive in imparting better abrasion resistance and improved impact resistance to concrete when conventional aggregates were replaced by PWA. It was difficult to ascertain the relative performance of different types of plastics for a particular performance indicator due to a lack of consistency in test methodologies and variations in mix compositions. However, the existing, investigated data presents enough evidence to state that composites containing PET show better performance against chloride migration, impact loads, and abrasive actions and the worst performance in absorption, permeability, and shrinkage characteristics when compared to other types of plastics. It is rather interesting to note that PVC aggregates are better at chloride shielding but show poor resistance to

carbonation. EPS aggregates can minimize the deterioration of concrete subjected to freeze-thaw action and chemical attack. It can also control the relative strength loss of concrete at elevated temperatures.

The utilization of industrial waste in the form of HDS as aggregates in concrete has opened a new gateway to resolve the problems associated with waste management in the industrial sector. Extensive research studies in the concrete industry have assessed the potential of HDS from metal industries as an aggregate in concrete. The slags having a glassy surface texture, low surface porosity, and low water absorption as in the case of CPS, and SFS exhibit better rheology of concrete when used as a substitute for conventional aggregates. Furthermore, the studies have also indicated that the use of HDS aggregates replacing natural aggregates for optimum substitution levels of 40-50% by volume enhances the strength properties of concrete. This positive effect was attributed to the improved rheology of the mix, materialistic strength of HDS aggregates, and better bonding property of aggregates with the cement paste due to angular sharp edges and surface texture of slag. This behavior was prominent in the case of CPS, SSS, and EAFS. The concrete with HDS aggregate was categorized as "good" quality with UPV values ranging from 3500-4500 m/sec. Although the studies on the physical and mechanical properties of concrete have provided sufficient pieces of evidence of the benefit of using HDS in cement mixes, the investigations on the durability-related properties are yet to arrive at consensual inferences. The available studies have indicated better resistance of the mixes to ingress of water, chloride penetration, and strength deterioration at higher temperatures. However, some studies have shown that HDS modified concretes are prone to leaching problems, especially in the case of CPS and SFS concrete.

The concept of 'green concrete technology' is considered a major step towards the environmental sustainability initiative across the globe. This is directly related to the gigantic volumes of concrete manufactured and the environmental impacts associated with its production. Considering the established finding that the use of OPC binder in concrete contributes to 80-85% of the overall CO_2 emission from a given volume of concrete, the use of SCM like FLA, GBFS, LSF, etc. has been encouraged in the construction industry. Also, in an attempt to conserve the natural resources that are exhausted as aggregate fillers in concrete, the waste materials from the industrial and

construction sectors are utilized as aggregates in concrete. These 'green concrete' initiatives are assessed for their environmental impacts and compared with that of conventional concrete using a holistic approach of LCA in several studies across the globe. The studies have revealed a positive outcome of the usage of SCM in concrete as high-carbon-intensive material like OPC is substituted by low-carbon-intensive materials. However, it has been specifically mentioned that the benefit of the usage is subject to the decision regarding the allocation of impacts on the upstream side of the production of these SCM. Similar to the use of SCM in concrete, the use of industrial waste, such as RCA from CDW has also been audited for environmental impacts by several studies. In addition to the obvious advantage of natural resource saving, these studies also focused on the environmental impacts that might be implied in the process of obtaining concrete equivalent to the quality of conventional concrete. These implied impacts may be through several factors like usage of additional cement binder for strength replenishment, processing of the waste aggregates, additional transportation of waste aggregates, etc. The review of studies on LCA of concrete has revealed that it is a case-specific exercise linked to the geographical area of assessment, transportation distances of raw materials, selection of system boundary of assessment, and other variable factors like mix composition of concrete, strength requirements, etc. However, the holistic approach of the LCA method in ascertaining the environmental sustainability of concrete is undisputedly popular.

2.6 Research gaps in the literature

Extensive research works have been reported on the determination of the physical, mechanical, and durability characteristics of cementitious mixes containing various types of plastic materials replacing conventional aggregates, either partially or fully. However, some very salient aspects of such innovative concrete are demanding focus from the research fraternity.

It has been concluded by a few research studies that the use of PWA with gradation similar to the natural aggregates replaced by them may permit the replacement to the extent of 10-15% of volume without a significant effect on the mechanical performance of the mix. Such concretes have been experimented with only for the determination of mechanical properties and the durability characteristics of such concretes are yet to be explored. Furthermore, the surface treatment of PWA using certain

chemical surfactants like caustic soda, H_2O_2, and $H(ClO)_2$ is beneficial in the improvement of the bond characteristics of plastics with cement paste and improves the strength of concrete. Using this surface treatment in the case of graded PWA may permit aggregate substitution above the determined volumes of 10-15%. Also, the investigations on the use of mineral admixtures like FLA, SF, and nanomaterials in concretes containing plastic waste are in their preliminary stages. This use of mineral admixtures in plastic incorporated concretes need a thorough investigation as it may provide a new dimension in obtaining sustainable concrete with dual benefit i.e., recycling of non-biodegradable waste like plastic and achieving reduced environmental impacts through lowered cement consumption.

The investigations on the use of HDS as aggregates in cementitious mixes have given an optimistic outcome about the mechanical performance of the modified mixes. Even the codal provisions in IS 456-2000 permit the use of such HDS up to 25% by weight in reinforced cement concrete (IS 456, 2000). The ability of HDS to improve the mechanical strength of the modified concretes has been successfully applied to replenish the strength lost in concrete containing weak aggregates such as RCA. Considering the degradation in the mechanical performance of concrete containing PWA, it is possible to utilize HDS as ternary aggregate in plastic incorporated mixes with natural aggregates. The authors did not come across any such experimentation till recent times.

The sustainability assessment of green concrete using LCA methodology is gaining popularity nowadays for its systematic approach in the evaluation of step-by-step environmental impacts throughout the life cycle of concrete. The use of this methodology to assess the environmental impacts of concrete with SCM as a substitute for cementitious components and RCA from CDW as alternative aggregates is well appreciated. However, LCA of concrete with HDS and other alternative materials like plastic is not available in the literature in considerable volumes. The development of a life cycle inventory of such materials as ingredients in concrete is in the seeding stage of LCA studies.

Chapter 3

Materials and Mix proportions

3.1 General

The current study is aimed at making cement mortar and concrete mixes with PET sand (PET-Sand) as a fine aggregate replacing natural sand (N-Sand). The research specifically aims at obtaining the mixes in which it is possible to replace higher volumes of N-Sand with PET-Sand. The review of literature on the use of PWA in Chapter 2 has confirmed the finding that irrespective of the type of plastic used, there is degradation in the strength of the composites, especially at higher replacement levels of N-Sand. To mitigate this negative effect, the current research proposes to blend the N-Sand with industrial waste in the form of HDS. This innovative proposal finds its roots in the review of literature on cement mixes with HDS aggregates. The majority of the previous studies showed that the use of an optimum volume of HDS as aggregate fillers enhances the functional performance of concrete in comparison to conventional mixes without HDS aggregates. Considering the availability and economic viability, the current research proposes to blend SFS as a fine aggregate with the N-Sand and subsequently incorporate PET-Sand inside the mix. With OPC as the basic binding material, the research also proposes to use SCM in the form of FLA with a hypothesis that the use of FLA provides an environmental advantage in addition to the functional performance of concrete.

As an integral part of the experimental program of the current research, it is imperative to have detailed information on the characteristics of the materials used in the mixes. It is also mandatory to verify whether the materials conform to the specifications as per relevant Indian standards and/or international standards. To perform the laboratory investigation on mortar and concrete mixes, the scheme of experimentation i.e., mix proportions of the proposed composites should be decided beforehand to proceed with the experimentation. This chapter deals with the material characterization and finalization of the scheme of experimentation of the research.

3.2 Material Characterization

This section gives the details of the properties of all the materials used in the current study. These materials include OPC, FLA, N-Sand, NCA, PET-Sand, SFS sand (SFS-Sand), admixture, and mixing water. The properties specifically related to the objective of the current study have been determined and have been verified for acceptance as per relevant code provisions.

3.2.1 Binders

Ordinary Portland cement (OPC 53 grade) manufactured by Associated Cement Companies (ACC) was used as the primary binding material in the current research. FLA confirming to IS 3812: 2013 is used as SCM in the current study (IS 3812, 2013). FLA was procured from Dirk India Private Limited, a subsidiary of Ambuja Cements Ltd. Nashik, Maharashtra, India which is commercially available as POZZOCRETE 60.

Various tests were conducted to ascertain the physical and chemical characteristics of OPC and FLA and their acceptance as per relevant standards. These physical and chemical properties of the OPC used in the current study are summarized in Table 3.1. The chemical characteristics of FLA are summarized in Table 3.2. The obtained results are also validated for the requirements as per IS 269-2015 and IS 3812-2013 for acceptance in the case of OPC and FLA respectively (IS 269,2015; IS 3812, 2013).

The particle sizes of OPC and FLA particles in a given volume were determined using Mastersizer 2000 E Ver. 5.60 of Malvern Instruments Ltd. fitted with a Scirocco sample handling unit. This particle size distribution of OPC and FLA particles is presented in Fig. 3.1.

Scanning Electron Microscopy (SEM) and Energy Dispersive X-ray Spectroscopy (EDS) analyses of OPC and FLA were performed by examining the binder samples using JEOL-JSM-6360 L V SEM. The SEM and EDS micrographs of OPC and FLA are presented in Fig. 3.2 and Fig. 3.3. SEM micrographs show that the OPC particles are irregular showing angularity and sharper edges. On the other hand, the FLA microstructure shows that the particles are spherical in shape. The micrographs confirm the particle size distribution of binder particles as presented in Fig. 3.1.

Table 3.1 Physical and chemical characteristics of OPC

Sr. No.		Characteristics	Test as per IS	Results	Requirements as per IS 269:2015
1.		Physical characteristics			
	a.	Fineness			
		By dry Sieving, %	IS 4031 (Part 1): 1996	5.6	Not greater than 10
		Blaines Air Permeability, m^2/kg	IS 4031 (Part 2): 1999	306	Not less than 225
	b.	Soundness (Le Chatelier), mm	IS 4031 (Part 3): 1988	1.0	Not greater than 10
	c.	Setting time	IS 4031 (Part 5): 1988		
		Initial setting time, min		170	Not less than 30
		Final setting time, min		220	Not greater than 600
	d.	Compressive strength, MPa	IS 4031 (Part 6): 1988		
		72 ± 1h (3 days)		35.5	Not less than 27
		168 ± 2h (7 days)		45.5	Not less than 37
		672 ± 4h (28 days)		58.0	Not less than 53
	e.	Specific Gravity	IS 2720 (Part 3): 1980	3.15	-
	f.	Normal consistency, %	IS 4031 (Part 4): 1988	28.25	-
2.		Chemical characteristics	IS 4032: 1985		
	a.	Lime Saturation Factor		0.91	0.8-1.20
	b.	Ratio of percentage of alumina to that of iron oxide (Al_2O_3/Fe_2O_3)		1.28	Not less than 0.66
	c.	Insoluble residue, %		0.50	Not more than 5%
	d.	Magnesia, %		1.00	Not more than 6%
	e.	Sulphuric anhydride, %		2.90	Not more than 3.5%
	f.	Total loss on ignition, %		1.60	Not more than 4%
	g.	Chloride content (%)		0.010	Not more than 0.1%

Table 3.2 Physical and chemical characteristics of FLA

Sr. No.		Characteristics	Test as per IS	Results	Requirements as per IS 3812:2013
1.		Physical characteristics	IS 1727: 2015		
	a.	Fineness			
		Blaines Air Permeability, m^2/kg		372	Not less than 320
		Residue over sieve of 45 µm, %		15.42	Not more than 34%
	b.	Compressive strength, MPa			
		672 ± 4h (28 days)		53.80	Not less than 80 % strength of plain cement mortar
	c.	Specific gravity		2.28	-
2.		Chemical characteristics	IS 1727: 2015		
	a.	$SiO_2 + Al_2O_3 + Fe_2O_3$		83.50 %	Not less than 70 %
	b.	SiO_2		52.25 %	Not less than 35 %
	c.	MgO		2.19 %	Not more than 5 %
	d.	SO_3		0.76 %	Not more than 3 %
	e.	Loss on ignition		1.02 %	Not more than 5 %

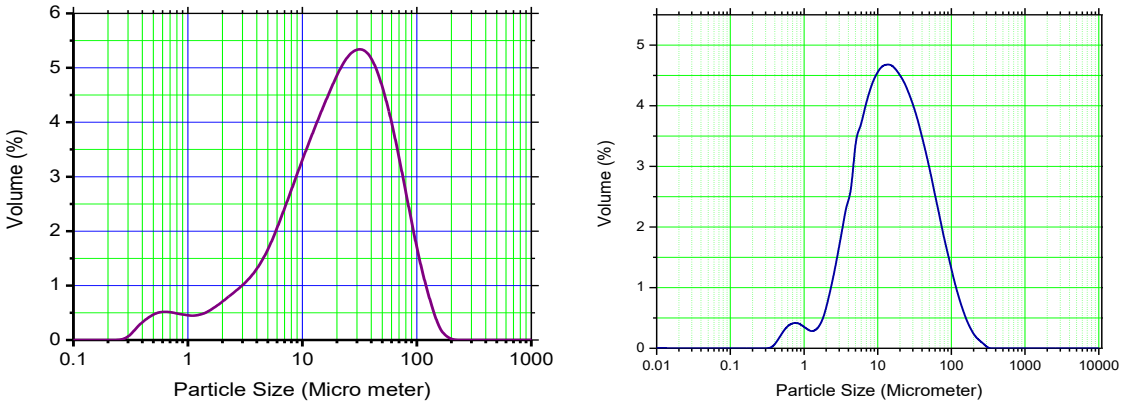

Fig. 3.1 Particle size distribution of binder (a) OPC (b) FLA

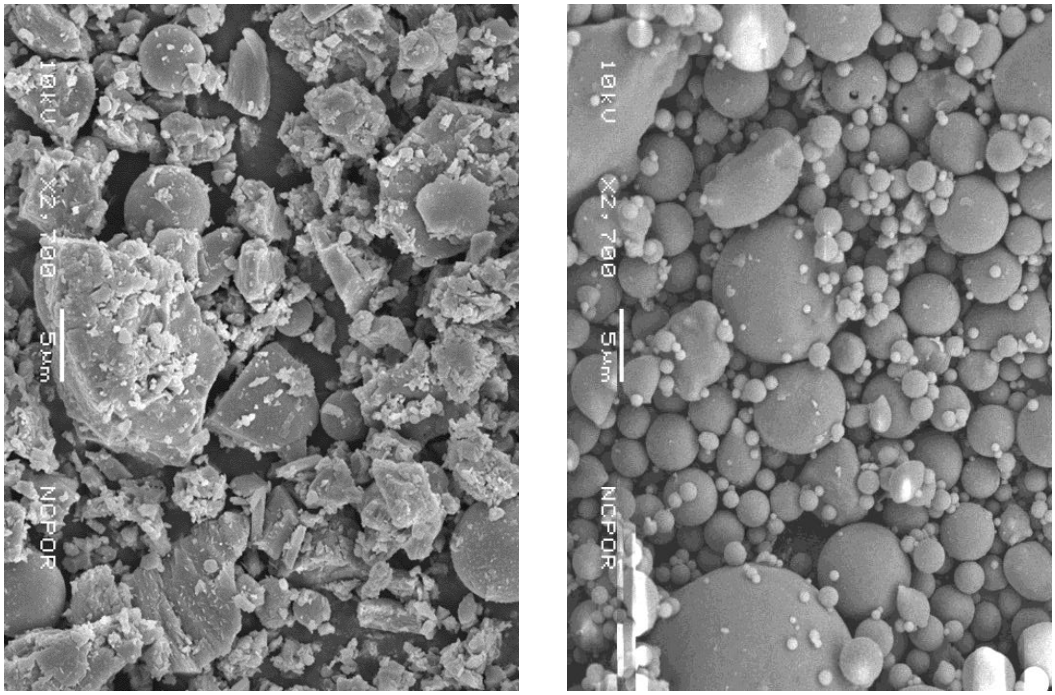

Fig. 3.2 SEM images of the binders (a) OPC (b) FLA

The results of the EDS analysis of OPC and FLA are shown in Fig. 3.3. The spectrum of EDS analysis of OPC confirms the presence of significant amounts of calcium and silica oxides with traces of alumina, ferrous, magnesium, and sulphur oxides. On the other hand, FLA shows a major share of silica and alumina oxides with traces of ferrous, magnesium, and sulphur oxides.

The chemical oxide composition of OPC and FLA is summarized in Table 3.3. This composition is in agreement with the values depicted by spectrums of EDS analysis for both binders.

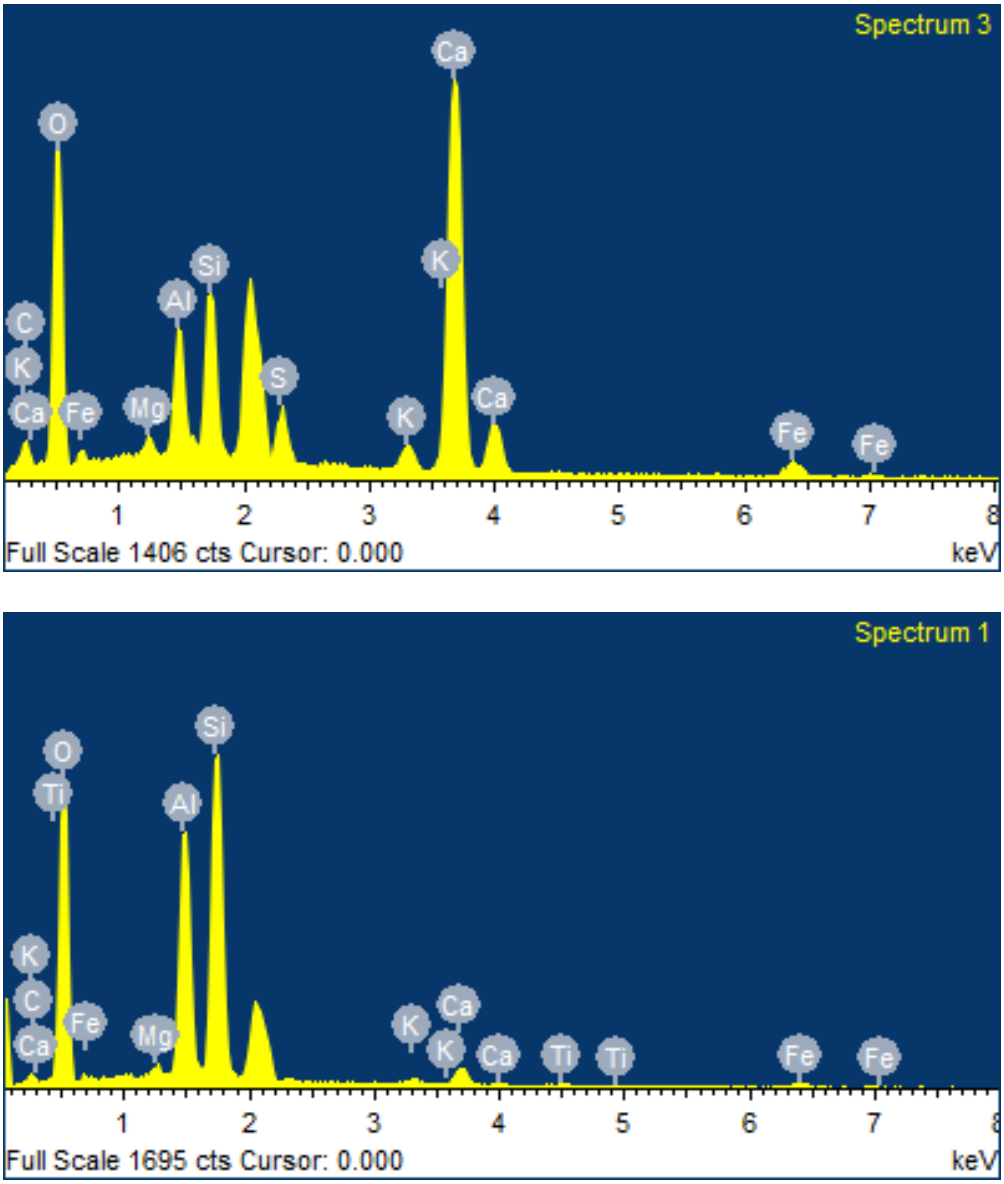

Fig. 3.3 EDS spectrum of binders (a) OPC (b) FLA

Table 3.3 Chemical (oxide) composition of binders

Binder	Oxide (%)					
	SiO_2	Al_2O_3	Fe_2O_3	CaO	SO_3	MgO
OPC	21.36	5.39	3.81	62.25	2.33	2.15
FLA	56.41	24.90	7.99	4.12	0.50	1.47

3.2.2 Fine aggregates

The primary objective of the current research is the replacement of N-Sand in conventional concrete with PET-Sand to avail the environmental benefit of resource conservation and efficient plastic waste management. In addition to the research

objectives, the methodology of research in Chapter 1 proposed the use of HDS in the form of SFS-sand as fine aggregate in the mix with a hypothesis that HDS aggregate component will compensate for the strength lost by the mix due to plastic inclusion. Therefore, the mix compositions investigated in the current study look forward to a ternary blend of fine aggregates, i.e., N-Sand, SFS-Sand, and PET-Sand. A clear understanding of the properties of all three types of fine aggregates is a very important aspect in designing the compositions of the mix. The physical properties, particle sizes, and other properties of these aggregates relevant to the current investigation are determined according to the code provisions.

Crushed sand obtained from the Tamba Metal Quarry, Old Goa, Goa (India) is used as N-sand in the current study. SFS-Sand was supplied from Hindustan Zinc Limited, Chanderiya plant, Rajasthan, India. PET-Sand was procured from M/s. Ubhayodaya plastic recycling Industries, Navi Mumbai. PET-Sand is a product of mechanical recycling of small and large PET bottles. Discarded PET bottles were collected and shredded into flakes. Bottle caps and label papers were removed to obtain only PET material. Using a specially designed shredder (see Fig. 3.4), PET bottles of different sizes and colors are minced to achieve extremely small diameters of particles that can pass a 4.75mm Sieve. Fig. 3.5 shows the photographic view of N-Sand, SFS-Sand, and PET-Sand.

The physical properties of the fine aggregates are determined as per the procedure laid down by IS 2386 (Part 3): 1963, Methods of tests for aggregates for concrete (IS 2386(3), 1963). The results of the physical properties of N-Sand, SFS-Sand, and PET-Sand are presented in Table 3.4. Particle size distribution or the gradation of fine aggregates is determined by IS 2386 (Part 1): 1963, Methods of tests for Aggregates for Concrete (IS 2386(1), 1963). The particle size distribution in terms of percentage finer than standard sieve size for three types of fine aggregates are summarized in Table 3.5. The classification of fine aggregates according to grading zone criteria as per IS 383:2016 is an indicator of the feasibility of the use of aggregates in mortar and concrete. Relative gradation of the three types of aggregates to the upper and lower limits of Zone II is presented in Fig. 3.6. It can be seen that all the aggregates obtained for the current study confirm Zone II grading of sand as per IS 383:2016 (IS 383, 2016).

Fig. 3.4 Shredding machine to make PET sand

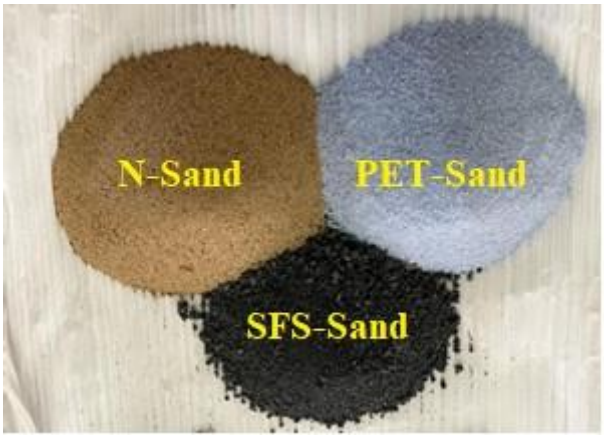

Fig. 3.5 Photographic view of fine aggregates

Table 3.4 Physical properties of fine aggregates

Sr. No.	Property	Fine aggregate type		
		Natural Sand	PET sand	SFS sand
1.	Specific gravity	2.82	1.32	3.28
2.	Water absorption (%)	1.60	0.0	0.84
3.	Bulk Density (kg/m^3)			
	Loose bulk density	1628	497	1894
	Dry rodded density	1820	591	1964

Table 3.5 Particle size grading for fine aggregates

Sieve size	Percentage finer (%)		
	Natural Sand	PET Sand	SFS sand
4.75mm	99.16	100	100
2.36mm	72.74	100	88.08
1.18mm	45.91	98.75	70.07
600µ	32.41	54.63	54.62
300µ	21.57	10.25	40.38
150µ	12.87	0.75	31.46
75µ	7.66	0.13	26.77

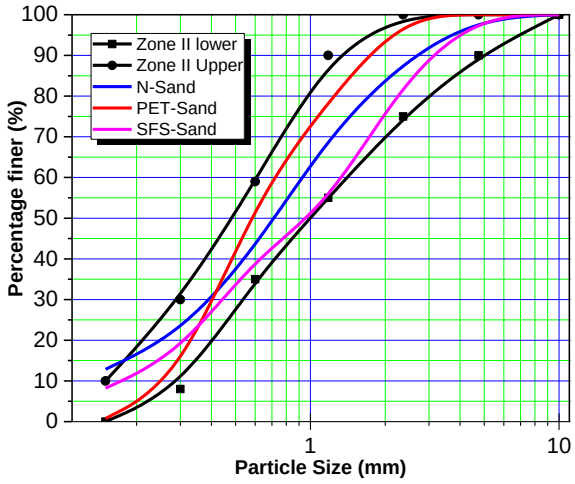

Fig. 3.6 Grading of fine aggregates comparative to Zone II limits as per IS 383:2016

PET-Sand and SFS-Sand were also observed under a microscopic scale to understand the shape and surface characteristics of the innovative aggregates. The SEM images of PET-Sand and SFS-Sand particles are presented in Fig. 3.7. From Fig. 3.7(a), it can be seen that shredded PET particles are non-uniform with angular and mercenary shapes. Fig. 3.7(b) shows an SEM image of the SFS aggregate particle. The image shows spherical needle-like protuberance along with large open cavities. These particles appear to be irregularly shaped compared to the sand particles which are found to be regular having smooth surfaces. The visual observation of SFS-Sand depicts a glassy surface texture. The chemical composition of the SFS-Sand was also analyzed using EDS analysis. The results of the analysis are presented in Table 3.6 and Fig. 3.8.

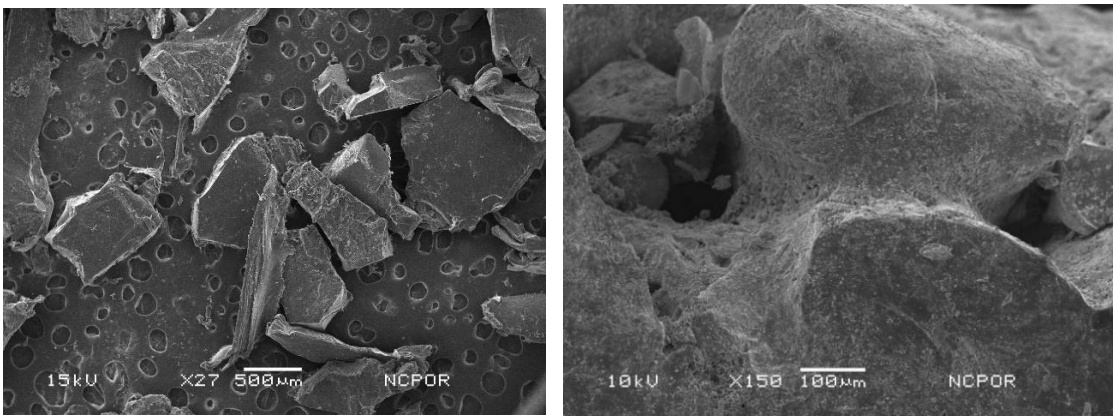

Fig. 3.7 SEM images of fine aggregates (a) PET-Sand (b) SFS-Sand

Table 3.6 Chemical composition of SFS-Sand

Aggregate	Element (weight %)							
	SiO_2	MgO	Al_2O_3	Fe_2O_3	CaO	K_2O	ZnO	FeS_2
SFS-Sand	13.06	1.15	2.75	18.68	26.51	0.91	5.47	1.32

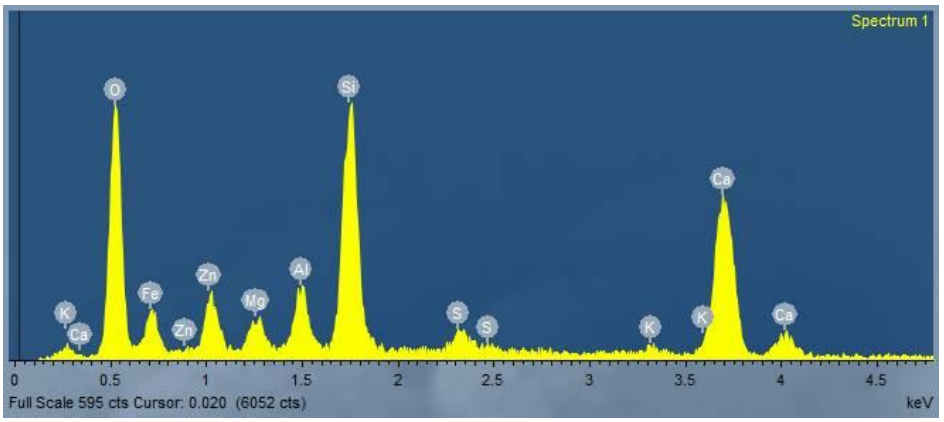

Fig. 3. 8 EDS spectrum of SFS-Sand particle

3.2.3 Coarse aggregates

Natural basaltic aggregates of 20mm maximum size of aggregates procured from M/s. Nanu sand, Goa was used as NCA for making concrete in the proposed research. The photographic view of aggregates is shown in Fig. 3.9. The physical and mechanical properties of NCA are determined as per the specifications by IS 2386: 1963 which are summarized in Table 3.7. The particle size distribution details for 20mm and 12.5mm nominal aggregate sizes are presented in Table 3.8. This distribution is depicted graphically in Fig. 3.10 for corresponding nominal sizes.

Fig. 3.9 Photographic view of coarse aggregates

Table 3.7 Physical and mechanical properties of coarse aggregates

Sr. No.	Property	Coarse aggregate type	
		20mm	12.5mm
1.	Specific gravity	2.84	2.84
2.	Water absorption (%)	0.45	0.48
3.	Aggregate crushing value	19.60	18.60
4.	Aggregate impact value	15.40	17.20
5.	Aggregate abrasion value	16.70	14.30
6.	Bulk Density (kg/m^3)		
	Loose bulk Density	1534	1569
	Dry rodded Density	1745	1800

Table 3.8 Particle size distribution of coarse aggregate

Aggregate	Sieve size (% finer)						
	40mm	20mm	16mm	12.5mm	10mm	4.75mm	2.36mm
20mm	100	82.3	52.8	35.6	0.24	0.04	0.0
12.5mm	-	-	100	99.6	82.4	7.80	1.0

3.2.4 Admixture

A commercially available Poly-Carboxylic Ethers (PCE) based superplasticizer was used for enhancement of the workability of the mixes in the current research. It was procured from Concrete Additives and Chemicals Pvt. Ltd. (CAC). The manufacturer's inputs mentioned the specific gravity and pH value of the admixture as 1.145 and 6

respectively. The admixture confirmed the requirements as per IS 9103:1999 (IS 9103,1999).

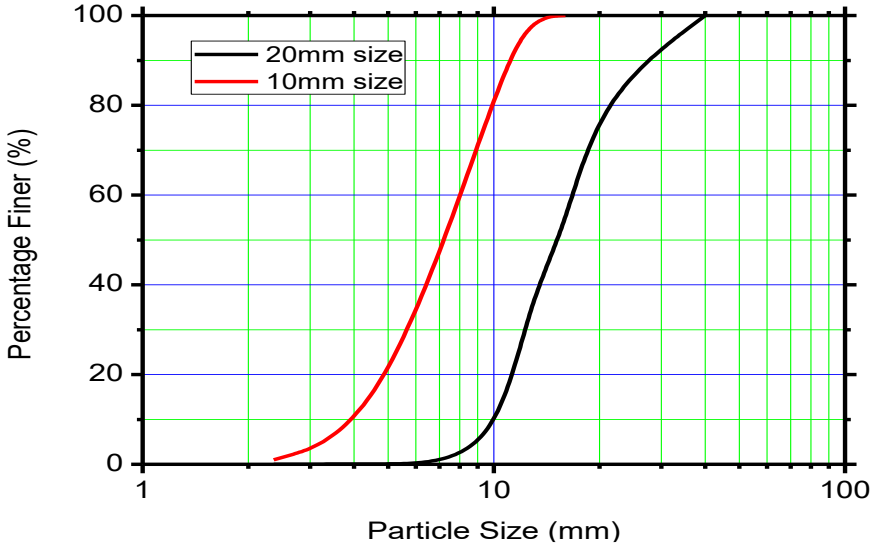

Fig. 3.10 Particle size distribution of coarse aggregates

3.2.5 Water

Tap water available in the laboratory was used as mixing water for the preparation of mortar and concrete. Tap water is used for the curing of mortar and concrete specimens maintaining an ambient temperature of 25 – 27 °C. Water used for curing is replaced with fresh tap water every seven days.

3.3 Mix proportions

The comprehensive review of investigations of cement mixes containing PWA in Chapter 2 has revealed that the natural aggregates in conventional cementitious mixes are replaced with plastic waste alone in incremental proportions by volume/weight. However, the current study is a novel approach to plastic valorization in which the PET-Sand replaces the fine aggregate volume which comprises a blend of N-Sand and SFS-Sand. Therefore, the investigations in the current study include two different iterations in aggregate replacement. They are 1) the substitution of PET-Sand for N-Sand for various volume proportions on lines similar to the studies already reviewed in the literature and 2) the substitution of PET-Sand for the blended fine aggregate consisting of N-Sand and SFS-Sand.

The findings in the literature have concluded that there is an optimum level of substitution of N-sand by HDS aggregates beyond which there is a decline in strength attenuation of the mix. Therefore, the determination of the optimum substitution level of SFS-Sand is the pre-requirement of the current experimental program before the formulation of mortar and concrete mixes. This optimum substitution level for mortar and concrete mixes is determined in the laboratory from compressive strength tests on mortar and concrete specimens. The experimental program and the results of the investigation to determine optimum substitution levels SFS-Sand for mortar and concrete mix are presented in **Appendix A** and **Appendix B** respectively. From the results, it is noted that maximum strength gain is observed in the mortar and concrete mix when N-Sand is replaced by SFS-Sand for volumes of 50% and 40% respectively.

Research studies in polymer aggregate concrete have shown that the use of mineral admixture in the form of FLA may also control the strength reduction in PWCC. As reported in the literature, the spherical shape of FLA particles increases the flow ability of concrete, leading to a denser mix with higher strength. PET with FLA has a larger crystalline degree and FLA particles act as nucleation centers for the crystallization of PET improving the strength characteristics of the PET mix (Duta et al., 2011). The environmental benefit of using FLA as a partial replacement for OPC is well-known in the life cycle of concrete. Considering these major benefits, the current investigation is further extended to formulate design mixes with FLA as a supplementary binder by 30% of the weight of OPC. Therefore, three tiers of cementitious composites are investigated in the current study. The details of mix proportions for these three tiers of mortar and concrete are presented in the following sections.

3.3.1 Mix proportions for cement mortar

Two different mix proportions for cement mortar having binder to fine aggregate ratios 1:3 and 1:5 are formulated in the current investigation. These different mix proportions are selected to verify the consistency of the results of the experimentation and also to understand the effect of the increase in the PWA-to-binder ratio on various properties of the modified mixes. As already discussed in the previous section, in addition to the control mix, the scheme of experimentation consists of three tiers of mortar mixes. This three-tier mix formulation can be summarized as follows:

1) Tier I- Mortar mix with OPC binder (100%) and volumetric substitution of PET-Sand to replace N-Sand in the mix,
2) Tier II- Mortar mix with OPC binder (100%) and volumetric substitution of PET-Sand to replace the blended volume of N-Sand (50%) and SFS-Sand (50%), and
3) Tier III- Mortar mix with OPC (70%) and FLA (30%) and volumetric substitution of PET-Sand to replace the blended volume of N-Sand (50%) and SFS-Sand (50%).

It is pertinent to note that 50% volume of SFS-Sand is considered in the blended volume of fine aggregates in Tier II and Tier III by the discussions already presented in § 3.3 and the experimental results in **Appendix A**. The control mix is formulated for 1:3 and 1:5 mix proportions without the utilization of PET-Sand to replace the fine aggregate fraction. The three-tier mix proportions were formulated by incorporation of 10%, 15%, 20%, and 25% volumetric replacement of fine aggregates by PET-Sand for each tier of the experimental scheme. All the mixes are prepared with a constant water/binder ratio (w/b ratio) of 0.45. The admixture dosage for the control mortar in both the mix proportions is selected such that the flow value is sufficiently higher in the range of 200 ± 10mm. A higher flow value for the control mix was selected to avoid stiffer mixes at higher replacement levels of PET-Sand where it is difficult to note the variations in the flow values.

Table 3.8 presents the composition of the control mortar mix with only N-Sand as fine aggregate. Table 3.9-3.11 presents the mix compositions for three tiers of mortar. The percentage ratio of the OPC and FLA is considered as a proportion of 100% weight of binding material and the percentage ratio of N-Sand, PET-Sand, and SFS-Sand is considered as the proportion of 100% volume of total fine aggregates in the mix.

Mortar mixes are identified with identities consisting of three terms. The first term indicates the type of composite, the second term indicates the binder used, and the third term indicates the fine aggregates used as substitutes in the mix. M_X-C-P0, M_X-C-P10, M_X-C-P15,… are the identities given for the control mix and Tier I mixes of the experimentation. In these identities, the first abbreviation 'M_X' refers to Mortar mix (X=3 or 5 for 1:3 or 1:5 mix respectively), the second abbreviation 'C' refers to cement binder, and the third abbreviation is purposefully related to PET-Sand content in the mix. 'P'

refers to PET-Sand and the number that follows the abbreviation 'P' indicates the percentage volume content of PET in the mix. In the second tier of experimentation, SFS-Sand is blended with N-Sand. To indicate this blending, the abbreviation 'S' (without suffixing any numerical value since blending is constant i.e., 50%) is prefixed to 'P' and it is followed by the substitution ratio of PET-Sand. E.g., M_5-C-SP20 identifies the mortar of 1:5 mix proportion with 100% OPC binder in which fine aggregate blend of SFS-Sand and N-sand is replaced for 20% volume by PET-Sand. Furthermore, in the third tier, the suffix of the alphabet 'F' to the abbreviation 'C' in the first term signifies that the mixes are formulated on the lines of the second tier, except for the change that the binder content is a blend of OPC and FLA (30% by weight of cement). E.g., mix M_3-CF-SP25 indicates the mortar of 1:3 mix proportion with 70% cement and 30% FLA binder in which fine aggregate blend of SFS-Sand and N-sand is replaced by 25% PET-Sand by volume.

The actual quantities of the materials used for various mortar mixes are presented in **Appendix C**.

Table 3.9 Mix proportions for control mortar (OPC/N-Sand)

Mix Identity	Binder (100%)		Fine aggregate (100%)			Admixture as per mix (% wt. of binder)	
	OPC	FLA	PET-Sand	N-Sand	SFS-Sand	1:3 mix	1:5 mix
M_X-C-P0	100	0	0	100	0	0.60	0.90

(X=3 for 1:3 mix and X=5 for 1:5 mix)

Table 3.10 Mix proportions for Tier I mortar (OPC/ N-Sand + PET-Sand)

Mix Identity	Binder (100%)		Fine aggregate (100%)			Admixture as per mix (% wt. of binder)	
	OPC	FLA	PET-Sand	N-Sand	SFS-Sand	1:3 mix	1:5 mix
M_X-C-P10	100	0	10	90	0	0.60	0.90
M_X-C-P15	100	0	15	85	0	0.60	0.90
M_X-C-P20	100	0	20	80	0	0.60	0.90
M_X-C-P25	100	0	25	75	0	0.60	0.90

(X=3 for 1:3 mix and X=5 for 1:5 mix)

Table 3.11 Mix proportions for Tier II mortar (OPC/ N-Sand + SFS-Sand + PET-Sand)

Mix Identity	Binder (100%)		Fine aggregate (100%)			Admixture as per mix (% wt. of binder)	
	OPC	FLA	PET-Sand	N-Sand	SFS-Sand	1:3 mix	1:5 mix
M_X -C-SP0	100	0	0	50	50	0.60	0.90
M_X -C-SP10	100	0	10	45	45	0.60	0.90
M_X -C-SP15	100	0	15	42.5	42.5	0.60	0.90
M_X -C-SP20	100	0	20	40	40	0.60	0.90
M_X -C-SP25	100	0	25	37.5	37.5	0.60	0.90

(X=3 for 1:3 mix and X=5 for 1:5 mix)

Table 3.12 Mix proportions for Tier III mortar (OPC+FLA/ N-Sand + SFS-Sand + PET-Sand)

Mix Identity	Binder (100%)		Fine aggregate (100%)			Admixture as per mix (% wt. of binder)	
	OPC	FLA	PET-Sand	N-Sand	SFS-Sand	1:3 mix	1:5 mix
M_X -CF-SP0	70	30	0	50	50	0.60	0.90
M_X -CF-SP10	70	30	10	45	45	0.60	0.90
M_X -CF-SP15	70	30	15	42.5	42.5	0.60	0.90
M_X -CF-SP20	70	30	20	40	40	0.60	0.90
M_X -CF-SP25	70	30	25	37.5	37.5	0.60	0.90

(X=3 for 1:3 mix and X=5 for 1:5 mix)

3.3.2 Mix proportions for cement concrete

To investigate the effect of the incorporation of PET-Sand on the fresh and hardened properties of concrete mix, two different grades of concrete are selected. M30 and M50 grade concretes are designed with w/c of 0.44 and 0.39 respectively. These different mix proportions are selected to verify the consistency of the results of the experimentation and also to understand the effect of the w/c and strength grade on the properties of concrete with PWA. The investigation of concrete mixes with PET-Sand has followed a similar program of experimentation as in the case of mortar mixes. Without any change in NCA composition, the concrete mixes are designed with PET-Sand substituted for N-sand or a blend of N-Sand and SFS-Sand in volumetric ratios of 10%, 15%, 20%, and 25%. Accordingly, concrete mixes also follow a three-tier investigation program as below:

1) Tier I- Concrete mix with OPC binder (100%) and volumetric substitution of PET-Sand to replace N-Sand in the mix,
2) Tier II- Concrete mix with OPC binder (100%) and volumetric substitution of PET-Sand to replace the blended volume of N-Sand (60%) and SFS-Sand (40%), and
3) Tier III- Concrete mix with OPC (70%) and FLA (30%) and volumetric substitution of PET-Sand to replace the blended volume of N-Sand (60%) and SFS-Sand (40%).

It is pertinent to note that 40% volume of SFS-Sand is considered in the blended volume of fine aggregates in the second and third tier by the discussions already presented in § 3.3 and the experimental results presented in **Appendix B**. The control mix is formulated for M30 and M50 grades of concrete without the utilization of PET-Sand to replace the fine aggregate fraction. The admixture dosage for the control concrete in both the strength grades is selected such that the slump value is sufficiently higher in the range of 180 ± 10mm. A higher slump value for the control mix was selected to avoid stiffer mixes at higher replacement levels of PET-Sand where it is difficult to note the variations in the slump values.

Table 3.13 presents the composition of the control concrete mix with only conventional aggregates. Table 3.14-3.16 presents the mix compositions for three tiers of concrete, The percentage ratio of the OPC and FLA is considered as a proportion of 100% weight of binding material, and the percentage ratio of N-Sand, PET-Sand, and SFS-Sand is considered as the proportion of 100% volume of total fine aggregates in the mix.

Concrete mixes are identified with identities similar to those discussed in the case of mortar mixes in section 3.3.1. To differentiate from the mortar mixes, the concrete mixes are indicated with the first term 'C_Y' instead of 'M_X' in the case of mortar mixes. Alphabet 'C' in the first term refers to the 'concrete mix' and the subscript 'Y' is used to indicate the strength grade of concrete (Y= 30 for M30 grade; Y=50 for M50 grade).

Table 3.13 Mix proportions for control concrete (OPC/N-Sand)

Mix Identity	Binder (100%)		Fine aggregate (100%)			Coarse aggregate (100%)	Admixture as per mix (% wt. of binder)	
	OPC	FLA	PET-Sand	N-Sand	SFS-Sand	NCA	M30	M50
C_Y-C-P0	100	0	0	100	0	100	0.70	0.60

(Y=30 for M30 mix and Y=50 for M50 mix)

Table 3.14 Mix proportions for Tier I concrete (OPC/ N-Sand+PET-Sand)

Mix Identity	Binder (100%)		Fine aggregate (100%)			Coarse aggregate (100%)	Admixture as per mix (% wt. of binder)	
	OPC	FLA	PET-Sand	N-Sand	SFS-Sand	NCA	M30	M50
C_Y-C-P10	100	0	10	90	0	100	0.70	0.60
C_Y-C-P15	100	0	15	85	0	100	0.70	0.60
C_Y-C-P20	100	0	20	80	0	100	0.70	0.60
C_Y-C-P25	100	0	25	75	0	100	0.70	0.60

(Y=30 for M30 mix and Y=50 for M50 mix)

Table 3.15 Mix proportions for Tier II concrete (OPC/ N-Sand+PET-Sand+SFS-Sand)

Mix Identity	Binder (100%)		Fine aggregate (100%)			Coarse aggregate (100%)	Admixture as per mix (% wt. of binder)	
	OPC	FLA	PET-Sand	N-Sand	SFS-Sand	NCA	M30	M50
C_Y-C-SP0	100	0	0	60	40	100	0.70	0.60
C_Y-C-SP10	100	0	10	54	36	100	0.70	0.60
C_Y-C-SP15	100	0	15	51	34	100	0.70	0.60
C_Y-C-SP20	100	0	20	48	32	100	0.70	0.60
C_Y-C-SP25	100	0	25	45	30	100	0.70	0.60

(Y=30 for M30 mix and Y=50 for M50 mix)

Table 3.16 Mix proportions for Tier III concrete (OPC+FA/ N-Sand+PET-Sand+SFS-Sand)

Mix Identity	Binder (100%)		Fine aggregate (100%)			Coarse aggregate (100%)	Admixture as per mix (% wt. of binder)	
	OPC	FLA	PET-Sand	N-Sand	SFS-Sand	NCA	M30	M50
C_Y-CF-SP0	70	30	0	60	40	100	0.70	0.60
C_Y-CF-SP10	70	30	10	54	36	100	0.70	0.60
C_Y-CF-SP15	70	30	15	51	34	100	0.70	0.60
C_Y-CF-SP20	70	30	20	48	32	100	0.70	0.60
C_Y-CF-SP25	70	30	25	45	30	100	0.70	0.60

(Y=30 for M30 mix and Y=50 for M50 mix)

The mix designs are formulated as per the specifications of IS 10262-2019 (IS 10262, 2019). The actual quantities of the materials used for various concrete mixes are presented in **Appendix D**.

Chapter 4

Methodology

4.1 Introduction

The cement mortar and concrete mixes prepared as per the scheme of experimentation discussed in § 3.3 in Chapter 3 are tested in the laboratory for various properties in the fresh and hardened states. Most of the tests are performed by the relevant testing procedures described as per Bureau of Indian standards. A few tests are also performed as per European testing procedures. This chapter deals with the description of the testing procedures adopted for ascertaining the physical, mechanical, and durability characteristics of cement mortar and concrete prepared in the current study. In addition to the laboratory testing, the assessment of the environmental sustainability of the formulated cement mortar and concrete mixes is a noteworthy objective of the current research. Therefore, the methodology of LCA used for the assessment is also discussed in this chapter.

4.2 Tests on cement mortar

Various tests are performed on cement mortar to determine its properties in fresh and hardened states. The tests include workability, bulk density, compressive strength, flexural strength, and sorptivity. The experimental procedure for conducting these tests is discussed in the following sections.

4.2.1 Workability of mortar

The workability test of cement mortar is performed by IS:2386 (Part 6)-1963 using a flow table. A mold 60mm in height having a base diameter of 100mm and a top diameter of 70mm is placed in the center of the flow table. It is filled with the mortar in two layers by uniformly tamping each layer 20 times with a standard tamping rod. By drawing the straight edge of a trowel, the mortar is cut off to a plane surface, to flush with the top of the mould. Excess mortar if any is removed from the top of the mould and the area at the base of the mould is cleaned thoroughly with a cloth. The mold is lifted from

the mortar after one minute of mixing operation and immediately the table is jolted through a height of 12.5mm ten times in 6 seconds. The average flow is measured on at least four spread diameters of the mortar at approximately equal angles (IS 2386(6), 1963).

4.2.2 Bulk density of mortar

The test for the determination of the fresh density of cement mortar is performed by BS EN 1015-6 (BS 1015-6, 2019). The test involves the calculation of the mass of the mortar in a calibrating container of known volume. The method of filling and compacting the mortar within the container is based on the flow value of the fresh mortar as determined by the flow table test.

1) If the mixture is stiff having a flow value of less than 140mm, the calibrating container is filled till it is overflowing. It is then vibrated on a vibrating table with the addition of more quantity if required until no further settlement of material is observed.
2) For a plastic mortar having a flow value between 140mm to 200mm, the container is first filled with mortar up to 50% of the height. It is then tilted 30mm on alternate sides and dropped 10 times on a solid base. Subsequently, the container is filled to the full height with similar compaction efforts.
3) For a soft mortar having a flow value greater than 200mm, the container is filled with mortar until it is overflowing. Then the edges are wiped clean with a damp cloth.

The container is weighed to the accuracy of 1 gram. Fresh density (ρ) is calculated by using the formula:

$$\rho = \frac{W_2 - W_1}{V} \quad \text{..... Eq. (4.1)}$$

where W_1 = Weight of container; W_2 = Weight of container + mortar; V= Volume of container

The bulk density of hardened mortar is determined by BS EN 1015-10 (EN 1015-10, 2019). Three test samples of regular shape are prepared from fresh mortar and cured by BS EN 1015-11 (EN 1015-10,2019). The hardened test samples are dried at a

temperature of 70º C and the dry weight is found to the nearest 0.1 gram (W_{dry}). The volume (V_d) of the dry specimen is determined using the buoyancy balance method. The test specimens are immersed in water and the weight is noted after a period of immersion and the process is repeated until the saturated weight does not differ by more than 0.2%. The saturated weight is recorded to the nearest 0.1 gram (W_{sat}). The test specimens are then weighed in water (using a stirrup attachment to the balance). The weight of the immersed test specimens is recorded to the nearest 0.1 gram (W_i). The volume (V_d) is calculated using the formula:

$$V_d = \frac{W_{sat} - W_i}{\rho_w} \quad \text{.....Eq. (4.2)}$$

where ρ_w= density of water; kg/m^3.

The dry density of the mortar (ρ_d) is calculated using the formula:

$$\rho_d = \frac{W_{dry}}{V_d} \quad \text{..... Eq. (4.3)}$$

The average dry density of three test samples is noted to the nearest 10 kg/m^3.

4.2.3 Compressive strength of mortar

The compressive strength of mortar specimens is determined according to the recommendations as per IS 2386 (Part 6):1963. After the completion of the flow test, the mortar is placed in 7.06 cm cube moulds in two layers. Each layer of the mortar is tamped with 25 strokes of tamping rod and the moulds are filled to overflowing. The moulds are kept in a moist closet for curing. In 3 to 4 hours after moulding, the specimens are struck off to a smooth surface and again kept in the moist closet. The specimens are removed from the mould 20 to 24 hours after moulding and stored in water for curing till the test period.

On attaining the test period, the specimens are removed from the storage water. Each specimen is surface dried and loose sand grains or incrustations are removed from the faces that come in contact with the bearing plates of the testing machine. The specimen is kept at the center of the upper bearing plate and the load is applied, without interruption, to failure at such a rate that the maximum load will be reached in not less than 20 nor more than 80 seconds.

The results are presented as an average of three test specimens and also the age of testing. The result is recorded to the nearest 0.05 N/mm^2 and the average of the set of results is reported to the nearest 0.1 N/mm^2 (IS 2386(6), 1963).

4.2.4 Flexural strength of mortar

The flexural strength of hardened mortar is determined by the procedure prescribed in BS EN 1015-11 (EN 1015-11,2019). Prismatic mortar specimens of size 160mm x 40mm x 40 mm are obtained using a mould assembly that can house three specimens. The mould is filled in two layers of mortar with each layer compacted with 25 strokes of the tamper. The specimens are cured in a curing chamber for an age of 28 days.

The flexural strength is measured by the three-point loading method. The schematic diagram of the test setup is shown in Fig. 4.1. The prism is placed on two supporting rollers and the third loading roller is located above the test specimen and at midspan between the two supporting rollers. The prism is placed in such a way that one of its faces, which has been cast against the steel mould, is in contact with the supporting rollers. The load (W) is applied to the test specimens at the rate of 50 N/sec such that failure is affected in a period of thirty to ninety seconds. The flexural strength (*f*) is determined using the formula:

$$f = \frac{1.5\,WL}{bd^2} \quad \text{.....Eq. (4.4)}$$

Where b and d are the internal dimensions of the mould; L = distance between the supporting rollers.

The result is recorded to the nearest 0.05 N/mm^2 and the average of the set of is results reported to the nearest 0.1 N/mm^2.

4.2.5 Sorptivity test of mortar

The test was performed according to Choi et al. (2009) and Gouasmi et al. (2019) and the procedure recommended by RILEM publications in Sabir et al. (1998) (Choi et al., 2009; Gouasmi et al., 2019; Sabir et al., 1998). It is the measurement of the rate of absorption of water by capillary suction of unsaturated mortars when placed in contact with water with no application of hydraulic pressure.

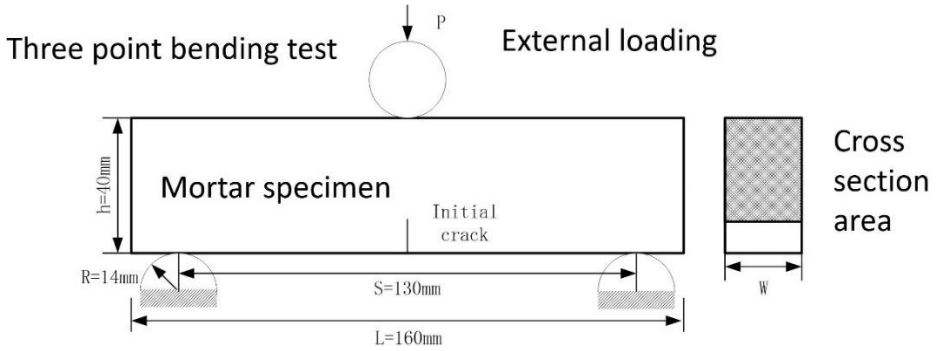

Fig. 4.1 Flexural strength test of mortar specimens

Cubic specimens, of dimensions 50mm x 50mm x 50mm are used for the test. The specimens are preconditioned in an oven at 105º C until they attain a constant mass. A small layer of the face of each cube is sliced off to expose the capillary pores on the face selected for contact with water. The other lateral faces of the cubes are impregnated with epoxy resin to seal the entry of water from the faces other than the one that is selected. The cubic specimens are placed on small supports in a tank containing water, in such a way that water reaches only 5mm of the height of the specimen as shown in Fig. 4.2.

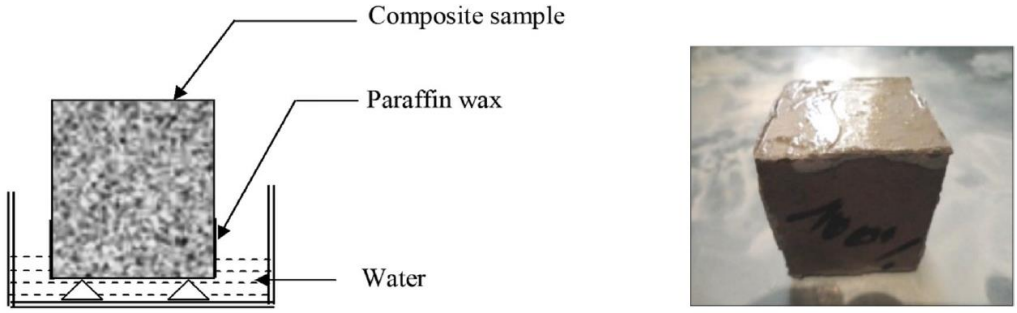

Fig. 4.2 Arrangement of sorptivity test on mortar

The increase in mass of the test specimen is measured as a function of time i.e., at 1, 4, 9, 16, 25, 36, 49, and 64 min. The capillary water absorption coefficient is then calculated using the following formula:

$$\frac{Q}{A} = S\sqrt{t} \quad \text{..... Eq. (4.5)}$$

Where Q is the cumulative volume of water absorbed in cm^3; A is the area of the inflow surface of the specimen in contact with water in cm^2; t is the time expressed in seconds and S is the sorptivity coefficient of the specimen in $cm/(sec)^{1/2}$.

4.3 Tests on cement concrete

Various tests are performed on cement concrete to determine its properties in fresh and hardened states. The physical and mechanical tests include workability, bulk density, compressive strength, tensile strength, flexural strength, modulus of elasticity, UPV, and sorptivity. Also, durability-related properties of concrete vis-à-vis water absorption, permeability, chloride migration, and the effect of exposure to aggressive environments such as elevated temperatures are investigated in the current study. The experimental procedure for conducting these tests is discussed in the following sections.

4.3.1 Workability Test on Concrete

The workability of the concrete was determined using a slump test on concrete by IS 1199-2018 (IS 1199,2018). The mould in the form of the frustum of a cone is used for the test. Internally, the cone has a bottom diameter of 20 cm, a top diameter of 10 cm, and a height of 30 cm. The tamping rod of steel or other suitable material, 16 mm in diameter, 0.6 m long, and rounded at one end is used for compaction purposes.

The mould is thoroughly cleaned from the inside to avoid any superfluous moisture or remains of any set concrete before the commencement of the test. The mould is then placed on a smooth, horizontal, rigid, and non-absorbent surface. A carefully leveled metal plate can be used for this purpose. The mould is filled in four layers by firmly holding it in place with the help of attached handles. Each layer is tamped with twenty-five strokes of the rounded end of the tamping rod in such a way that the strokes are uniformly distributed over the cross-section of the mould. After proper compaction, the top layer is struck off level with a trowel or tamping rod such that the mould is exactly filled. Any overflown mortar from the mix is cleaned carefully. The mould is then immediately removed from the concrete by raising it slowly and carefully in a vertical direction. This allows the concrete to subside. The slump is measured immediately by determining the difference between the height of the mould and that of the highest point of the specimen being tested. The above operations are completed within a period of two minutes after sampling the mix.

The slump measured is recorded in terms of millimeters of subsidence of the specimen during the test. If the slump specimen collapses or shears off laterally, the results are considered incorrect and the test is repeated with another sample.

4.3.2 Bulk density of concrete

The density of concrete was determined in terms of weight per cubic meter of concrete in the freshly mixed state as well as the hardened state.

The weight per cubic meter of freshly mixed concrete was determined as per IS 1199-2018 (IS 1199, 2018). A calibrated measure of 250 mm inside diameter and 280 mm inside height is used. The capacity of the measure is obtained in cubic meters by dividing the weight of water required to fill the measure by the unit weight of water, i.e., 1000 grams/litre. The measure is filled with concrete after mixing, in such a way as to produce full compaction of the concrete with neither segregation nor excessive laitance. The concrete is filled into the measure in layers approximately 5 cm deep and each layer is compacted by hand using a standard tamping steel bar weighing 1.8 kg, 38 cm long, and having a square ramming face. The exterior surface of the cylinder is tapped smartly 10 to 15 times or until no large bubbles of air appear on the surface of the compacted layer. After the top layer is compacted, the surface of the concrete is struck off-level with the top of the measure. All excess concrete is then cleaned from the exterior and the filled measure is weighed. The weight per cubic meter of freshly mixed concrete is calculated by dividing the weight of fully compacted concrete in the measure by the volume of the measure and is recorded in kg/m^3.

The bulk density of hardened concrete is determined using the experimental procedure on similar lines with mortar samples. This test uses three test samples of 15cm x 15cm x 15cm cast according to the recommendations by IS: 516-2021 (IS 516,2021). The average dry density of three test samples is noted to the nearest 10 kg/m^3.

4.3.3 Compressive Strength of Concrete

The compressive strength of concrete is determined as per the recommendations by IS:516 (2021) (IS 516,2021).

Cubical-shaped test specimens of 150 mm x 150 mm x 150 mm are prepared for the compression test with standard cube moulds as prescribed in the standards. The procedure for making and curing the test specimens in respect of sampling of materials, preparation of materials, proportioning, weighing, mixing, workability, compaction, and curing is followed in all respects with the requirements given as per IS:516-2021 (IS

516,2021). The joints between the sections of the mould and contact surfaces between the bottom of the mould and the base plate are thinly coated with mould oil to prevent any escape of water from the mix during the filling of the concrete. Also, the internal surfaces of the assembled mould are coated with mould oil to prevent the adhesion of concrete. The concrete is filled into the moulds in layers approximately 50 mm deep ensuring a symmetrical distribution of the concrete within the mould. Each layer is compacted by vibration using a suitable vibrating table until the specified condition is attained. After the top layer has been compacted, the surface of the concrete is finished level with the top of the mould, using a trowel, and covered with a glass or metal plate to prevent evaporation.

The test specimen is stored in the moist air of at least 90 percent relative humidity and at a temperature of 27° ± 2°C for 24 hours ± l hour from the time of addition of water to the dry ingredients. Then the specimens are marked and removed from the moulds and immediately submerged in clean, fresh water and kept there until taken out just before the test. The water in which the specimens are submerged is renewed every seven days and shall be maintained at a temperature of 27° ± 2°C.

The concrete specimens are tested at ages 3, 7, 28, 56, and 90 days. The dimensions of the specimens to the nearest 0-2 mm and their weight are noted before testing. The compression testing is done on the machine from EIE Instruments Pvt. Ltd. make of 5000kN capacity. The load is applied at a rate of approximately 5.15 kN/Sec until the resistance of the specimen to the increasing load breaks down and no greater load can be sustained. The maximum load applied to the specimen is then recorded and the appearance of the concrete and any unusual features in the type of failure is noted.

The measured compressive strength of the specimen is calculated by dividing the maximum load applied to the specimen during the test by the cross-sectional area, calculated from the mean dimensions of the section, and expressed to the nearest kg/cm^2. The average compressive strength of three samples is taken as the representative of the batch.

4.3.4 Splitting Tensile Strength of Concrete

The splitting tensile strength of concrete is performed as per the recommendations by IS 516: 2021 (IS 516,2021). The cylindrical specimens of 150 mm in diameter and 300 mm long are used for the test. The procedure for making and curing tension test specimens in respect of sampling of materials, preparation of materials, proportioning, weighing, mixing, workability, compaction, and curing is followed in all respects with the requirements given as per IS 516-2021 (IS 516,2021). Three test specimens at 28 days of age are tested. The mass and dimension of the specimen are noted before testing.

The test is performed using a compression testing machine with cylindrical specimens placed in a centering jig with steel loading pieces. The load is applied without shock and increased continuously at a nominal rate within the range of 1.2 N/ (mm^2/min) to 2.4 N/ (mm^2/min) until failure. The maximum load (P) applied is then recorded. The appearance of concrete and any unusual features in the type of failure is also noted. The splitting tensile strength (f_t) of the specimen is calculated to the nearest 0.05 N/mm^2 using the following formula:

$$f_t = \frac{2P}{\pi l d} \quad \text{..... Eq. (4.6)}$$

Where P = maximum load applied to the specimen (N)

l = Length of the specimen (in mm),

d = Cross-sectional dimension (in mm)

4.3.5 Flexural Strength of Concrete

The flexural strength of concrete is determined as per the code provisions given by IS: 516-2021 (IS 516,2021). The specimens of size 150 mm x 150mm x 700 mm are cast for the flexure test. The procedure of preparation of materials, casting of specimens in the flexure test moulds, and curing is followed as in the case of the compressive strength test. The specimen is supported on two steel rollers of the testing machine which are so mounted that the distance from center to center is 60 cm. The load is applied through two similar rollers mounted at the third point of the supporting spans, which are spaced 20cm center to center.

Test specimens stored in water are tested immediately upon removal from the water whilst they are still in a wet condition. The dimensions of each specimen are noted before testing. The specimen is loaded with the two-point loads in such a way that the load is applied to the uppermost surface as cast in the mould. The axis of the specimen is carefully aligned with the axis of the loading device. The load is applied with a steady incremental rate such that the extreme fiber stress increases at approximately 7-10 kg/cm^2/min. The load is increased till the failure of the specimen, and the maximum load (*P*) causing the failure of the specimen is noted. The fractured faces of the concrete and the failure pattern are carefully examined for any unusual features.

The flexural strength of the concrete specimen is expressed as the modulus of rupture *(f_b)*. The calculation of 'f_b' depends upon the distance *(a)* between the line of fracture and the nearer support measured on the center line of the tensile side of the specimen. Accordingly, 'f_b' is calculated as follows:

$$f_b = \frac{P \times l}{b \times d^2}$$ (When a > 20 cm) …….. Eq. (4.7)

$$f_b = \frac{3P \times a}{b \times d^2}$$ (When a < 20 cm but greater than 17 cm) …….. Eq. (4.8)

If 'a' is less than 17 cm the results of the test are discarded.

Where b = width of the specimen (cm),

d = depth in cm of the specimen at the point of failure (cm),

l = length in cm of the span on which the specimen was supported (cm)

4.3.6 Modulus of elasticity of concrete

The modulus of elasticity of the concrete specimens in compression is determined using the procedure laid down by IS:516-2021 (IS 516,2021). Concrete specimens of 150 mm diameter and 300 mm length are used for the test. The procedure of preparation of materials, casting of specimens, and curing is followed as in the case of the compressive strength test. Three test specimens at 28 days of age are tested to determine the modulus of elasticity.

The average compressive strength of concrete is determined first as preliminary data for the elastic modulus test as per the procedure already discussed in § 4.3.3. To begin with the test, the specimens are removed from the curing tank and immediately

placed in the test apparatus with extensometers provided for the measurement of strain in the specimen for a given stress value. In the first cycle, the load is applied continuously at the rate of 140 kg/cm^2/min. until a stress value equal to (C+5) kg/cm^2 is reached, where C is one-third of the average compressive strength of concrete calculated preliminarily. The load is maintained at the applied stress at least for one minute and then gradually reduced to an average stress of 1.5 kg/cm^2 when the extensometer readings are taken. In the second cycle, the load is applied again until the stress level of (C+1.5) kg/cm^2 is reached. The load is maintained for at least one minute and extensometer readings are taken. The load is again reduced gradually and readings are taken at 1.5 kg/cm^2. The load is applied again in the third cycle and extensometer readings are taken at ten equal increments of stress up to an average stress of (C+1.5) kg/cm^2. If the strain observations in the second and third cycles differ by more than 5 percent, the loading cycle is repeated until the difference in strain between consecutive cycles at (C+1.5) kg/cm^2 does not exceed 5 percent.

The strain values at the various loads in the last two cycles are calculated individually for each extensometer and the results are plotted graphically against the stress. The slope of the straight lines obtained from the plot is found and the average value is determined. This average value nearest to 1.00 kg/cm^2 is recorded as the modulus of elasticity of concrete.

4.3.7 Ultrasonic Pulse Velocity of Concrete

The UPV test on concrete is performed as per the test procedure covered in IS 516 (Part 5):2018 (IS 516(5), 2018). The test works on the principle that, when an ultrasonic pulse is induced into the concrete from a transducer, it undergoes multiple reflections at the boundaries of the different material phases within the concrete. The receiving transducer detects the onset of the longitudinal waves, which is the fastest.

Using the apparatus prescribed in the standard, the ultrasonic pulse is produced in the concrete using a transducer which is held in contact with one surface of the concrete member under test. This pulse of vibration is converted into an electrical signal by the second transducer held in contact with the other surface of the concrete member. Knowing the path length of travel of the pulse (L), the transit time (T) of the pulse is measured

using an electronic timing circuit. The UPV (V) is determined in m/sec by using the formula:

$$V = \frac{L}{T} \text{..... Eq. (4.9)}$$

4.3.8 Sorptivity of concrete

The sorptivity test on concrete specimens is performed as per the procedure covered in ASTM C 1585-20 (ASTM C1585,2020). This test is used to determine the water absorption rate by cement concrete by measuring the increase in the mass of the specimen due to the absorption of water as a function of time when only one surface is exposed to water absorption and all other surfaces are sealed.

The standard test specimens are discs of 100 ± 6 mm diameter and a length of 50 ± 3 mm, obtained by cutting the concrete cylinders at a suitable depth. The tests are performed on at least two specimens to deliver the average value of results. The test specimens are placed in the specimen conditioning chamber at a temperature of 50 ± 2°C and relative humidity of 80 ± 3 % for 3 days. The average diameter of the sample is measured to the nearest 0.1 mm by taking measurements of at least four diameters at the faces exposed to water. Each specimen is then kept inside a separate sealable polyethylene container. The container is stored at 23 ± 2°C for at least 15 days before the start of the absorption procedure. After removal from the storage containers, the side surfaces of the specimen are sealed with a suitable sealant. The face that is not exposed to water is sealed using a plastic sheet. The initial weight of the sealed specimen is measured to the nearest 0.01 g and is recorded as the initial weight for water absorption calculations. The support device meeting the requirements as per standard is placed at the bottom of the pan and the pan is filled with water such that the water level is 1 to 3 mm above the top of the support device constantly throughout the test. The specimen is placed on the support device with the test surface exposed to the water as shown in Fig. 4.3. The time and date of initial contact with water are recorded. To determine the capillary water absorption as a function of time, the weight of the sample is recorded at the time intervals of 60 seconds, 5 mins, 10 mins, 20 mins, 30 mins, and 60 mins, every hour up to 6 hours with tolerances as per standards. The weight is measured to the nearest 0.01 g within 15 seconds of the removal of the sample from the pan.

Using the above observations, the absorption (I) is determined (in mm) using the following formula:

$$I = \frac{w_t}{a \times \rho_w} \quad \text{..... Eq. (4.10)}$$

where, w_t = the change in specimen weight in grams, at the time t,

a = the exposed area of the specimen, in mm^2, and

ρ_w = the density of the water in g/mm^3

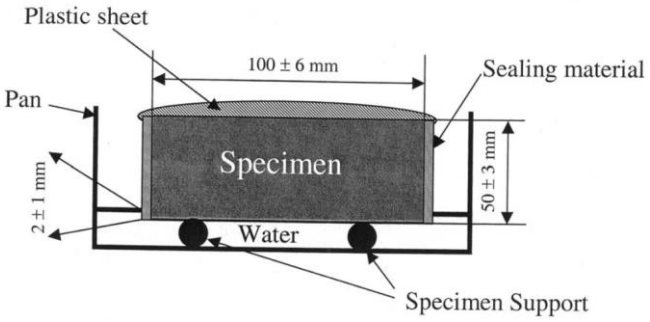

Fig. 4.3 Arrangements for the rate of water absorption test

Absorption I is plotted against the square root of time ($t^{1/2}$). The best-fit line is obtained to this I plotted against the square root of time $t^{1/2}$. The slope of this line is obtained using least squares, linear regression analysis for all points from 1 minute to 6 hours. This slope indicates the initial rate of water absorption of the sample and is recorded as the sorptivity coefficient of the concrete sample in $mm/(hour)^{1/2}$.

4.3.9 Water permeability of concrete

This test is used to determine the depth of penetration of water under pressure in the hardened concrete specimens. The test is performed as per the experimental setup and procedure prescribed in BS EN 12390–8:2019 (EN 12390, 2019). The test involves placing concrete specimens in suitable equipment such that water pressure can be applied on the test surface for a specified period and can be read at all times. The typical test arrangement is shown in Fig. 4.4.

Cubical test specimens of 150 mm size of 28 days curing age are used for the test. The surface to be exposed to the water pressure is roughened with a wire brush immediately after de-moulding the specimen before the curing process. The specimen is placed in the apparatus such that water pressure is applied on the non-trowelled surface.

A water pressure of (500 ± 50) kPa is applied for (72 ± 2) h. Care should be taken to see that no leakage is observed on the faces not exposed to water pressure. The specimen is removed from the apparatus and the face subjected to the water pressure is wiped off to remove excess water. The specimen is split in half, in a direction perpendicular to this face. When the water penetration front is visible, the maximum depth of penetration under the test area is measured and recorded to the nearest millimeter.

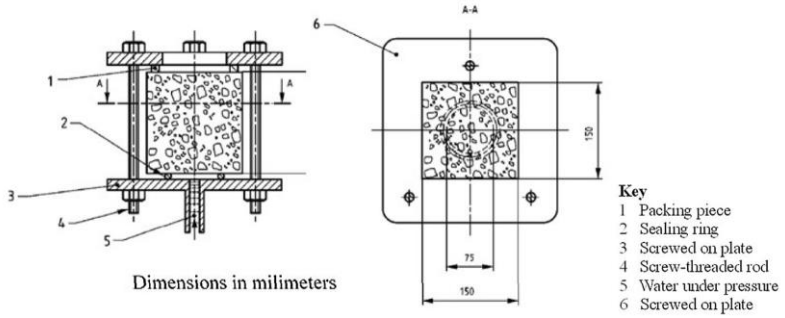

Fig. 4.4 Specimen arrangement for water permeability test (BS EN 12390-8-2019)

4.3.10 Chloride migration coefficient of concrete

The chloride migration coefficient of concrete is obtained from non-steady-state migration experiments as per NT Build 492 (NT Build, 492). The chloride migration coefficient is a measure of the resistance of the tested material to chloride penetration. The test is based on the principle that the application of an external electrical potential across the specimen forces the chloride ions outside to migrate into the specimen. Axially splitting the specimen and spraying a silver nitrate solution on the split sections enable the measurement of chloride penetration depth due to the visible white silver nitrate solution.

Three cylindrical specimens with a diameter of 100mm and a thickness of 50 mm, sliced from cast cylinders with a minimum length of 200 mm are used for the test. Each test specimen is prepared by first cutting the cylinder into two halves (i.e., into two Ø100 × 100 mm cylinders), and then cutting a 50 ± 2 mm thick slice from one half. The end surface that is nearer to the cut i.e., the middle surface is the one to be exposed to the chloride solution (catholyte). The thickness of each specimen is measured with a slide caliper to an accuracy of 0.1mm. The specimens are brushed and washed to remove any burrs from the surfaces and the excess water is wiped off to make the surface dry. They

are placed in the vacuum container for vacuum treatment with the exposed end surfaces. The vacuum is maintained for three hours and the container is filled with saturated $Ca(OH)_2$ solution to immerse all the specimens. After another hour of vacuum treatment, the air is allowed to re-enter the container. The specimens are kept in the solution for further 18 ± 2 hours.

The catholyte reservoir is filled with about 12 litres of 10 % NaCl solution. The rubber sleeve is fitted on the specimen and it is secured with two clamps (see Fig. 4.5). If the curved surface of the specimen is not smooth, or there are defects on the curved surface a line of silicone sealant is applied to improve the tightness to prevent leakages.

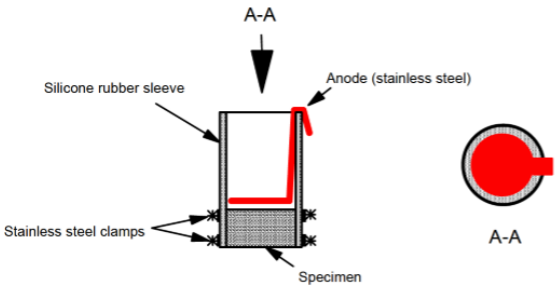

Fig. 4.5 Rubber sleeve assembled with specimen, clamps, and anode

The specimen is placed on the plastic support in the catholyte reservoir as shown in Fig.4.6. The sleeve above the specimen is filled with 300 ml anolyte solution (0.3 M NaOH) and the anode is immersed in the anolyte solution. The cathode is connected to the negative pole and the anode is connected to the positive pole of the power supply. The voltage is preset at 30 V, and the initial current through each specimen is recorded. The initial temperature is recorded in each anolyte solution, as shown by the thermometer or thermocouple. According to the initial current an appropriate test duration is chosen as per guidelines. The final current and temperature are recorded before concluding the test. To measure the chloride penetration depth, the specimen is disassembled, rinsed with tap water, and split axially into two pieces. 0.1 M silver nitrate solution is sprayed onto the freshly split sections. After about 15 minutes, when the white silver chloride precipitation on the split surface is visible, the penetration depth is measured, from the center to both edges at intervals of 10 mm to obtain seven depths. The depth is measured to an accuracy of 0.1 mm.

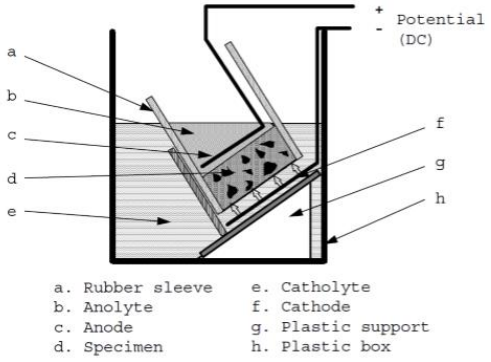

Fig. 4.6 Specimen placement for Chloride migration test

The non-steady state migration coefficient is obtained using the following equation:

$$D_{nssm} = \frac{0.0239(273+T)L}{(U-2)t}\left\{X_d - 0.0238\sqrt{\frac{(273+T)L\,X_d}{U-2}}\right\} \quad \text{..... Eq. (4.11)}$$

Where, D_{nssm}: non-steady-state migration coefficient, $\times 10^{-12}$ m^2/s;

U: absolute value of the applied voltage, V;

T: average value of the initial and final temperatures in the anolyte solution, °C;

L: thickness of the specimen, mm;

X_d: average value of the penetration depths, mm;

t: test duration, hour.

4.3.11 Resistance of Concrete to elevated temperature

The effect of elevated temperature on concrete containing PWA in the current study was studied by the determination of residual compressive strength characteristics of concrete after subjecting the specimens to elevated temperatures.

Cubic concrete specimens of 100 mm size were used for the test that were cast and cured for 28 days as per the standard procedure by IS 516-2021 (IS 516, 2021). A muffle furnace with a maximum temperature of 1200ºC was used to conduct the test. Three representative concrete cube specimens from each batch were chosen. The cubes were subjected to temperatures of 200°C, 400°C and 600°C in the muffle furnace with the rate of increase in temperature as 5°C/min. On reaching the expected temperature, each specimen was kept at that temperature for a period of 60 minutes. After removal from the furnace, the specimens were air-cooled in the laboratory atmosphere for 24 hours

before testing for residual properties. Subsequently, the compressive strength of the samples was determined as per the procedure described in § 4.3.3.

4.4 Sustainability assessment using LCA

As per ISO 14040, Life Cycle Assessment (LCA) is defined as the "compilation and evaluation of the inputs, outputs and the potential environmental impacts of a product system throughout its life cycle". LCA is also defined as the "consecutive and interlinked stages of a product system, from raw materials acquisition or generation from natural resources to final disposition" (ISO 14040, 2006). It is a well-appreciated holistic method adopted in sustainability assessment. This method is very popular in the environmental assessment of the construction products like concrete in which the life cycle can be subdivided into small unit processes from the raw material extraction to the final disposal after its useful life (Colangelo et al., 2018a; X. Li et al., 2010; Ortiz et al., 2009; Vieira et al., 2016).

The ISO 14040 (2006) and ISO 14044 (2006) standard defines the methodology of LCA in four systematic and well-defined phases (ISO 14040, 2006; ISO 14044, 2006). These four phases are interlinked and interdependent as shown in Fig. 4.7 and discussed in detail in the following sections. These phases include:

1) Goal and scope definition – It involves the definition and description of the product, process, or activity to be assessed. It also involves the establishment of the objective and the context as well identification of boundaries in which the assessment is to be made;
2) Inventory analysis– It involves the identification and quantification of the energy and raw material inputs of the process;
3) Impact assessment- It involves the assessment of human and ecological impacts of the usage of energy and raw materials as identified in the inventory analysis and
4) Interpretation- It involves the evaluation of the results of inventory analysis and the establishment of the relationship between the process flows and the environmental impacts.

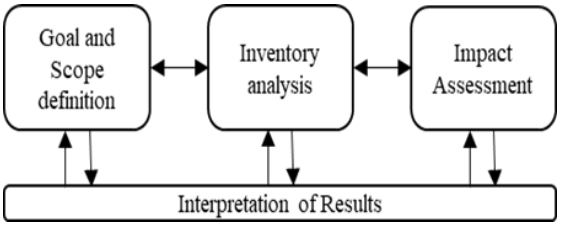

Fig. 4.7 Methodology of LCA (ISO 14040, 2006)

4.4.1 Goal and Scope Definition

Goal and scope definition involves two important tasks defining the FU of assessment and establishing the system boundary (Marinkovic 2013).

The FU is the key parameter in the assessment of the quantification of environmental impact as it allows the comparative analysis of two products on functional equivalence. It provides the basis for the quantification of all input and output data for the given product or process (Panesar et al. 2017). In the case of concrete, the simplest and the basic FU is the unit volume or unit mass. However, consideration of unit volume or unit mass as the sole FU may not yield logical results when a comparative analysis of concretes containing different mix proportions, especially variable binder contents, is analyzed. Therefore, the incorporation of functional parameter/s like strength and/or durability in addition to the basic FU, in other words, the use of a complex FU is desired for comparative environmental assessments of concretes with diverse material composition as in the case of the current study. It also implies that the selection of different functional units for the same concrete shall deliver different outcomes of LCA (Reap et al. 2008).

Similarly, the establishment of system boundary is also an important task in the LCA of any product. In the life cycle of a typical product like concrete, there are a series of unit processes from the extraction of raw materials to the disposal or reuse of concrete after its useful service life. Although it is possible to consider the entire life cycle of concrete for LCA, the methodology offers the flexibility of exclusion of some phases of the life cycle depending on the scope and objective of the analysis. Therefore, the decision regarding which life cycle process/es of concrete is/are to be included in or excluded from the analysis is an important aspect of the LCA of concrete. This decision defines the

system boundary for the analysis. To have uniformity in consideration of system boundary, the life cycle of concrete is divided into three prominent phases:

1) Cradle-to-gate phase- This phase includes the manufacturing phase of concrete. It includes material and energy inputs related to the extraction, processing, and transportation of basic raw materials from the source to the batching plant and the manufacturing process of concrete in the concrete-making plant.
2) Gate to grave phase- This phase includes the activities related to the life span of concrete from its manufacture at the concrete plant to its end-of-life destination in a disposal site or recycling unit after the useful service life. Thus, it includes the transportation and placing of ready concrete for the intended use at the site, its application, maintenance, repairs, replacement, and refurbishment during its useful service life, and the post-service life stages i.e., demolition of concrete, transportation of debris to the disposal site or the recycling units.
3) Grave to cradle phase- This phase includes the activities related to processing the demolished concrete for the reuse and recovery of the material for recycling.

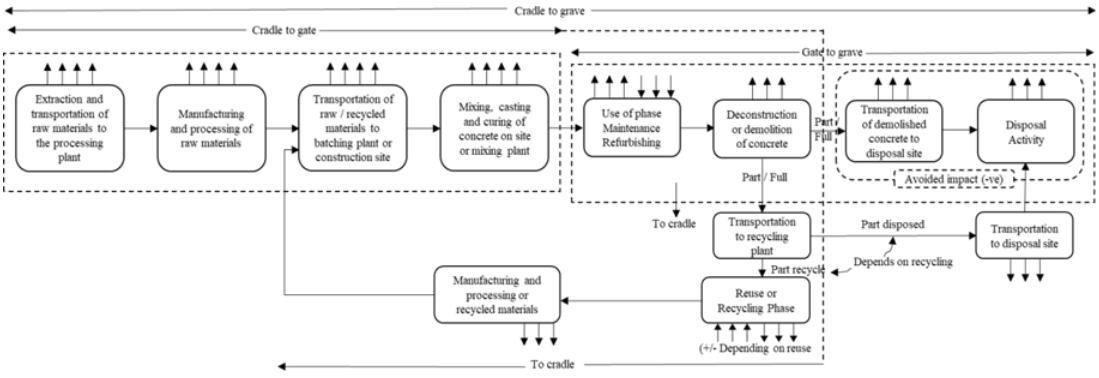

Fig. 4.8 Flow diagram showing life cycle phases of concrete and system boundaries

One or more of these three prominent phases may form part of the system boundary of the LCA of concrete. Accordingly, the three most generalized system boundaries namely, ‘cradle to gate’, ‘cradle to grave’, and ‘cradle-to-cradle system boundaries are widely accepted in LCA exercise. The flow diagram of the concrete life cycle in Fig. 4.8 shows the process demarcation of these three system boundaries. The selection of a system boundary for LCA is mostly indicated on such a flow diagram by enclosing the processes included in the analysis in a closed boundary. The other processes

are kept outside the enclosed area as they are not included in the domain of the goal and scope of LCA analysis (Silvestre et al. 2014).

4.4.2 Life cycle inventory (LCI)

This is the foundational step for any assessment of the environmental impacts of a product. This phase identifies and quantifies every input or output of materials or energy included within the system boundary. The primary objective of this phase is the collection of high-quality data. It involves the development of a methodology for data collection. This methodology includes the establishment of data quality objectives based on the objectives of the LCA, identification of sources of data (literature, industry, government database, etc.), creation of a methodology for management of poor quality or missing data, and compilation of data for the product, process or activity being analyzed (Seto, 2015). It is noteworthy that the LCA of any material is influenced by local conditions but the life cycle inventory of that material is a global database (Anastasiou et al., 2017). LCI aims at describing product-specific and impact-specific parameters required for a holistic LCA study. A comprehensive, broad, and credible LCI, thus determines the credibility of the LCA of any product (Petek Gursel et al. 2014).

It is evident from the aforesaid discussions that the LCI of any product is an assimilation of the LCI of all the raw materials which go into making the product. If these materials are used in their primary life, their LCI can be very well defined considering all the phases of the life cycle of the materials. However, if any material is consumed in its secondary lifespan i.e., after exhausting its primary useful service life, there arise questions about whether to consider the primary life or the secondary life processes in data assimilation of LCI. This dilemma is quite common in the case of green concrete products which aim at the utilization of waste materials or byproducts from the industrial sector inside the concrete. E.g., SCM like FLA is a byproduct from the combustion of coal in the production of electricity. So, when FLA is used in concrete mixes, the LCI of FLA demands the decision about whether to allocate environmental impact from electricity production to FLA or consider it as waste without any allocation of environmental impact. Furthermore, if it is decided to allocate the upstream impacts of coal combustion to the products in downstream chain links i.e., electricity and FLA, the methodology also demands the determination of the ratio in which these impacts shall be

distributed. This process of the distribution of impacts in a multifunctional process to the products and byproducts on the downstream chain link is called allocation (Chen et al., 2010; Seto et al., 2017). The impact allocated to the byproduct is a fraction of the total impact associated with the primary process from which it is generated. This fraction of impact is called the allocation coefficient. The allocation coefficient depends on the modes of allocation as listed below:

1) No allocation- In this mode of allocation, the byproduct is considered as a total waste without any allotment of impact from the primary process and thus, the allocation coefficient is considered zero.

2) Mass allocation- In this mode of allocation, the impact from the upstream is allocated to the main product and byproduct in the ratio of their masses. Therefore, the mass allocation coefficient is the ratio of the mass of the byproduct to the total mass of the main product and byproduct.

3) Economic allocation- In this mode of allocation, the impact from the upstream is allocated to the main product and byproduct in the ratio of their economic values or revenues. Therefore, the economic allocation coefficient is the ratio of the economic value of the byproduct to the total economic value of the main product and byproduct (Chen et al., 2010; S. Marinković et al., 2017).

4.4.3 Life Cycle Impact Assessment (LCIA)

This phase of LCA aims at the evaluation of potential human health and environmental impacts resulting from various inputs and outputs identified in the LCI of the product. As per ISO 14044 (2006), LCIA involves two mandatory steps, namely selection, and classification of impact categories and characterization (ISO 14044, 2006). The selection and classification of the impact category aim at defining the environmental impacts by their impact pathway and an impact indicator. The characterization aims at quantitative modeling of each impact in terms of impact score with a common unit to all contributions for that particular impact category (ILCD, 2010). Global warming potential (GWP), Acidification potential (AP), Abiotic depletion potential (ADP), Eutrophication potential (EP), Cumulative energy demand (CED), Ozone depletion potential (ODP), Photochemical oxidant creation potential (POCP), Human Health (HH), Toxicity

Potential (TP), Ecosystem Depletion (ECO) and Resource Depletion (RD) are the some of the core impact categories and indicators listed in European standard EN 15804 (2012) (EN 15804, 2012).

The LCIA also allows the choice of impact assessment methods. These methods are categorized as problem-oriented methods and damage-oriented methods. In the problem-oriented method, the impacts caused by each process in the flow line are simply grouped based on certain environmental problems. In this method, the impact category indicator lies between life cycle inventory results and the category endpoint. So, it is the quantification of category indicators but not an indicator of actual environmental damage. Thus, they are also called midpoint impacts. On the other hand, the damage-oriented method carries the calculation further to quantify actual damage caused to the environment or human beings. These impacts are also called endpoint impacts. E.g., the emission of GHG causes climate change problems. In the case of the problem-oriented method or midpoint impact method, this greenhouse gas impact is quantified in terms of GWP value (in kg-CO_2 eq). To express these impacts in terms of the damage-oriented method, the impact is further extended to quantify damage to human health in terms of disability-adjusted life years (DALYs) or damage to the ecosystem in terms of the extinction rate of species (SPECIES.YR) (Blankendaal et al. 2014; Van den Heede and De Belie 2017; Rybaczewska-Blażejowska and Palekhov 2018).

Table 4.1 Frequently used LCIA methodologies (Source: ILCD, 2010)

LCIA Methodology	Approach	Web Access	Country of origin
CML 2002	Midpoint	http://www.leidenuniv.nl/cml/ssp/projects/lca2/lca2.html	Netherlands
IPCC 2007	Midpoint	http://www.ipcc.ch/publications_and_data/publications_and_data.htm	United Kingdom
Eco-indicator 99	Endpoint	www.pre.nl/eco-indicator99	Netherlands
Impact 2002+	Midpoint and Endpoint	http://www.sph.umich.edu/riskcenter/jolliet/index.htm	Switzerland
TRACI	Midpoint	http://www.epa.gov/ORD/NRMRL/std/sab/traci/	USA
ReCipe	Midpoint and Endpoint	www.lcia-recipe.net	Netherlands
Ecopoints 2006	Endpoint	http://www.e2mc.com/BUWAL297%20english.pdf	Switzerland

The life cycle impact assessment methodologies are developed in different countries with these midpoints and/or endpoint approaches. The various methodologies all over the globe are presented in the Manual ‘‘Analysis of Existing EI Assessment Methodologies for Use in Life Cycle Assessment (LCA)” (ILCD, 2010). Table 4.1 provides the details of the most frequently used LCIA methodologies with details regarding country of origin, source, and web access details.

4.4.4 Interpretation of Results

This is the final step of the LCA of any product. The key objective is to evaluate the results obtained from the analysis concerning completeness, consistency, and sensitivity (Josa et al., 2005; Koroneos and Th Dompros, 2009; Seto, 2015).

4.5 Procedure for Environmental impact calculation

Irrespective of the selection of system boundary, the environmental impact per unit of volume cement composite, considering all phases of its life cycle can be given by equation (4.12):

$$Net\ EI = EI_{raw\ materials} + EI_{transport} + EI_{production} + EI_{maintenance+use} + EI_{demolition} + EI_{disposal} + EI_{recycling\ process} - EI_{avoided\ impacts}$$

…… Eq. (4.12)

The environmental impact of each of these processes/activities can be calculated as follows:

The impact of all the raw materials[a] utilized in the manufacturing of the composite can be estimated using equation (4.13).

$$EI_{raw\ materials} = \sum [Q_i \times (E_{RM})_i] \quad (i = 1, 2, 3 \ldots N \text{ for all the raw materials})$$

…… Eq. (4.13)

[[a]The Society of Environmental Toxicology and Chemistry (SETAC) provides the guidelines for the consideration of material inputs to a process. The raw material is excluded from material inputs if 1) The material accounts for less than 1% of the total mass of the product, 2) The material does not consume significant energy, and 3) The material does not contribute to any toxic emissions (SETAC, 1993). These guidelines permit the exclusion of process inputs like admixtures from the analysis(Faleschini et al. 2014).]

Where Q is the quantity of each raw material per unit volume of the composite and E_{RM} is the emission factor[b] for a given impact category per unit quantity of corresponding raw material.

The total emission resulting from transportation for various activities in the concrete cycle can be obtained using equation (4.14).

$$EI_{transport} = EI_{RM-TR} + EI_{CT-TR} + EI_{DC-TR} + EI_{RC-TR} \quad \text{..... Eq. (4.14)}$$

Where EI_{RM-TR} = Total Impact due to the transportation of all the raw materials to the batching plant,

EI_{CT-TR} = Total Impact due to the transportation of manufactured composite to the placement site,

EI_{DC-TR} = Total Impact due to the transportation of demolished concrete to the disposal site or recycling plant, *and*

EI_{RC-TR} = Total Impact due to the transportation of RAC to batching plant in case of the cradle-to-cradle system boundary.

The total impact due to the transport of raw materials, demolished concrete, and RAC can be estimated using equation (4.15).

$$EI_{RM-TR/DC-TR/RC-TR} = \sum [Q_j \times D_j \times (E_{TR})_j] \quad \text{..... Eq. (4.15)}$$

(j=1, 2, 3...N for the raw materials, demolished concrete, disposable concrete, RAC, etc.)

Where Q is the quantity of each material per unit volume of composite, D is the distance transported (km) and E_{TR} is the impact factor per unit quantity of raw material per unit distance (unit/t.km) which depends upon the transportation equipment used for the corresponding materials.

The total impact from the transportation of manufactured concrete to the placement site is mostly estimated relative to the density of concrete as indicated in equation (4.16).

$$EI_{CT-TR} = \delta_{CT} \times D_{CT} \times E_{TR} \quad \text{..... Eq. (4.16)}$$

[b The allocation of impact for the byproducts from a primary process as discussed in § 4.4.2 is done at this stage of analysis by considering the allocation coefficient from the primary process.]

Where δ_{CT} is the density of the composite, D_{CT} is the transportation distance to the placement site, and E_{TR} is the impact factor (unit/t.km) which depends upon the transportation equipment.

The manufacturing activity of the composite, maintenance activities during the use phase, demolition activity, disposal process, and/or recycling phases are all energy-consuming phases. The environmental impact for all these phases is directly proportional to the quantified amount of energy source (fuel and/or power) consumed in carrying out each process per unit volume of the composite. The impact of these phases can be calculated using equation (4.17):

$$EI_{production/maintenance\ /demolition/recycling} = \sum [P_k \times (E_p)_k] \quad \text{..... Eq. (4.17)}$$

(k= 1, 2, 3....N for the energy sources used for the corresponding process like electricity, fuel, etc.)

Where P is the quantified consumption of energy from the used source per unit volume of concrete (E.g., kWh of electricity or litres of oil per unit volume) and Ep is the impact factor per unit energy consumption (unit /kWh of electricity or unit impact/litre of Oil)

Any material consumption during the use phase for maintenance, repairs, or refurbishment should be analyzed for its impact and accounted for per unit volume of the repaired composite.

Finally, the avoided impacts due to recycling if any should be determined depending upon energy consumption for processing and transportation of the recycled volume of the composites which otherwise would have been disposed of in landfills.

4.5.1 Databases and Software

From the methodical procedure of estimation of environmental impact for a given system boundary of the life cycle of a product, it is clear that the quantification of material and energy inputs is an essential requirement. These material quantities and energy inputs are then multiplied by the respective impact factor for the material and energy consumed to obtain the total environmental impact for the given category. To obtain reliable results, the value of the impact factors is a key factor in the LCA process. The determination of these impact factors for each input is a complex and laborious process (Vieira et al. 2016).

Considerable efforts have been put to develop databases of such impact factors for a particular process in the life cycle of concrete. Although these databases are in a regional context, they may be used on a global scale to get a sufficient idea of the impact of a process. These databases have also paved a path for the development of software tools for impact assessment. The details about the most common databases with their regional context and software tools using the database are presented in Table 4.2. These tools are facilitating an efficient and less time-consuming analysis (Ding, 2008; Martínez et al., 2015). These software tools are well-equipped to generate the results of LCA in tabular formats along with graphical presentations. The Ecoinvent database is the most popularly used and internationally accepted database for the LCA of concrete (Marinković et al., 2013).

Table 4.2 Databases and software tools for LCA
{Sources:(Khasreen et al. 2009; Vieira et al. 2016)}

Database	Software tool	Web Access	Country
Bath data	x	People.bath.ac.uk/cj219	UK
Bousted	Boustead	www.boustead-consulting.co.uk	UK
Ecoinvent	x	www.pre.nl/ecoinvent	Switzerland
x	Ecoit	www.pre.nl	Netherlands
ELCD	x	http://lca.jrc.eceuropa.eu	EU
GaBi	GaBi	www.gabi-software.com	Germany
GEMIS	GEMIS	http://www.oeko.de/service/gemis/en/	Germany
JEMAI	JEMAI	www.jemai.or.jp/english/index.cfm	Japan
SimaPro	SimaPro	www.pre.nl	Netherlands
Spin	x	http://195.215.251.229/Dotnetnuke/	Sweden
TEAM	TEAM	www.ecobilan.com	France
Umberto	Umberto	www.umberto.de	Germany
USLCI data	x	www.nrel.gov/lci	USA

Chapter 5

Test Results and Discussions

5.1 Introduction

Various laboratory tests were conducted to understand the rheological, physical, mechanical, and durability-related properties of cement mortar and concrete mixes proposed in the current research. The mix proportions for the cement composites and the experimental procedures followed for the performance of the tests as per relevant standards are already discussed in Chapter 4. This chapter exclusively deals with the results of the laboratory tests on mortar and concrete mixes. Elaborative discussions on the performance characteristics of the composites have been presented for each performance indicator. The results obtained from the experimental investigations have been validated with the findings in the literature.

5.2 Workability of Mortar and Concrete

Workability is the relative ease or difficulty of placing and consolidating a cementitious mix. It is directly related to the stiffness and homogeneity of the mix. It also refers to the consistency and compaction characteristics of the composites, which are vital for the potential strength and durability of concrete. In the current research, the workability of fresh mortar and fresh concrete is determined in terms of flow and slump values, respectively.

5.2.1 Workability of Cement Mortar

The workability of the mortar mixes of different mix proportions in terms of flow values is presented in Table 5.1. The baseline mixes with no PET sand for 1:3 and 1:5 mix proportions are prepared with flow values of 160-170 mm to have a noticeable variation in flow value after subsequent incremental substitution of PET-Sand. The mix containing 100% N-Sand as fine aggregate is considered the control mix for all purposes. Fig. 5.1 exhibits the variation of flow values for different mortar mixes with the substitution of PET-Sand.

Table 5.1 Workability (flow value) of mortar mixes

Identification	1:3 mix		1:5 mix	
	Flow	± Δ%*	Flow	± Δ%*
Control Mix (OPC/N-Sand)				
M_x-C-P0	180	0	175	0
Tier I Mortar (OPC/N-Sand+PET-Sand)				
M_x-C-P10	170	-5.60	160	-8.60
M_x-C-P15	155	-13.90	150	-14.30
M_x-C-P20	150	-16.70	140	-20.00
M_x-C-P25	140	-22.20	120	-31.40
Tier II mortar (OPC/N-Sand+SFS-Sand+PET-Sand)				
M_x-C-SP0	190	+5.60	185	+5.70
M_x-C-SP10	180	0.00	170	-2.90
M_x-C-SP15	175	-2.80	155	-11.40
M_x-C-SP20	160	-11.10	145	-17.10
M_x-C-SP25	150	-16.70	130	-25.70
Tier III mortar (OPC+FLA/N-Sand+SFS-Sand+PET-Sand)				
M_x-CF-SP0	205	+13.90	200	+14.30
M_x-CF-SP10	195	+8.30	180	+2.90
M_x-CF-SP15	190	+5.60	165	-5.70
M_x-CF-SP20	170	-5.60	145	-17.10
M_x-CF-SP25	160	-11.10	140	-20.00

(x=3 for 1:3 mix and x=5 for 1:5 mix)
(*Negative value indicates a decrease in slump relative to control mix)

5.2.2 Workability of Cement Concrete

The measure of the workability or consistency of concrete is its slump. The slump flow test is the simplest and most widely used test. Slump value is a design consideration that is inversely proportional to the stiffness of the mix (Saikia and De Brito, 2012). The slump value is necessary for the design of the concrete mix and it is the counterpoint of the mixture hardness. The straightforward correlation - the higher the slump flow value, the greater its ability to fill formwork under its weight - makes it very easy to use and interpret the results.

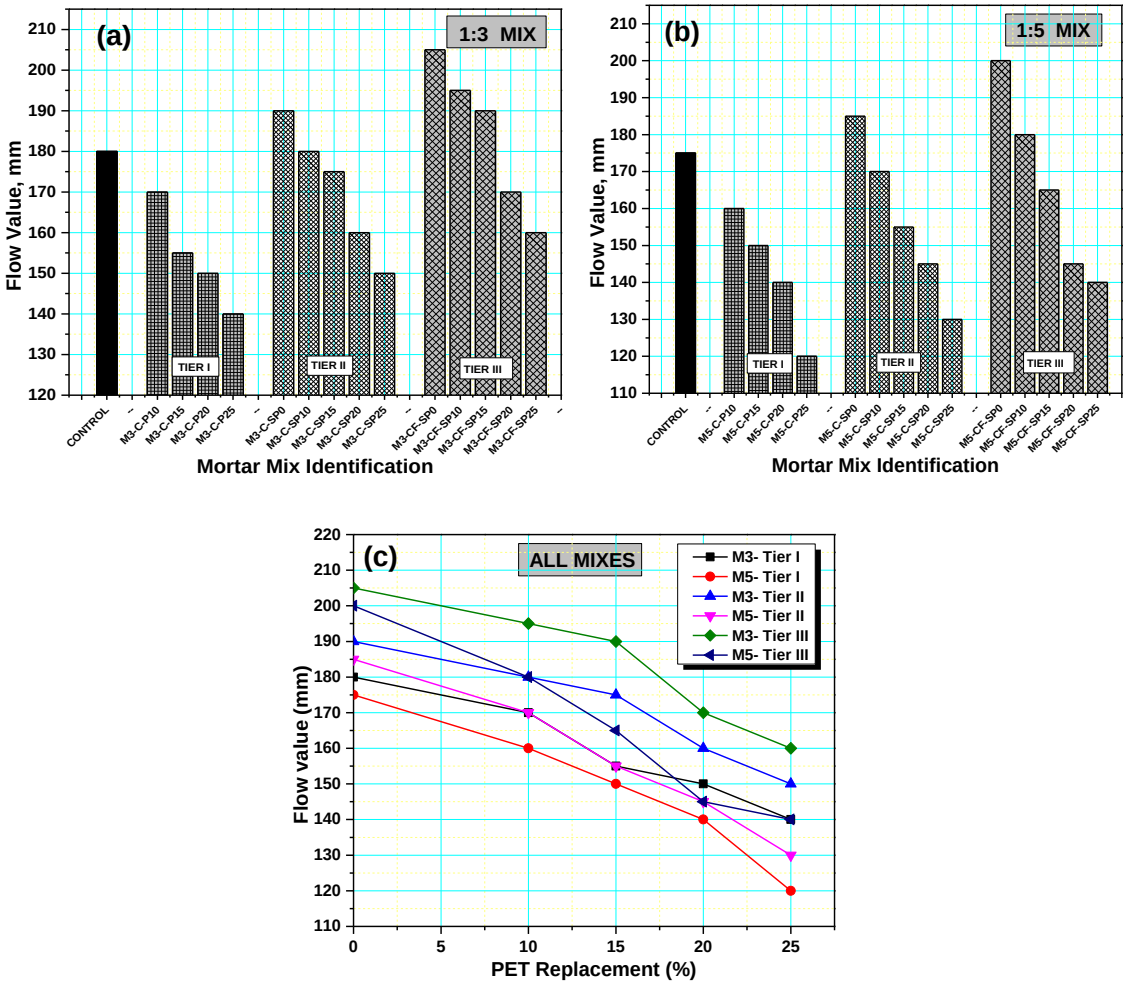

Fig. 5.1 Flow values of mortar mix (a) 1:3 mix (b) 1:5 mix (c) All mortar mixes

The slump values for various concrete mixes tested in the current research are summarized in Table 5.2. The variations in the consistency of the mixes with the increase in PET-Sand content and the positive effect of the use of SFS-Sand and FLA are evident from the graphical presentation of slump values in Fig. 5.2.

5.2.3 Discussions

The flow values of mortar mixes and the slump values of the concrete mixes for all proportions provide sufficient evidence to claim that the fluidity or workability of the composites decreases with an increase in PET content.

The results showed that the workability of Tier I mixes for mortar and concrete mixes decreased by 22% to 33% for a replacement of 25% of N-sand by PET-Sand, the loss being more in concrete mixes than the mortar mixes. The loss in workability of the

composites with the increase in PET-Sand is attributed to the increased internal friction between the PET particles and the binder paste (Ferreira et al. 2012). This is because of the angular and non-uniform shape of the PET particles. Such mercenary shapes of particles have a higher specific surface area demanding more cement paste for lubrication in comparison with N-sand units which they replace (Ismail and AL-Hashmi, 2008; Rahmani et al., 2013; Saikia and De Brito, 2014; R. Saxena et al., 2020). Nibudey et al. (2013) have stated that the presence of PET particles with an aspect ratio higher than 50 causes a pronounced negative effect on workability and in the current research, more than 45% of particles are coarser than 600µ size increasing the possibility of a considerable amount of PET particles having an aspect ratio in that range (Nibudey et al., 2013).

Table 5.2 Workability (Slump) values for concrete mixes

Identification	M30 mix		M50 mix	
	Slump	± Δ%*	Slump	± Δ%*
Control Mix (OPC/N-Sand)				
C_Y-C-P0	170	0.00	175	0.00
Tier I Concrete (OPC/ N-Sand+PET-Sand)				
C_Y-C-P10	155	-8.80	175	0.00
C_Y-C-P15	140	-17.60	170	-2.90
C_Y-C-P20	125	-26.50	155	-11.40
C_Y-C-P25	115	-32.40	135	-22.90
Tier II Concrete (OPC/N-Sand+SFS-Sand+PET-Sand)				
C_Y-C-SP0	175	+2.90	185	+5.70
C_Y-C-SP10	165	-2.90	180	+2.90
C_Y-C-SP15	150	-11.80	170	-2.90
C_Y-C-SP20	135	-20.60	160	-8.60
C_Y-C-SP25	120	-29.40	140	-20.00
Tier III Concrete (OPC+FLA/N-Sand+SFS-Sand+PET-Sand)				
C_Y-CF-SP0	180	+5.90	200	+14.30
C_Y-CF-SP10	175	+2.90	190	+8.60
C_Y-CF-SP15	155	-8.80	180	+2.90
C_Y-CF-SP20	140	-17.60	175	0.00
C_Y-CF-SP25	130	-23.50	150	-14.30

($_Y$=30 for M30 mix, $_Y$=50 for M50 mix)
(*Negative value indicates a decrease in slump relative to control mix)

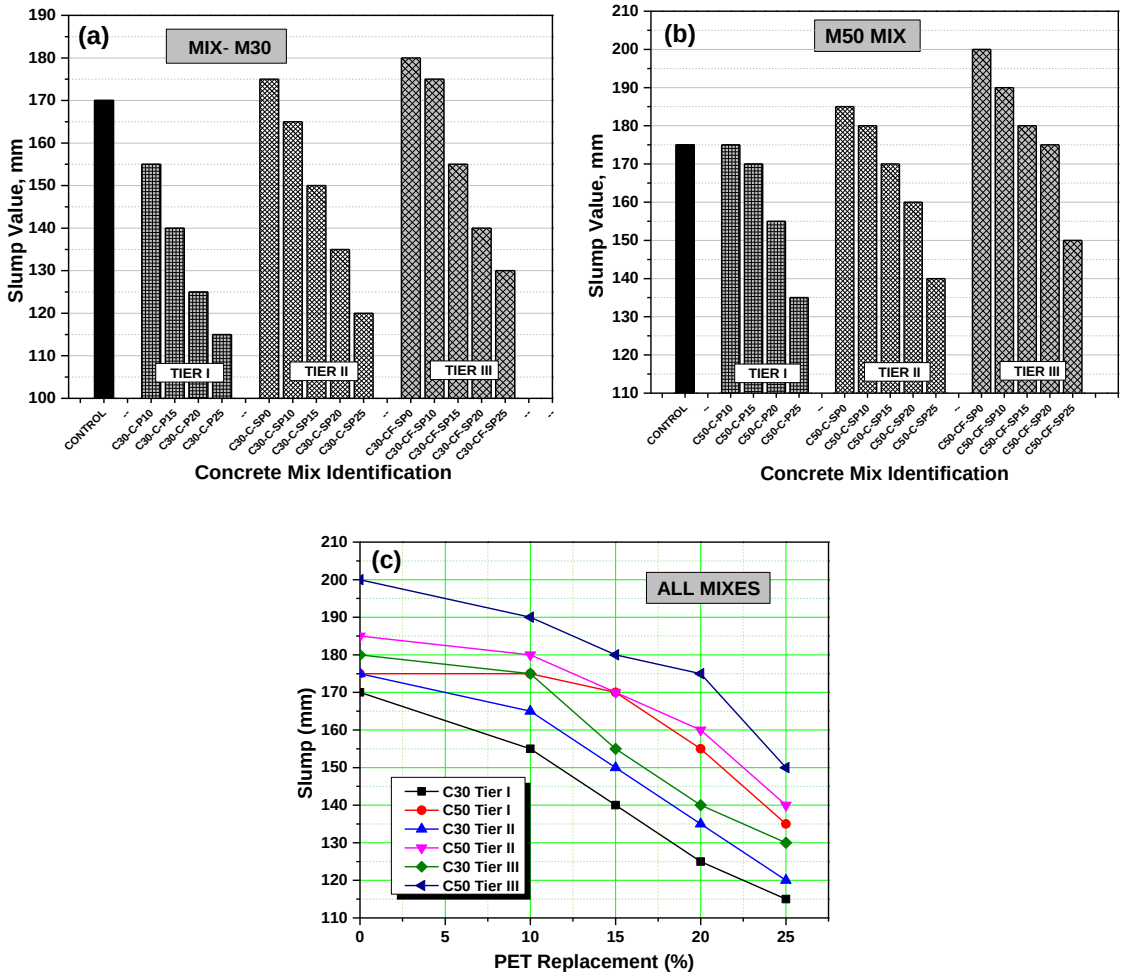

Fig. 5.2 Workability (Slump) values for Concrete mixes (a) M30 mix (b) M50 mix (c) All mixes

The results also reveal that leaner mixes show a higher loss in workability than richer mixes. This is attributed to a lower cement-to-aggregate ratio and consequently lower paste intensity in the leaner mix. This observation also reflects the adverse effects of an increase in the water-cement ratio on the flow ability of the concrete mixes. This can be appreciated from the fact that the M30 mix having a w/c of 0.44 shows a higher slump loss than the M50 mix having a w/c of 0.39. When the w/c is higher, the excess water in the mix is not absorbed by PET particles due to their hydrophobic nature, unlike N-Sand. Therefore, the water content of the blend is not reduced. As the cement paste is not in direct contact with PET particles, the water film around each particle entraps air which is detrimental to the flow ability of the mix. This additional water which does not participate in the cement hydration process increases the porosity, and therefore, reduces the workability of the mix. This observation is in agreement with the findings by Albano

et al. (2009). Rahmani et al. (2013) also presented a similar effect of the PET content and w/c on the flow characteristics of concrete. The authors showed that there is a 40% decrease in slump value for the 20% substitution of N-sand by PET.

The addition of SFS-Sand as fine aggregate in the mix affected an increase in the workability to the extent of 6% higher than the baseline mix for mortar and concrete in Tier II mixes. This effect is attributed to the smooth and glassy surface texture of SFS-Sand which offered a better lubricating effect inside the mix. This effect was also complimented by the low water absorption by the SFS particles providing more water for better mobility of the mix. The higher density of SFS aggregates is also considered a contributing factor in the increase of flow ability of the mixes (Gencel et al. 2012).

The addition of FLA as an SCM enhanced the workability of the mixes as exhibited by the results of Tier III mixes of mortar and concrete. This behavior is due to the spherical shape of FLA particles, already been confirmed by SEM results in material characterization studies. These particles reduce the internal friction inside the matrix by the ball-bearing effect. Also, the use of FLA to replace OPC by weight proportions results in an increase in the paste volume of the binder as the specific weight of FLA is lower than OPC. This causes better pore filling inside the mix facilitating the better flow of the mix (Akcaözoglu and Atis, 2011). Tier III mixes exhibit a combined effect of SFS slag and FLA on the workability of the composites. The results reveal that the incorporation of SFS-Sand and FLA could control the loss in workability due to the incorporation of PET-Sand. The mixes having 10-15% volume of PET-Sand exhibited workability similar to the control mix. At higher incorporation levels of PET-Sand, the workability loss was minimized to the extent of 8-11% in comparison to Tier I mixes with conventional materials i.e., OPC and N-Sand.

The results of all three tiers confirm the trend of a decrease in workability of the composites with the increase in plastic content in the mix. It is expected that the free water content of the mix would increase due to low absorption values of PET-Sand and SFS-Sand in comparison to N-Sand that is replaced. This free water does not necessarily contribute to the improvement in workability due to the non-uniform and mercenary shapes of PET-Sand. In addition to the increase in their surface area, the random orientations of these sharp-edged particles introduce locking effects inducing resistance

to the flow of the mass. This effect is more prominent for the mixes with higher plastic contents. Furthermore, the air entrapped around the PET particles due to their hydrophobic nature contributes to this resistance to flow leading to substantial decrease in workability at higher replacement ratios.

5.3 Bulk density of mortar and concrete

Density is one of the important parameters, which can control many physical properties in cement composites and it is mainly controlled by the amount and density of aggregate inside the mixes (Kan and Demirboğa, 2009a). It is quite obvious that, if any of the natural aggregates in concrete is replaced with any alternative aggregate having a specific weight different from that of natural aggregate, it would substantially alter the overall density of the mix, for the primary reason that aggregates occupy major volumes inside the cementitious mixes. The current study incorporates PET wastes having a specific weight of 48% of the natural aggregate it replaces. Therefore, this variation in the specific weight is expected to have a significant effect on the density of the mixes.

The bulk density of mortar and concrete mixes for different mix proportions in different tiers as proposed in the methodology of research was determined in the fresh state immediately after making concrete as well as the hardened state after 28 days of water curing. The incorporation of PET-Sand in conventional mixes and novel mixes with SFS-Sand showed a significant effect on the density of mortar and concrete samples.

5.3.1 Bulk density of mortar

The density of the mortar in the fresh state and hardened state after 28 days of curing are tabulated in Table 5.3. The variations in these density values with the increased substitution of PET-Sand and for all three tiers of the mixes are presented in Fig. 5.3 and 5.4. It can be concluded that there is a decrease in the density of the mortar with the increase in PET content inside the mix. For OPC mortars with N-Sand, a replacement of 25% N-sand by PET caused a decrease of 11% in the density values of the mortar. As observed in Tier II mixes, the use of SFS-Sand compensated for the decrease in the density of mortar due to PET substitution, and mortar with 10-15% PET-Sand possessed the density of the control mix when SFS-Sand was incorporated in the mix. The density values of the mixes were not significantly affected by the incorporation of FLA in the

mix, as observed from the results of Tier III mixes. Nonetheless, there was a decrease in density values by 0.5-1.0% due to the lower specific weight of FLA compared to OPC.

Table 5.3 Fresh and dry density (kg/m^3) of mortar mixes

Mix	1:3 mix				1:5 mix			
	Fresh Density	± Δ %	Dry Density	± Δ %	Fresh Density	± Δ %	Dry Density	± Δ %
Control Mix (OPC/N-Sand)								
Mx-C-P0	2450	0.00	2401	0.00	2410	0.00	2353	0.00
Tier I Mortar (OPC/N-Sand+PET-Sand)								
Mx-C-P10	2401	-2.00	2353	-2.00	2356	-2.20	2308	-1.90
Mx-C-P15	2339	-4.50	2276	-5.20	2293	-4.90	2239	-4.80
Mx-C-P20	2264	-7.60	2219	-7.60	2254	-6.50	2185	-7.10
Mx-C-P25	2188	-10.70	2126	-11.50	2157	-10.50	2083	-11.50
Tier II mortar (OPC/N-Sand+SFS-Sand+PET-Sand)								
Mx-C-SP0	2534	+3.40	2502	+4.20	2482	+3.00	2422	+2.90
Mx-C-SP10	2432	-0.70	2394	-0.30	2385	-1.00	2337	-0.70
Mx-C-SP15	2381	-2.80	2321	-3.30	2310	-4.10	2293	-2.50
Mx-C-SP20	2302	-6.00	2246	-6.50	2276	-5.60	2213	-5.90
Mx-C-SP25	2231	-8.90	2189	-8.80	2194	-9.00	2123	-9.80
Tier III mortar (OPC+FLA/N-Sand+SFS-Sand+PET-Sand)								
Mx-CF-SP0	2512	+2.50	2486	+3.50	2460	+2.10	2388	+1.50
Mx-CF-SP10	2434	-0.70	2375	-1.10	2362	-2.00	2308	-1.90
Mx-CF-SP15	2361	-3.60	2288	-4.70	2322	-3.70	2254	-4.20
Mx-CF-SP20	2282	-6.90	2231	-7.10	2251	-6.60	2204	-6.30
Mx-CF-SP25	2209	-9.80	2159	-10.10	2179	-9.60	2117	-10.00

($_X$=3 for 1:3 mix, $_X$=5 for 1:5 mix)

5.3.2 Bulk density of concrete

The fresh and dry bulk density values for various concrete mixes in the current research are presented in Table 5.4. The results showed that there is a 6.5 - 8% decrease in the density of concrete when 25% of N-Sand volume was substituted by PET-Sand for concrete in Tier I with OPC and N-Sand. On incorporation of SFS-Sand in the Tier II concrete mixes, the loss in density was controlled due to the higher density of SFS than the N-Sand. The use of FLA in the third tier did not show any significant difference in

density values from that of tier II mixes. The variations in density values are presented in Fig. 5.5 and 5.6.

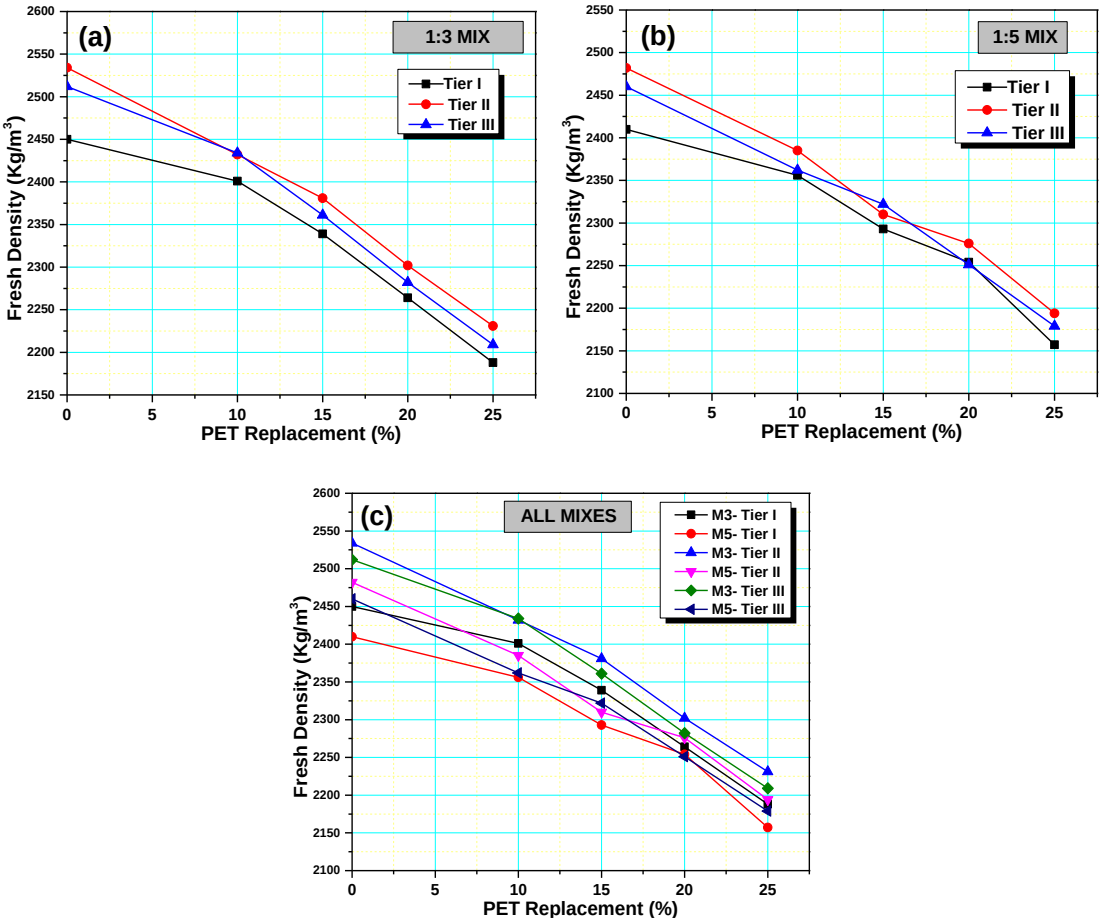

Fig. 5.3 Fresh density of mortar (a) 1:3 mix (b) 1:5 mix and (c) All mortar mixes

5.3.3 Discussions

The results on fresh and dry density values of mortar and concrete mixes studied in the current research confirm that the density of the composites decreases with the increase in PET content of the mix. The observation is attributed to the fact that PET particles have a lower specific weight compared to N-Sand particles as evident from the material characterization results presented earlier in Table 3.4. For tier I mixes a reduction of 10.5% - 11.5% in density was noted for mortar samples, while concrete samples showed a reduction of 6.5 to 8% in the density values for a maximum volume substitution of 25% PET waste.

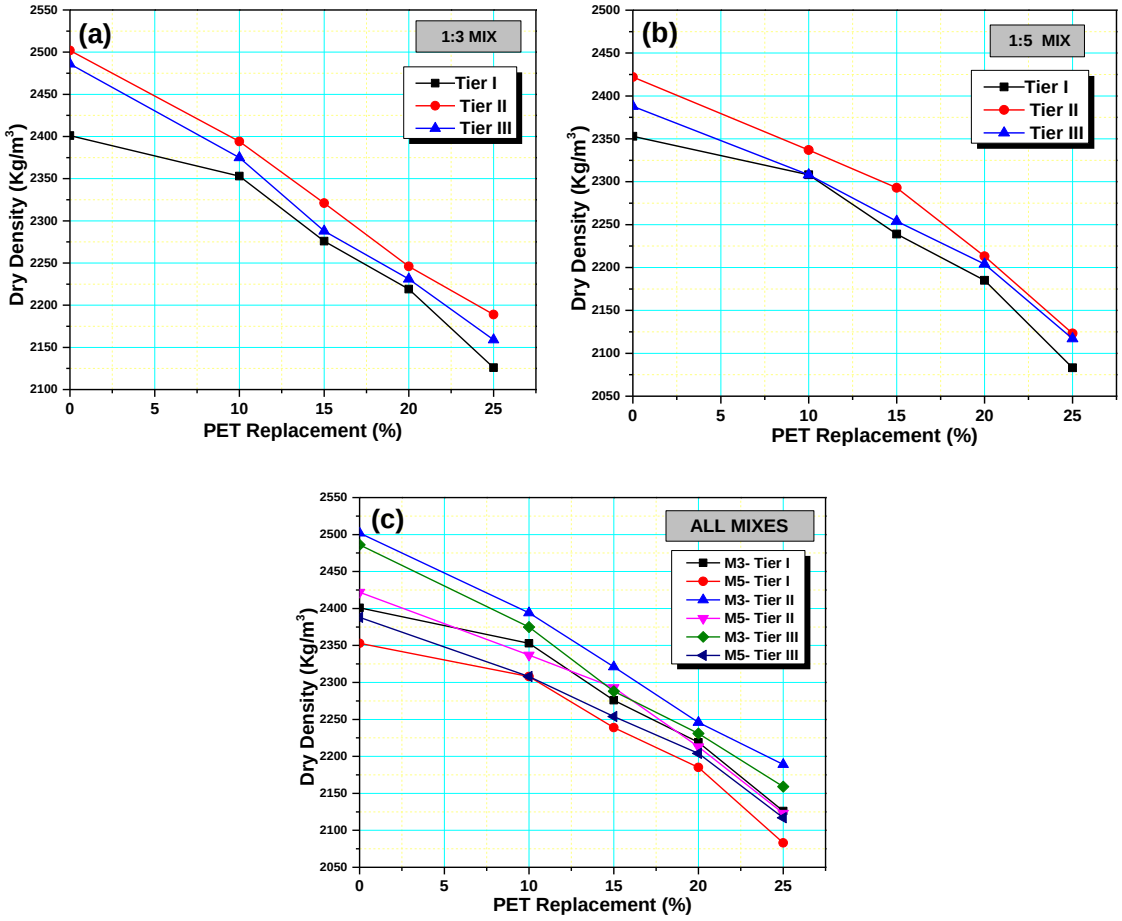

Fig. 5.4 Dry density of mortar mix (a) 1:3 mix (c) 1:5 mix and (c) All mortar mixes

The results have proved the literature finding that regardless of type and size, the use of plastic aggregate generally results in a decrease in the density of the concrete (Saikia and De Brito, 2012). Such behavior can be primarily attributed to the fact that the plastic aggregate is lighter than N-Sand. Another prominent reason for the decline in the density of the plastic-incorporated cement mixes is the increase in porosity in the microstructure of the mixes. Iucolano et al. (2013) have reported an increase in the open porosity of mortars by 13% over reference mortars when plastic waste of 33% is included in the mix. This increase in porosity is due to the resistance of the plastic particles to the formation of a cohesive mix (Iucolano et al. 2013). Also, negligibly low water absorption by plastic particles leads to void spaces around plastic grains when the unabsorbed water evaporates out. Several authors reported that plastic aggregates exhibit a series of drawbacks, mainly due to their poor chemical compatibility with inorganic matrix, which could lead to the formation of microcavities responsible for the increase of porosity (Frigione, 2010; Ismail and AL-Hashmi, 2008; Siddique et al., 2008). So, it is not the

lower specific weight of the plastic waste that solely decreases the density, but the porosity induced by the plastic waste also adds to the reduction of the density of cement mixes in the dry state.

Table 5.4 Fresh and dry density (kg/m^3) of concrete mixes

Mix	M30 mix				M50 mix			
	Fresh Density	± Δ %	Dry Density	± Δ %	Fresh Density	± Δ %	Dry Density	± Δ %
Control Mix (OPC/N-Sand)								
C_Y-C-P0	2484	0.00	2426	0.00	2507	0.00	2448	0.00
Tier I Concrete (OPC/N-Sand+PET-Sand)								
C_Y-C-P10	2424	-2.40	2357	-2.80	2456	-2.00	2410	0.00
C_Y-C-P15	2396	-3.50	2299	-5.20	2418	-3.60	2349	-1.60
C_Y-C-P20	2360	-5.00	2271	-6.40	2376	-5.20	2321	-4.00
C_Y-C-P25	2322	-6.50	2231	-8.00	2337	-6.80	2276	-5.20
Tier II Concrete (OPC/N-Sand+SFS-Sand+PET-Sand)								
C_Y-C-SP0	2543	+2.40	2487	+2.50	2568	+2.40	2507	+2.40
C_Y-C-SP10	2469	-0.60	2406	-0.80	2526	+0.80	2446	-0.10
C_Y-C-SP15	2434	-2.00	2361	-2.70	2498	-0.40	2415	-1.30
C_Y-C-SP20	2395	-3.60	2330	-4.00	2458	-2.00	2373	-3.10
C_Y-C-SP25	2358	-5.10	2267	-6.60	2413	-3.7	2318	-5.30
Tier III Concrete (OPC+FLA/N-Sand+SFS-Sand+PET-Sand)								
C_Y-CF-SP0	2529	+1.80	2474	+2.00	2553	+1.80	2487	+1.60
C_Y-CF-SP10	2467	-0.70	2391	-1.40	2507	0.00	2433	-0.60
C_Y-CF-SP15	2434	-2.00	2357	-2.80	2477	-1.20	2404	-1.80
C_Y-CF-SP20	2406	-3.10	2315	-4.60	2429	-3.10	2322	-5.10
C_Y-CF-SP25	2356	-5.20	2261	-6.80	2406	-4.00	2288	-6.50

($_Y$=30 for M30 mix, $_Y$=50 for M50 mix)

The addition of SFS-Sand by optimum replacement volumes in mortar and concrete increases the density of the baseline mix without PET. Although the higher specific weight of the SFS aggregates is the primary cause of the increase in density, it may not be considered the exclusive cause. Ouda and Abdel-Gawwad (2017) stated that the micropores on the surface of the slag aggregates get filled with the cement matrix with a better interlock between the cement paste and aggregate particles. This results in a decrease in porosity and an increase in the density of the global mass (Ouda and Abdel-Gawwad, 2017). Therefore, SFS particles partially compensate for the density loss caused

by the substitution of PET-Sand in the tier II mixes. The SFS inclusion mitigates the density reduction by 1-2% compared to the tier I mixes. However, the rate of reduction of density with PET content is not affected significantly.

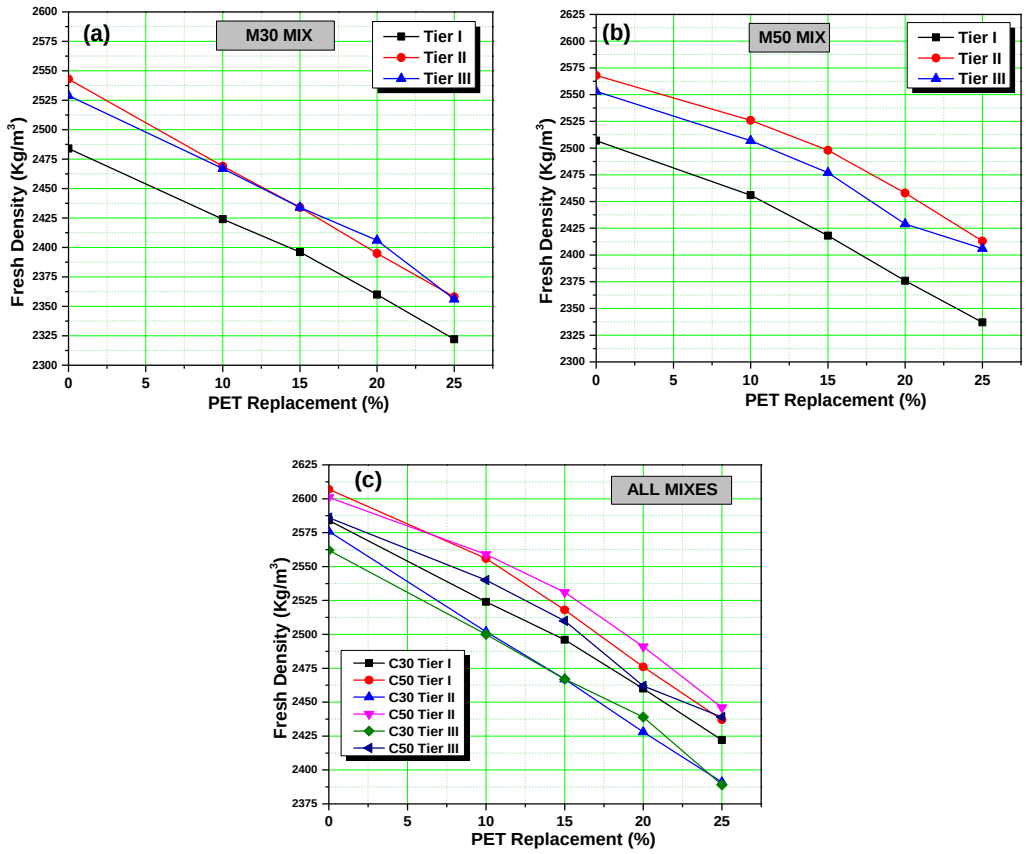

Fig. 5.5 Fresh Density of Concrete mixes (a) M30 mix (c) M50 mix (c) All mixes

A significant decrease in density values was expected in tier III mixes over tier II mixes due to the lower specific weight of FLA particles than the cement particles. However, there was a marginal difference in the density values. This may be explained by the compensating effect of better compaction of tier III mixes having better workability characteristics due to FLA.

5.4 Compressive strength of mortar and concrete

Compressive strength is a property of paramount importance in the evaluation of the quality and performance of cement composites. It is the face value of the material which decides the functional suitability of any cement product in the construction industry. Most of the properties of concrete or cement-related products are directly related to compressive strength. The current study is a novel approach to using PET-Sand, a

material having a low modulus of elasticity, and low density, but a higher tensile strength than N-Sand which it replaces in the cement mixes. Thus, understanding the compressive strength characteristics of the PET-modified cement product would be a guiding parameter in assessing its technical suitability.

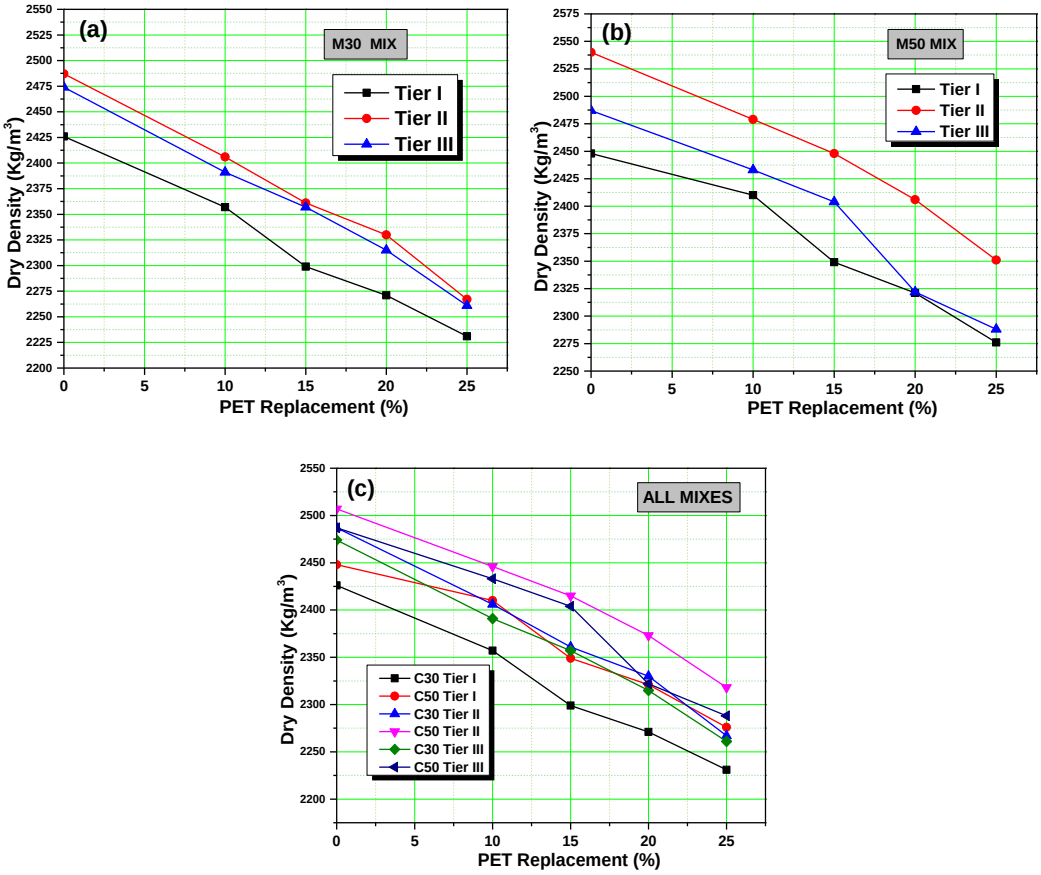

Fig. 5.6 Dry Density of Concrete mixes (a) M30 mix (b) M50 mix (c) All mixes

The compressive strength results of mortar and concrete mix for different mix proportions in the three tiers as per the scheme of experimentation are provided in the following sections. The results are provided for 3 days, 7 days, 28 days, 56 days and 90 days of age. The 90 days age strength has been considered with a hypothesis that the effect of FLA on the strength properties of the cement mixes is visible at older ages of curing. The graphical representations and the discussions on the results have been provided to reveal the variations in strength characteristics of the novel composites.

5.4.1 Compressive Strength of Mortar

The compressive strength of mortar specimens for different mixes containing varying proportions of PET-Sand in three different tiers of experimentation is presented in Table 5.5. As already discussed, the mix with OPC binder and N-Sand as the fine aggregate is considered a control mix for all purposes. The variation in strength values of the mortar about the substitution volumes of PET-Sand and the age of the specimens are summarized in Fig. 5.7 to Fig. 5.9.

Table 5.5 Compressive strength (N/mm^2) of mortar mixes

Mix	1:3 mix				1:5 mix			
	3 days	7 days	28 days	90 days	3 days	7 days	28 days	90 days
Control Mix (OPC/N-Sand)								
Mx-C-P0	31.41	36.79	45.07	47.84	26.31	34.29	40.71	42.56
Tier I Mortar (OPC/N-Sand+PET-Sand)								
Mx-C-P10	30.51	35.68	43.47	46.24	25.68	32.78	38.9	41.24
Mx-C-P15	28.76	33.51	40.99	43.26	23.47	30.29	35.78	37.10
Mx-C-P20	25.99	31.14	37.66	38.98	20.87	27.08	32.9	34.20
Mx-C-P25	22.00	27.23	32.04	34.82	17.02	22.34	26.13	27.28
Tier II mortar (OPC/N-Sand+SFS-Sand+PET-Sand)								
Mx-C-SP0	33.74	40.56	50.64	52.69	28.86	37.24	45.68	45.87
Mx-C-SP10	33.25	38.77	48.36	50.46	26.98	35.93	43.22	43.45
Mx-C-SP15	31.64	36.45	44.68	47.19	24.97	32.84	38.72	39.1
Mx-C-SP20	27.62	32.14	40.19	42.30	22.64	28.56	34.84	36.24
Mx-C-SP25	23.59	28.32	35.62	37.96	19.86	25.81	31.56	29.97
Tier III mortar (OPC+FLA/N-Sand+SFS-Sand+PET-Sand)								
Mx-CF-SP0	28.41	35.86	47.12	52.34	24.60	34.6	43.65	46.24
Mx-CF-SP10	27.94	36.97	45.42	50.12	22.10	32.64	42.12	44.76
Mx-CF-SP15	24.10	34.88	43.65	47.54	19.01	31.01	36.80	41.56
Mx-CF-SP20	23.39	32.40	39.10	43.65	18.00	28.40	33.12	37.48
Mx-CF-SP25	20.40	25.32	34.80	38.97	16.40	24.40	28.98	33.42

($_X$=3 for 1:3 mix, $_X$=5 for 1:5 mix)

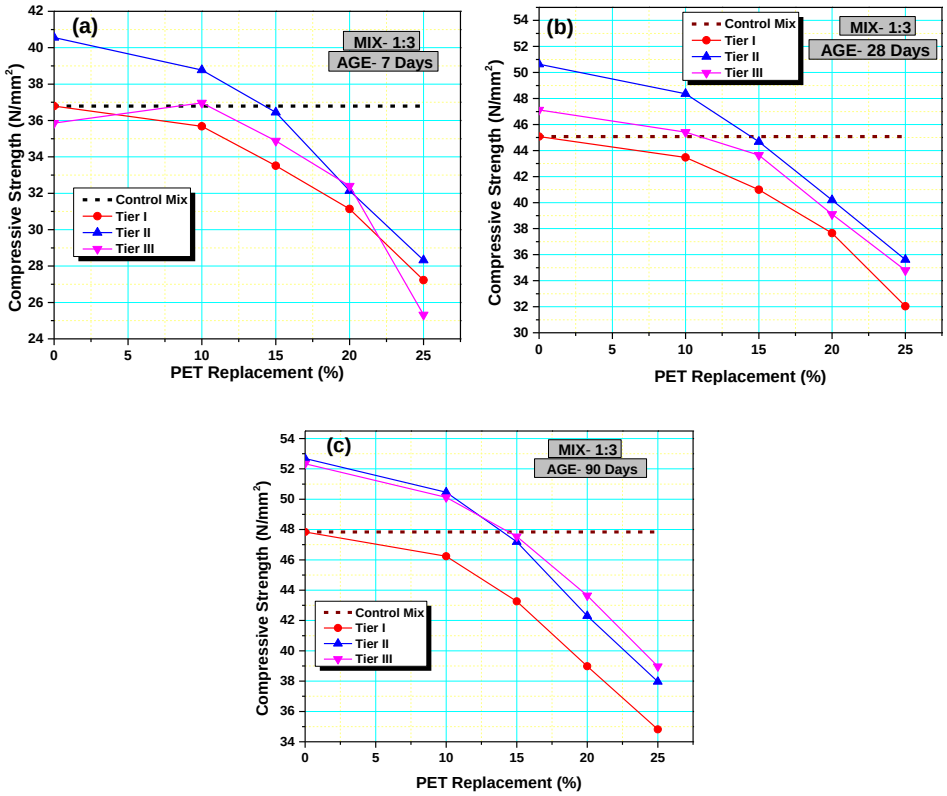

Fig. 5.7 Compressive strength of 1:3 mortar mix (a) 7 days, (b) 28 days, and (c) 90 days

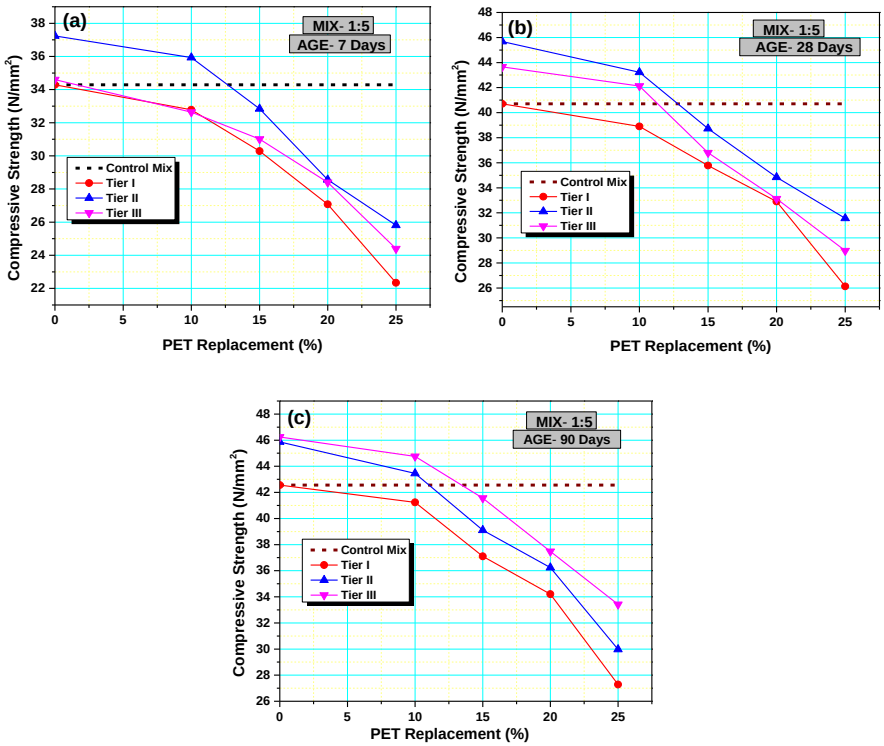

Fig. 5.8 Compressive strength of 1:5 mortar mix (a) 7 days, (b) 28 days, and (c) 90 days

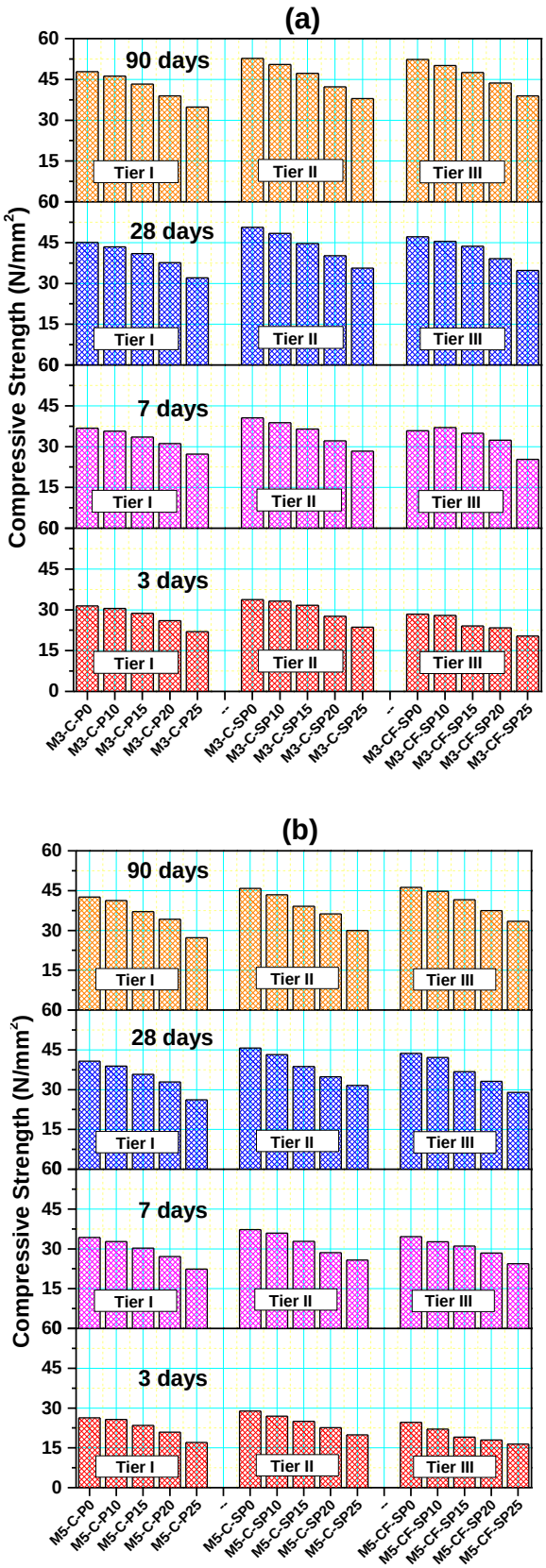

Fig. 5.9 Variation of Compressive strength of mortar with PET-Sand at different ages

(a) 1:3 mix (b) 1:5 mix

5.4.2 Compressive Strength of Concrete

The compressive strength of concrete specimens for different mixes containing varying proportions of PET-Sand in three different tiers of experimentation is presented in Table 5.6. The concrete mix with OPC as the sole binder and N-Sand as the fine aggregate is considered a control mix for all purposes. The variation in strength values of the concrete about the substitution volumes of PET-Sand for various ages of concrete is summarized in the plots presented in Fig. 5.10 to Fig. 5.12.

Table 5.6 Compressive strength (N/mm^2) of concrete mixes

Mix	M30 mix				M50 mix			
	7 days	28 days	56 days	90 days	7 days	28 days	56 days	90 days
Control Mix (OPC/N-Sand)								
C_Y-C-P0	29.86	40.6	42.42	44.6	48.86	62.60	64.73	66.12
Tier I Concrete (OPC/N-Sand+PET-Sand)								
C_Y-C-P10	29.35	40.84	42.84	44.9	49.54	63.80	65.64	67.42
C_Y-C-P15	28.51	38.56	39.82	39.94	45.68	59.67	59.12	62.20
C_Y-C-P20	26.54	33.40	34.15	35.04	43.65	54.30	55.20	57.48
C_Y-C-P25	22.64	29.80	30.82	32.58	38.22	50.42	50.40	51.96
Tier II Concrete (OPC/N-Sand+SFS-Sand+PET-Sand)								
C_Y-C-SP0	32.56	44.79	47.12	49.26	54.98	69.78	72.65	73.25
C_Y-C-SP10	32.82	44.68	43.78	47.46	49.72	66.24	68.58	69.90
C_Y-C-SP15	30.24	41.86	41.26	42.86	48.40	63.92	64.70	66.10
C_Y-C-SP20	27.25	36.54	35.10	37.20	46.10	58.31	59.10	61.42
C_Y-C-SP25	24.63	32.80	32.90	34.80	42.20	52.61	53.44	54.26
Tier III Concrete (OPC+FLA/N-Sand+SFS-Sand+PET-Sand)								
C_Y-CF-SP0	27.56	41.20	45.75	49.52	47.95	64.52	68.97	71.26
C_Y-CF-SP10	26.45	41.60	44.67	47.28	44.56	62.35	66.52	68.94
C_Y-CF-SP15	24.23	39.20	42.56	45.44	41.56	58.64	63.54	66.84
C_Y-CF-SP20	23.56	34.20	38.64	41.24	38.98	51.26	58.16	59.47
C_Y-CF-SP25	21.84	30.20	34.24	37.19	36.21	48.69	52.96	54.55

($_Y$=30 for M30 mix, $_Y$=50 for M50 mix)

5.4.3 Discussions

The results of compressive strength of mortar and concrete specimens containing increasing volumes of PET-Sand as a partial substitute to N-Sand show the effect of the replacement ratios, age of curing, the effect of blending of SFS as fine aggregate with N-

sand, and the effect of using FLA as an SCM with OPC. The compressive strength behavior of the novel composites can be explained for each tier separately to appreciate the effect of each factor.

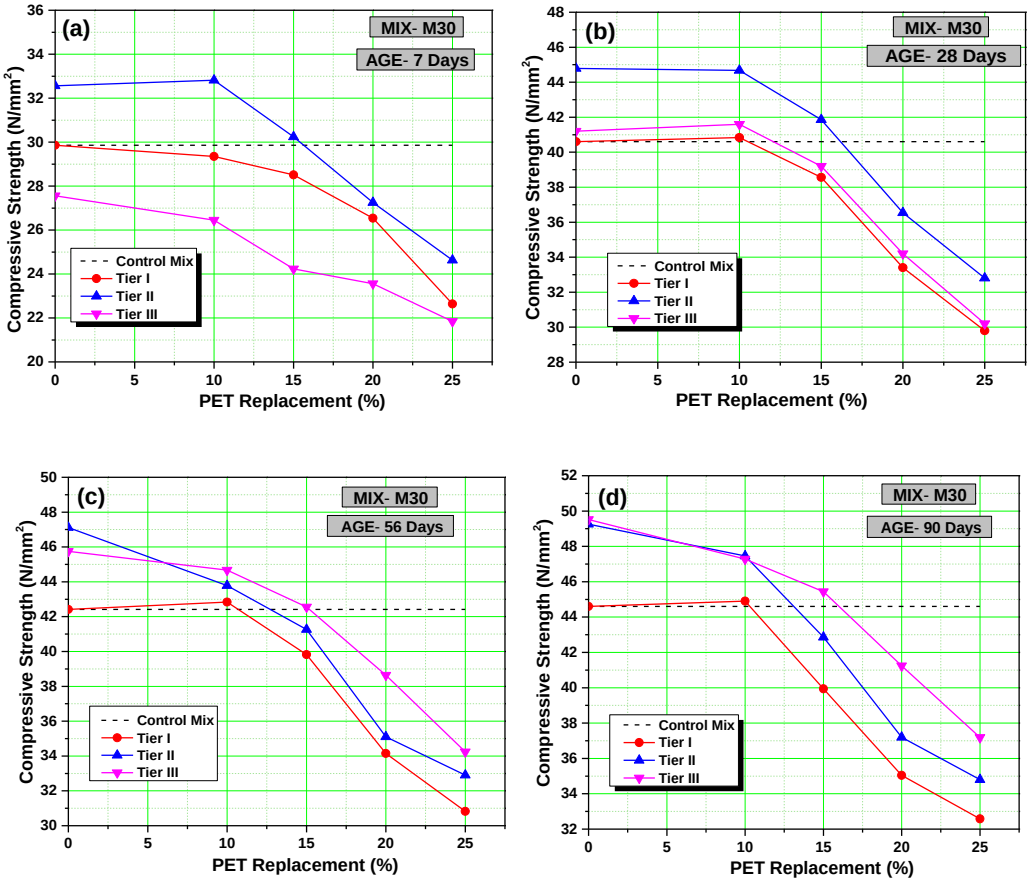

Fig. 5.10 Compressive strength of M30 Grade concrete with PET-Sand (a) 7 Days (b) 28 Days (c) 56 Days (d) 90 Days

Tier I specimens of mortar and concrete reveal the effect of substitution ratios of PET-Sand on the compressive strength of OPC-bonded mixes. The compressive strength of the mixes decreased significantly with the increase in PET-Sand content regardless of the type of composite, period of curing, and the w/c ratio of the mix. For the replacement of 25% of the volume of N-Sand by PET-Sand, mortar specimens for 1:3 and 1:5 mix proportions showed a decrease in strength of 29% and 36% respectively. A similar effect was also observed in the case of M30 and M50 grade concretes where 25% volume replacement of N-Sand showed a decrease of 27% and 22% respectively.

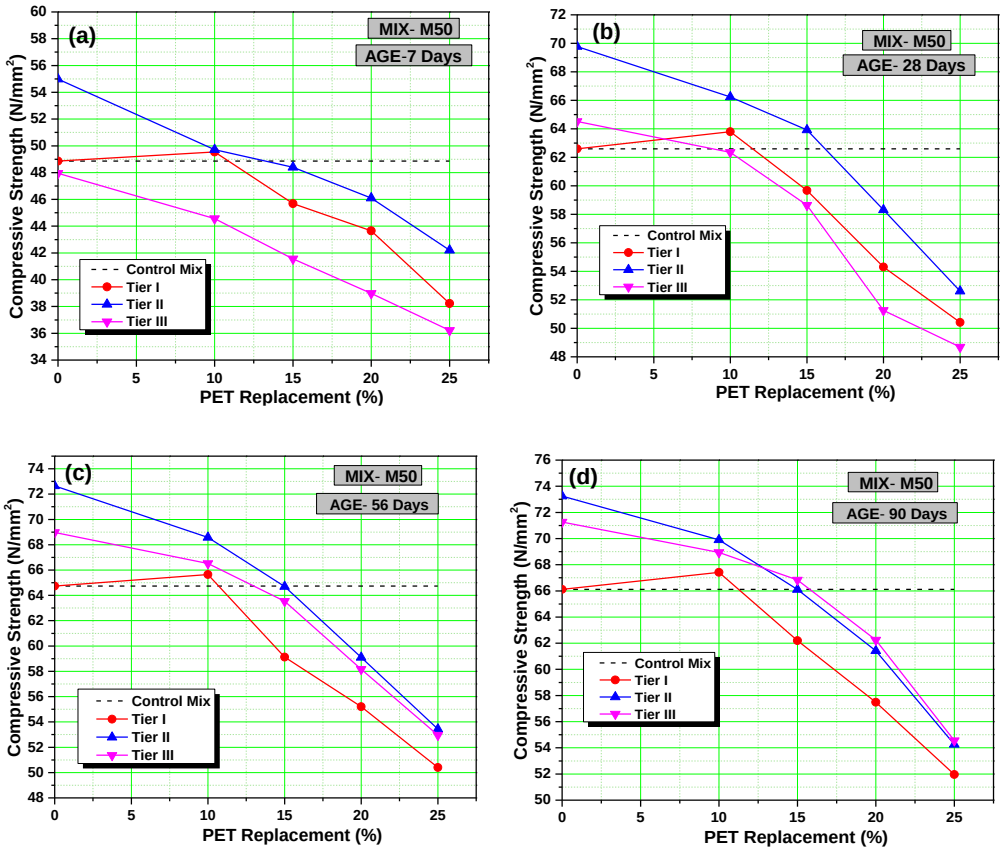

Fig. 5.11 Compressive strength of M50 Grade concrete with PET-Sand (a) 7 Days (b) 28 Days (c) 56 Days (d) 90 Days

The reduction in compressive strength with the increase in PET inclusions is influenced by one or more of the following factors.

1) The main reason for the drastic reduction in compressive strength of PET-modified specimens is the weak adhesion between the plastic fragments and the cementitious matrix due to the smooth texture of the PET particles.
2) The inclusion of plastic results in a highly porous mix with a noticeable increase in air content inside the mix. This increase in porosity is a result of several associated factors like reduced workability, the hydrophobic nature of PET particles, the water-cement ratio of the mix, etc. The results of rheological studies of fresh mixes have confirmed the resistance offered by PET particles to the flowability of the mixes, especially at higher replacement levels. This leads to the formation of honeycombs inside the mix.

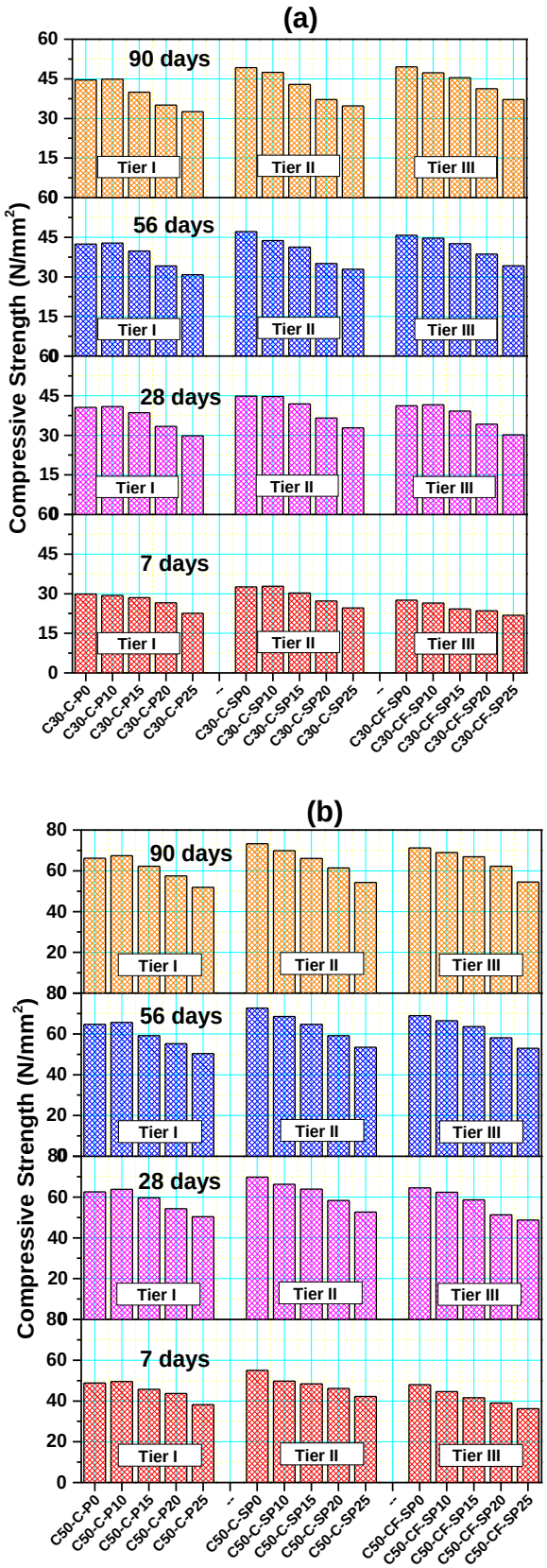

Fig. 5. 12 Variation of Compressive strength of concrete with PET-Sand at different ages (a) M30 mix (b) M50 mix

3) The plastic fragments possess lower strength than N-Sand. The lower stiffness values of the plastic fragments influence the strength of the mixes.
4) The hydrophobic nature of plastic limits the cement hydration reactions at the surface of the plastic units (Abed et al. 2021). In the case of natural aggregates, water-cement paste gets absorbed in the pore spaces on the surface of aggregates. These are the minute cement hydration sites where the mortar components get clogged. On the contrary, such absorption of water and cement does not occur on the surface of plastic fragments due to the low intrinsic porosity and hydrophobic nature of plastic. This feature prevents impregnation and subsequent crystallization of binder paste therein (Correia et al. 2014). So, there is a weak ITZ at the interface between the cement paste and plastic aggregate which is confirmed by the SEM images presented in § 5.13.

The leaner mixes showed a higher reduction in strength than the richer mixes. The 28-day strength for 25% volume of PET for M30 grade (w/c ratio= 0.44) concrete was 26.6% lower than the control mix, whereas, for M50 grade (w/c ratio= 0.39) concrete the reduction was found to be 20%. This effect may be attributed to two factors i.e., the w/c ratio of the mix and the ratio of PET to binder intensity inside the mix. The results have shown that the higher the w/c ratio of the mix, the higher the rate of strength reduction of the mix for a given percentage inclusion of PET-Sand. This finding is in agreement with the study by Frigione (2010) in which mixes with two different w/c ratios were analyzed with two different cement contents (Frigione 2010). This may be attributed to the availability of excess water in the mix which does not participate in the cement hydration process. This excess water subsequently evaporates out leaving behind small diameter channels like capillaries adding to the porosity of the composites, ultimately affecting the strength (Albano et al. 2009). Secondly, it can also be concluded that the higher the ratio of PET to binder intensity inside a mix, the more the rate of strength reduction at a given replacement level of PET. In the present study, the leaner mixes exhibited a higher ratio of PET to binder intensity and thus exhibited higher strength reduction than the richer mixes. This observation is in agreement with the study presented by Mohammed Joarder et al. (2019) which showed that 30% volume of PET coarse aggregate causes a strength reduction of 20% and 33% in 1:1.5:3 and 1:2:4 mix respectively(Mohammed Joarder et al. 2019).

The results showed that there was no effect of PET inclusion on the strength gain with age and the rate of gain of strength was similar to the control mixes in both mortar and concrete samples. An early gain of strength was noticed for most of the PET-incorporated mixes. This may be attributed to the lower thermal conductivity of PET aggregates. This reduces the loss of heat generated by the cement hydration process, thereby creating better hydration conditions for the paste and assisting strength gain (Saikia and De Brito, 2013).

At a lower substitution level of 10% volume of PET-Sand, the compressive strength values were not affected significantly. Mortar mixes showed a 3-4% reduction in strength, while the concrete mixes showed a strength increase of 0-1.5%, more prominently for the richer M50 mix. These findings complement the results presented by several other investigations in the literature (Aguayo et al., 2016; Azhdarpour et al., 2016; Babafemi et al., 2022; Yang et al., 2015). Azhdarpour et al. (2016) in an investigation advocated that at a lower percentage of substitution, PET particles interfere with the failure process. The presence of elongated and sheet-shaped PET fragments at the starting points of failure tolerates a part of the applied stress before their separation from the matrix. So, a portion of induced shear stress is converted to tensile stress which is utilized to overcome the tensile strength of plastic fragments. This effect diminishes with the increase in the volume of plastic pieces because the effect of the decrease in cohesion dominates at the points of failure due to the smooth surface and flat-shaped PET particles (Azhdarpour et al. 2016). Aguayo et al. (2016) observed that at low substitution levels, the replacement of hard sand with soft inclusions led to an increase in compressive strength. With the aid of numerical simulations, they attributed such behavior to stress redistribution between soft and hard inclusions (i.e., sand). The authors stated that at moderate replacement levels, there is stress transfer to the strong (sand) inclusions causing a delay in the failure process (Aguayo et al., 2016). Jaskowska-Lemańska et al. (2022) claimed that the decrease in the strength of concrete with PET aggregates is due to the increased softness of the material compared to natural aggregates. The authors also proved that PET units in the mix act like air voids in the cement matrix and the cracks initiate around these particles(Jaskowska-Lemańska et al. 2022).

It is observed that failure under compressive stress is more gradual and it depends upon the plastic content. As the plastic content increases the failure tends to be more ductile. The reference concrete exhibited a brittle failure. The failure modes of concrete with PET indicated that the synthetic sand could prevent larger deformation. It can be assumed that PET particles produce a softening behavior inside cement mixes.

The tier II mixes utilized a blend of N-Sand and SFS-Sand as fine aggregates, the latter being used with optimum substitution levels of 50% and 40% in mortar and concrete respectively. The baseline mix in this tier with 0% PET showed a strength enhancement of 12-12.5% for mortar and 11-12% for concrete mixes in comparison to the control mix. Subsequently, the incorporation of PET sand reduced the compressive strength of the mixes of Tier II as well. However, the SFS aggregates partially compensated for the loss of strength. In the comparison of Tier I mixes with 25% PET replacement, the use of SFS-Sand in the mixes could lower the reduction in strength by 8-12.5% for mortar mixes and 5-6% for concrete mixes at 28 days of aging.

This strength enhancement in Tier II mixes is attributed to the physical characteristics of the SFS aggregates. The angular, sharp edges of the slag aggregates improve the cohesion of the concrete matrix. Also, the surface texture improves the bond between cement paste and aggregates. The porous texture of slag aggregates causes enhanced interlocking and improvement in the transition zone of the aggregate-paste interface. So, there is a better mechanical bite force and cohesive force than N-Sand resulting in higher bonding strength with cement paste. The SFS aggregates are stronger than the N-Sand which is replaced. SFS particles have better compressibility than N-Sand. Therefore, these aggregates partially relieve the stress concentration. The increase in workability of the mixes due to the addition of SFS offers better compaction conditions for the mixes, thereby improving the strength of the mixes. One of the major causes for the strength degradation in PET aggregate mixes is the excess water available in the mixes due to the hydrophobic nature of the PET particles which do not participate in a hydration reaction. SFS slag is characterized by surface roughness and microcavities as evident from the SEM images presented in the material characterization of the current study. These microcavities are the minute water-absorptive pockets. These pockets not only reduce the free water in the concrete mix but may also lower the effective w/c ratio of the

mix. Tripathi and Chaudhary (2016) further claim that this water held in the microcavities initially is gradually released and used at later ages for the hydration process (Tripathi and Chaudhary, 2016). Therefore, the strength lost due to the PET inclusions is mitigated partially. Additionally, the hydration products of cement can penetrate these microcavities or fine wrinkles of SFS surfaces, giving several hook bonds between matrix and aggregates further contributing to the mitigation of strength loss.

In the case of Tier III mixes having a blend of 70% OPC and 30% FLA as the binder material, the strength gain with age follows the traditionally witnessed pattern observed in FLA blended mixes. The mortar and concrete mixes showed a delay in strength gain with age. This is attributed to the slow reactivity of FLA at early ages. FLA has comparatively lower fineness and lower pozzolanic activity than OPC. FLA is responsible for the reduction of the heat of hydration in concrete. Therefore, it requires higher curing periods for the completion of the hydration process. The poor development of strength in the FLA blended mixes at early curing periods is a well-known fact in the literature (Atiş, 2005; Cong Kou et al., 2007). It has been stated that the early strength development in the case of purely OPC blended mixes is due to the amount of C_3S in OPC. The replacement of OPC by any pozzolanic SCM like FLA reduces the quantity of C_3S in the mixes directly affecting the strength-gaining ability of the composites at early ages (Herki, 2017b). However, at longer curing periods of 90 days, the delayed pozzolanic reaction of FLA could attain strength values better than the strength values of the control mix as well as the Tier I and Tier II mix. The loss in strength at 25% replacement of PET-Sand was reduced by 4-8% compared to Tier I mixes. This may be attributed to the pore-filling effect of FLA particles in the matrix and better compaction characteristics of the mix due to the enhanced workability of the mix already confirmed by the rheological tests. These findings are in agreement with the studies presented by Sadrmomtazi et al. (2016).

5.5 Flexural Strength of Mortar and Concrete

Flexural strength is the capacity of a material to resist deformation under flexural load. It is also called a modulus of rupture. It is the maximum bending stress that can be applied to a material before it yields. In other words, it is the measure of the greatest stress inside the material at the time of the collapse. The flexural strength of mortar and concrete

in the current study has been determined by transverse bending tests for specimens at 28 days of age.

5.5.1 Flexural strength of mortar

The results of the flexural strength of mortar specimens in three different tiers for 1:3 and 1:5 mix proportions are summarized in Table 5.7 with percentage variation in results relative to the strength of the control mix. Fig. 5.13 exhibits the effect of the rate of substitution of PET waste on the flexural strength of the mixes in different tiers for both the mix proportions.

Table 5.7 Flexural strength (N/mm^2) of mortar mixes

Identification	1:3 mix		1:5 mix	
	Flexural Strength	± Δ%	Flexural Strength	± Δ%
Control Mix (OPC/N-Sand)				
M_x-C-P0	6.04	0.00	5.29	0.00
Tier I Mortar (OPC/N-Sand+PET-Sand)				
M_x-C-P10	6.18	+2.30	5.21	-1.50
M_x-C-P15	5.82	-3.60	4.97	-6.00
M_x-C-P20	5.04	-16.60	4.48	-15.30
M_x-C-P25	4.72	-21.90	4.19	-20.80
Tier II mortar (OPC/N-Sand+SFS-Sand+PET-Sand)				
M_x-C-SP0	6.53	+8.10	5.76	+8.9
M_x-C-SP10	6.62	+9.60	5.81	+9.8
M_x-C-SP15	6.28	+4.00	5.20	-1.70
M_x-C-SP20	5.68	-6.00	4.71	-11.00
M_x-C-SP25	4.96	-17.90	4.31	-18.50
Tier III mortar (OPC+FLA/N-Sand+SFS-Sand+PET-Sand)				
M_x-CF-SP0	6.12	+1.30	5.59	5.70
M_x-CF-SP10	6.04	0.00	5.19	-1.90
M_x-CF-SP15	5.84	-3.30	4.82	-8.90
M_x-CF-SP20	5.10	-15.60	4.38	-17.20
M_x-CF-SP25	4.69	-22.40	3.94	-25.50

(x=3 for 1:3 mix and x=5 for 1:5 mix)

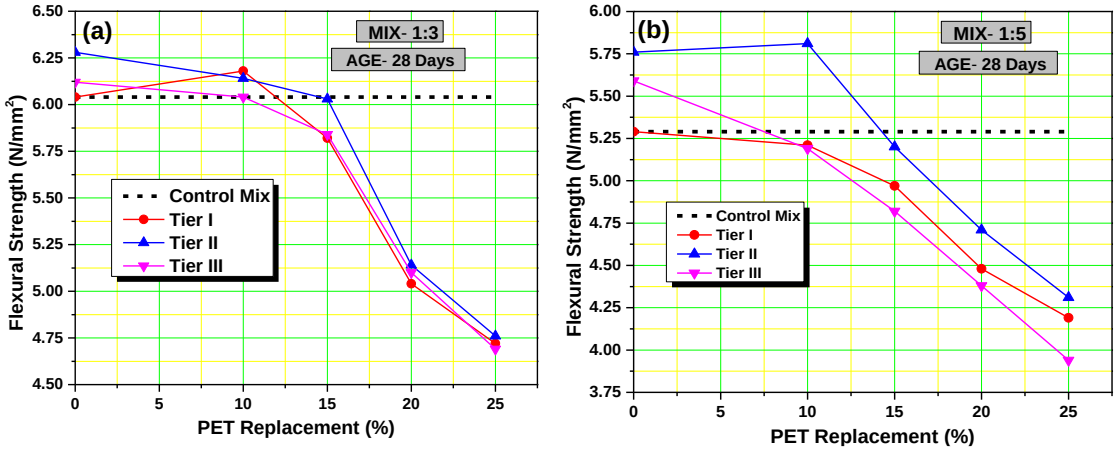

Fig. 5.13 Flexural strength of mortar mix (a) 1:3 mix and (b) 1:5 mix

5.5.2 Flexural Strength of Concrete

The results of the flexural strength of concrete specimens in three different tiers for M30 and M50 mix proportions are summarized in Table 5.8 with percentage variation in results relative to the strength of the control mix. Fig. 5.14 exhibits the effect of the rate of substitution of PET waste on the flexural strength of the mixes in different tiers for both the mix proportions.

5.5.3 Discussions

From the observed values of flexural strength of mortar and concrete mixes of tier I samples, there was enough evidence to claim that the increase in PET content beyond 10% volume degrades the flexural strength of the composites. A noticeable resistance to the yielding failure was observed at a lower substitution level of up to 10% volume of PET-Sand. At this percentage substitution, the richer 1:3 mortar mix showed an enhancement in strength by 2.30%, while the 1:5 mortar mix exhibited a decline in strength by 1.50%. A similar trend was observed for concrete specimens depicting a decline of 0.5% in flexural strength in the M30 mix and a gain in strength of 2.10% in the case of the M50 mix. The slight increase in flexural strength may be attributed to the considerable tensile strength of PET particles which were present at the starting point of failure. At these low PET ratios, plastic fragments were situated at the starting points of failure and they locked both sides of these points to each other, leading to an enhanced flexural behavior. Babafemi et al. (2018) claimed that a small fraction of the waste plastics has a shape similar to short fibers, and can bridge the crack to a certain extent, providing

the material with some post-peak toughening (Babafemi et al. 2018). The flexural strength declined sharply when substitution ratios exceeded 10% of fine aggregate volume. Azhdarpour et al. (2016) claimed that as PET volumes increase, the locking effect diminishes because there is an accumulation of particles next to each other, directly affecting the cohesion between the cement paste and PET fragments (Azhdarpour et al. 2016). This effect was noticed through the decline in flexural strength by 18-22% for 25% substitution of PET in mortar and concrete. It can be seen that flexural strength reduction follows a similar trend as in the case of compressive strength. However, the loss in flexural strength is lower as compared to the loss in compressive strength due to the incorporation of PET.

Table 5.8 Flexural strength (N/mm^2) of concrete mixes

Identification	M30 mix		M50 mix	
	Flexural Strength	± Δ%	Flexural Strength	± Δ%
Control Mix (OPC/N-Sand)				
C_Y-C-P0	5.12	0.00	7.52	0.00
Tier I Concrete (OPC/ N-Sand+PET-Sand)				
C_Y-C-P10	5.10	-0.40	7.68	+2.10
C_Y-C-P15	4.74	-7.40	7.14	-5.10
C_Y-C-P20	4.21	-17.80	6.70	-10.90
C_Y-C-P25	3.96	-22.70	6.15	-18.20
Tier II Concrete (OPC/N-Sand+SFS-Sand+PET-Sand)				
C_Y-C-SP0	5.29	+3.30	7.98	+6.10
C_Y-C-SP10	5.38	+5.10	8.06	+7.20
C_Y-C-SP15	5.07	-1.00	7.62	+1.30
C_Y-C-SP20	4.62	-9.80	6.93	-7.80
C_Y-C-SP25	4.25	-17.00	6.58	-12.50
Tier III Concrete (OPC+FLA/N-Sand+SFS-Sand+PET-Sand)				
C_Y-CF-SP0	5.24	+2.30	7.79	+3.60
C_Y-CF-SP10	5.22	+2.00	7.94	+5.60
C_Y-CF-SP15	4.93	-3.70	7.58	+0.80
C_Y-CF-SP20	4.48	-12.50	6.74	-10.40
C_Y-CF-SP25	4.16	-18.70	6.44	-14.40

($_Y$=30 for M30 mix, $_Y$=50 for M50 mix)

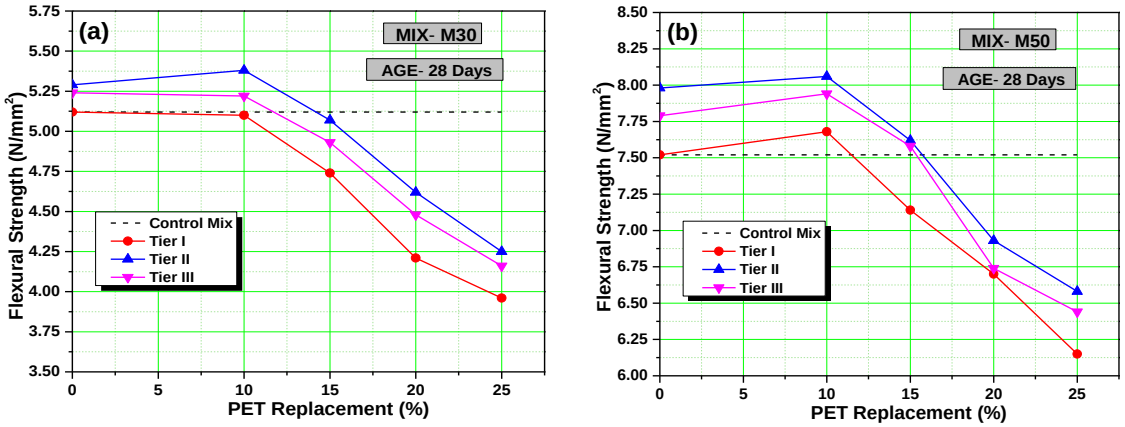

Fig. 5.14 Flexural Strength of concrete mixes (a) M30 (b) M50

From the failure patterns of the specimens, it was observed that there was no brittle failure of the PET-incorporated specimens. The specimens did not split into two pieces like the control specimen. This may be due to the bridging of fine cracks by the PET particles. Hannawi et al. (2010a) state that the plastic aggregates prolong the crack propagation interval. This is because the plastic-matrix interface act as an obstacle to the propagation of micro crack by the vacuum available at the interface. This decreases the stress concentration and delays the coalescence of the micro-cracks (Hannawi et al., 2010a).

The tier II mixes of mortar and concrete showed flexural strength trends similar to those observed in the case of compressive strength. The blending of SFS aggregates could enhance the flexural behavior of the mixes. The improvement in flexural strength of the mixes due to slag incorporation was of lower magnitude than the improvement witnessed in compressive strength values. The baseline mixes in tier II with 0% PET-Sand showed an increase of 8-9% in mortar samples and 3-6% in concrete samples, the range being 11-12% in the case of compressive strength values. At 10% incorporation of PET-Sand, a synergetic effect of better bond characteristics of SFS aggregates (as discussed in the compressive strength essay) and bridging action of PET fragments led to enhanced flexural performance in the composites with flexural strength enhancement in the range of 8-10%. The mixes in Tier II showed a better flexural performance than Tier I mixes. For a maximum substitution level of 25%, the strength recovery of 2.5-5% over Tier I mixes was observed in the investigation. In this tier, the mixes with 15% PET inclusions exhibited the flexural strength behavior of the control mix for both composites.

In the case of Tier III mixes in which FLA was used as SCM with OPC, the results showed trends similar to Tier II mixes. However, due to the slow reactivity of FLA at early ages, the strength development was moderately inferior to the tier II mixes. The 28-day flexural strength values for mortar specimens with 25% PET sand were 22.4% and 25.5% lower than the control mix for the 1:3 and 1:5 mix respectively. For M30 and M50 grade concrete samples the corresponding reduction was 18.7% and 14.4% respectively. The flexural strength behavior is governed by the same factors that decide the response of the composites to compressive loading.

5.6 Splitting Tensile Strength of Concrete

Concrete is a material that exhibits poor resistance to tensile loading due to its brittle behavior. The measurement of the tensile strength of concrete is a difficult or rather impossible task as it is difficult to subject the specimens to truly axial loads in direct tension. Thus, the tensile behavior of concrete is determined by using indirect testing methods (Almeshal, et al., 2020b). It is determined as the tensile stress developed in the cylindrical concrete specimen when it splits across the vertical diameter under the action of compressive loads.

The splitting tensile strength test results for concrete specimens for M30 and M50 grade concrete for three tiers of mixes are summarized in Table 5.9 and Fig. 5.15.

5.6.1 Discussions

The outputs of the experimental determination of the split tensile strength of Tier I mixes highlighted that the strength dwindled with the increase in PET waste content, especially at higher levels of substitution beyond 10% volume. At lower volumes, there was a slight improvement in the tensile strength of the mixes. This is attributed to the higher tensile strength of PET particles compared to the other components in the concrete mix. The results showed that at 25% PET replacement, there was a reduction of 26.30% and 22.60% in tensile strength for M30 and M50 grade concrete respectively. At higher replacement ratios the lack of adhesion between the PET particles and cement paste is the decisive factor causing a reduction in the tensile strength of the concrete. The explanation for the loss of compressive strength and flexural strength in the concrete specimens due to the inclusion of PWA applies to the tensile strength as well. An increase in the ratio

between tensile strength and compressive strength was noted for concrete specimens with increasing PET content. This shows that the inclusion of PET in concrete increases the toughness behavior. From the pattern of failure, it was noted that PET particles prevented the sudden failure of the specimens and an additional loading was sustained by the samples even after the cracking phenomenon. Like flexural strength samples, the specimens with PET did not separate into two pieces under loading, probably due to the ability of PET fragments to bridge the cracks and transfer the applied load. Some PET particles were observed on the cracked surface which were debonded from the matrix without undergoing intrinsic material failure.

Table 5.9 Split tensile strength (N/mm^2) of concrete mixes

Identification	M30 mix		M50 mix	
	Split tensile strength	± Δ%	Split tensile strength	± Δ%
Control Mix (OPC/N-Sand)				
C_Y-C-P0	3.04	0.00	5.17	0.00
Tier I Concrete (OPC/ N-Sand+PET-Sand)				
C_Y-C-P10	3.05	+0.30	5.34	+3.30
C_Y-C-P15	2.82	-7.20	4.93	-4.60
C_Y-C-P20	2.61	-14.10	4.58	-11.40
C_Y-C-P25	2.24	-26.30	4.00	-22.60
Tier II Concrete (OPC/N-Sand+SFS-Sand+PET-Sand)				
C_Y-C-SP0	3.38	+11.20	5.69	+10.10
C_Y-C-SP10	3.26	+7.20	5.66	+9.50
C_Y-C-SP15	3.10	+2.00	5.19	+0.40
C_Y-C-SP20	2.86	-5.90	4.84	-6.40
C_Y-C-SP25	2.42	-20.40	4.31	-16.60
Tier III Concrete (OPC+FLA/N-Sand+SFS-Sand+PET-Sand)				
C_Y-CF-SP0	3.08	+1.30	5.32	+2.90
C_Y-CF-SP10	3.05	+0.30	5.32	+2.90
C_Y-CF-SP15	2.92	-3.90	5.04	-2.50
C_Y-CF-SP20	2.72	-10.50	4.51	-12.80
C_Y-CF-SP25	2.50	-17.80	4.36	-15.70

($_Y$=30 for M30 mix, $_Y$=50 for M50 mix)

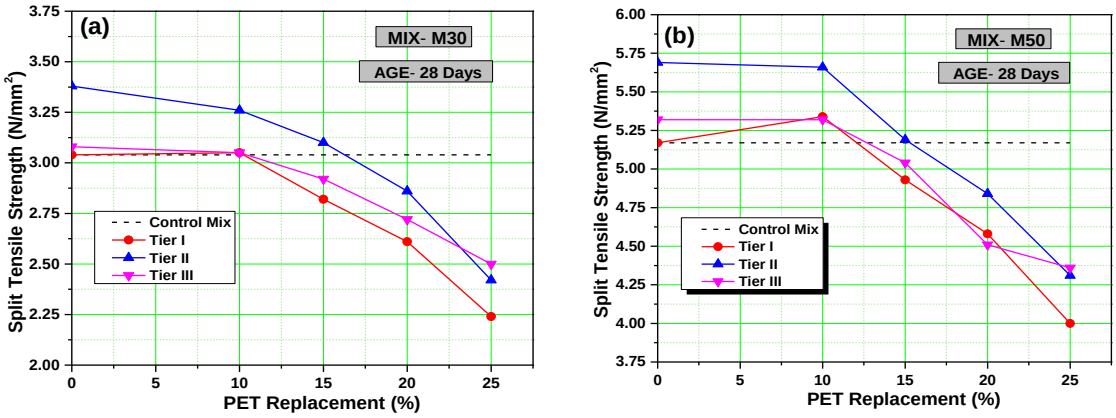

Fig. 5. 15 Split tensile strength of concrete mixes (a) M30 mix (b) M50 mix

For Tier II concrete samples, the results for tensile strength followed the trends observed in the case of compressive and flexural strength behavior. The explanation for the observed behavior as discussed for compressive strength can be applied to tensile strength too. The mixes with a 15% volume of PET-Sand showed tensile strength equivalent to the control mix due to the strength gain caused by the incorporation of SFS aggregates. The effect of SFS was also evident from the replenishment of tensile strength in the case of mixes with 25% PET in Tier II. There was a net recovery of 6% in the tensile strength in this mix compared to the corresponding mix in Tier I concrete for both grades of concrete.

For tier III mixes with FLA as a supplementary binder showed a response to tensile test similar to the tier II mixes. No significant variation in results was noticed in tensile strength at 28 days of age due to moderate reactivity of FLA at that age. Concrete with 10% PET in this tier matched the tensile behavior of the control mix. The mix with 25% PET in both grades showed an average decline of 17% compared to the control mix with an OPC binder, N-Sand, and no PET aggregates.

5.7 Modulus of elasticity of concrete

The modulus of elasticity is the ratio of stress to strain for hardened concrete. The deformation produced in concrete is influenced by the type of aggregate fillers in the concrete. It is directly related to the elastic deformation of the aggregates. It is the parameter to determine the stiffness of concrete.

The results of the modulus of elasticity of concrete specimens containing increasing proportions of PET-Sand are summarized in Table 5.10 and Fig. 5.16 for all the tiers of concrete for M30 and M50 grades.

Table 5.10 Modulus of elasticity (GPa) of concrete mixes

Identification	M30 mix		M50 mix	
	Modulus of elasticity	± Δ%	Modulus of elasticity	± Δ%
Control Mix (OPC/N-Sand)				
C_Y-C-P0	30.84	0.00	39.68	0.00
Tier I Concrete (OPC/ N-Sand+PET-Sand)				
C_Y-C-P10	30.64	-0.60	40.22	+1.40
C_Y-C-P15	29.12	-5.60	39.22	-1.20
C_Y-C-P20	27.67	-10.30	36.44	-8.20
C_Y-C-P25	24.22	-21.50	33.25	-16.20
Tier II Concrete (OPC/N-Sand+SFS-Sand+PET-Sand)				
C_Y-C-SP0	33.76	+9.50	42.26	+6.50
C_Y-C-SP10	32.56	+5.60	40.52	+2.10
C_Y-C-SP15	31.54	+2.30	39.94	+0.70
C_Y-C-SP20	28.66	-7.10	38.12	-3.90
C_Y-C-SP25	25.68	-16.70	34.68	-12.60
Tier III Concrete (OPC+FLA/N-Sand+SFS-Sand+PET-Sand)				
C_Y-CF-SP0	31.56	+2.30	40.22	+1.40
C_Y-CF-SP10	32.46	+5.30	39.86	+0.50
C_Y-CF-SP15	29.54	-4.20	37.80	-4.70
C_Y-CF-SP20	27.46	-11.00	34.24	-13.70
C_Y-CF-SP25	25.25	-18.10	33.76	-14.90

($_Y$=30 for M30 mix, $_Y$=50 for M50 mix)

5.7.1 Discussions

Similar to the results of the compressive strength, the modulus of elasticity of concrete containing PET-Sand showed a reduction in values with increasing plastic aggregates in the mix. Tier I concrete showed a gradual reduction in elasticity modulus values extending to 21.5% lower than the control mix when a 25% volume of PET was incorporated into the mix. The main reason for the drop in elastic modulus is the low elastic modulus of PET aggregates. The plastic fragments are comparatively more flexible

than natural aggregates. The incorporation of such a material makes concrete more deformable leading to a decline in its elasticity modulus. This behavior is in agreement with the theory of composite materials, which states that the elastic behavior of the composite depends mainly on the elastic properties of the constituent materials and their relative proportions in the composite (Babafemi et al. 2018). The drop in elasticity modulus can also be linked to an increase in the porosity of the composites with the increase in plastic inclusions due to various reasons already discussed under the explanation for the compressive strength behavior of PET-modified concrete. It can be seen that the drop in elastic modulus for low-strength concrete with a higher water-cement ratio is more than for high-strength concrete with a low water-cement ratio. This is linked to the porosity increase in concrete with a higher water-cement ratio. Furthermore, it can be noticed that the decrease in elastic modulus is lower than the corresponding decrease in compressive strength. This signifies that compressive failure is influenced by stress concentrations in the weaker ITZ surrounding the plastic particles and elasticity depends on the constituents and their proportions in the mix (Babafemi et al. 2018). The decrease in elastic modulus is also attributed to the weak adhesion between the plastic and cement matrix due to the smooth and less porous surface of plastic aggregates.

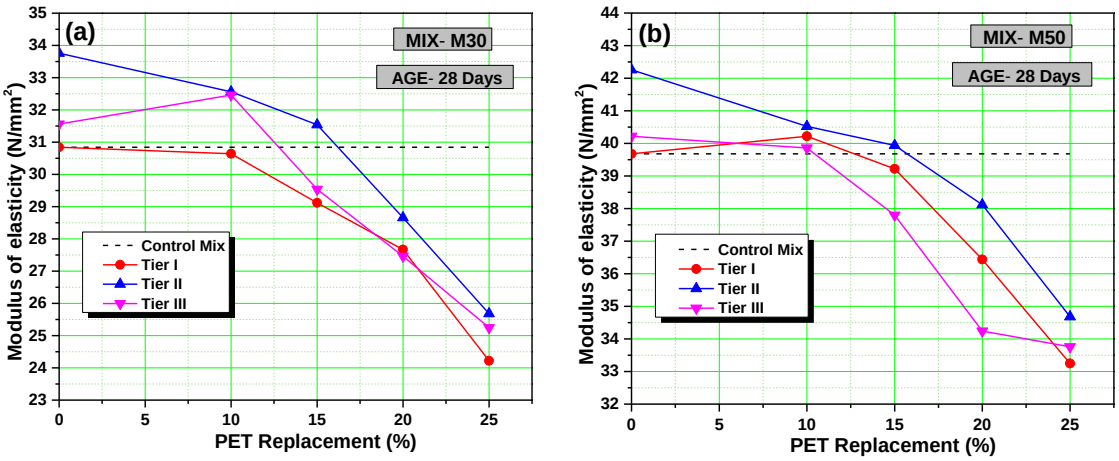

Fig. 5.16 Modulus of elasticity of concrete mixes (a) M30 mix (b) M50 mix

The utilization of SFS-Sand in Tier II concrete improved the modulus of elasticity of concrete due to improved strength of the blended aggregate and also improvement in bond characteristics between aggregates and cement paste. These high-density aggregates could mitigate the loss in modulus of elasticity caused by PET inclusion in the mixes. The loss in elastic modulus for 25% PET inclusion was reduced from 21.50% to 16.70% in

M30 concrete and from 16.20% to 12.60% in M50 grade concrete. The explanations for improvement in strength with SFS aggregates are also applicable to the elastic behavior of concrete too. Similar to Tier I mixes, the reduction in elastic modulus with PET volumes is observed to be lower than the corresponding reduction in compressive strength.

The tier III mixes with FLA as a supplementary binder and blended aggregate containing N-Sand and SFS-Sand also witnessed a decline in modulus of elasticity with an increase in PET content in the mix. However, the gain in elasticity due to the incorporation of SFS, as observed in tier II mixes was partially sacrificed due to the lower early strength development of FLA in the mix. Mixes in tier III with 25% PET showed a further decrease of 1.4% and 2.3% in elastic modulus over tier II mixes for M30 and M50 grade concrete.

5.8 Ultrasonic Pulse Velocity (UPV) of Concrete

UPV of concrete is an indicator of the homogeneity and structure of concrete and is determined using a non-destructive test. The UPV value of concrete can give an idea about the strength and durability of concrete. It is used in structural surveys to detect cracking or deterioration in concrete, determine the existence of cracks and voids and assess the relative quality and uniformity of concrete.

The results of the UPV test on concrete samples at 28 days and 90 days of age are summarized in Table 5.11 and a plot of UPV value against the percentage substitution of PET-Sand is presented in Fig. 5.17 and 5.18.

5.8.1 Discussions

The results of the UPV test show that there is a decline in UPV at every substitution of N-Sand by PET waste at both the curing regimes, i.e., 28 days and 90 days. The effect is significantly visible in the case of Tier I concrete. At 28 days of curing, the decline in UPV is approximately 30% for a 25% volume substitution of PET waste for M30 grade concrete. It is a known fact that the ultrasonic wave propagation speed is influenced by the porosity of the material which is dependent on the density and elastic properties of the material (Akçaözoğlu et al. 2013). Results of bulk density and modulus of elasticity of concrete containing PET have shown that as the PET content in the mix

increases, there is a sharp decrease in density and elasticity values. The decrease in UPV with the increase in PET content confirms the correlation between these parameters. The decrease in UPV is mainly due to the lack of compactness in the case of PET-modified mixes. The addition of PET increases the porosity of concrete due to the formation of air pockets or cavities inside the concrete. These cavities cause the attenuation of the ultrasonic waves due to the acoustic impedance. The incident wave passes through three different materials, i.e., concrete matrix, PET, and voids. This wave is partially reflected and partially transmitted. This causes a reduction in the velocity of waves. This effect is further aggravated by the poor elasticity of PET inclusions. The more the volume of PET, there is an increased reduction in the UPV of the mix. The results also show that the corresponding loss in UPV for M50 grade concrete was 2-3% lower than M30 grade concrete. This indicates a better microstructure of higher-strength concrete with a lower w/c ratio than low-strength concrete with a higher w/c ratio. This also signifies that the PET mixes with higher w/c ratios have higher void contents. These voids are the result of the evaporation of excess water available in the mix due to the hydrophobic nature of plastics. These voids contribute to the constriction in UPV. The increase in UPV with age is due to the same reasons that are responsible for strength gain in concrete with curing time. It is due to the physical-chemical changes that occur in the concrete consequent to the better hydration reactions that occur inside the mix at prolonged curing periods.

Tier II mixes are characterized by an improved microstructure due to the incorporation of SFS-Sand having a better interlocking with the cement matrix compared to N-Sand. The effect is already confirmed through the improved compressive strength of the mixes in Tier II. The UPV results of Tier II mixes also showed an increase in velocity values, however, the increase was proportionally lower than that of compressive strength values. This increase in UPV of the mixes is attributed to the ability of the slag to provide a relatively denser concrete than Tier I mixes. M50 grade concrete presented relatively higher pulse velocity than M30 grade concrete. The M30-grade concrete with 25% PET in Tier II mixes showed a reduction of 27.5% and 26.2% compared to the control mix at 28 days and 90 days respectively. The corresponding values were 25.6% and 23.6% for M50-grade concrete. These values are 2.6-4.0% higher than the corresponding values of Tier I mixes depicting the better quality of Tier II mixes in comparison to Tier I mixes.

Table 5.11 Ultrasonic Pulse Velocity (m/sec) of concrete mixes

Mix	M30 mix				M50 mix			
	28 days	±Δ%	90 days	±Δ%	28 days	±Δ%	90 days	±Δ%
Control Mix (OPC/N-Sand)								
C_Y-C-P0	4318	0.00	4364	0.00	4896	0.00	4919	0.00
Tier I Concrete (OPC/N-Sand+PET-Sand)								
C_Y-C-P10	4202	-2.70	4267	-2.20	4806	-1.80	4826	-1.90
C_Y-C-P15	4008	-7.20	4062	-6.90	4447	-9.20	4421	-10.10
C_Y-C-P20	3621	-16.10	3652	-16.30	3964	-19.00	3986	-19.00
C_Y-C-P25	3426	-20.70	3482	-20.20	3680	-24.80	3702	-24.70
Tier II Concrete (OPC/N-Sand+SFS-Sand+PET-Sand)								
C_Y-C-SP0	4396	+1.80	4405	+0.90	4920	+0.50	5196	+5.60
C_Y-C-SP10	4324	+0.10	4389	+0.60	4906	+0.20	4926	+0.10
C_Y-C-SP15	4122	-4.50	4256	-2.50	4568	-6.70	4586	-6.80
C_Y-C-SP20	3818	-11.6	3986	-8.70	4106	-16.10	4138	-15.90
C_Y-C-SP25	3516	-18.6	3542	-18.80	3808	-22.20	3896	-20.80
Tier III Concrete (OPC+FLA/N-Sand+SFS-Sand+PET-Sand)								
C_Y-CF-SP0	4364	+1.10	4428	+1.50	4829	-1.40	5123	+4.10
C_Y-CF-SP10	4294	-0.60	4398	+0.80	4562	-6.80	4985	+1.30
C_Y-CF-SP15	4042	-6.40	4325	-0.90	4351	-11.10	4732	-3.80
C_Y-CF-SP20	3866	-10.50	4008	-8.20	3927	-19.80	4363	-11.30
C_Y-CF-SP25	3562	-17.50	3594	-17.60	3748	-23.40	4086	-16.90

($_Y$=30 for M30 mix, $_Y$=50 for M50 mix)

The pulse velocity values of tier III mixes with FLA as a supplementary binder follow a similar trend of decline in UPV values with the increase in PET volume inside the concrete. However, the UPV at an earlier curing regime is reduced substantially due to the slow reactivity of FLA. This is evident from a decrease of 32.80% in UPV value compared to the control mix in the M30 mix when 25% N-Sand is replaced by PET-Sand. The delayed reaction of FLA is reflected through the improved values of UPV at 90 days of the age of concrete. An improvement in UPV values by 3-6% above Tier I and Tier II mixes depicts that at older ages concrete with SFS aggregates and FLA as a supplementary binding component can improve the quality of PET-modified concrete.

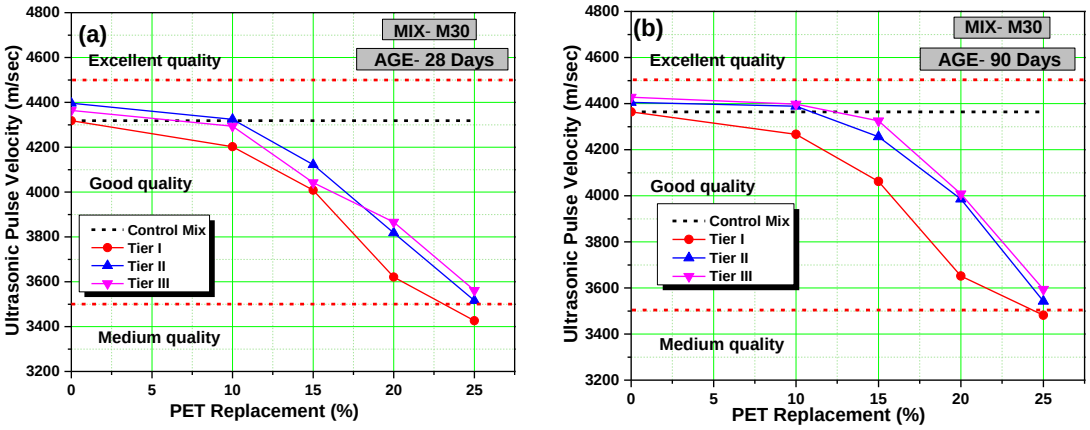

Fig. 5.17 Ultrasonic pulse velocity of M30 grade concrete (a) 28 days (b) 90 days

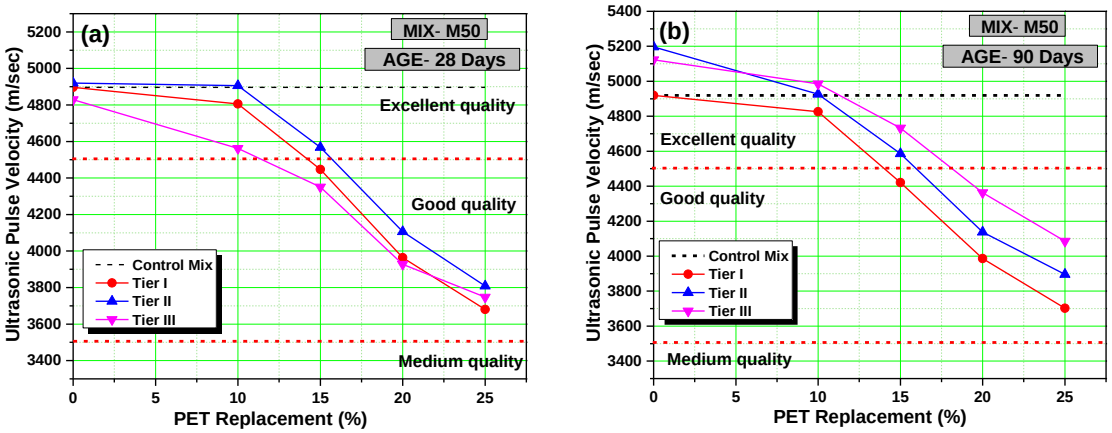

Fig. 5.18 Ultrasonic pulse velocity of M50 grade concrete (a) 28 days (b) 90 days

The Indian standard IS 516 (Part 5)-2018 suggests a guideline for practical evaluation of grading of concrete as shown in Table 5.12 (IS 516(5), 2018). The values of UPV for the Tier I mixes allow the categorization of the concrete as “good” quality, although there is a reduction in the values due to the incorporation of PET. Considering the values of pulse velocities at 90 days curing age the mixes up to 10% PET in M50 grade concrete exhibited the quality of “excellent” concrete as per IS specification in Table 5.12. On the other hand, the M30 mixes 20-25% PET could be rated as “medium” quality concrete.

5.9 Sorptivity of mortar and concrete

The sorptivity is one of the important parameters that indicate the porosity of the cementitious mixes. It is also related to the absorption kinetics of the mixes. It is the rate of water absorption by capillary suction exposed to water without applying any hydraulic

pressure. The sorptivity test for the mortar and concrete samples has been performed for the samples at 28 days of curing.

Table 5.12 Quality grading of concrete based on UPV values (IS 516(5), 2018)

Sr. No.	UPV (m/sec)	Concrete grading
1.	Above 4500	Excellent
2.	3500-4500	Good
3.	3000-3500	Medium
4.	Below 3000	Doubtful

5.9.1 Sorptivity of mortar

The sorptivity coefficients of mortar samples of 1:3 and 1:5 mix proportions for all three tiers are summarized in Table 5.13. The plots of sorptivity values against PET replacement ratios are presented in Fig. 5.19.

5.9.2 Sorptivity of concrete

The sorptivity coefficients of concrete samples of M30 and M50 grade mix proportions for all three tiers are summarized in Table 5.14. The plots of sorptivity values against PET replacement ratios are presented in Fig. 5.20.

5.9.3 Discussions

The sorptivity values of the cement composites indicate the liquid transfer behavior inside the mass. This behavior is directly related to the extent of porosity inside the mortar or concrete structure. The increase in porosity of the cement composites after the incorporation of PET has been discussed extensively in the current research through literature surveys as well as through explanations for the deterioration of the mechanical strength of composites. The results for the sorptivity of mortar and concrete specimens also agree with the finding that the porosity of cementitious mixes increases with the increase in plastic content inside the mix. This is evident from the linear increase in the sorptivity of mortar and concrete mixes with the increase in the substitution rate of PET. For tier I mortar mixes, a 25% replacement of N-Sand by PET-Sand showed an increase of sorptivity coefficient by 19.2% for the 1:3 mix and 21.1% for the 1:5 mix. In the case of Tier I concrete mixes the corresponding increase was found to be 13.5% and 9.20% for M30 and M50 grade concrete respectively. This increase is attributed to the increase

in porosity of the composites caused due to one or more of the following reasons: 1) the hydrophobic nature of PET particles causing availability of unreactive water inside the mix and subsequently generating void pockets after evaporation of free water; 2) the weak adhesion between PET and cement paste, and the resulting weak ITZ around the PET particles; 3) the difficulty in mixing and compaction due to the heterogeneous nature of plastic species in the otherwise homogenous mix (Bhagat and Savoikar, 2022). The porous openings are the preferential paths for the transport of water along the boundaries between the cement matrix and PET species.

Table 5.13 Sorptivity (x 10^{-3} cm/$sec^{1/2}$) of mortar mixes

Identification	1:3 mix		1:5 mix	
	Sorptivity coefficient	± Δ%	Sorptivity coefficient	± Δ%
Control Mix (OPC/N-Sand)				
M_x-C-P0	6.04	0.00	6.07	0.00
Tier I Mortar (OPC/N-Sand+PET-Sand)				
M_x-C-P10	6.18	+2.30	6.12	+0.80
M_x-C-P15	6.29	+4.10	6.38	+5.10
M_x-C-P20	6.58	+8.90	6.64	+9.40
M_x-C-P25	6.96	+15.20	7.24	+19.30
Tier II mortar (OPC/N-Sand+SFS-Sand+PET-Sand)				
M_x-C-SP0	5.76	-4.60	6.14	+1.20
M_x-C-SP10	6.04	0.00	6.20	+2.10
M_x-C-SP15	6.22	+3.00	6.33	+4.30
M_x-C-SP20	6.58	+8.90	6.62	+9.10
M_x-C-SP25	6.94	+14.90	7.01	+15.50
Tier III mortar (OPC+FLA/N-Sand+SFS-Sand+PET-Sand)				
M_x-CF-SP0	5.72	-5.30	6.02	-0.80
M_x-CF-SP10	6.00	-0.70	6.10	+0.50
M_x-CF-SP15	6.10	+1.00	6.30	+3.80
M_x-CF-SP20	6.37	+5.50	6.64	+9.40
M_x-CF-SP25	6.59	+9.10	6.96	+14.70

(x=3 for 1:3 mix and x=5 for 1:5 mix)

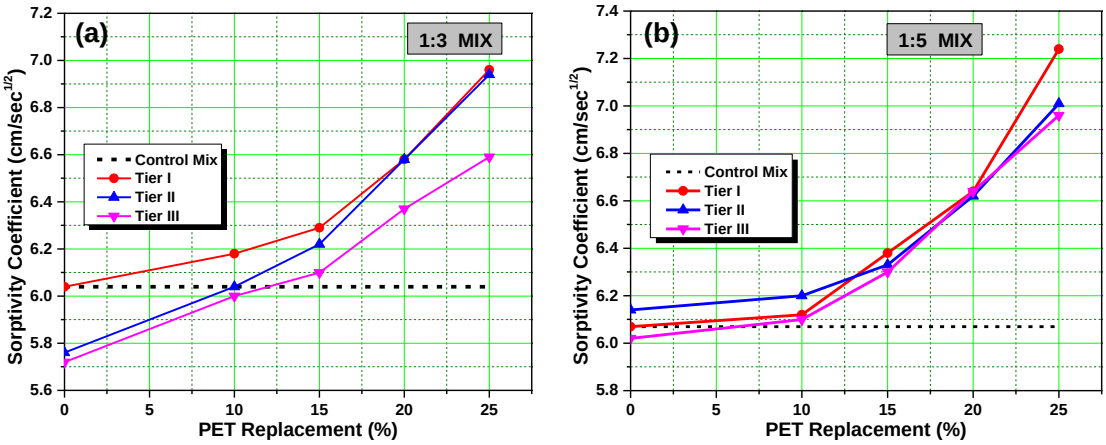

Fig. 5.19 Sorptivity coefficient of mortar mix (a) 1:3 mix and (b) 1:5 mix

Table 5.14 Sorptivity (x 10^{-3} cm/$sec^{1/2}$) of concrete mixes

Identification	M30 mix		M50 mix	
	Sorptivity coefficient	± Δ%	Sorptivity coefficient	± Δ%
Control Mix (OPC/N-Sand)				
C_Y-C-P0	5.62	0.00	5.24	0.00
Tier I Concrete (OPC/ N-Sand+PET-Sand)				
C_Y-C-P10	5.74	+2.10	5.31	+1.30
C_Y-C-P15	5.96	+6.00	5.39	+2.90
C_Y-C-P20	6.14	+9.30	5.50	+5.00
C_Y-C-P25	6.38	+13.50	5.72	+9.20
Tier II Concrete (OPC/N-Sand+SFS-Sand+PET-Sand)				
C_Y-C-SP0	5.27	-6.20	5.04	-3.80
C_Y-C-SP10	5.32	-5.30	5.12	-2.30
C_Y-C-SP15	5.52	-1.80	5.26	+0.40
C_Y-C-SP20	5.84	+3.90	5.44	+3.80
C_Y-C-SP25	6.10	+8.50	5.62	+7.30
Tier III Concrete (OPC+FLA/N-Sand+SFS-Sand+PET-Sand)				
C_Y-CF-SP0	5.54	-1.40	5.04	-3.80
C_Y-CF-SP10	5.62	+0.00	5.14	-1.90
C_Y-CF-SP15	5.79	+3.00	5.26	+0.40
C_Y-CF-SP20	5.94	+5.70	5.46	+4.20
C_Y-CF-SP25	6.18	+10.00	5.67	+8.20

($_Y$=30 for M30 mix, $_Y$=50 for M50 mix)

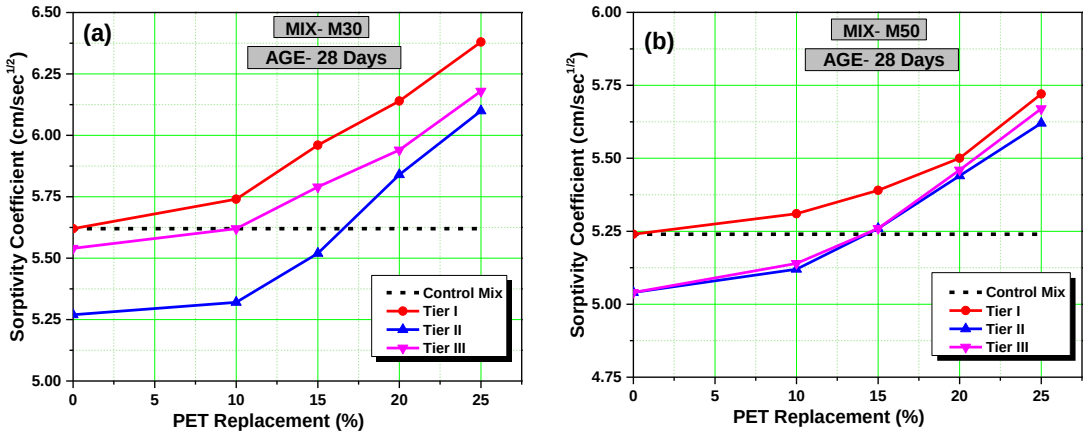

Fig. 5.20 Sorptivity coefficient of concrete mixes (a) M30 (b) M50

For corresponding percentage replacement ratios of PET, the Tier II mixes showed reduced capillary absorption relative to the Tier I mix. The incorporation of SFS slag in the mixes could improve the workability of the mix and provide a compact mass of the composites compared to the Tier I mix. In addition, the improved bond between the fine aggregates and the cement pastes due to SFS incorporation also contributed to the decrease in relative absorption. The results also advocated the finding that low-strength concrete exhibits higher capillary absorption and vice versa (Babu and Babu, 2004). In the case of Tier II mixes of mortar, the mix with 10% PET showed sorptivity values closer to the control mix, whereas, the concrete mixes maintained the control mix sorptivity till the 15% incorporation of PET sand.

Tier III mixes of mortar and concrete exhibited sorptivity values intermediate between Tier I and Tier II mixes for corresponding PET substitution levels. The use of FLA in the mix together with SFS could give better compaction due to enhanced workability. Moreover, the use of FLA could deliver additional paste in comparison to cement binder allowing improved pore-filling effect. However, the proportionate reduction in sorptivity values was hindered by incomplete hydration of FLA at 28 days of curing. It is expected that at prolonged curing regimes, the capillary absorption may decrease substantially for Tier III mixes due to the better reactivity of FLA at older ages. Such a complementary effect of using EAF slag and FLA in concrete containing CDW was presented by Anastasiou et al. (2014). The authors showed a reduction in capillary absorption by 14% between control concrete and concrete containing CDW, EAF slag, and FLA supplementary binder (Anastasiou et al., 2014). In the case of PET fine

aggregate concrete, Sadrmomtazi et al. (2016) also reported the positive influence of FLA in reducing water transportation behavior. The water absorption by immersion was reduced by 18% due to the addition of FLA (Sadrmomtazi et al., 2016).

5.10 Permeability of concrete

Permeability of concrete is the property that indicates the vulnerability of the material to the ingress of aggressive forms of chemical species. It is one of the important durability-related parameters of concrete. It also indicates the susceptibility of concrete to the permeation of gases such as carbon dioxide and other suspended ions that might lead to undesirable effects on the long-term performance of cementitious mixes and reinforcement embedded within the mixes (Bhagat and Savoikar, 2022; Mercante et al., 2018; H. Mohammed et al., 2020a). The results of the permeability test conducted on concrete samples for 28 days and 90 days curing regime are presented in Table 5.15 and Fig. 5.21 and 5.22. The test is performed as per the procedure prescribed in BS EN 12390–8:2019 (EN 12390, 2019). This standard provides permeability values in terms of the depth of penetration of water under pressure in millimetres.

5.10.1 Discussions

The permeability of water under pressure for concrete specimens for M30 and M50 grades showed an increasing trend with the increase in PET content of the mixes, irrespective of the tier of the mix. The attributes for the observed increase are the same factors that explained the increase in sorptivity of the mixes with increasing contents of plastics. The increase in porosity and an affected ITZ due to plastic inclusions is the main reason for the increase in permeability of the specimens. The disrupted ITZ between plastic and cement paste acts as a bridge between the pores already existing in the global mass of the composite assisting the transfer of water through it.

Accordingly, Tier I mixes showed permeability values ranging from 8.40 mm to 15.80 mm at 28 days of the age of concrete for PET dosage from 0% to 25%. The prolonged curing allowed better pore refinement and improved microstructure of concrete resulting in lower values of permeability at 90 days of the age of concrete. The studies on permeability characteristics of plastic-incorporated concrete are scanty. For PET-based concrete, Saxena et al. (2020) presented significantly higher values of water penetration

between 40-70mm for 10-15% weight replacement of fine aggregates by PET waste(R. Saxena et al., 2020).

Table 5.15 Permeability (mm) of concrete mixes

Identification	M30 mix		M50 mix	
	28 days	90 days	28 days	90 days
Control Mix (OPC/N-Sand)				
C_Y-C-P0	8.40	7.60	8.40	6.80
Tier I Concrete (OPC/ N-Sand+PET-Sand)				
C_Y-C-P10	10.40	10.00	10.20	8.50
C_Y-C-P15	10.90	10.60	10.60	8.90
C_Y-C-P20	14.20	13.70	14.20	13.20
C_Y-C-P25	15.80	15.50	15.70	14.90
Tier II Concrete (OPC/N-Sand+SFS-Sand+PET-Sand)				
C_Y-C-SP0	8.20	8.00	8.20	7.60
C_Y-C-SP10	11.00	9.50	8.40	8.10
C_Y-C-SP15	10.80	10.60	10.80	10.20
C_Y-C-SP20	13.90	12.80	11.20	10.70
C_Y-C-SP25	15.40	13.80	13.20	12.60
Tier III Concrete (OPC+FLA/N-Sand+SFS-Sand+PET-Sand)				
C_Y-CF-SP0	8.80	7.80	8.40	6.40
C_Y-CF-SP10	9.50	8.20	8.70	7.20
C_Y-CF-SP15	11.60	9.00	10.60	8.40
C_Y-CF-SP20	14.50	11.90	12.30	10.10
C_Y-CF-SP25	15.90	13.40	14.70	12.40

($_Y$=30 for M30 mix, $_Y$=50 for M50 mix)

Considering the significant effect of SFS on the mechanical properties of concrete, Tier II mixes were expected to provide a significant reduction in permeability. However, at 28 days of age, the mixes in Tier II exhibited permeability values in a range very close to Tier I mixes for corresponding replacement ratios of PET. At the older age of 90 days, the mixes showed better resistance to permeability relative to Tier I mixes.

At an earlier curing age of 28 days, the Tier III mixes also showed permeability behavior similar to Tier I mixes. Although the mixes with SFS-Sand and FLA had better compaction abilities due to increased workability, the moderate reactivity of FLA

compared to OPC at an earlier age could not offer the benefit of improved microstructure at an early age. This benefit was observed at an older curing regime of 90 days and the mixes showed permeability values of 13.40 mm and 12.40 mm for M30 and M50 grade concrete mixes for 25% substitution of N-Sand by PET-Sand. Comparing these values with the corresponding results of Tier I mixes which reads as 15.50 mm and 14.90 mm, it can be said that the use of FLA and SFS-Sand in the PET-modified mixes can improve the resistance of the concrete to the permeability of liquids, especially at older curing periods.

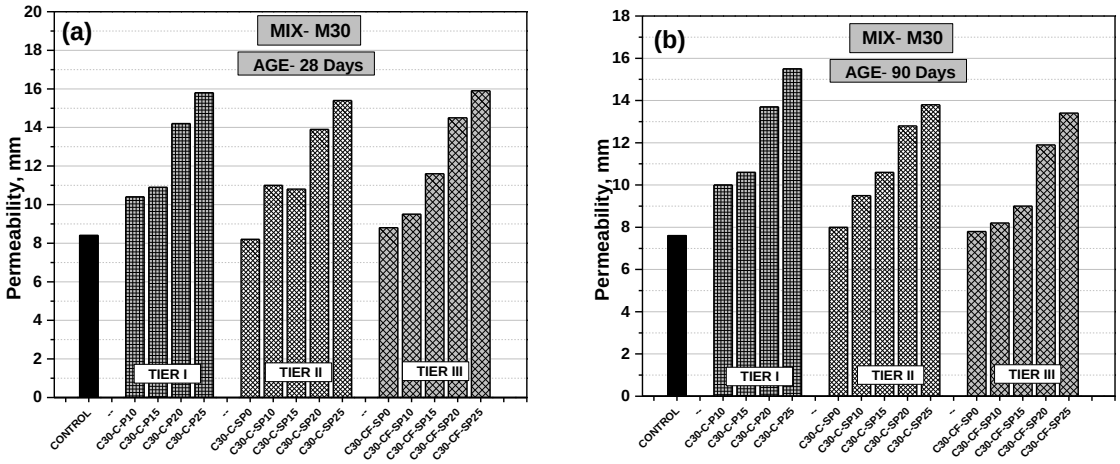

Fig. 5.21 Permeability of M30 concrete mix (a) 28 days (b) 90 days

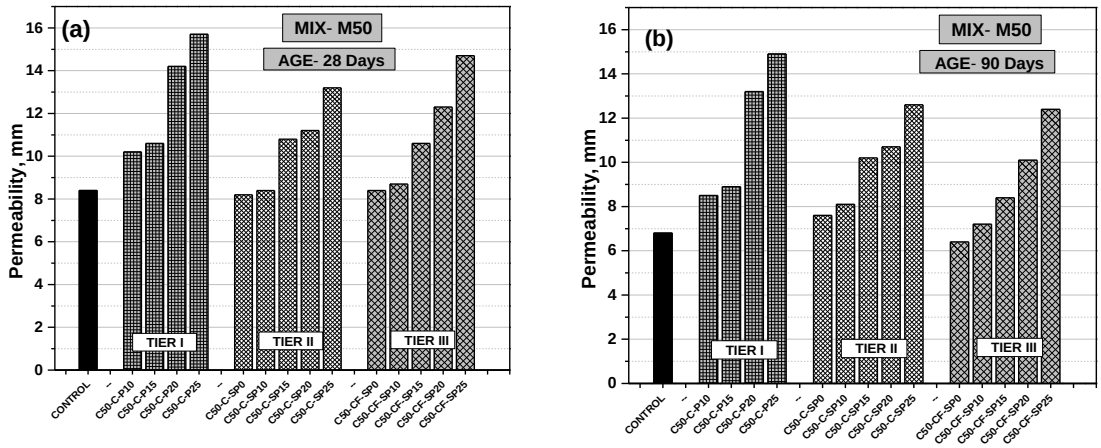

Fig. 5.22 Permeability of M50 concrete mix (a) 28 days (b) 90 days

5.11 Chloride Migration in Concrete

Chloride migration is known to be one of the indicative parameters of durability and long-term service life of concrete, especially when the concrete is reinforced.

Chloride migration in concrete can cause de-passivation of steel reinforcement, initiating corrosion of steel and ultimately interfering with the serviceability of the concrete structure (Bhagat and Savoikar, 2022). It is known that chloride migration is dependent on the absorption, porosity, and permeability of concrete mass. The observations about these parameters in the current research point to the hypothesis that chloride migration increases with the increase in PET proportion in the mix. However, the hypothesis is not supported by the experimental results. The chloride migration coefficients for both grades of concrete are presented in Table 5.16 and also summarized in Fig. 5.23 and 5.24.

Table 5.16 Chloride migration coefficient ($\times 10^{-12}$ m^2/s) of concrete mixes

Mix	M30 mix				M50 mix			
	28 days	±Δ%	90 days	±Δ%	28 days	±Δ%	90 days	±Δ%
Control Mix (OPC/N-Sand)								
C_Y-C-P0	9.64	0.00	8.94	0.00	7.30	0.00	6.24	0.00
Tier I Concrete (OPC/N-Sand+PET-Sand)								
C_Y-C-P10	8.82	-8.50	8.26	-7.60	6.92	-5.20	6.02	-16.20
C_Y-C-P15	8.14	-15.60	7.96	-11.00	6.04	-17.30	5.48	-23.70
C_Y-C-P20	7.82	-18.90	7.46	-16.60	5.20	-28.80	5.01	-30.20
C_Y-C-P25	8.64	-10.40	8.36	-6.50	5.69	-22.10	5.32	-25.90
Tier II Concrete (OPC/N-Sand+SFS-Sand+PET-Sand)								
C_Y-C-SP0	9.96	+3.30	9.76	+9.20	7.12	-2.50	7.42	+3.30
C_Y-C-SP10	8.88	-7.90	8.04	-10.10	6.12	-16.20	6.82	-5.00
C_Y-C-SP15	8.16	-15.40	8.02	-10.30	5.86	-19.70	5.73	-20.20
C_Y-C-SP20	7.88	-18.30	7.26	-18.80	5.25	-28.10	4.94	-31.20
C_Y-C-SP25	8.28	-14.10	7.96	-11.00	5.82	-20.30	5.22	-27.30
Tier III Concrete (OPC+FLA/N-Sand+SFS-Sand+PET-Sand)								
C_Y-CF-SP0	8.86	-8.10	8.64	-3.40	7.46	+2.20	6.30	+1.00
C_Y-CF-SP10	7.42	-23.00	7.04	-21.30	6.22	-14.80	5.81	-6.90
C_Y-CF-SP15	6.87	-28.70	6.54	-26.80	5.04	-31.00	4.85	-22.30
C_Y-CF-SP20	5.79	-39.90	5.60	-37.40	4.94	-32.30	4.64	-25.60
C_Y-CF-SP25	7.20	-25.30	6.72	-24.80	5.62	-23.00	4.94	-20.80

($_Y$=30 for M30 mix, $_Y$=50 for M50 mix)

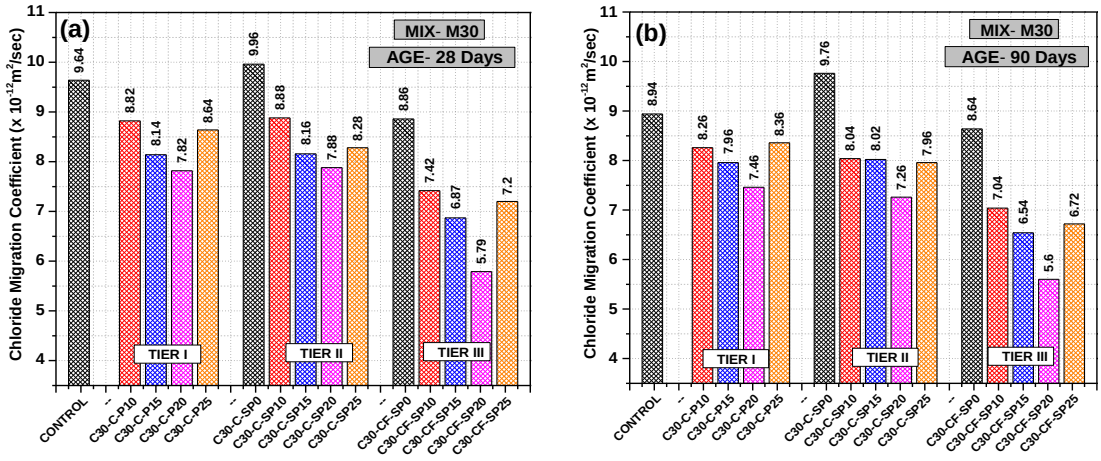

Fig. 5.23 Chloride migration coefficients of M30 mix (a) 28 days (b) 90 days

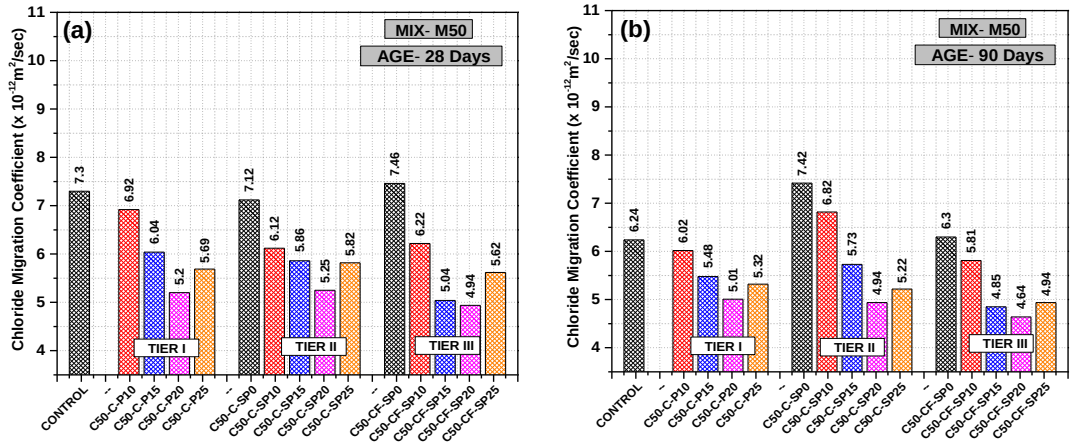

Fig. 5.24 Chloride migration coefficients of M50 mix (a) 28 days (b) 90 days

5.11.1 Discussions

In general, the mechanism of chloride ion diffusion is the process of ion exchange between the aggressive diffusing solution and interstitial solution inside the concrete. Therefore, generally, it can be stated that more the porosity inside the concrete, the more chloride ion diffusion. The explanations presented for the degradation of the mechanical performance of concrete in the current research have repeatedly mentioned that the increase in porosity of the composites due to the incorporation of plastic species is the major factor responsible for the quality degradation. The severity of the effect increases with the increase in the plastic content inside the mix. This aspect hints at the finding that the chloride migration in the concrete may increase with an increase in plastic content. However, the results have presented a contrary outcome for all the mixes up to 20%

substitution of PET waste. The chloride migration coefficient showed a declining trend with an increase in plastic volumes from 10% to 20%. This reduction in chloride migration is attributed to the impervious nature of PET particles. The impervious nature of PET particles is considered to be a hindrance to the passage of chloride ion transfer, thereby causing a diminution in chloride migration. This attribute has been ubiquitously accepted by a few studies conducted on concrete containing PET, PP, and PVC aggregates (Alqahtani et al., 2018; Gouasmi et al., 2019; Kou et al., 2009; Shanmugapriya and Santhi, 2017). The results disagree with the findings by Silva et al. (2013) in the case of PET aggregates and Faraj et al. (2019) in the case of PP aggregates. Both these studies have reported an increase in chloride penetration with the increase in plastic content in concrete. It is noteworthy that this disagreement is valid for up to 20% substitution of PET sand and the chloride migration coefficient increases at a 25% replacement ratio. This observation signifies that the effect of disrupting the chloride ion transfer diminishes beyond 20% PET substitution. It may be due to the increase in porosity of the mixes which may suppress the chloride shielding effect of PET (Faraj et al. 2019; Silva et al. 2013). Such a behavior has been advocated by an experimental study by Senhadji et al. (2015) for concrete containing PVC aggregates. The authors found that, until a threshold substitution level of 50%, the chloride penetration decreased with an increase in PVC content, and thereafter the values increased by 3% for 70% substitution volume (Senhadji et al. 2015).

Tier I and Tier II mixes showed a similar response to chloride migration with a marginal difference in the coefficients relative to control mixes for the corresponding substitution levels of PET. It could be seen that there was no significant effect of SFS-Sand on the chloride migration characteristics and the shielding effect of PET played a major role in deciding the behavior.

The use of pozzolanic admixture in the form of FLA showed a significant reduction in chloride migration for all the mixes up to the threshold substitution level of 20% volume of PET. A reduction of 25-40% in chloride migration coefficient was reported relative to the control mix for 20% PET replacement in Tier III mixes. This is related to the enhancement of the chloride binding capacity of the ingredients of concrete by FLA in addition to the pore-filling effect. The chloride binding is mobilized through

the reaction of C_3A present in the hydrated cement paste that reacts with chloride ions. This leads to the generation of products like Friedel's salt ($3CaO\ Al_2O_3\ CaCl_2.\ 10H_2O$), inhibiting the movement of chloride ions. This reaction is further favored by the presence of alumina in the FLA-OPC mix and better hydration conditions due to the availability of excess free water in the mix, thanks to the hydrophobic nature of PET particles (Babu and Babu, 2004). From the results, it can be concluded that Tier III mixes with OPC-FLA binder blend and SFS-PET aggregate blend may provide better shielding against chloride ion passage and control de-passivation and corrosion of reinforcement in reinforced concrete members.

5.12 Resistance of concrete to elevated temperature

Concrete is a material that is known for the heterogeneous nature of the constituent materials of which it is made. Due to this fact, the response of concrete when exposed to elevated temperatures is very complex. At higher temperatures, concrete is subjected to a series of physical changes and chemical reactions having a direct impact on the mechanical performance of concrete. For concrete containing plastic species as aggregates, the exposure to elevated temperature is a testing time of its functionality because the decomposition temperature of plastics is significantly lower than the natural aggregate which is replaced. In the current research, concrete samples of M30 and M50 grade concrete cured for 90 days are exposed to elevated temperatures of 200ºC, 400ºC, and 600ºC. The residual compressive strength of the samples is determined at these three temperatures and compared with the strength of the corresponding mixes at ambient room temperature.

Table 5.17 summarizes the results of the residual compressive strength of the concrete samples of M30 and M50 grades in all three tiers at different thermal exposure conditions. The results are also presented graphically in Fig. 5.25 and 5.26 to exhibit the variation in residual strength of each tier of mix containing different PET proportions for different temperature exposures.

5.12.1 Discussions

From the results available on the residual compressive strength of the concrete mixes for both grades of concrete, it can be concluded that regardless of the composition,

the exposure of the mixes to elevated temperatures caused a drastic reduction in their compressive strength. The effect of thermal exposure was analyzed through the proportionate decrease in strength of a particular mix in relation to the compressive strength of that mix at the ambient temperature of 30ºC. For M30 grade concrete, the strength degradation was 20%, 23%, and 19% for Tier I, Tier II, and Tier III mixes respectively, the maximum decrease being reported for 25% PET inclusion in all the tiers. At 400ºC exposure, 25% PET-Sand caused a strength reduction of 37%, 44%, and 35% for Tier I, Tier II, and Tier III mixes respectively. At 600º C, Tier I and Tier II mixes with 25% PET-Sand were subjected to severe cracking before the completion of exposure time with their corners detached from the samples with explosive sound (see Fig. 5.25). However, Tier III samples with 25% were subjected to 55% strength loss at 600º C.

Table 5.17 Residual compressive strength (N/mm^2) of concrete mixes at different thermal exposures

Mix	M30 mix				M50 mix			
	30ºC	200ºC	400ºC	600ºC	30ºC	200ºC	400ºC	600ºC
Control Mix (OPC/N-Sand)								
C_Y-C-P0	43.80	40.84	36.40	30.86	65.20	62.84	58.26	50.46
Tier I Concrete (OPC/N-Sand+PET-Sand)								
C_Y-C-P10	44.60	40.52	35.86	30.24	66.04	60.82	54.32	48.67
C_Y-C-P15	38.64	33.84	28.45	24.10	62.14	56.64	50.32	44.26
C_Y-C-P20	35.02	28.64	24.16	17.82	57.02	47.62	40.02	32.46
C_Y-C-P25	32.08	25.62	20.22	-	50.84	42.26	33.84	24.28
Tier II Concrete (OPC/N-Sand+SFS-Sand+PET-Sand)								
C_Y-C-SP0	48.56	43.52	38.18	33.24	71.56	68.94	60.26	52.46
C_Y-C-SP10	47.38	42.21	37.62	31.1	68.20	61.64	56.72	47.62
C_Y-C-SP15	42.50	35.62	31.46	26.54	65.84	57.64	51.28	43.22
C_Y-C-SP20	37.24	30.24	24.32	21.46	60.20	50.36	42.62	35.25
C_Y-C-SP25	34.24	26.42	19.24	-	53.76	42.56	33.21	23.22
Tier III Concrete (OPC+FLA/N-Sand+SFS-Sand+PET-Sand)								
C_Y-CF-SP0	49.68	46.92	43.56	38.64	72.34	70.52	64.28	56.34
C_Y-CF-SP10	46.95	44.10	38.42	32.26	68.52	65.25	59.64	48.62
C_Y-CF-SP15	45.62	41.10	35.48	30.24	65.76	60.18	52.32	45.27
C_Y-CF-SP20	40.96	34.56	30.28	25.64	61.02	53.2	45.82	38.69
C_Y-CF-SP25	37.04	30.04	24.22	16.54	54.29	44.61	36.24	26.42

($_Y$=30 for M30 mix, $_Y$=50 for M50 mix)

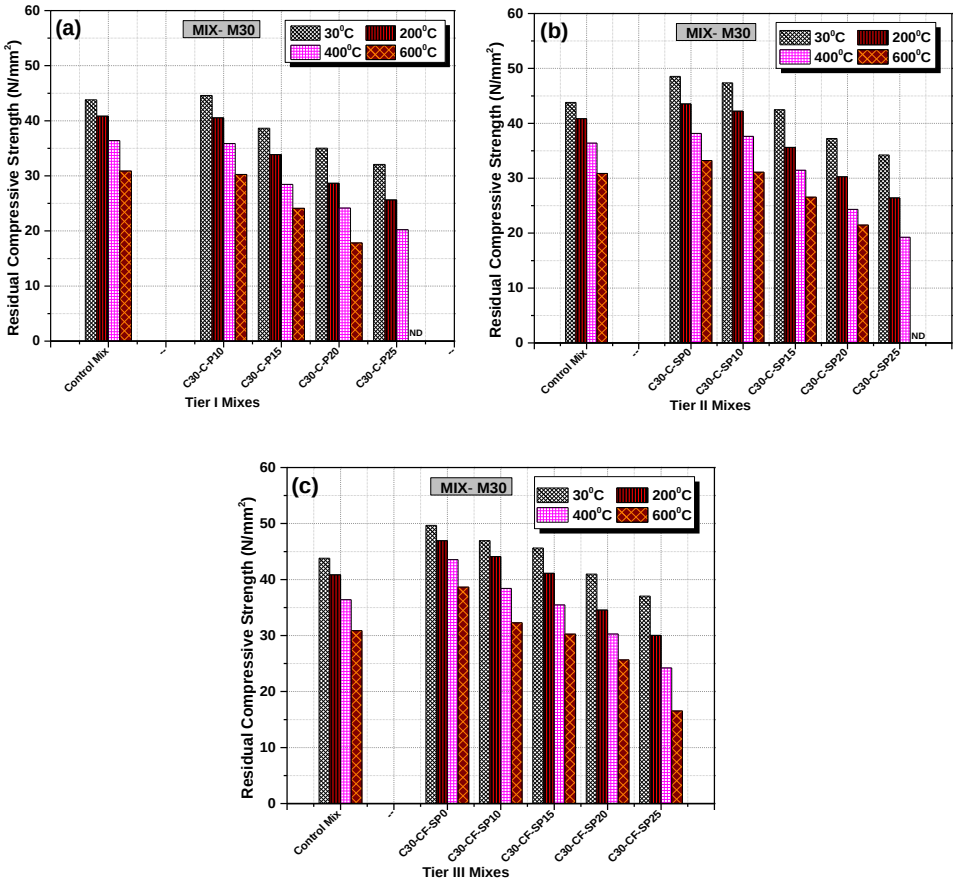

Fig. 5.25 Residual compressive strength of M30 Grade concrete at elevated temperature exposure conditions (a) Tier I (b) Tier II (c) Tier III

M50-grade concrete with a lower w/c ratio exhibited a lower strength loss than M30-grade concrete. For M50 grade concrete, at 200º C, the strength reduction was 17%, 21%, and 18% for Tier I, Tier II, and Tier III mixes respectively. However, the corresponding values at 400º C were 33%, 38%, and 33%. At 600º C, the strength deterioration extended to 52%, 57%, and 51% for the respective tiers.

The degradation in the strength of the concrete on exposure to elevated temperatures is due to the thermal gradient as well as different physical and chemical transformations inside the concrete. Similar to the negative effect on other properties, the porosity induced in concrete due to the incorporation of PET affects the behavior of concrete against thermal exposure too. The enhanced porousness of concrete due to PET causes an imbalanced thermal gradient inside the concrete mass initiating crack development inside the concrete. Also, volumetric changes are induced inside concrete due to the dehydration of cement paste. This effect is predominant in the case of a lower

range of elevated temperature, i.e., 200º C. However, at a temperature of 400º C, the effect is further aggravated due to the thermodegradative nature of PET. It is because the decomposition temperature of PET lies between 350ºC to 450ºC. So, when this decomposition temperature of PET is surpassed, volatile products are formed inside the concrete mass which leads to a further increase in porosity and associated thermal stress inside the mass. Furthermore, Albano et al. (2009) stated that there can be a reaction of involatile products inside the concrete leading to the formation of internal cavities which are the sites of stress concentration (Albano et al. 2009). All these factors are responsible for strength deterioration at higher temperatures. There are certain possibilities that the water vapors entrapped in the cavities or holes are not discharged out. These water vapors not only initiate cracking due to the build-up of pore pressure but can lead to explosive fissuring of specimens as observed in the cases of 25% PET mixes of tier I and tier II compositions for M30 grade concrete.

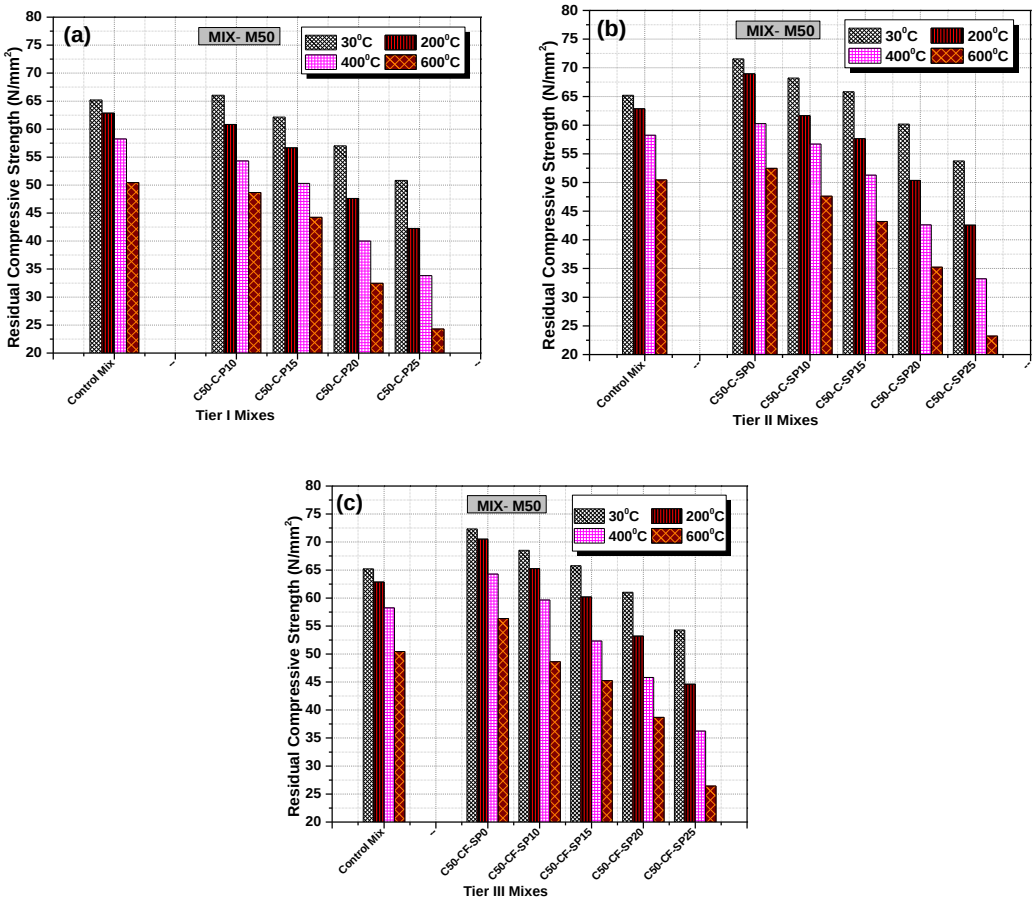

Fig. 5.26 Residual compressive strength of M50 Grade concrete at elevated temperature exposure conditions (a) Tier I (b) Tier II (c) Tier III

A drastic reduction in residual compressive strength is noticed at 600ºC exposure condition. The increase in temperature in this range causes a major chemical change in concrete microstructure. At around 400º C, the C-S-H gel and $Ca(OH)_2$ crystals in the paste start decomposing causing irreversible damage to the internal structure of the concrete. This causes strength degradation in concrete. Furthermore, at significantly higher temperatures of 600º C, the majority of C-S-H gel and $Ca(OH)_2$ crystals get decomposed with severe damage to the microstructure of concrete causing further reduction in residual strength (Wang et al., 2017). In addition to these factors, for plastic-modified concrete, Saxena et al. (2018) explained that when PET undergoes thermal decomposition, there is a splitting of ester links to form vinyl easter and carboxylic acid-ended oligomers (Martín-Gulló et al. 2001). These oligomers further decompose in the gas phase to form CO, CO_2, hydrocarbons, aliphatic aldehydes, aromatic hydrocarbons, acids, ketones, and esters (Bednas et al., 1981). The formation of these products is responsible for the void formation and thermal cracking of concrete.

The comparative analysis of the residual compressive strengths of the three tiers of concrete revealed that the Tier III concrete with FLA as a supplementary binder and optimum blend of SFS-Sand with N-sand performed better than the Tier I and Tier II mixes. This enhanced performance of the Tier III mix can be attributed to the contribution of FLA in providing a relatively less porous concrete mass due to the pore-filling effect and higher paste volumes than OPC mixes. Among Tier I and Tier II mixes, the strength degradation in Tier II mixes was reported to be higher. This may be due to the higher thermal conductivity of SFS aggregates than N-Sand and the higher thermal gradient set up inside the mass. Also, higher-strength concrete of M50 grade exhibited lower strength degradation than M30 grade concrete. This observation was in agreement with the findings by Albano et al. (2009).

Most of the specimens showed cracks on their surface. The length and width of cracks were more for specimens exposed to higher temperatures. Few specimens showed signs of spalling, mostly localized at the corners of the specimens. The surface colors of the specimens were subjected to significant changes. Some specimens showed brown/black stains on the surface due to incomplete combustion of some plastic waste particles. While some specimens showed voids on the surface due to the decomposition

of PET particles. The photographic images of a few samples exposed to elevated temperatures are presented in Fig. 5.27.

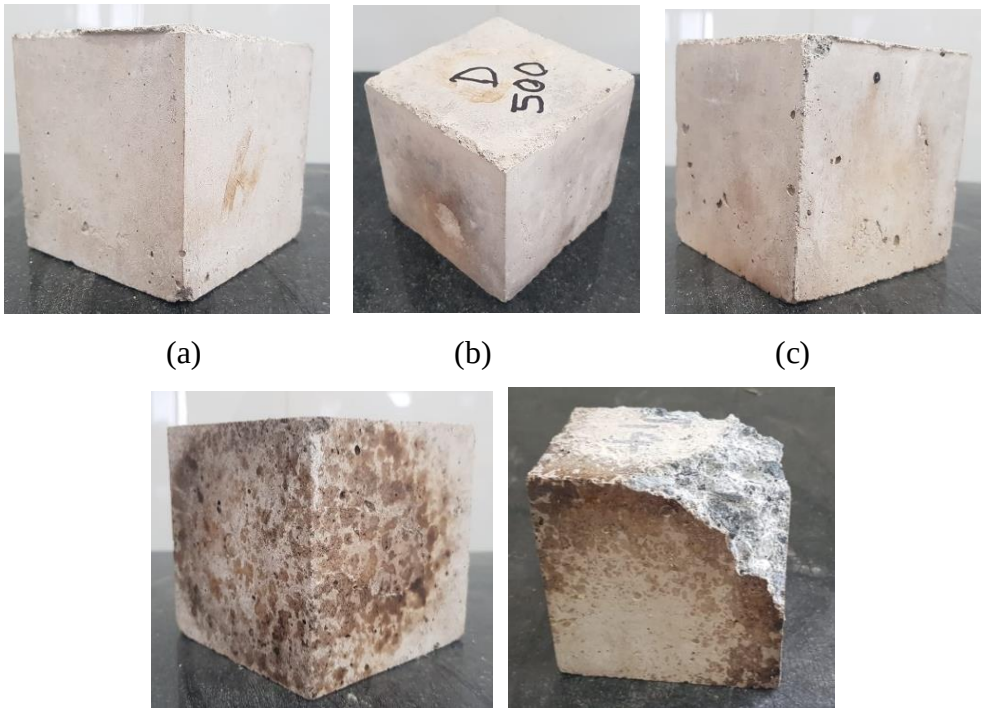

(a) (b) (c)

(d) (e)

Fig. 5.27 Tier I concrete samples exposed to elevated temperatures of 600ºC (a) Control mix (b) 10% PET (c) 15% (d) 20% PET (e) 25% PET

5.13 Microstructure Analysis of Concrete

The use of PWA in cement composites is seen to have a serious influence on a range of properties of cement mortar and concrete. Considering the smoothness of the surface of PET particles and their hydrophobic nature, the hypothetical assumption of weak ITZ around PET inclusions was considered the main attribute for negative influence on the strength and durability characteristics. A microscopic study of this zone was necessary to accept the hypothesis. The SEM images of several samples showed that the addition of PET-Sand or SFS-Sand in a conventional mix does not modify, in any visually observable way the microstructure of the matrix of the composite. It is the connection between the polymer phase and cementitious matrix that forms the area of interest in the microstructure analysis. The SEM images of the concrete samples are presented in Fig 5.28.

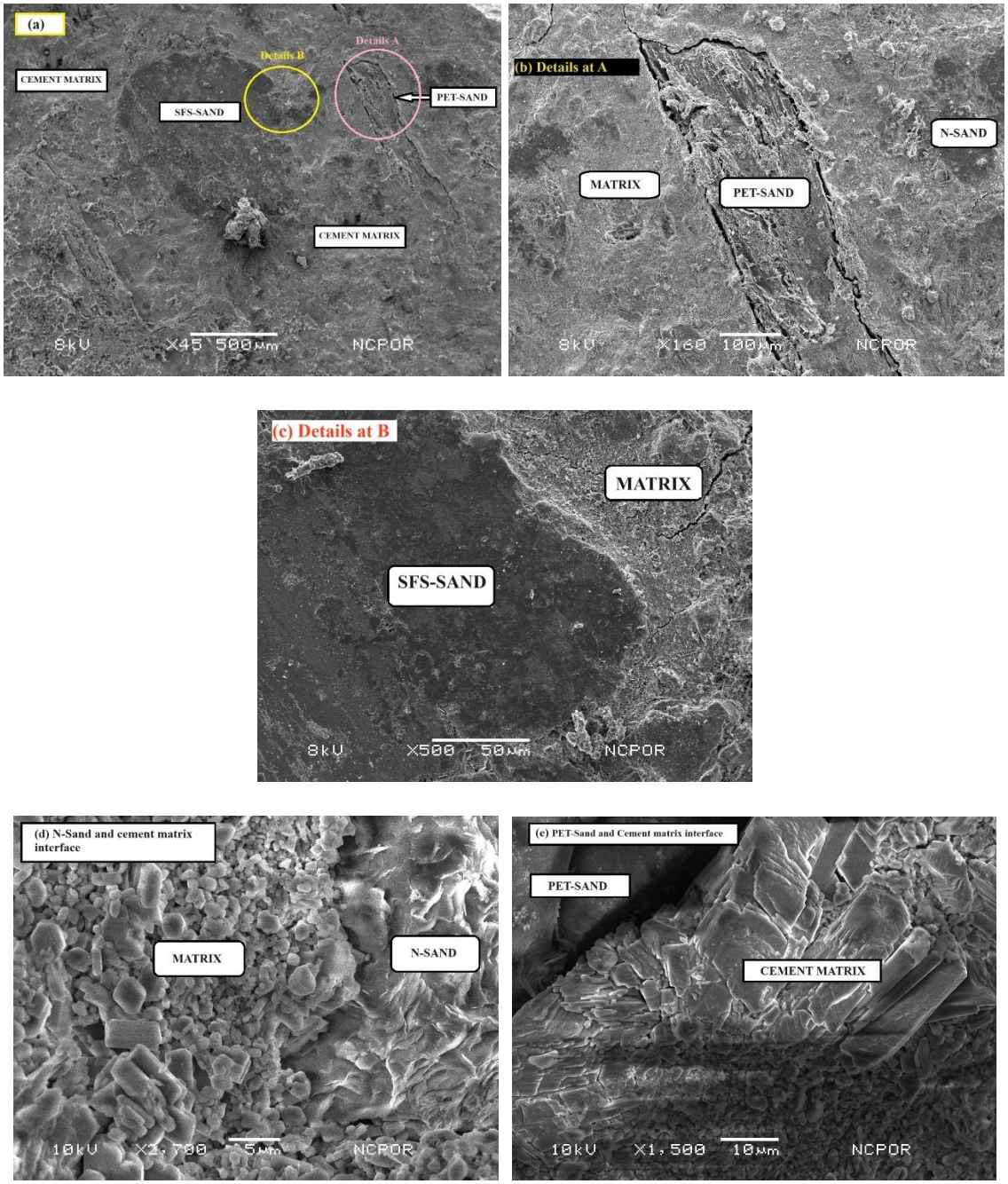

Fig. 5.28 SEM images of cement concrete mix with PET and SFS aggregate

With a magnification of X45 for Tier III sample with 25% PET waste, the SEM image in Fig. 5.28 (a) shows the typical transition zone variations in the cases of PET aggregate, N-Sand, and SFS-Sand. The ITZ between PET particles and cement paste shows a tendency to be wider than that of the other two aggregates. Magnification (X160 and X300) of the region around PET particle as presented in Fig. 5.28 (b) easily shows weak adhesion between the matrix and plastic filament. A gap of 5-10µm can be observed

between the matrix and PET particle edges. This is mainly due to the hydrophobic nature of plastic inclusions that prevents hydration reactions at the outskirts of the plastic particles, resulting in weak transition zones. These bad connections are the failure zones during the mechanical loading on the composites and the entry points for the absorption/permeability of fluids. The observations presented in the current research are found to comply with microscopic observations by several research studies in the past (Badache et al., 2018; Choi et al., 2005; Galvão et al., 2011; Gavela et al., 2004.; Gouasmi et al., 2019; Safi et al., 2013). On the other hand, it is observed in Fig. 5.28 (d) that the connection zone between SFS-Sand and cement paste is dense enough without any weak linkage. It indicates a better bond between SFS and cement paste responsible for enhanced performance of SFS-seeded mixes. At higher magnification ranges (X1500 and X2700) hydration products around the N-Sand particle and PET particle are presented in Fig. 5.28 (e) and 5.28 (f) respectively. It is pertinent to note that hydration products are not influenced by substitution ratios of waste aggregates.

Chapter 6

Mathematical Modeling and Validation

6.1 Introduction

As discussed in the literature review in Chapter 2, the extensive laboratory investigations on PWCC in the past have exhibited ubiquitous conclusions about most of the physical and mechanical properties. Nonetheless, dissension does exist in some of the properties. Given this, the current study demands validation of the results for various properties. This Chapter is devoted to validating the results with the findings of experimental outcomes on the PWCC in the literature. Notably, the scheme of experimentation in the current study permits the validation of results for Tier I mixes only. Tier II mixes are based on an innovative approach of seeding the mix with optimum content of SFS-Sand along with varying proportions of PET-Sand. Furthermore, the Tier III mix was also a modification of the Tier II mix by partial replacement of OPC in the mix by FLA. Being an unprecedented approach, direct validation was not possible for the results of Tier II and Tier III mixes.

In addition to the validation, this chapter also deals with the analysis of results of various physical and mechanical properties for a possible correlation between the properties and suggests mathematical models for possible relationships. These relationships have been devised considering the results for all three tiers of concrete. The mathematical models are also compared with the relationships presented by other researchers and validated with standards like CEB-FIP, ACI codes, and Eurocode.

6.2 Workability

The decrease in workability of mortar and concrete mixes as seen in the current study is agreed upon by several research studies accommodating different forms of PWA as presented in Fig. 6.1. In the case of PET-modified concrete mixes, for 20% replacement of natural aggregates, workability reduction of 30-32% was shown by several studies (Almeshal et al.,2020a; Jaskowska-Lemańska et al., 2022; Saxena et al., 2020). For the

same replacement level, Batayneh et al. (2007) showed a 25% reduction in workability (Batayneh et al. 2007). A reduction of 25-30% in workability was presented for the 25% incorporation of PP aggregates (Coppola et al., 2016; Ozbakkaloglu et al., 2017; Záleská et al., 2018). However, some studies showed comparatively higher increases in workability values in the 42-50% range for 20% inclusion of PWA (Albano et al. 2009; Senthil Kumar and Baskar 2015).

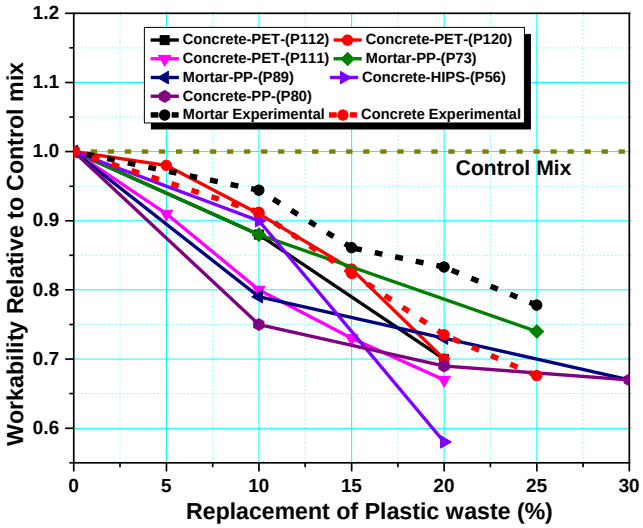

Fig. 6.1 Validation of results of workability

6.3 Bulk density

The trends of decline in density values of PWCC from the literature are in agreement with the current study and are evident from the results of a few studies presented in Fig. 6.2. It proves that regardless of the types of plastics, there is a gradual decrease in density values with the increase in plastic content. In addition to the studies depicted in Fig. 6.2, a few other studies also showed identical variations in density values with variations in plastic volumes (Ferreira et al., 2012; Rai et al., 2012). Azhdarpour et al. (2016), Chen et al. (2019), and Ghernouti et al. (2014) showed that the density of concrete was reduced by 9%, 14%, and 13% for concrete containing 30%, 40%, and 50% of plastic waste as aggregate respectively(Azhdarpour et al., 2016; Chen et al., 2019; Ghernouti et al., 2014).

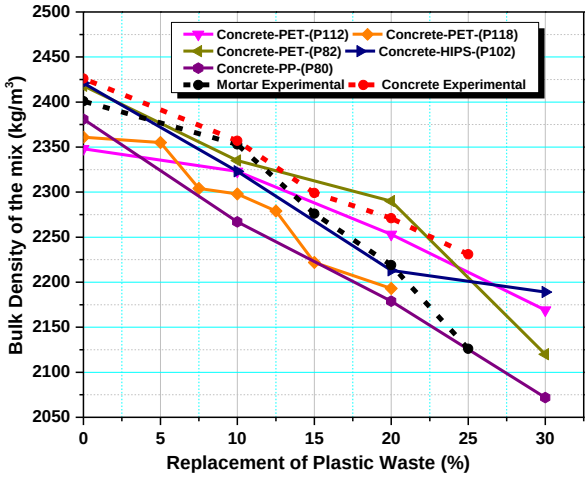

Fig. 6.2 Validation of results of bulk density

6.4 Compressive Strength

The results of the compressive strength of tier I mixes in current research can be validated with the findings from similar research studies in the literature. A display of a comparative analysis of these results for mortar and concrete mixes is available in Fig. 6.3.

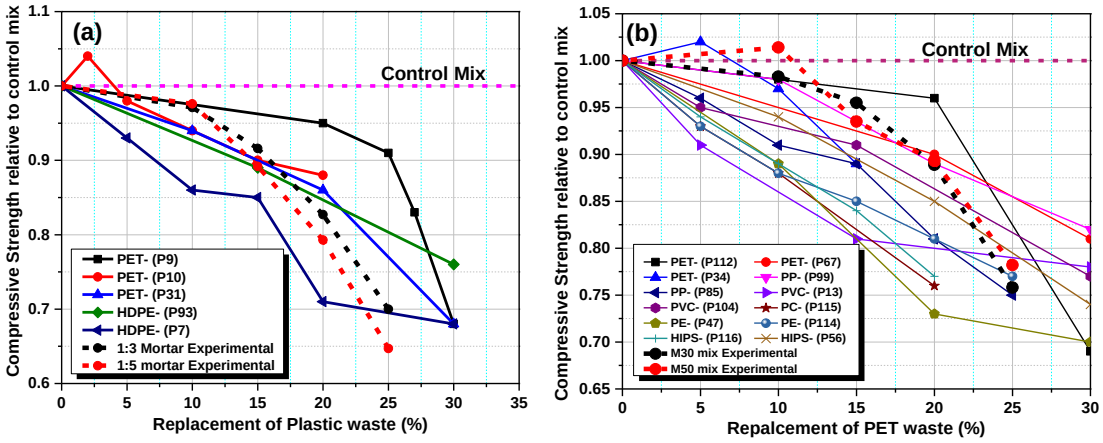

Fig. 6.3 Validation of results of compressive strength (a) Mortar (b) Concrete

In addition to the studies presented in Fig. 6.3, for mortar mixes Hannawi et al. (2010b) showed that a volumetric substitution of 20% PET fine aggregates lowers the compressive strength values by 47% in comparison to the conventional mix (Hannawi et al., 2010b). Da Silva et al. (2014) recorded a decrease in strength by 20% and 50% for a replacement of 15% PET in pallet form and flaky form respectively. However, Safi et al.

(2013) and Abed et al. (2021) showed a decrease in strength by 14% and 33% for a replacement ratio of 25% by weight of fine aggregates (Abed et al. 2021; Safi et al. 2013). In case of concrete mixtures too, several studies have shown that substitution of natural fine aggregates by 15-25% leads to a reduction in compressive strength by 30-40% in comparison to the control mix (Albano et al., 2009; Azhdarpour et al., 2016; Correia et al., 2014; Gavela et al., 2004; Ismail and AL-Hashmi, 2008; Wicaksono et al., 2018). Rahmani et al. (2013) and Saikia and De Brito (2014) showed a lower reduction in strength values as compared to other studies in the range of 10%-22% for a replacement ratio of 15% by volume of fine aggregates (Rahmani et al., 2013; Saikia and De Brito, 2014).

6.4.1 Relationship between Dry Density and Compressive Strength

The relationships between dry density and compressive strength of cement composites at 28 days of aging are illustrated in Fig. 6.4 and 6.5. It can be seen that the mortar mixes exhibit an increase in compressive strength with the increase in density values of the mix. A very strong R-squared correlation is observed between the density and compressive strength of all the mortar mixes in three different tiers.

Similar to the relationship in the mortar specimens, the concrete mixes also showed polynomial relationships with a strong correlation coefficient as presented in Table 6.1.

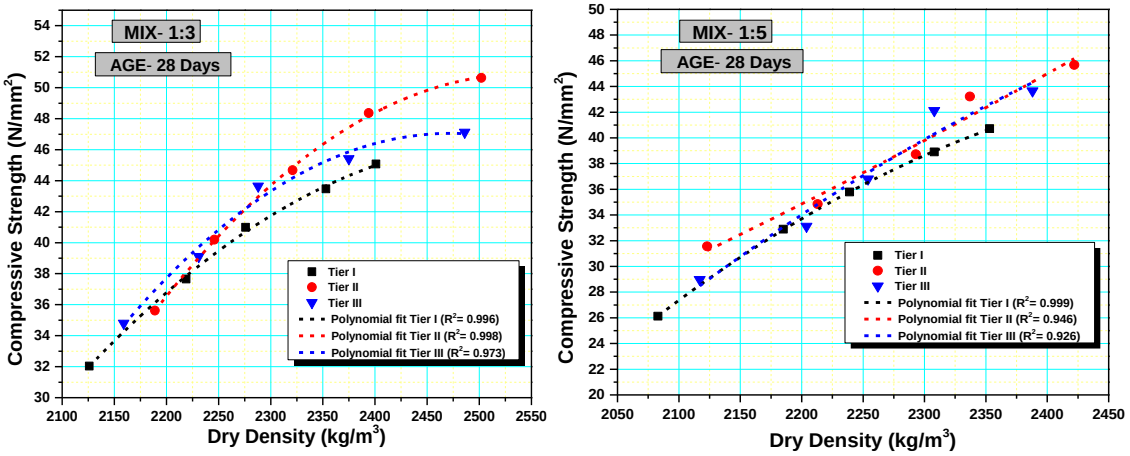

Fig. 6.4 Relationship between dry density and compressive strength of mortar (a) 1:3 mix (b) 1:5 mix

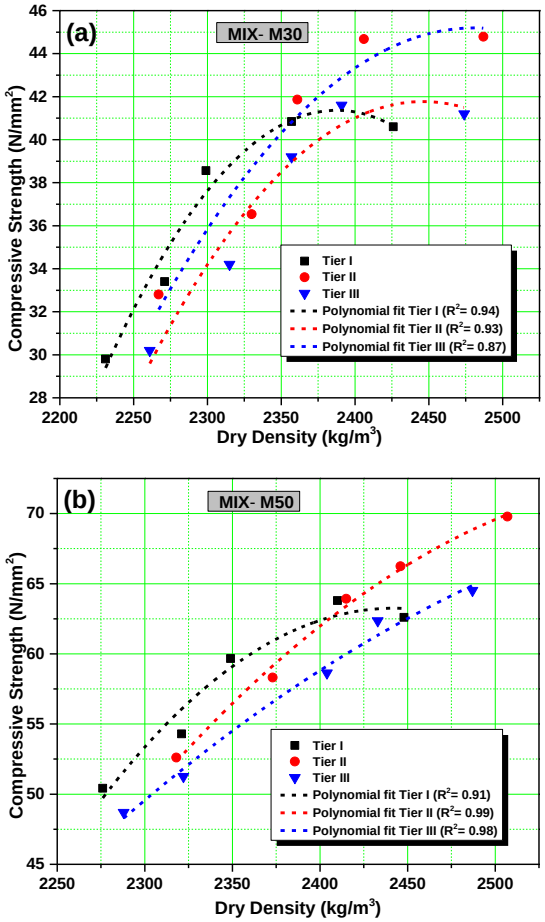

Fig. 6.5 Relationship between dry density and compressive strength of concrete (a) M30 mix (b) M50 mix

Table 6.1 Mathematical equations for the relationship between dry density and compressive strength

Composite	Mix	Tier	Relationship	Equation	Correlation coefficient (R^2)
Mortar	1:3	Tier I	Polynomial	$y = -605.87+0.435x-8.57E-05x^2$	0.996
		Tier II	Polynomial	$y = -737.31+0.62x-12.19E-05x^2$	0.998
		Tier III	Polynomial	$y = -724.53+0.624x-12.63E-05x^2$	0.973
	1:5	Tier I	Polynomial	$y = -432.92+0.367x-7.08E-05x^2$	0.999
		Tier II	Polynomial	$y = -6.89-0.01x+1.32E-05x^2$	0.946
		Tier III	Polynomial	$y = -320.20+0.259x-4.45E-05x^2$	0.926
Concrete	M30	Tier I	Polynomial	$y = -2747.14+2.34x-4.89E-04x^2$	0.936
		Tier II	Polynomial	$y = -2085.02+1.74x-3.55E-04x^2$	0.928
		Tier III	Polynomial	$y = -1720.75+1.42x-2.87E-04x^2$	0.875
	M50	Tier I	Polynomial	$y = -2866.94+2.40x-4.91E-04x^2$	0.914
		Tier II	Polynomial	$y = -1492.16+1.20x-2.29E-04x^2$	0.988
		Tier III	Polynomial	$y = -841.25+0.67x-1.23E-04x^2$	0.980

6.5 Flexural Strength

The results of the flexural strength of composites obtained in the current work were in close agreement with the findings of other studies in the literature. In the case of mortar composites, Hannawi et al. (2010b) reported a decrease in flexural strength by 15% when 20% sand was replaced by PET aggregates. The findings by Abed et al. (2021) and Safi et al. (2013) showed a reduction in flexural strength by 28-39% for substitution levels of 20-25% by weight. In the case of concrete mixes, the findings of the current research were in total agreement with the results provided by several research works (Harini et al., 2015; Ismail and AL-Hashmi, 2008; Rahmani et al., 2013; Saikia and De Brito, 2014; Umasabor and Daniel, 2020). The findings by Gavela et al. (2004), Hossain et al. (2016a), Sadrmomtazi et al. (2016), and Saxena et al. (2020) however, present a higher reduction in flexural strengths in the range of 40-50% for replacement ratios of 20-30% PET waste(Gavela et al.,2004; Hossain et al., 2016a; Sadrmomtazi et al., 2016; Saxena et al., 2020). In addition to these studies, the agreement of the current investigation with other historical works with different forms of plastics is also illustrated in Fig. 6.6.

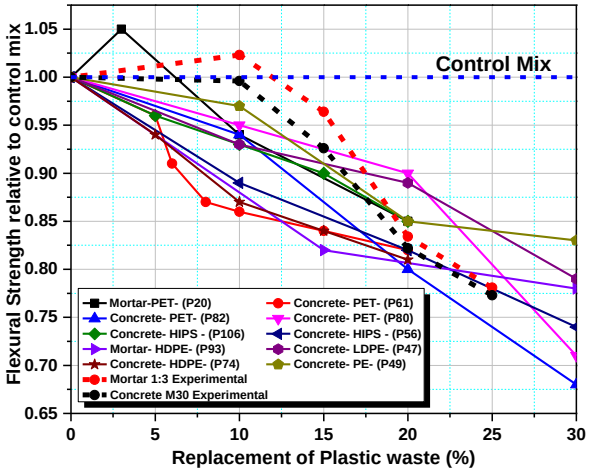

Fig. 6.6 Validation of results of flexural strength

6.5.1 Relationship between flexural strength and compressive strength

The relationships between flexural strength and compressive strength for the mortar and concrete mixes are obtained for the experimental results and the mathematical models are suggested. These models are compared with the other research studies and models suggested by the relevant codes.

Fig. 6.7 illustrates the relationship for the mortar mixes. A regression analysis was performed on the test data to formulate the relationship for obtaining the flexural strength values and equations 6.1 and 6.2 were obtained for 1:3 and 1:5 mixes with R^2 values of 0.906 and 0.916 respectively.

$$f_s = 0.1161 f_c + 0.8453 \text{…..... Eq. (6.1)}$$

$$f_s = 0.09787 f_c + 1.3144 \text{……Eq. (6.2)}$$

The relationships are compared with the models given by given by other studies for PET and PP aggregates used as fine fractions in mortar mixes. From Fig. 6.7 it can be seen that the models presented by Akçaözoğlu and Ulu (2014) and Abed et al. (2021) underestimate the results for flexural strength in comparison to the models suggested by current research(Abed et al. 2021; Akçaözoğlu and Ulu 2014). On the other hand, the relationship for PP aggregates as presented by Coppola et al. (2016) exhibits higher values of flexural strength for given compressive stress(B. Coppola et al., 2016).

Similar to the mortar mixes, the relationships are also obtained for concrete mixes. The mathematical equations for M30 and M50 grade concrete are given in equations 6.3 and 6.4 respectively. The correlation coefficients 0.982 and 0.953 indicates a strong linear relationship between compressive strength and flexural strength.

$$f_s = 0.1306 f_c + 0.7456 \text{…..Eq. (6.3)}$$

$$f_s = 0.8871 f_c - 0.3232 \text{…..Eq. (6.4)}$$

The mathematical model suggested in the current research is compared with the models obtained by other studies in the past. In addition to these models, the relationship illustrated in ACI 318- 19 (ACI, 2019) and Eurocode 2 (BSI, 2004) is also presented for a comparative analysis of the expression suggested by the current study. The power relation as suggested by ACI 318-19 and Eurocode 2 are given in equations 6.5 and 6.6 respectively.

$$f_s = 0.62 {f_c}^{0.5} \text{…..Eq. (6.5)}$$

$$f_s = 0.435 {f_c}^{2/3} \text{…..Eq. (6.6)}$$

The comparative analysis of mathematical models for concrete mixes is presented in Fig. 6.8. It can be seen that the model suggested for M30 grade concrete overestimates the flexural values in comparison to most of the models presented by previous studies including those suggested by ACI 318-19 and the Eurocode 2 (ACI, 2019; BSI, 2004). On the other hand, for M50 grade concrete, the suggested model presents the experimental to the predicted ratio of flexural strength close to 1 in the case of the model prescribed by ACI 318-19. All the other models seem to overestimate the flexural strength of mixes for all PET replacement ratios in all the tiers of concrete.

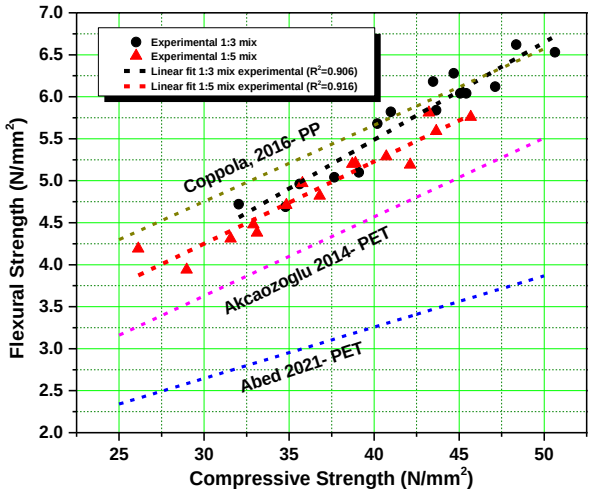

Fig. 6.7 Relationship between compressive strength and flexural strength of mortar

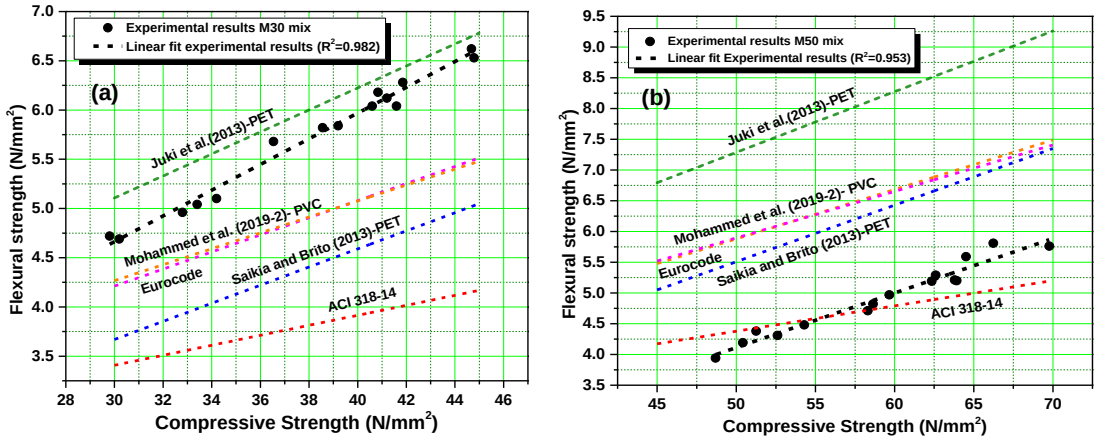

Fig. 6.8 Relationship between compressive strength and flexural strength of concrete (a) M30 mix (b) M50 mix

6.6 Splitting Tensile Strength

Several studies conducted on PET blended concrete samples have shown a behavior similar to the current research when tested for investigation of tensile behavior. Studies have shown that 10-20% replacement of fine aggregates in conventional concrete leads to a reduction of 11-30% in tensile strength (Albano et al., 2009; Aswatama et al., 2018; Babafemi et al., 2022; Rahmani et al., 2013; Saikia and De Brito, 2013). Few authors also showed that the tensile strength loss may extend beyond 35% for 20% replacement of PET particles in flaky form (Correia et al., 2014; Hossain et al., 2016a; Jaskowska-Lemańska et al., 2022). The variation in tensile strength of concrete with varying proportions of plastic contents for the experimental work and literature studies is illustrated in Fig. 6.9 which shows a good agreement in the outcomes.

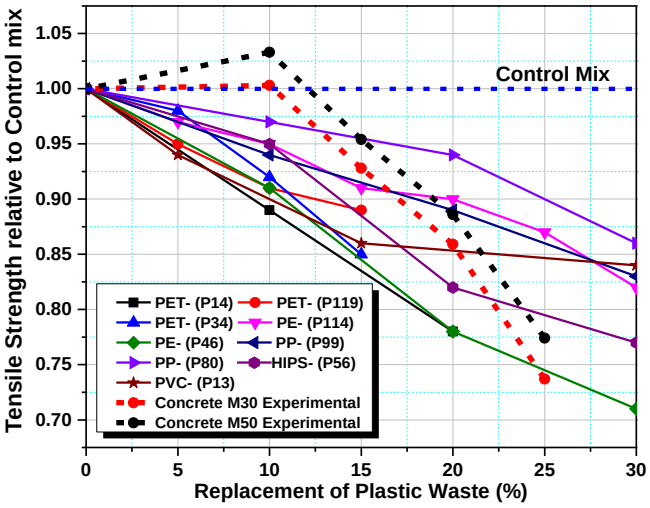

Fig. 6.9 Validation of results of tensile strength

6.6.1 Relationship between split tensile strength and compressive strength

Prior studies on concrete containing PET waste in the past have shown that there exists a definite relationship between splitting tensile strength and compressive strength. Although the relationship is empirical, it gives a sufficiently reliable model for the estimation of tensile strength as a function of compressive strength. Such an empirical formulation has been established for the current study and compared with the models presented by some of the previous studies. These relationships for M30 and M50 mixes are presented in Fig. 6.10 (a) and (b). Equations 6.7 and 6.8 gives the mathematical relationship for M30 and M50 mixes. Both these equations exhibit a strong correlation

between compressive strength and tensile strength with R^2 values of 0.942 and 0.922 respectively.

$$f_t = 0.06337 f_c + 0.4610 \text{…….....Eq. (6.7)}$$

$$f_t = 0.07620 f_c + 0.4441 \text{…….....Eq. (6.8)}$$

The experimental results and the mathematical model established for the current research are compared with the models presented by other researchers for concrete specimens with PET fine aggregates. For M30-grade concrete, it can be seen that the present model is in close agreement with the formulation provided by Saikia and De Brito, (2013). The other research models seem to overestimate the tensile strength values (Almeshal et al., 2020a; Juki et al., 2013). However, for higher strength values as obtained for M50 grade concrete, the current model is in total agreement with the models presented by past studies (Fig. 6.10b).

The experimental results are also validated for the empirical models given by CEB-FIP guidelines, ACI code, and Eurocode (ACI, 2019; BSI 2004; CEB-FIP, 1993). The upper and lower limits for tensile strength according to CEB- FIP guidelines are given as per equations 6.9 and 6.10.

$$f_t = 1.85\left(\frac{f_c}{10}\right)^{0.67} \text{…….....Eq. (6.9)}$$

$$f_t = 0.95\left(\frac{f_c}{10}\right)^{0.67} \text{…….....Eq. (6.10)}$$

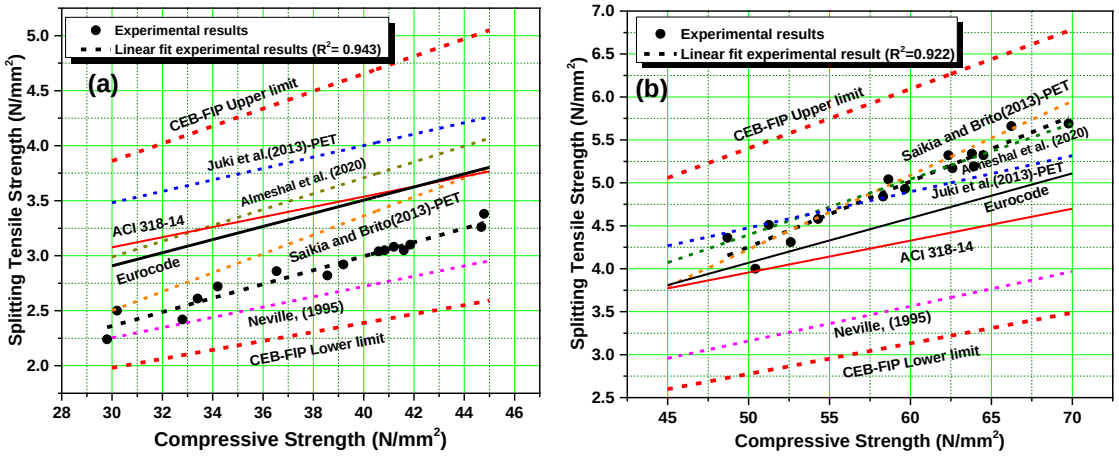

Fig. 6.10 Relationship between compressive strength and tensile strength of concrete (a) M30 mix (b) M50 mix

For both mixes the experimental results are within the bounds suggested by CEB-FIP guidelines. For lower strength values the ACI 318-19 and Eurocode 2 formulations seem to overestimate the tensile strength values. On the other hand, for higher strength values, in the case of M50 grade concrete, the models present lower values of tensile strength as compared to the experimental results. The current results are also compared with the model presented by Neville (1995) for normal concrete as per equation 6.11 (Neville, 1995).

$$f_s = 0.23 {f_c}^{0.67} \text{.....Eq. (6.11)}$$

6.7 Modulus of Elasticity

Several studies in the past have presented the effect of the substitution of PET fine aggregates on the modulus of elasticity of concrete. The results of the current research are in close agreement with most of the studies. For a substitution of 10-15% of natural sand with PET aggregates a reduction in modulus of elasticity to the extent of 14-24% is reported in the literature (Aswatama et al. 2018; Correia et al. 2014; Ferreira et al. 2012; Guilherme et al. 2012; Rahmani et al. 2013). A substitution of 20-25% natural fine aggregates by volume was reported to have reduced elasticity modulus between 30-40% (Albano et al., 2009; Hannawi et al., 2010a; Jaskowska-Lemańska et al., 2022; Sadrmomtazi et al., 2016). Fig. 6.11 shows that the other forms of plastics also show a similar effect on the modulus of elasticity like PET aggregates. A slight variation in modulus of elasticity values with varying proportions of plastic contents for the literature studies and the experimental data can be seen for plastic contents up to 15% replacement levels. Elasticity values are comparatively higher than the results depicted by literature studies. This variation may be attributed to a relatively compact mass of concrete achieved in the current work, thanks to the gradation of PET-Sand that is similar to the N-Sand replaced.

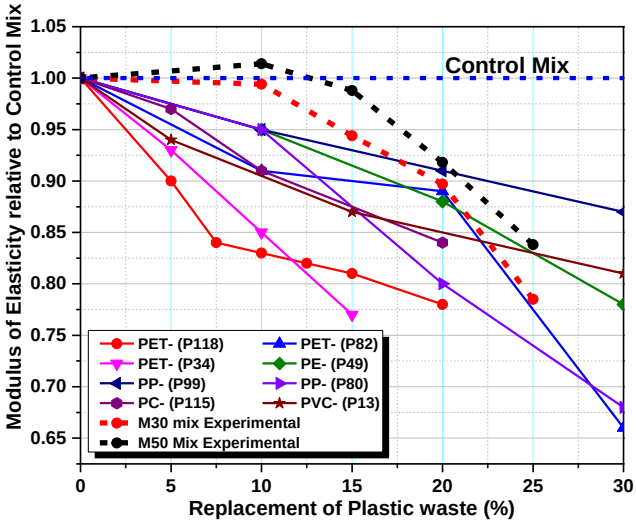

Fig. 6.11 Validation of results of modulus of elasticity

6.7.1 Relationship Between Compressive Strength and Modulus of Elasticity

Similar to the relationship of tensile strength and flexural strength as a function of compressive strength, a mathematical model is also deduced for modulus of elasticity as a function of compressive strength for the experimental results obtained for all the tiers of concrete in M30 and M50 grade. A linear relationship exists between the modulus of elasticity and compressive strength with strong correlation coefficients as shown in Fig. 6.12 (a) and (b). It can be seen that the modulus of elasticity increases with the increase in compressive strength. The mathematical model depicting the relationship for M30 and M50 grades of concrete is presented in equations 6.12 and 6.13 respectively. The correlation coefficients R^2 are found to be 0.960 and 0.966 respectively.

$$E_c = 0.57584 f_c + 7.505 \text{…….....Eq. (6.12)}$$

$$E_c = 0.43865 f_c + 12.0718 \text{…….....Eq. (6.13)}$$

The above mathematical formulations suggested in the current research are compared with the formulations presented by other research works conducted to experiment with the utilization of plastic waste in concrete. The experimental results of the present study and the correlations are compared with the studies on concrete containing PET (Hannawi et al., 2010a), LDPE (Alqahtani et al., 2017), and PVC (Haghighatnejad et al., 2016; Kou et al., 2009; A. A. Mohammed et al., 2019) aggregates. It can be seen that the relationship given by Hannawi et al. (2010a) for PET concrete

correlates well with the model suggested for M30 concrete in current research. However, in comparison to the M50 mix, the same model overestimates the elastic modulus. The models proposed by Haghighatnejad et al. (2016) and Mohammed et al. (2019) for PVC-based concrete seem to present considerable overestimates of elastic modulus, whereas, the relationship given by Kou et al. (2009) presents considerably safer values of modulus of elasticity compared to the current test data.

The proposed correlations are also validated with the models suggested by ACI 318-19 and CEB- FIP guidelines (ACI, 2019; CEB-FIP, 1993). ACI 318-19 presents the correlation for elastic modulus as a function of compressive strength (f_c, in N/mm^2) along with the incorporation of the density parameter of concrete (γ_d, in kg/m^3) as given in equation 6.14.

$$E_c = 43 \times 10^{-6} \times (\gamma_d{}^{1.5}) \times f_c{}^{0.5} \text{.....Eq. (6.14)}$$

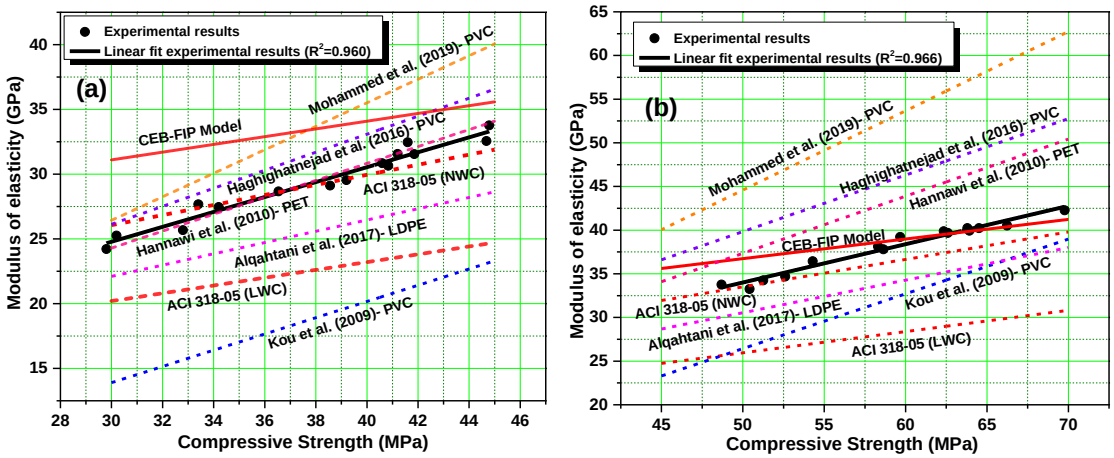

Fig. 6.12 Relationship between compressive strength and modulus of elasticity of concrete (a) M30 mix (b) M50 mix

The relationships for normal weight concrete (NWC) and lightweight concrete (LWC) are obtained considering density values as 2300 kg/m^3 and 1940 kg/m^3 respectively. It can be seen that the test data is in close agreement with the model about NWC as per ACI 318-19. Similarly, another relationship given as per the CEB-FIP model (equation 6.14) is also analyzed for validation of the experimental data. It can be seen that for strength values up to 45 MPa, the CEB-FIP model seems to overestimate the elasticity values compared to test data. However, for higher strength values, the model presents a better correlation with the test data.

6.8 Ultrasonic Pulse Velocity

The results of UPV for Tier I mixes are in close agreement with prior studies conducted for concrete mixes containing PET aggregates. The current study indicates a reduction in UPV in direct proportion to the substitution ratio of PET. This proportionate decrease in UPV is also exhibited by several studies. Correia et al. (2014) and Sadrmomtazi et al. (2016) showed that a replacement of 15% of sand by PET leads to a loss of 16-19% in UPV. Gavela et al. (2004) and Ismail Khalil and Jumaa Khalaf (2017) reported a reduction of 33% in UPV for replacement volumes of 30% of natural fines. Exceptionally, Akçaözoğlu et al. (2013), Azhdarpour et al. (2016) and Jaskowska-Lemańska et al. (2022) showed a lesser reduction in UPV compared to the replacement ratio. This close agreement of the experimental UPV results with the literature data is evident from the illustration in Fig. 6.13.

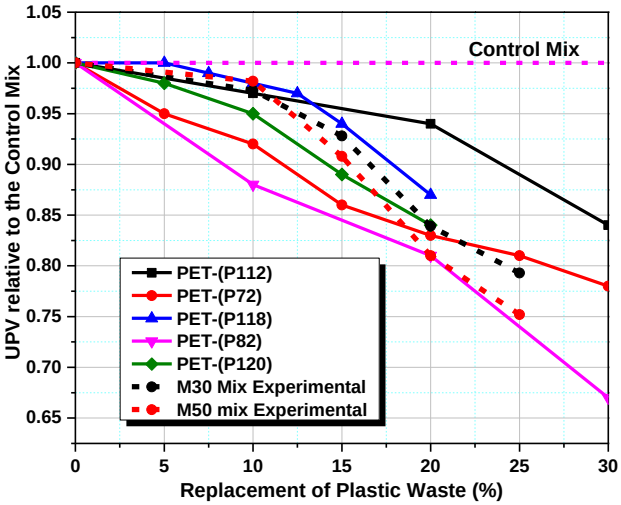

Fig. 6.13 Validation of results of UPV

6.8.1 Relationship between compressive strength and UPV of concrete

The experimental results of the UPV test on the concrete specimens are analyzed for a possible relationship with compressive strength at 28 days of age. Fig. 6.14 shows a strong mathematical correlation between UPV and compressive strength of M30 and M50 grade concrete. There is a linear increase in compressive strength with the increase in UPV value and the relationship for M30 and M50 grade concrete can be expressed by equations 6.15 and 6.16. The regression coefficient R^2 is found to be 0.907 and 0.910

respectively. These relationships indicate that UPV can be considered potentially useful in the prediction of the compressive strength of PET-modified concrete mixes.

$$f_c = 0.01396(UPV) + 17.672 \text{…....Eq. (6.15)}$$

$$f_c = 0.1333(UPV) + 0.90527 \text{…....Eq. (6.16)}$$

The above relationships are compared with the mathematical correlations available in the literature for concrete containing different forms of PWA. It can be seen that for the M30 grade, the model for the experimental results presents conservative results in comparison to all the selected studies except for the study on HDPE aggregate concrete by Badache et al. (2018). The results were in a relatively closer correlation with the study by Akçaözoğlu et al. (2013) for PET-incorporated concrete. However, the other models underestimated the strength values (Albano et al., 2009; Almeshal et al., 2020a; Sadrmomtazi et al., 2016; Senhadji et al., 2015). For the M50 grade of concrete, the relationship proposed by current research seems to overestimate the strength values in comparison to all the models suggested by other research studies selected for validation.

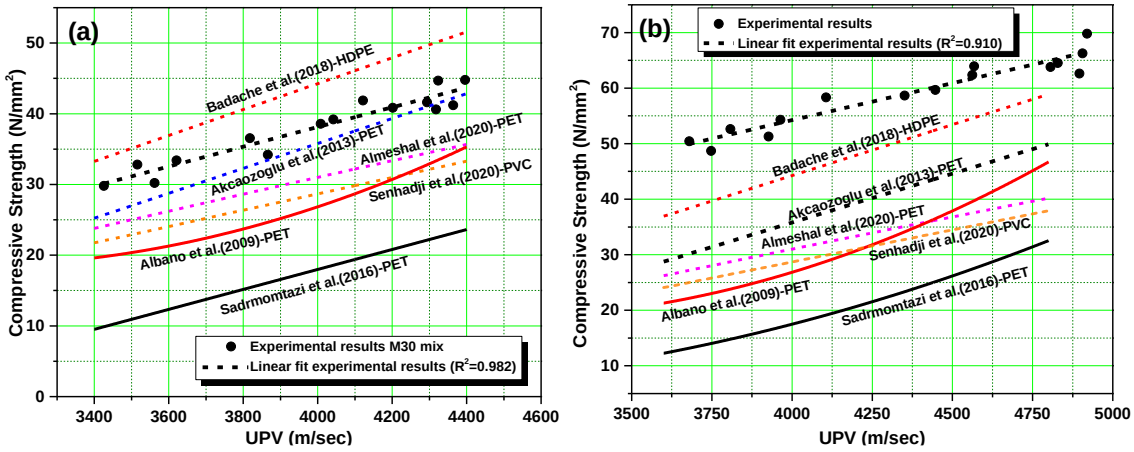

Fig. 6.14 Relationship between compressive strength and UPV of concrete (a) M30 mix (b) M50 mix

6.9 Sorptivity

Most of the studies on cement composites containing PET inclusions as aggregates have performed water transfer behavior investigation by determination of absorption by immersion techniques (Albano et al., 2009; Correia et al., 2014; Hossain et al., 2016a; Sadrmomtazi et al., 2016). Only a few studies determined the capillary

absorption characteristics of PET-modified composites. The results presented by A. M. Da Silva et al. (2014) for mortar specimens showed that sand replacement by 15% volume with PET pallets and flakes increases the capillary absorption by 13% and 10% respectively. For a similar percentage replacement in concrete, Silva et al. (2013) showed that the capillary absorption increased by 13% and 31% when specimens were cured in laboratory and outdoor environments respectively. The absorption characteristics of PWCC available in the literature for different plastic forms also exhibit similar absorption trends in most of the cases as illustrated in Fig. 6.15. The results provided by Coppola et al. (2018) and Faraj et al. (2019) for PP aggregates are worth a mention for validation of the results of the current study (Coppola et al., 2018; Faraj et al., 2019).

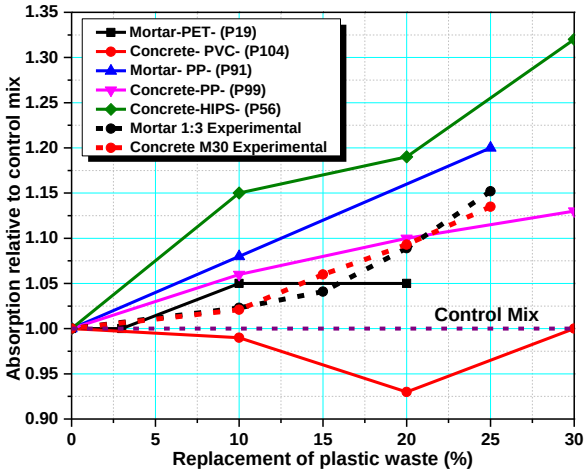

Fig. 6.15 Validation of results of absorption characteristics

6.9.1 Relationship between Sorptivity and Density of Composites

A regression analysis is performed for the results of the sorptivity test with the results of compressive strength and dry density of the composites at 28 days of age. High dispersion in values is observed for compressive strength results giving a very weak correlation with sorptivity values. However, a strong relationship is observed between sorptivity values and dry density values as shown in Fig. 6.16 and 6.17.

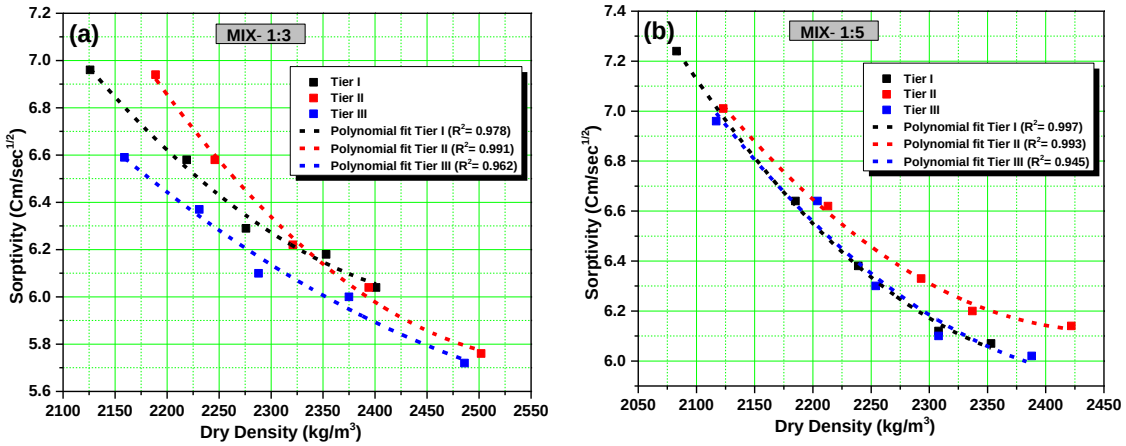

Fig. 6.16 Relationship between dry density and sorptivity of mortar (a) 1:3 mix (b) 1:5 mix

It can be seen that as the density of the mix increases, the sorptivity value goes on decreasing. The increase in density is related to a reduction in PET volumes inside the mix. The lower the PET content, the lesser the porosity which decreases the capillary absorption. The relationship between the parameters satisfies a polynomial equation as presented in Table 6.2. All the relationships show a high correlation factor indicating a significantly strong relationship between dry density and sorptivity.

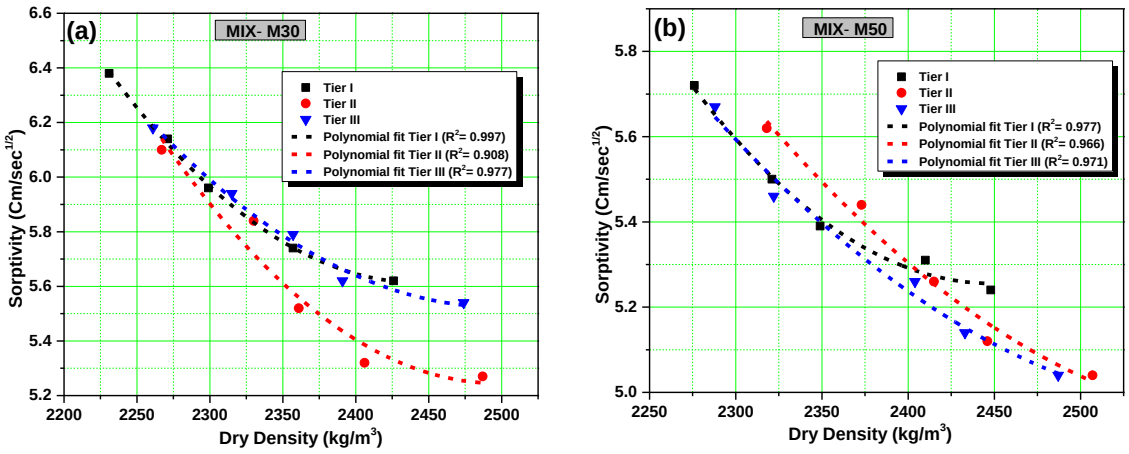

Fig. 6.17 Relationship between dry density and sorptivity of concrete (a) M30 mix (b) M50 mix

Table 6.2 Mathematical equations for the relationship between dry density and sorptivity

Composite	Mix	Tier	Relationship	Equation	Correlation coefficient (R^2)
Mortar	1:3	Tier I	Polynomial	$y = 6.629E\text{-}06x^2\text{-}0.0333x+47.846$	0.978
		Tier II	Polynomial	$y = 7.875E\text{-}06x^2\text{-}0.0406x+58.092$	0.991
		Tier III	Polynomial	$y = 3.169E\text{-}06x^2\text{-}0.0173x+29.239$	0.962
	1:5	Tier I	Polynomial	$y = 9.977E\text{-}06x^2\text{-}0.0487x+65.354$	0.997
		Tier II	Polynomial	$y = 8.416E\text{-}06x^2\text{-}0.0412x+56.632$	0.993
		Tier III	Polynomial	$y = 8.154E\text{-}06x^2\text{-}0.0404x+56.036$	0.945
Concrete	M30	Tier I	Polynomial	$y = 1.710E\text{-}05x^2\text{-}0.0836x+107.73$	0.998
		Tier II	Polynomial	$y = 1.683E\text{-}05x^2\text{-}0.0841x+110.24$	0.908
		Tier III	Polynomial	$y = 1.170E\text{-}05x^2\text{-}0.0585x+78.637$	0.977
	M50	Tier I	Polynomial	$y = 1.532E\text{-}05x^2\text{-}0.0751x+97.144$	0.977
		Tier II	Polynomial	$y = 0.766E\text{-}05x^2\text{-}0.0402x+57.636$	0.966
		Tier III	Polynomial	$y = 0.719E\text{-}05x^2\text{-}0.0373x+53.458$	0.971

6.10 Permeability

Not many studies have reported on the permeability characteristics of PET-modified cement composites in the literature. Saxena et al. (2020) presented significantly higher values of water penetration, 3.38 times higher than the control mix compared to 1.92 times as observed in the current experiment with 25% PET-Sand (R. Saxena et al., 2020). The relative permeability values for PP aggregates by Coppola et al. (2018) and Faraj et al. (2019) fully agree with the current investigation for a replacement ratio of 15% volume as illustrated in Fig. 6.18(Coppola et al., 2018; Faraj et al., 2019).

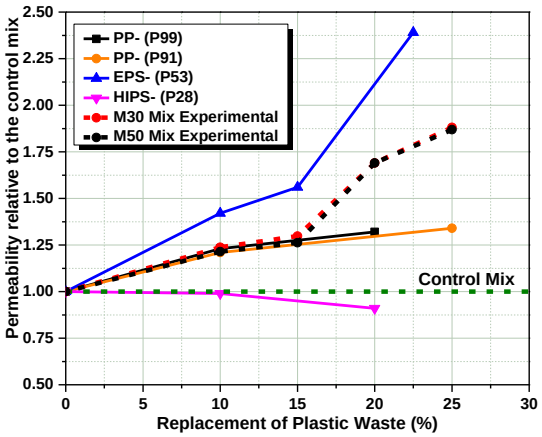

Fig. 6.18 Validation of results of permeability

6.11 Chloride migration

The comparison of the results of chloride migration for the current study with the results from the literature is presented in Fig.6.19. The decrease in chloride migration value with the increase in PET-Sand followed the pattern indicated by previous studies by Senhadji et al. (2015) and Kou et al. (2009). However, the threshold substitution level beyond which chloride migration increased was quite lower than that indicated by two studies. The current study disagreed with the finding by Alqahtani et al. (2018) that chloride migration goes on decreasing with the increase in plastic content.

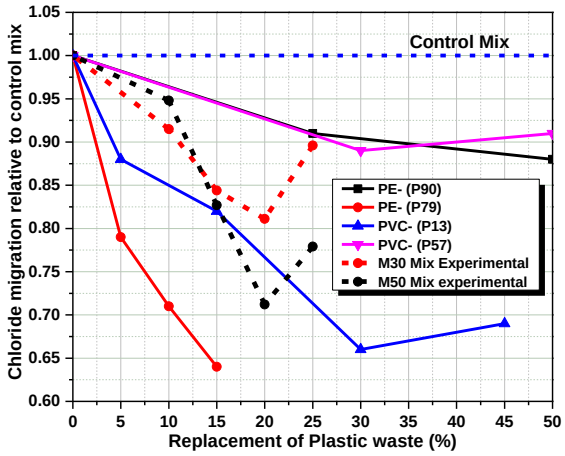

Fig. 6.19 Validation of results of chloride migration

6.12 Resistance to elevated temperatures

The outcome of the current investigation of the residual strength of the concrete composites after exposure to elevated temperatures showed an agreement with the results presented by Correia et al. (2014) and Guilherme et al. (2012). Both studies reported a strength degradation of 65-70% at 600º C in comparison to a 56% loss in strength observed in the current study. The results fully agree with the findings by Sojobi and Owamah (2014) for the exposure of specimens with 25% PET at 200ºC.

Chapter 7

Sustainability Assessment

7.1 Introduction

The current research is an attempt to utilize and reuse plastic waste material as an alternative to N-Sand inside cementitious mixes. It is an innovative attempt of achieving sustainability in the manufacturing of cement-related products and a promising step toward green concrete technology. It is pertinent to note that the quantitative substitution of waste materials in the concrete-making process cannot be certified as a sustainable and green approach unless the resulting innovative concrete exhibits functional performance equivalent to the one obtained using conventional ingredients. Most importantly, the production process of such innovative concrete should not cause any damage to the environment. Therefore, the question is; is it possible to obtain functional structural concrete with alternative waste materials and if this is possible, can this waste utilization technique provide energy savings and reduce the environmental impact of its production?

The rheological, mechanical, and durability characteristics of the innovative concrete mixes made in three tiers have been discussed in Chapter 5 of the current thesis. The results of the mechanical and durability characteristics of these novel concrete mixes have provided enough evidence of the possibility of obtaining functional structural concrete for certain substitution ratios of N-Sand by PET-Sand. These findings have placed on record the achievement of sustainability through recycling plastic waste and saving natural resources quantitatively. However, the saving in embodied energy or the reduction in associated environmental impacts in the process remains questionable unless proved by a systematic life cycle analysis of the materials and their utilization process in the system. The current research proposes the use of LCA methodology as per ISO 14040:2006 to analyze the environmental impacts associated with the production of novel concretes and compare them with the impacts caused due to the production of traditional ones (ISO 14040, 2006).

7.2 Results of sustainability assessment

The methodology of LCA as per ISO 14040:2006 defines four systematic and well-defined phases in which the results of impact assessment are presented. This study follows these four well-known phases in the presentation of the results of the analysis. These four phases include goal and scope definition, life cycle inventory analysis, life cycle impact assessment, and interpretation of results (ISO 14040, 2006). These four phases are already discussed in detail in § 4.4 in Chapter 4.

7.2.1 Goal and scope definition

The primary objective of the current study is to identify and evaluate the environmental impact associated with the making of concrete with PET-Sand. In the first stage of the investigation, concrete mixes with OPC as the sole binding material were investigated by replacing N-Sand in the mix with increasing PET content in ratios of 10%, 15%, 20%, and 25% by volume. This constituted the first tier (Tier I) of experimentation with concrete. Considering the degradation of the performance of Tier I mixes with increasing content of PET-Sand, the scheme of experimentation in current research proposed the utilization of HDS from the zinc manufacturing industry (i.e., SFS) as a supplementary aggregate material that can compensate for the quality degradation of concrete due to PET inclusion. This proposal constituted the second tier (Tier II) of experimentation. Furthermore, it was proposed to use pozzolanic admixtures in Tier II mixes by replacement of OPC with FLA by weight proportion of 30%. This proposal was floated based on the hypothesis that the use of SCM provides a significant environmental advantage by the reduction in the quantity of OPC in the composites, the latter being the giant contributor to the environmental impact. In other words, the modification in binder content of tier II mixes constituted the third tier (Tier III) of investigation. The goal of the LCA is the analysis of the environmental life cycle impacts of these three-tiered mixes for a selected FU. The selection of a FU and the decision regarding the system boundary of assessment are two critical steps of the analysis.

7.2.1.1 Functional Unit of Analysis

The concrete mixes in the present study are analyzed for environmental impacts by considering the material and energy flows required to obtain $1m^3$ of concrete. These environmental impacts are compared with those associated with manufacturing $1m^3$ of

conventional concrete. The comparison of the environmental impact of concrete mixes for identical volumes cannot be justified unless the mixes in question have a similar functional performance. The compressive strength of concrete is the index property associated with the mechanical performance of a concrete mix. Therefore, compressive strength of 40 N/mm^2 and 60 N/mm^2 is considered a component of the functional unit of the environmental analysis of concrete. Although the compressive strength values at 28 days of age signify the characteristic strength of concrete, the use of SCM like FLA has indicated the strength gain in concrete at older ages, unlike OPC concretes which achieve nearly ultimate strength at 28 days of aging. To utilize the advantage of strength gain of SCM at older ages, 90 days of compressive strength in concrete is considered in the FU for the current analysis. To summarize, $1m^3$ of concrete having a compressive strength of 40 N/mm^2 and 60 N/mm^2 at 90 days of curing is selected as the FU of LCA. Accordingly, concrete mixes are designated as 'FU40 mix' and 'FU60 mix' respectively.

7.2.1.2 System boundary of analysis

The system boundary is a presentation of inputs of energy and material profiles and outputs arising from the processing and production of concrete. The system boundary of the present study includes the material profiles from the stage of extraction of raw materials, the energy demand for processing of raw materials, and the transportation of raw materials to the concrete manufacturing site. The cradle-to-gate approach was used for the concrete production process. The cradle-to-gate method included the production of ingredients of concrete like cement, and other raw materials like extraction of natural aggregates and their processing, water exploitation, transportation, and energy consumption in the production process of concrete. Alternative materials like FLA, SFS-Sand, and PET-Sand are used in the present study to obtain environmentally friendly concrete. The allocation of impacts caused by these alternative materials is avoided by system expansion or the so-called consequential modeling approach. It means that no upstream environmental burden from the production of alternative materials is taken into the system boundary of the production of green concrete. However, if the alternative waste material requires any downstream processing, it is taken into account for the analysis. Ex. Use of PET waste in concrete as fine aggregate requires a two-stage approach, such as washing and shredding of PET to make it suitable for use in concrete.

In the case of SFS slag, a similar approach is adopted to process the slag as fine aggregates.

Figure 7.1 summarizes the system boundary considered for environmental analysis of all three tiers of concrete including control concrete. The black solid line in the system boundary indicates the impact on the corresponding life phase of concrete, while the black line with alphabet 'T' indicates the impact of transportation of the particular ingredient from the raw material manufacturing point to the concrete manufacturing plant. The dotted lines show the avoided environmental impacts due to the utilization of waste materials like SFS, PET, and FLA as concrete ingredients. In the case of SFS-Sand the avoided impacts are from avoided landfilling, whereas in the case of PET waste, the avoided impacts are either from avoided landfilling or incineration of plastics. The avoided impacts are taken as environmental credits and can be deducted from the total impact related to making a new concrete mix.

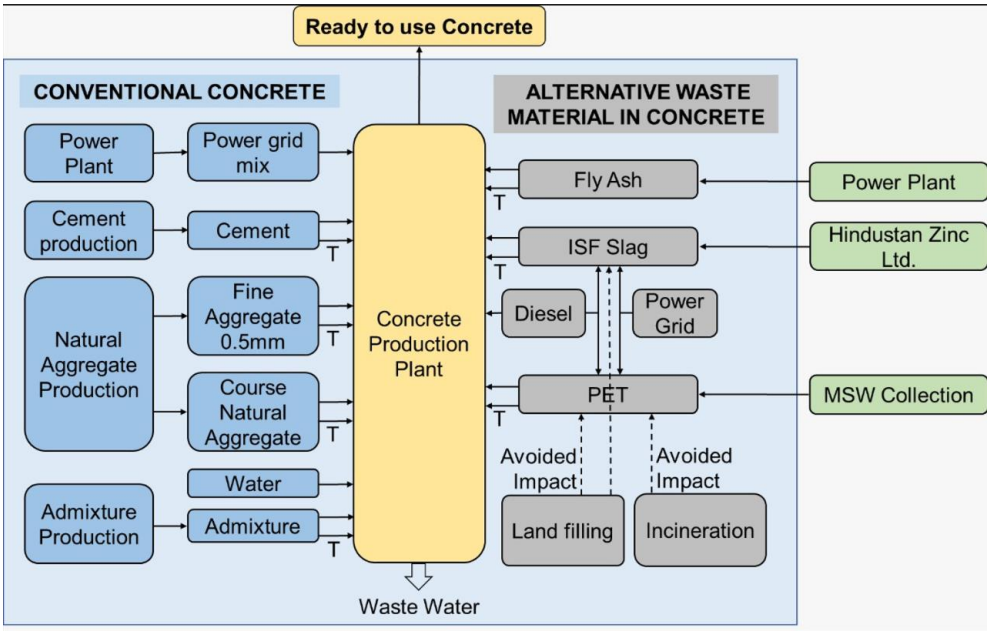

Fig. 7.1 System boundary of LCA of concrete

7.2.1.3 Impact Categories for the Analysis

The life cycle environmental impact of all the concrete mixes was investigated through the analysis of the environmental impact categories that are required for Environmental Product Declarations (EPD) by EN 15804 (EN 15804, 2012). Only seven impact categories were considered. These categories include ADP, GWP, ODP, POCP,

AP, EP and use of non-renewable primary energy resources (PE-NRe). The first six impact categories were analyzed according to the methodology of the Institute of Environmental Sciences (CML) from Leiden University, Netherlands, one of the most commonly applied in practice (Jiménez et al., 2015). The last impact category (PE-NRe) was analyzed according to the Cumulative Energy Demand (CED) method.

7.2.1.4 Assumptions of LCA and its Limitations

The LCA methodology followed in the current research is based on certain assumptions. These assumptions are a source of limitations of the assessment process. The assumptions and corresponding limitations are as follows:

1) Analysis accounts for only seven environmental impact categories. Some impact categories are not considered, particularly those categories that are not very significant or used to assess the impact of construction-related processes. Ex. toxicity potentials are avoided in the current analysis.
2) Due to the unavailability of information, some emissions like diffuse dust emissions related to different stages of production and extraction of raw materials are not accounted for in the analysis. E.g., dust emissions in the case of extraction processes at quarries are not considered in the analysis. Nonetheless, these emissions are also considered insignificant and thus usually disregarded.
3) The life cycle of concrete is considered for cradle-to-gate system boundary and the transportation of concrete to the placement site and its applications and maintenance during service life and demolition and disposal of concrete after its useful life is not considered in the analysis. As a result, the carbon uptake by the concrete during its use face and after its useful life and demolition is not considered a part of the system boundary in the current analysis. This carbon capture may reduce the net global warming potential estimated for the entire life cycle of concrete.
4) The data on the production of some raw materials like N-Sand, NCA were estimated from the raw data available from the local industries about energy consumption by the firm in terms of electricity, and fuel consumption. The data may differ if any other firm is chosen. The impact factors for each impact category

are obtained based on the impact factors per unit consumption of energy or fuel as available in the literature.

5) In the case of some raw materials or other chain-linked processes, it was not possible to have site-specific data collection to estimate the environmental impacts of a product or process. In such cases, databases from SimaPro software (Ecoinvent 3 and ELCD) available in the literature were used. The data from these databases present some uncertainty because they are generic.
6) No allocation approach is adopted for SFS-Sand used as blending aggregate and FLA used as a supplementary binder in concrete production. If mass allocation or economic allocation is adopted the outcome of LCA may differ from the current investigation.
7) The avoided impacts of landfilling of SFS-Sand and landfilling/incineration of PET waste are not considered in the current analysis. This facet of the analysis hints at the overestimation of the impacts.
8) As the data for each impact category for most of the raw materials or the chain-linked processes are sourced from the literature in generic form, the LCA study in current research demands validation of the outcome in the local as well as global context. However, the current research is a novel approach in the concrete technology sector without any precedence. Therefore, it was not possible to validate the outcome of the LCA study, except for the conventional mixes.

7.2.2 Life cycle inventory analysis (LCIA)

The inventory analysis is an important step in the LCA. It refers to the collection of data for each unit process included in the system boundary of the concrete. It is the assimilation of data regarding all relevant inputs and outputs of energy and mass flows identified in every activity within that system boundary. It also includes data on emissions to air water and land. The inventory analysis involves the determination of impact coefficients for all the unit processes leading to making a particular concrete. As discussed, these unit processes may be the activities related to the extraction of raw materials for concrete, the transportation of raw materials to the concrete-making plant, energy inputs on concrete production, etc.

The data about material and energy flows for all the activities considered in the study were obtained from various sources. The information regarding the life cycle of raw materials required for conventional concrete like cement, admixtures, and water was obtained from the International Environmental Product Declaration (EPD) for the respective material. The information regarding alternative materials like PET sand, SFS aggregate, and FLA was obtained from the literature studies. Incomplete and missing data or data that could not be accessed was obtained from secondary data sets such as the Ecoinvent v.3 database.

The inventory analysis in the present study for cradle to gate approach is performed in the following stages:

1) Inventory analysis of raw materials used in the concrete
2) Inventory analysis of transport of ingredients to the concrete plant
3) Inventory analysis of the concrete production process

The inventory analysis of raw materials includes the data for the binder materials used in the concrete mixes i.e., OPC and FLA, fine aggregates used i.e., N-Sand, SFS-Sand, and PET-Sand, NCA obtained for basalt quarries, water and the admixture used. The inventory analysis for the transportation of ingredients is performed independently of the type of material transported. It is expressed in terms of the tonnage or hauling capacity of the mode of transport and the distance traveled in terms of ton.km or kg.km. The inventory analysis of concrete production is site-specific, a one-time analysis of material and energy inputs and outputs involved in the mechanical process of manufacturing of $1m^3$ of concrete.

7.2.2.1 Inventory analysis for binders- OPC and FLA

The main constituent of cement is the Portland cement clinker which accounts for 95% of the total constituents of cement. The remaining 5% is composed of minor additional components. Clinker is produced from raw materials like limestone and clay. These materials are crushed, homogenized, and fed into a rotary kiln. These raw materials are sintered at a temperature of 1450º C to form clinkers which consist of calcium, silicium, aluminuim, and iron-oxides. In the next phase, calcium sulfate in the form of gypsum and other minor constituents are added to improve the physical properties of cement such as setting, workability, or water retention. As per EPD data, Ultratech OPC

used in current research is composed of 92.03% clinker, 3.76% gypsum, and 4.22% additional constituents (EPD, Ultra tech India,2020).

The EPD for OPC is presented in the Indian context of cement production. Fig. 7.2 shows the production system of a typical cement industry in India. The selection of system boundary influences the impact assessment of cement production. Two different system boundaries can be considered cement LCA: Ground to gate and gate to gate. In the current EPD, a gate-to-gate system boundary is considered. The third system boundary i.e., Cement Sustainability Initiative (CSI) or Global Cement and Concrete Association (GCCA) is used with certain processes as shown in Fig. 7.2. Ground-to-gate system boundary was used in the current analysis. The cement infrastructure (i.e., buildings, plant, and equipment) and energy and water consumption for office operation were beyond the scope of the analysis.

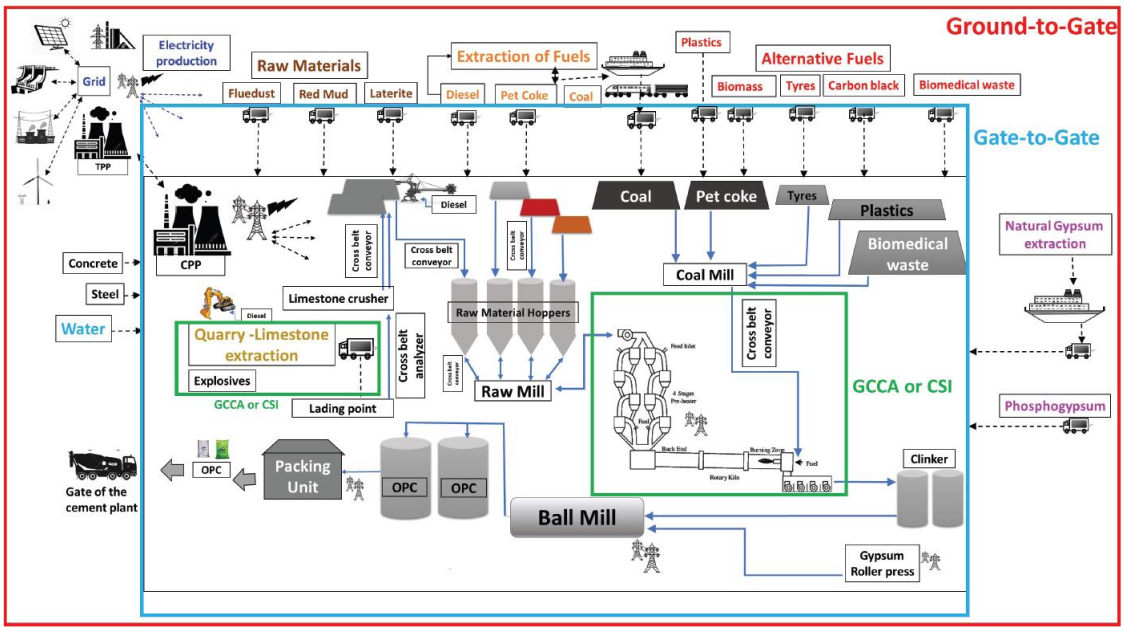

Fig. 7.2 Typical cement production process in India and system boundary (Source: Basavaraj and Gettu, 2022)

The cement production process begins with the extraction of raw materials, namely limestone, clay, gypsum, and other additional constituents from the respective mining quarries and their subsequent transportation to the manufacturing plants. The means of transport depend on the context (e.g., a conveyor belt, truck, boat, train, etc.). Various energy inputs are involved in raw material extraction and transportation. The use

of explosives for the mining process and diesel consumption for drilling, crushing, and transportation of raw materials are the frontline energy inputs in this process.

The preparation of the raw material input is the second stage of cement manufacture. The limestone obtained after the mining process is usually crushed with a jaw crusher and subsequently by a hammer crusher. An impact crusher is used to grind clay and laterite. The crushed clay and laterite are thoroughly mixed with limestone and this mixed material is fed to the raw mill at the required proportions. This mixture is milled in the raw mill to provide the desired 'raw material input'. At this stage, the coarse particles of raw material are channeled back to the raw mill for grinding purposes. The fine particles are channeled to the raw mill silo where the mixture is blended and stored. Electricity is the main energy input in this raw meal preparation stage.

The calcination process is the third and most energy-intensive stage of cement production. This is the stage where the mixture of raw materials is exposed to a high temperature within the kiln and clinker formation takes place through a chemical reaction. In recent times, a preheater and pre-calciner kiln is used for the process which consumes a relatively lower amount of energy. The raw meal is fed to the preheater cyclones where the mixture undergoes drying and partial calcination. The pre-heater uses hot air from the kiln for drying purposes through bottom-up processes. This is the stage where oxides are formed and CO_2 is released into the atmosphere. Pre-calciner facilitates almost 60-65% of primary calcination. It utilizes almost 40% of the fuel energy. Usually, coal and natural gas fuel mixes are used in kilns for heating the raw meal to about 1400-1500º C. As a waste management hierarchy, alternative fuels are also used nowadays as shown in Fig. 7.2. Calcination stage is the highest GHG-emission stage in the entire process. The hot clinker is then cooled down in air-quenching coolers, also the heat recovery centers from which the heat is channeled to the pre-heater and cyclone separators.

In the fourth and final stage, clinker is blended with gypsum and the mixture is ground in the cement mill. The fine grey powder obtained from the cement mill is stored in silos and supplied to the market in bags or bulk-loaded trucks.

The main inputs and outputs at each stage of analysis are summarized in Fig. 7.3. For the Indian context, the LCA data for cement is obtained from the EPD of Ultratech Cement Limited. This EPD is prepared by ISO 14025 and EN 15804:2012+A2:2019. The

LCA study carried out for developing this EPD is done as per ISO 14040 and ISO 14044 requirements. The environmental impacts associated with the production of 1 tonne of OPC as sourced from EPD of Ultratech Cements, India for the selected impact categories have been presented in Table 7.1. To validate the data presented for the Indian context, the data obtained from the International EPD systems through a comprehensive review is also presented in Table 7.1. This database is obtained to enable the authors to select the impact factors for OPC to perform LCA in agreement with the international system.

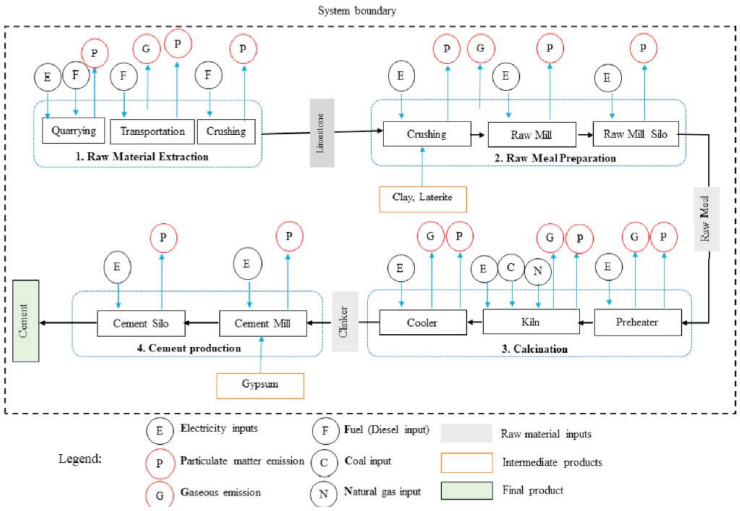

Fig. 7.3 Summary of energy inputs and system outputs for cement production

Table 7.1 Environmental impact factors for the production of 1 ton of OPC

Reference	Chen et al. (2010)	Müller et al. (2014)	De Schepper et al. (2014)	Song et al. (2016)	Stafford et al. (2016)	Braga et al. (2017)	ECRA, 2015	Kurda et al. (2018a)	Marinković et al., (2017)	EPD, Ultratech, (2015)
Regional Context	France	Germany	Netherlands	China	Portugal	Portugal	European Union	European Union	Serbia	India
ADP kg sb eq.	1.59E+00	-	1.60E+00	2.65E-06	1.81E+00	3.83E+00	1.00E-03	1.00E-03	-	9.80E-06
GWP kg CO_2 eq.	8.44E+02	6.91E+02	8.30E+02	6.78E+02	6.32E+02	9.26E+02	8.98E+02	8.98E+02	8.87E+02	9.96E+02
ODP kg CFC-11eq.	2.28E-05	1.50E-05	2.40E-05	6.15E-07	-	9.47E-05	1.21E-07	-	-	1.53E-10
POCP kgC_2H_4eq.	4.26E-02	1.00E-01	4.50E-02	1.28E-01	1.58E-01	7.48E-02	1.42E-01	1.42E-01	1.56E-01	2.84E+00
AP kgSO_2 eq.	1.15E+00	8.30E-01	1.20E+00	2.51E+00	1.97E+00	2.54E+00	1.48E+00	1.48E+00	5.30E+00	3.58E+00
EP kgPO_4^{2-} eq.	1.73E-01	1.20E-01	2.75E-01	1.59E-01	3.54E-01	3.50E-01	2.11E-01	2.11E-01	3.00E-01	1.27E-04
PE- NRe MJ	6.42E+03	2.45E+03	6.87E+03	-	-	5.64E+03	3.70E+03	3.70E+03	-	5.96E+03
PE-Re MJ	-	6.58E+01	-	-	-	2.03E+02	2.22E+02	-	1.26E+03	7.75E+01

The product category rules for most of the international EPD of renowned concrete manufacturing industries recognize FLA as waste products recovered material. Therefore, the environmental impacts allocated to FLA are limited to the treatment and transportation required to use it as a concrete material input. It is a byproduct or waste obtained from the primary production of electricity from a coal-fired plant. This byproduct is subjected to secondary processes to make it suitable as a cement concrete component. Figure 7.4 shows a schematic view of the secondary processing of fly ash along with the primary production process of electricity through the power plant as presented by (Chen et al., 2010). In the primary production process of electricity, the ashes are removed from the exhaust gases of coal power plants by an electromagnetic process. These ashes are concentrated to obtain raw FLA. In the secondary process, FLA is dried and stocked, before being used as a cement additive (Chen et al., 2010).

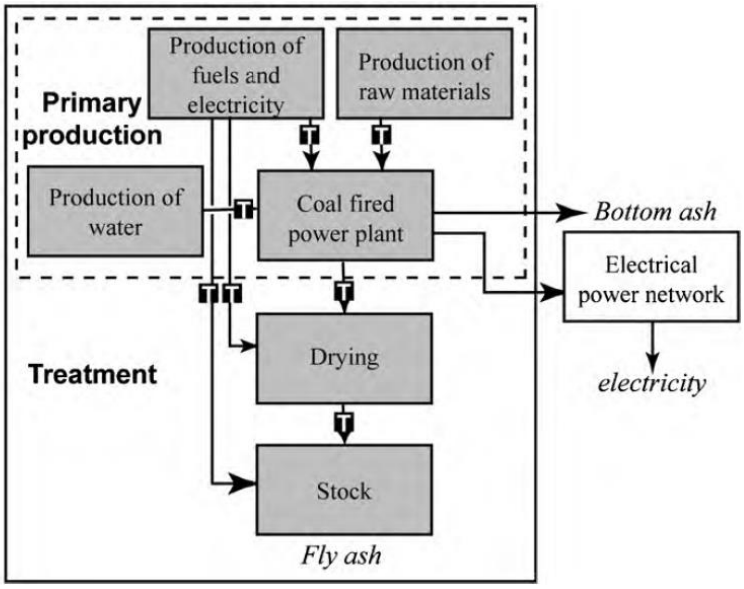

Fig. 7.4 Primary and secondary processes in Fly ash production (Source: Chen et al., (2010))

It can be seen that the secondary processing of fly ash incurs energy expenses through fuel and electricity for drying and stockpiling of fly ash. Chen et al. (2010) have presented the inputs for the secondary treatment of raw FLA to enable it to be used as SCM. It is stated that 6.82×10^{-3} kWh of electricity, 0.29 MJ of Gasoline energy, and 1.03×10^{-6} m^3 of fuel are consumed for processing of 1kg of FLA. Transport emissions corresponding to 3.0×10^{-3} tkm for road transport in a truck are considered. The

environmental impacts corresponding to this secondary processing of FLA are presented in Table 7.2. These impacts are corresponding to the assumption that the FLA obtained is a waste without any allocated impact from the primary production of electricity (Chen et al., 2010). Thus, these impacts are categorized as 'no allocation' impacts as shown.

There exists a second school of thought about impact allocation to FLA. It is argued that, although fly ash is waste from electricity generation plants, it has emerged as a product whose use is certain, thanks to the concrete industry. Moreover, fly ash has attained economic value in the construction industry. This argument has evolved a strategy to allocate the impacts of the primary production of electricity to FLA. The study by Chen et al. (2010) determined the allocation coefficient of environmental impact based on the economic value and mass equivalents of fly ash and electricity produced. For a Frech production context, based on mass value and economic value allocation coefficients were determined as 12.4% and 1% respectively. The corresponding environmental impacts for 1 kg FLA were presented for both allocations (Chen et al., 2010). The allocated impacts for FLA are also provided by Teixeira et al. (2016) and EPD by Danish Technical Institute (DTI) (Teixeira et al., 2016; DTI, 2013). These impact factors are presented in Table 7.2.

Table 7.2 Environmental impact factors for the production of 1 kg of fly ash

Reference	(Chen et al., 2010)			Teixeira et al. (2016)	DTI EPD (2013)
Regional context	France			Portugal	Danish
Impact category	No allocation	Mass allocation	Economic allocation	Economic allocation	Economic allocation
ADP (kg sb eq.)	3.37E-04	3.25E-02	2.98E-03	-	3.29E-10
GWP (kg CO_2 eq.)	8.77E-03	4.18E+00	3.50E-01	1.01E-02	3.92E-03
ODP (kg CFC-11eq.)	5.58E-09	4.06E-08	8.45E-09	7.16E-11	9.88E-13
POCP (kgC_2H_4eq.)	3.22E-06	1.10E-03	9.34E-05	9.52E-07	5.49E-07
AP (kgSO_2 eq.)	5.53E-05	3.20E-02	2.67E-03	2.07E-05	7.26E-06
EP (kgPO_4^{2-}eq.)	8.23E-06	1.76E-03	1.52E-04	2.56E-07	1.05E-06
PE- NRe (MJ)	8.33E-01	8.35E-01	7.08E-02	1.99E-01	5.80E-02
PE-Re (MJ)	-	-	-	-	-

From the datasets of environmental impact for OPC in Table 7.1, it can be seen that there is a significant deviation between the impact values available for the Indian context (EPD Ultratech India, 2020) and the global averages. Secondly, no authentic data for impact factors for FLA in the Indian context is available at current dates for secondary processing of FLA. The use of impact factors for OPC in the Indian context and FLA in the foreign context may present a disparity in the quantification of the hypothetical benefit provided by SCM. For these two reasons, the use of impact factors for OPC in the Indian context as provided by the EPD of Ultratech Cements is discouraging. The data provided by Chen et al. (2010) is considered a reliable estimate of the impacts of FLA by most of the literature studies across the globe and is treated as generic. Therefore, the current research proposes to use the impact parameters provided by Chen et al. (2010) for OPC as well as FLA. Also, FLA is considered a waste without any allocation of impacts from the upstream chain of production of electricity and hence, the assessment uses a 'no allocation' approach. Table 7.3 provides a summary of the impact factors considered for 1 kg of binder components in the current analysis.

Table 7.3 Environmental impact factors for 1 kg of the binder component (Chen et al., 2010)

Impact	ADP	GWP	ODP	POCP	AP	EP	Pe- NRe	Pe- Re
Unit	kg sb eq.	Kg CO_2	KgCFC-11eq.	kgC_2H_4eq.	kgSO_2 eq.	kgPO_4^{2-}eq.	MJ	MJ
OPC	1.59E-03	8.44E-01	2.28E-08	4.26E-05	1.15E-03	1.73E-04	6.42E+00	-
FLA	3.37E-04	8.77E-03	5.58E-09	3.22E-06	5.53E-05	8.23E-06	8.33E-01	-

7.2.2.2 Inventory analysis for natural aggregates – N-Sand and NCA

The current study utilizes crushed sand from basalt quarry as fine natural aggregate and basaltic rock aggregates as the coarse aggregate fraction inside the concrete. Based on the cradle-to-gate theory the present study aims to establish an LCI for NFA and NCA based on site-specific data. The FU of the assessment of the present study is the production of 1 t each of fine and coarse natural aggregate fraction.

Figure 7.5 shows a typical aggregate production process in India. The life cycle of concrete aggregates consists of four main phases: exploration, extraction, processing, and transportation. The process starts with the site selection for exploration. On selection

of the site, the mining of aggregates is started with the removal of soil layers to expose the rocky strata from which the natural aggregates are extracted and processed.

The process starts with drilling holes into the rocks on the selected site. This is done by making perforations in the basalt rock using a drill rig supplied with the compressor. These holes are then partially filled with explosives. After blasting, the broken pieces of rock are extracted. If required, the size of the rocks is reduced to facilitate loading and transportation in trucks. The extracted basalt is loaded in a truck with a 28-ton capacity using a hydraulic excavator having a load capacity of $3m^3$. The distance from the quarry to the processing unit is assumed to be 40 km.

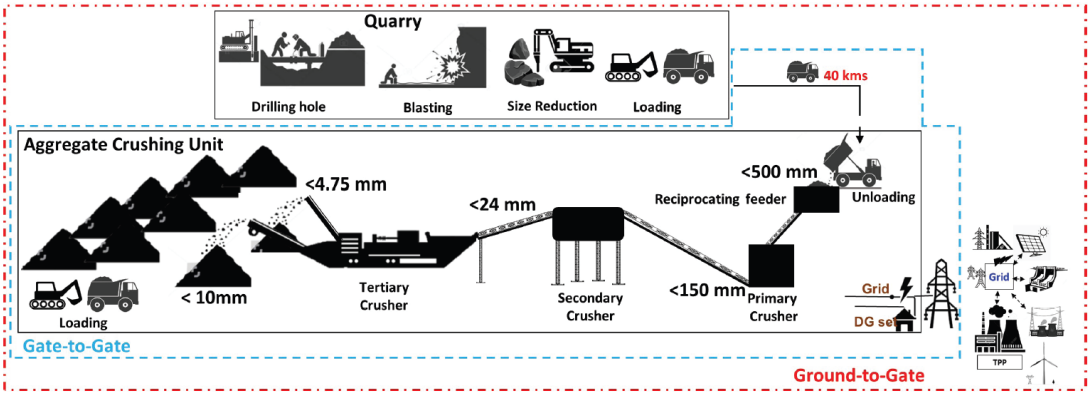

Fig. 7.5 Typical aggregate production process in India (Source: (Basavaraj and Gettu 2022))

At the processing unit, basalt is introduced into a vibrating feeder. It passes through a primary crusher where a natural basaltic aggregate with a particle size of 0-50mm is obtained. Subsequently, the material passes through a secondary crusher and a vibrating screen. This secondary crushing stage produces different size fractions of aggregates as per the site requirements. Then the material is admitted to the tertiary crusher provided with a vibrating screen. This tertiary crushing phase produces three different size fractions of aggregates i.e., 0-4.8 mm, 4.8-9.5 mm, and 9.5-19 mm. Several conveyor belts are used for the displacement of the material between the equipment. A humidification system is provided for the control of dust emissions. This process consumes electric energy for operation and oil for lubrication. The schematic diagram for natural aggregate production with system boundary is presented in Fig. 7.6.

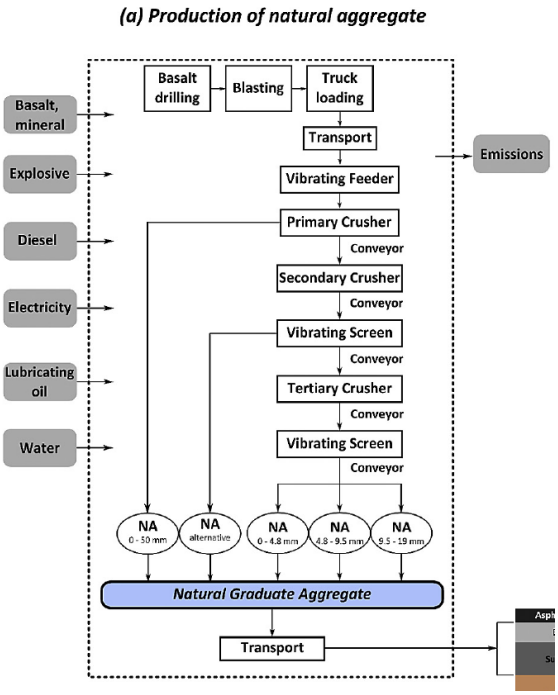

Fig. 7.6 Schematic diagram of natural aggregate production (Source: Rosado et al., (2017))

In a global context, many authors have provided site-specific data for the extraction of fine and coarse natural aggregates. Table 7.4 and 7.5 summarizes the site-specific data for the environmental impacts of obtaining 1 ton of crushed sand and natural coarse aggregate with the geographical context.

No authentic data about environmental impacts as per EN 15084 is available for natural aggregate production in the Indian context. The comprehensive literature review has revealed that the LCA studies of concrete in the Indian context are based on the generic emission details available through global databases and the site-specific data in the literature. From Tables 7.4 and 7.5, it is evident that the study by Braga et al. (2017) presented the impact coefficient for all the impact categories as per EN 15084. These impact coefficients given by Braga et al. (2017) were used for the LCA of concrete in the current study (Braga et al. 2017).

7.2.2.3 Inventory analysis for alternative fine aggregates- SFS and PET

SFS-Sand used in the current study is an industrial waste emerging from the zinc manufacturing industry M/s. Hindustan Zinc Limited. For the current study, SFS aggregates are considered total waste without any allocation of impacts from the upstream production process of zinc. However, the secondary processing of SFS aggregates incurs

environmental costs. No site-specific data is available from the industry regarding the emission details from this secondary processing. The zinc slag is obtained in sizes 100-350 mm. These lumps are pre-screened to obtain the lumps below 300 mm in size and subjected to crushing by passing over conveyor belts. The entire process involves the utilization of electrical energy. The process of secondary treatment of raw slag to convert it to sand-sized particles to be used in concrete is similar to the processing of EAF slag as presented by Faleschini et al. (2014). In a systematic LCA of this secondary processing, the authors have presented the data on emissions for various impact categories as per EN 15804 (Faleschini et al. 2014). This data has been presented in Table 7.6 for the functional unit of 1 ton of SFS-Sand.

Table 7.4 Environmental impact factors for 1 ton of crushed sand

Reference	Korre and Durrucan (2009)	Marinković et al. (2010)	Hossain et al. (2016b)	Braga et al. (2017)
Regional Context	UK	Serbia	Hong Kong	Portugal
ADP kg sb eq.	-	-	-	1.24E-06
GWP kg CO_2 eq.	3.29E+00	1.56E+03	3.30E+01	2.79E+01
ODP kg CFC-	4.50E-07	-	9.91E-07	2.26E-07
POCP kgC_2H_4eq.	1.20E-03	3.09E-01	-	9.06E-03
AP kgSO_2 eq.	1.89E-02	1.79E+01	1.90E-01	1.59E-01
EP kgPO_4^{2-}eq.	-	2.22E+00	-	3.54E-02
PE- NRe MJ	1.07E-03	-	5.18E+02	3.92E+02
PE-Re MJ	-	1.62E+01	-	4.52E-01

The use of PET as sand in concrete requires the processing of PET from the form in which it originates as a waste to a fine powder to match the characteristics of N-Sand. To obtain the sand-sized PET particles, the waste PET should be converted to flakes. These flakes are further shredded to obtain sand-sized PET particles. In the recycling sector, Arena et al., (2003) have presented the LCA of the phases of collection, compaction, sorting, processing, and conversion of waste PET into flakes. The typical flow diagram of LCA of PET waste from its collection to the transformation into PET

flakes for secondary use as presented by the authors has been presented in Fig. 7.7. The authors analyzed the material consumption, energy requirements, and environmental emissions for the entire process (Arena et al., 2003). However, the impact data was not by the parameters laid down by EN 15804, so could not be utilized in current research.

Table 7.5 Environmental impact factors for 1 ton of NCA

Reference	Sjunnesson (2005)	Korre and Durrucan (2009)	Marinković et al. (2010)	Tošić et al. (2015)	Hossain et al. (2016b)	Braga et al. (2017)	Rosado et al. (2017)
Regional Context	Sweden	UK	Serbia	Serbia	Hong Kong	Portugal	Brazil
ADP kg sb eq.	-	-	-	-	-	1.09E-06	-
GWP kg CO_2 eq.	1.60E+00	9.30E-01	1.56E+03	2.12E+00	3.20E+01	2.44E+01	2.00E+00
ODP kg CFC-11eq.	-	1.06E-07	-	-	9.88E-07	2.43E-07	2.62E-07
POCP kgC_2H_4eq.	1.70E-03	4.58E-04	3.09E-01	4.15E-04	-	7.83E-03	8.36E-04
AP kgSO_2 eq.	7.80E-04	5.85E-03	1.79E+01	2.42E-02	1.90E-01	1.44E-01	1.17E-02
EP kgPO_4^{2-}eq.	-	-	2.22E+00	3.01E-03	-	3.18E-02	7.15E-04
PE- NRe MJ	3.00E+01	4.35E-04	-	2.19E-02	4.96E+02	3.44E+02	-
PE-Re MJ	2.00E+01	-	1.62E+01	-	-	3.81E-01	-

Table 7.6 Impact factors for the production of 1 ton of SFS-Sand (Faleschini et al. 2014)

Impact	ADP	GWP	ODP	POCP	AP	EP	Pe- NRe	Pe- Re
Unit	kg sb eq.	Kg CO_2 eq.	KgCFC-11eq.	kgC_2H_4eq.	kgSO_2 eq.	kgPO_4^{2-}eq.	MJ	MJ
Impact factor	-	3.09E+00	3.82E-07	1.15E-03	1.86E-02	1.69E-03	-	-

The LCA of recycling PET bottles into flakes for the secondary use of PET waste has been presented by Aryan et al. (2019). The authors individually analyzed each phase of PET recycling and quantified energy requirements and emissions in the environment. The environmental impacts from the collection of waste to the processing of the waste into PET flakes for secondary use have been analyzed and presented confirming the guidelines laid as per EN 15804. The data has been provided for Dhanbad City of India (Aryan et al. 2019).

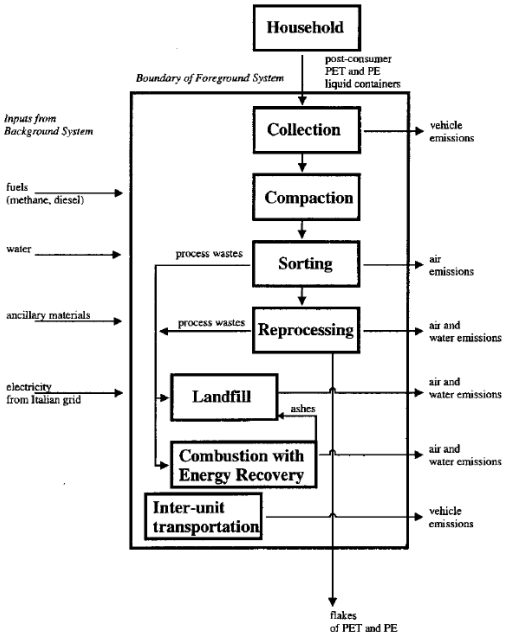

Fig. 7.7 Process flow diagram for recycling PET waste into flakes (Source: Arena et al., (2003))

The collection of plastic waste was done by rag-pickers and household waste collectors. No environmental burden or energy consumption was considered during the collection of plastic waste. This waste is either taken by hand cart/bicycle or in bags or sacks on their back and sold to small/medium scrap dealers. These dealers segregate this polymeric waste into various polymer forms like PET, PE, PP, PVC, etc. Then the segregated waste is stored in warehouses. PET waste is sent to large scrap dealers or material recovery facilities (MRF). The transportation of the waste to the MRFs is the first investment of energy in PET recycling. PET wastes are again segregated manually at MRF for discarding other types of plastic waste from PET. After segregation, PET wastes are compacted using a hydraulic machine and converted into PET bales. PET bales are made for convenience in the transportation of PET bottle wastes. Hydraulic baler consumes electricity of around 2.2 kWh/tonne of PET wastes. This is the second investment in energy for recycling PET waste. From the MRF facility, PET bales are received by the recycling industries. In the PET recycling unit, the baled PET is segregated and shredded. The labels and bottle caps are removed by film shredders. After that film shredders remove the labels and bottle caps. After segregation and shredding, PET wastes undergo cleaning using an automated washing line. Caustic soda (NaOH) is

mixed with hot water (60 to 70 °C) to remove any oil and clean PET wastes properly. Approximately 25 kg NaOH is used per tonne of PET waste. After washing, PET wastes are dried and the product comes out called PET flakes. Coal is used in the boiler, approximately 125 kg of coal is used per tonne of PET flakes. Around 12% of PET bottles are discarded during the recycling process, hence the recycling of 1 tonne of PET provides 880 kg of PET pellets or flakes. Aryan et al. (2019) provide the environmental impacts of recycling PET waste into PET flakes of size fractions of 5-50mm which are further processed to obtain secondary products. The current research aims at reducing the flakes to match the gradation of N-Sand (Aryan et al. 2019). This requires additional shredding beyond flake formation. To obtain the environmental impacts of the production of fine PET- Sand, the impact values presented by Aryan et al. (2019) have been increased by 10% to account for the additional electricity consumed in the process. The impact factors obtained are summarized in Table 7.7.

Table 7.7 Impact factors for the production of 1 kg PET sand

Impact	ADP	GWP	ODP	POCP	AP	EP	Pe- NRe	Pe- Re
Unit	kg sb eq.	Kg CO_2	KgCFC-11eq.	kgC_2H_4eq.	$kgSO_2$ eq.	$kgPO_4^{2-}$eq.	MJ	MJ
Impact factor	2.04E-06	9.60E-01	3.96E-09	4.37E-04	9.01E-03	1.28E-03	0.00E+00	-

7.2.2.4 Inventory analysis for water

Water is one of the major components required for the production of concrete and its components. Therefore, it is important to understand the environmental and energy burden of the production of potable water. For that purpose, most of the researchers consider a “cradle-to-gate” approach that ends in the final consumer as shown in Fig. 7.8.

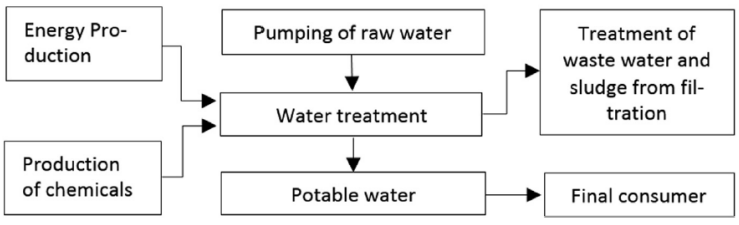

Fig. 7.8 System boundary of production of potable water

Table 7.8 summarizes the environmental impacts of the production of 1kg of potable water as presented by different studies across the globe using the Ecoinvent

database v3.0 included in Simapro software. The current research considered the values given by Braga et al. (2017) for the assessment of the environmental impacts of the novel concretes containing PET-Sand (Braga et al. 2017).

Table 7.8 Impact factors for the production of 1 kg water

Reference	Morales-Pinzon et al. (2011)	Cabejskova, (2012)	Braga et al. (2017)	Kurda et al., (2018b)
Regional Context	Colombia	Czech Republic	Portugal	European Union
ADP kg sb eq.	7.27E-05	1.18E-12	1.57E-11	1.57E-11
GWP kg CO_2 eq.	1.18E-02	7.82E-05	1.33E-04	0.00E+00
ODP kg CFC-11eq.	1.28E-08	1.18E-11	5.93E-12	-
POCP kgC_2H_4eq.	-	6.72E-09	4.99E-08	4.99E-08
AP kgSO_2 eq.	8.30E-05	1.47E-07	3.87E-08	3.87E-08
EP kgPO_4^{2-}eq.	-	7.02E-09	9.70E-07	9.70E-07
PE- NRe MJ	-	-	2.00E-03	2.00E-03
PE-Re MJ	-	-	1.80E-05	-

7.2.2.5 Inventory Analysis for Admixture

Polycarboxylic ether-based (PCE-based) admixture was used in the current study to improve the workability and compaction characteristics of concrete. Eco-profile for all main groups of superplasticizers (Sulphonated naphthalene formaldehyde, Sulphonated melamine formaldehyde, Vinyl copolymers, and Poly carboxylic ethers) was made available by the European Federation of Concrete admixtures Associations (EFCA) by the year 2015, through an Environmental Product Declaration (EPD) (EFCA, 2015). This data is preferred as generic data for most of the LCA studies on concrete irrespective of regional context. Therefore, the current research adopted the eco-profile of the production of 1kg of superplasticizer as per EFCA as listed in Table 7.9.

Table 7.9 Impact factors for the production of 1 kg of admixture (EFCA, 2015)

Impact	ADP	GWP	ODP	POCP	AP	EP	Pe- NRe	Pe- Re
Unit	kg sb eq.	Kg CO_2	KgCFC-11eq.	kgC_2H_4eq.	kgSO_2 eq.	kgPO_4^{2-}eq.	MJ	MJ
Impact	1.10E-06	1.88E+00	2.30E-10	3.12E-04	2.92E-03	1.03E-03	3.14E+01	1.51E+00

7.2.2.6 Inventory analysis of transportation of materials

The environmental impact of transportation of materials in the life cycle of concrete varies with the mode of transport selected for a particular material. It is related to the tonnage hauling capacity of the mode of transport. Depending upon the fuel consumption by the mode of transport, the environmental impact is defined for the transport of unit ton of material per km distance. ELCD core v.3 databases provides the environmental impact details for "Articulated lorry transport" different hauling capacities as cited in Kurda et al. (2018a). The present study assumes a heavy transport truck having a maximum capacity of 27 tons as a mode of transport for hauling the raw materials of concrete to the production plant (Kurda et al., 2018b). Table 7.10 presents the impact factors per tonne per km of the material hauled as per the datasets available in the ELCD core v.3 databases.

Table 7.10 Impact factors for material transport 1kg per km (Kurda et al., 2018a)

Impact	ADP	GWP	ODP	POCP	AP	EP	Pe- NRe	Pe- Re
Unit	kg sb eq.	Kg CO_2 eq.	KgCFC-11eq.	kgC_2H_4eq.	kgSO_2 eq.	kgPO_4^{2-}eq.	MJ	MJ
Impact factor	1.98E-12	4.98E-05	-	1.59E-08	2.24E-07	5.14E-08	6.73E-04	-

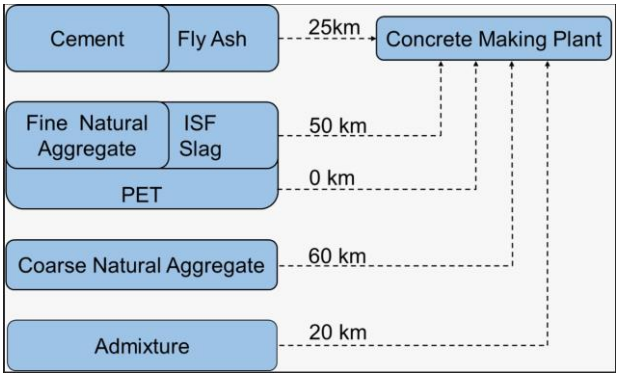

Fig. 7.9 Delivery distances of raw materials from the source to the concrete plant

The delivery distances of the raw materials between their source to the sink i.e., the production plant of concrete are very case specific. For this reason, a hypothetical case having nominal delivery distances of raw materials has been analyzed in the current study. Figure 7.9 shows the delivery distances of raw materials to the concrete production plant. The delivery distances of the alternative materials and the conventional materials are assumed to be equal to avoid the effect of the environmental burden of transportation

on the comparative analysis. The delivery distance of PET-Sand is taken as 'zero' for the baseline case for a better understanding of the environmental impact of utilizing PET for the assumed functional unit incorporating functional strength as one of the parameters.

7.2.2.7 Inventory analysis for the production of 1 m^3 of concrete

The environmental impacts in a concrete-making plant are the results of the energy consumption in the operation of the plant. Raw materials are mixed in elevated bins and placed directly into concrete trucks for final transport. This process is primarily powered by electricity, with small amounts of other fuels used on each site by small excavators used to move raw materials, etc. Electric mixing equipment is the most significant contributor to the emissions generated by concrete batching. Flower and Sanjayan (2017) audited six different batching plants in Australia to determine the energy consumption and production levels over 6 months and presented only the carbon emission data on the making of one cubic meter of concrete (Flower and Sanjayan, 2017). However, Braga et al. (2017) determined the environmental impacts of the production of $1m^3$ concrete for all the impact categories using the Baseline CML method in SimaPro software. Table 7.11 presents these impact values for the production of $1m^3$ of concrete as evaluated by Braga et al. (2017).

Table 7.11 Impact factors for the production of $1m^3$ of concrete (Braga et al. 2017)

Impact	ADP	GWP	ODP	POCP	AP	EP	Pe- NRe	Pe- Re
Unit	kg sb eq.	Kg CO_2	KgCFC-11eq.	kgC_2H_4eq.	$kgSO_2$ eq.	$kgPO_4^{2-}$eq.	MJ	MJ
Impact	5.50E-07	4.65E+00	2.08E-07	1.36E-03	3.40E-02	1.75E-03	67.81E+00	-

7.2.3 Life cycle impact analysis (LCIA)

Seven environmental categories were considered in the present study: ADP, GWP, ODP, AP, EP, POCP, and energy demand through PE-NRe. To obtain these results, the CML 2002 baseline method was used for the six first categories, and Cumulative Energy Demand for the last one, in the SimaPro. Table 7.12 presents an overview of these impact categories, viz. names, acronyms, and also the units used to quantify each of these impact categories. The impact factors for the respective category have also been included in the table as a ready reckoner in the LCIA of all the design mixes of the present study.

The current research deals with the environmental impact assessment of novel concrete mixes containing PET sand in varying proportions as a substitute aggregate for

N-Sand in three different tiers. The composition of the mixes in different tiers has been discussed in detail in the scheme of experimentation in Chapter 4. With the variations in the aggregate and the binder composition for the series of mixes, it is rather interesting to compare the environmental impacts and energy demand for all the mixes considering a $1m^3$ volume of concrete as the FU of assessment without any reference to the strength or other characteristics of concrete. This may be considered the preliminary exercise of LCIA in the current research. This assessment is performed with the hypothesis that the utilization of waste materials like PET, SFS, and FLA with lower embodied impacts and energy would lower the environmental and energy burden per unit volume compared to concrete with conventional ingredients. This preliminary assessment of concrete with unit volume as the sole FU is presented in § 7.2.3.1.

The use of waste materials as a substitute for conventional ingredients in concrete may provide an environmental advantage for a given volume of concrete. However, if this benefit is achieved at the cost of the quality of the concrete, the benefit is not justified. To overcome this limitation, the LCA methodology suggests the use of one or more quality parameter/s in the FU, in addition to the quantity of concrete. These additional parameters may be derived from the strength criteria or serviceability criteria of concrete. Most of the recent studies in the literature have considered compressive strength at 28 days as an additional parameter in the FU along with 1 m^3 volume of concrete (Kurda et al., 2018a; Mohammadi and South, 2017; Park et al., 2012; Proske et al., 2013). Few studies also use the service life of concrete as the FU (Van Den Heede et al. 2012; Van Den Heede and De Belie 2014; Pillai et al. 2019). The current study proposes to use the FU of $1m^3$ of concrete with compressive strength at a specified age. It means that for a logical comparison of the environmental impact of any mix in the experimental scheme for 1 m^3 volume, the compressive strength of that particular mix should be equal to the compressive strength of the control mix, at the specified age. In experimental attempts of obtaining green concrete mixes, it is difficult to obtain the mix proportions that deliver strength values in the range closer to that of control mixes. This fact makes comparative LCA analysis a difficult task. To minimize this difficulty and to enable a logical comparative analysis, Damineli et al. (2010) proposed a generalized term called impact intensity, e.g., GWP intensity, G_i, in kg-CO_2/m^3/MPa to relate GWP emission with the

compressive strength (f_c) for any type of mix for unit volume(Damineli et al. 2010). It is given by equation 7.1:

$$G_i = \frac{GWP}{f_c} \quad \text{.....eq. 7.1}$$

This impact intensity gives a normalized value of the impact concerning compressive strength at a specified age. This representative term can be very effectively used for a systematic and consistent comparison of the environmental impact of different mixes, especially in green concretes (Bhagat and Savoikar, 2021). This analysis is presented in § 7.2.3.2 for various mixes in the current research highlighting the benefits or drawbacks based on the outcomes of this analysis.

In the third version of the analysis, the impacts are calculated for a specific FU of $1m^3$ of concrete having a specific compressive strength. Based on the results of laboratory tests, mathematical models are devised to determine the replacement ratio of PET for each tier which can deliver concrete with specified strength at a specified age. The CML baseline impact indicators and energy consumption values are then compared with the control mix composition that can deliver the specified strength at the specified age. This analysis is presented in § 7.2.3.3.

7.2.3.1 Impact assessment for 1 m^3 of concrete

The scheme of experimentation in the current research investigated two grades of concrete, i.e., M30 and M50 grade of concrete. Three different tiers of mixes were formulated and tested for physical, mechanical, and durability-related properties. The mix compositions for both grades of concrete with three different tiers are summarized in **Appendix D**. Depending on the transportation distances of respective ingredients, it is possible to determine the total transportation burden in terms of kg.km unit. Based on the emission factors as per the CML baseline method and cumulative energy demand factors the impact values are determined for all seven impact categories. The results for all impact categories for the three tiers of mixes for both grades of concrete are presented in Tables 7.13 and 7.14. The variations in the environmental impact and cumulative energy demand for various mixes with different compositions of PET-Sand are also exhibited in Fig. 7.10 and 7.11 respectively.

Table 7.12 Impact categories and impact factors in LCA of concrete in the present study

Impact Category	Abiotic depletion	Climate change	Stratospheric ozone depletion	Photo-oxidant formation	Acidification	Eutrophication	Cumulative Energy Demand
Characterization factor	ADP	GWP	ODP	POCP	AP	EP	PE-Nre
Unit	kg sb eq.	kg CO_2 eq.	kgCFC-11eq.	kgC_2H_4eq.	kgSO_2 eq.	kgPO_4^{2-}eq.	MJ
Significance	Depletion of natural non-living resources (minerals and fossil fuels)	Deals with all GHGs that may cause the earth's temperature to rise and hurt the ecosystem and human health and material welfare	The ozone depletion produced by CFCs	Indicates the potential capacity of a volatile organic substance to produce ozone	Covers all impacts on soil, water, organisms, ecosystems and materials by acidifying pollutants (e.g., SO_2, NO_x, NH_x)	Covers all impacts of excessively high environmental levels of macronutrients (N, P) causing a shift in species composition and elevated biomass production in aquatic and terrestrial ecosystems	Consumption of energy contributing to the exhaustion of natural reserves of fossil (coal, petroleum, and natural gas) and nuclear (uranium) energy.
Cement OPC (kg)	1.59E-03	8.44E-01	2.28E-08	4.26E-05	1.15E-03	1.73E-04	6.42E+00
Fly ash (kg)	3.37E-04	8.77E-03	5.58E-09	3.22E-06	5.53E-05	8.23E-06	8.33E-01
Crushed Fine Aggregate (kg)	1.24E-09	2.79E-02	2.26E-10	9.06E-06	1.59E-04	3.54E-05	3.92E-01
ISF Slag (kg)	-	3.09E-03	3.82E-10	1.15E-06	1.86E-05	1.69E-06	-
PET waste (kg)	2.04E-06	9.60E-01	3.96E-09	4.37E-04	9.01E-03	1.28E-03	2.22E-02
Natural Coarse Aggregate (kg)	1.09E-09	2.44E-02	2.43E-10	7.83E-06	1.44E-04	3.18E-05	3.44E-01
Water (kg)	1.57E-11	1.33E-04	5.93E-12	4.99E-08	3.87E-08	9.70E-07	1.80E+01
Admixture (kg)	1.10E-06	1.88E+00	2.30E-10	3.12E-04	2.92E-03	1.03E-03	3.14E+01
Concrete making (m3)	5.50E-07	4.65E+0.00	-	1.36E-03	3.40E-02	1.75E-03	6.78E+01
Transportation (t.km)	1.98E-09	4.98E-02	-	1.59E-05	2.24E-04	5.14E-05	6.73E-01

Table 7.13 Baseline CML method results of impacts and energy demand for $1m^3$ concrete (M30 grade)

Impact	ADP x 10^{-1}	GWP x 10^{2}	ODP x 10^{-6}	POCP x 10^{-2}	AP x 10^{-1}	EP x 10^{-1}	PE- Nre x 10^{3}
Control Mix (OPC/N-Sand)							
C_{30}-C-P0	6.04	3.88	9.35	3.70	8.07	1.43	3.40
Tier I Concrete (OPC/N-Sand+PET-Sand)							
C_{30}-C-P10	6.04	4.19	9.47	5.14	11.07	1.85	3.37
C_{30}-C-P15	6.04	4.35	9.53	5.86	12.57	2.06	3.35
C_{30}-C-P20	6.04	4.50	9.59	6.59	14.07	2.26	3.34
C_{30}-C-P25	6.04	4.66	9.65	7.31	15.57	2.47	3.32
Tier II Concrete (OPC/N-Sand+SFS-Sand+PET-Sand)							
C_{30}-C-SP0	6.04	3.81	9.41	3.48	7.67	1.34	3.29
C_{30}-C-SP10	6.04	4.13	9.53	4.94	10.71	1.76	3.27
C_{30}-C-SP15	6.04	4.29	9.59	5.67	12.23	1.97	3.26
C_{30}-C-SP20	6.04	4.45	9.64	6.41	13.75	2.19	3.25
C_{30}-C-SP25	6.04	4.60	9.70	7.14	15.27	2.40	3.24
Tier III Concrete (OPC+FLA/N-Sand+SFS-Sand+PET-Sand)							
C_{30}-CF-SP0	4.61	2.84	7.43	2.96	6.31	1.12	2.62
C_{30}-CF-SP10	4.61	3.15	7.54	4.40	9.28	1.54	2.60
C_{30}-CF-SP15	4.61	3.31	7.60	5.11	10.77	1.75	2.59
C_{30}-CF-SP20	4.62	3.46	7.65	5.83	12.26	1.96	2.58
C_{30}-CF-SP25	4.62	3.62	7.71	6.55	13.75	2.16	2.57

There was no variation in ADP with the increase in PET replacement in Tier I and Tier II concretes relative to the control mix. However, a decrease of 24% values in ADP was observed in the case of Tier III mixes. It can be concluded that the inclusion of SFS and/or PET does not have any influence on the ADP of concrete mixes. The decline in ADP values of Tier III mixes is due to the replacement of OPC content in the mixes by FLA which exhibits an ADP impact 80% lower than the OPC. The trend of variations in ADP was the same irrespective of the grade of concrete, except for the fact that the values of ADP for mixes of M50 grade were higher than M30 grade concrete, thanks to the higher OPC content in the M50 mix.

All the tiers of concrete mixes showed a linear increase in the GWP with an increase in PET replacement. In comparison to the mix with no PET, an increase of 20% was noticed for the mix with 25% PET replacement for all the tiers. This increase is attributed to the CO_2 emission involved in the recycling of PET particles which is reported to be 0.96 kg CO_2 eq. per kg of PET shredded. The utilization of SFS-Sand in Tier II did not show a significant effect on the GWP of the mixes. However, in Tier III, the replacement of OPC by a weight ratio of 30% showed a significant decrease in the GWP values of the mixes. A GWP value 27% lower than the control mix was observed for the Tier III mix with no PET. However, the benefit was reduced to 7% when 25% of PET was included in the mix, incurring the environmental cost of recycling PET waste. This benefit was attributed to the lower emission coefficient of FLA, almost one order lower than OPC for no allocation approach. The results reveal that OPC contributes to almost 80-82% of the GWP of the control mix. This is in agreement with the findings in the literature (Gursel et al., 2016; S. Marinković et al., 2017; Vieira et al., 2016). However, due to the burden introduced by PET recycling, the share of contribution by OPC declined with the increase in PET substitution. For M50 grade concrete, the GWP values for concrete mixes were reported as 9-10% higher than M30 grade concrete for the corresponding mixes in the scheme of experimentation. This was attributed to the higher consumption of OPC in the higher-grade concrete mix.

The ODP values of the concrete mixes also showed an increasing trend with the increase in PET replacement, irrespective of the grade and the tier of concrete. An increase of 3-4% was observed in ODP values for the 25% replacement of N-Sand by PET waste. SFS inclusion did not cause a noticeable variation in ODP. However, tier III mixes with FLA showed a decline in values of ODP compared to the control mix. Tier III mix with 25% PET showed a decrease in ODP value by 18%, irrespective of the grade of concrete.

A sharp increase in values of POCP and AP was observed with an increase in PET substitution in concrete. An increase to the order of 17-20% for every 5% PET inclusion was noticed in these impacts. For the M30 grade mix, the Tier I concrete with 25% PET inclusion showed an increase in POCP and AP values by 97% and 93% respectively. For Tier II mixes, the blending of SFS with N-Sand could lower the values by 5-6%. In this

tier, the 25% PET mix presented POCP and AP values which are 93% and 89% higher than the control mix. The use of FLA as a binder and SFS-Sand in Tier III could show a saving of 20-22% in POCP and AP values. The increase in POCP and AP values for 25% PET-Sand mixes in Tier III relative to the control mix was found to be 77% and 70% respectively. For M50 grade concrete, the magnitude of impact for each mix was higher than the M30 grade. However, the increase in impact with an increase in PET for M50 grade concrete was 5-7% lower than M30 grade concrete.

Table 7.14 Baseline CML method results of impacts and energy demand for $1m^3$ concrete (M50 grade)

Impact	ADP x 10^{-1}	GWP x 10^{2}	ODP x 10^{-6}	POCP x 10^{-2}	AP x 10^{-1}	EP x 10^{-1}	PE- Nre x 10^{3}
Control Mix (OPC/N-Sand)							
C_{50}-C-P0	6.84	4.29	10.48	3.88	8.59	1.51	3.71
Tier I Concrete (OPC/N-Sand+PET-Sand)							
C_{50}-C-P10	6.84	4.60	10.60	5.30	11.53	1.92	3.68
C_{50}-C-P15	6.84	4.75	10.66	6.01	13.01	2.12	3.66
C_{50}-C-P20	6.84	4.90	10.72	6.71	14.48	2.32	3.64
C_{50}-C-P25	6.84	5.06	10.78	7.42	15.95	2.53	3.63
Tier II Concrete (OPC/N-Sand+SFS-Sand+PET-Sand)							
C_{50}-C-SP0	6.84	4.22	10.55	3.66	8.19	1.41	3.59
C_{50}-C-SP10	6.84	4.54	10.66	5.10	11.18	1.83	3.57
C_{50}-C-SP15	6.84	4.69	10.71	5.82	12.67	2.04	3.56
C_{50}-C-SP20	6.84	4.85	10.77	6.54	14.16	2.25	3.55
C_{50}-C-SP25	6.84	5.00	10.83	7.26	15.66	2.46	3.54
Tier III Concrete (OPC+FLA/N-Sand+SFS-Sand+PET-Sand)							
C_{50}-CF-SP0	5.22	3.13	8.31	3.12	6.72	1.18	2.86
C_{50}-CF-SP10	5.22	3.44	8.42	4.52	9.64	1.59	2.84
C_{50}-CF-SP15	5.22	3.59	8.48	5.22	11.09	1.80	2.83
C_{50}-CF-SP20	5.22	3.74	8.53	5.93	12.55	2.00	2.82
C_{50}-CF-SP25	5.22	3.90	8.59	6.63	14.01	2.21	2.81

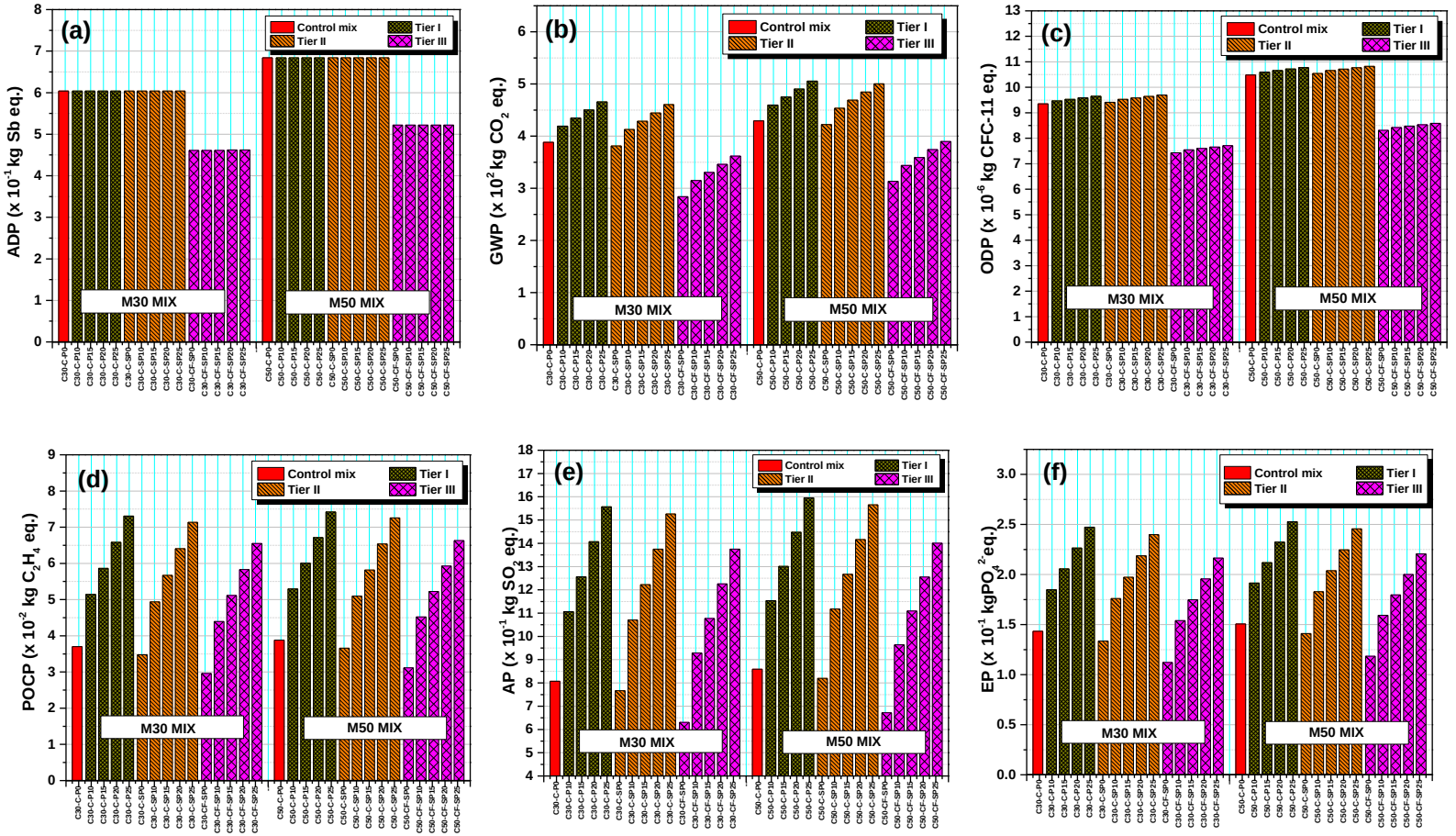

Fig. 7.10 Environmental impacts of concrete mixes per m^3 of concrete (a) ADP (b) GWP (c) ODP (d) POCP (e) AP (f) EP

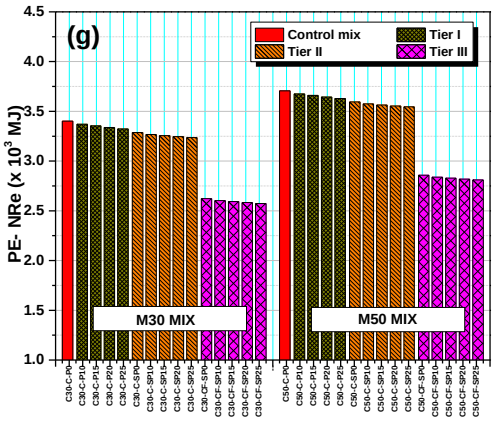

Fig. 7.11 Cumulative energy demand (PE-NRe) for 1m^3 concrete

A trend similar to POCP and AP was observed in the case of the EP impact indicator. For every 5% increase in PET inclusion, there was an increase of 14-15% EP impact. The use of SFS-Sand, as well as FLA, could lower the EP impact substantially. Tier I mix with 25% PET-Sand showed an increase of 73% in EP value when compared with a mix with no PET. However, the corresponding mixes in Tier II and Tier III showed a respective increase of 67% and 51% in EP values due to the lower contribution of SFS and FLA to eutrophication impact compared to N-Sand and OPC. Although M50 concrete mixes exhibited higher values of EP than M30 mixes, the increase in EP compared to the control mix due to the increase in PET volumes was lower than the corresponding increase in M30 concrete mixes.

The cumulative energy demand (non-renewable) decreased with the increase in PET content inside the concrete (See Fig. 7.11). Furthermore, the addition of SFS-Sand and FLA also showed significant savings in cumulative energy demand values. This is attributed to the use of alternative materials having lower embodied energy than the conventional ingredients inside the concrete. For both mix proportions i.e., M30 and M50, the saving in CED values for Tier I, Tier II, and Tier III mixes were 2%, 4%, and 24% respectively. This shows that the use of SCM such as FLA causes a significant reduction in the energy demand for concrete.

7.2.3.2 Impact Intensity with Respect to compressive strength

To determine the impact intensity of the control mix and the experimental green mixes with different compositions of PET-Sand, SFS-Sand, and FLA, the CML baseline impact indicator GWP is selected in the current research. The impact intensities are

determined for compressive strength values at three different ages, i.e., 28 days, 56 days, and 90 days. Table 7.15 summarizes these intensities for GWP for M30 and M50 grade concrete. The GWP intensity values are also presented graphically in Fig. 7.12 and 7.13 for a comparative analysis with the GWP intensity of the control mix.

Table 7.15 GWP impact intensity with respect to compressive strength for concrete

Mix	M30 mix			M50 mix		
	28 days	56 days	90 days	28 days	56 days	90 days
Control Mix (OPC/N-Sand)						
C_Y-C-P0	9.56	9.15	8.70	6.20	5.99	5.87
Tier I Concrete (OPC/N-Sand+PET-Sand)						
C_Y-C-P10	10.26	9.78	9.33	6.57	6.38	6.21
C_Y-C-P15	11.28	10.92	10.89	7.29	7.36	6.99
C_Y-C-P20	13.47	13.18	12.84	8.29	8.15	7.83
C_Y-C-P25	15.64	15.12	14.3	9.24	9.25	8.97
Tier II Concrete (OPC/N-Sand+SFS-Sand+PET-Sand)						
C_Y-C-SP0	8.51	8.09	7.73	5.46	5.24	5.20
C_Y-C-SP10	9.24	9.43	8.70	6.23	6.02	5.91
C_Y-C-SP15	10.25	10.40	10.01	6.71	6.63	6.49
C_Y-C-SP20	12.18	12.68	11.96	7.63	7.53	7.25
C_Y-C-SP25	14.02	13.98	13.22	8.74	8.61	8.48
Tier III Concrete (OPC+FLA/N-Sand+SFS-Sand+PET-Sand)						
C_Y-CF-SP0	6.89	6.21	5.74	4.40	4.12	3.99
C_Y-CF-SP10	7.57	7.05	6.66	5.05	4.74	4.57
C_Y-CF-SP15	8.44	7.78	7.28	5.64	5.21	4.95
C_Y-CF-SP20	10.12	8.95	8.39	6.75	5.95	5.56
C_Y-CF-SP25	11.99	10.57	9.73	7.43	6.84	6.64

($_Y$=30 for M30 mix, $_Y$=50 for M50 mix)

The results of the strength properties of concrete have confirmed the decline in the values of compressive strength of concrete with an increase in PET content in the mix. Furthermore, in the environmental impact analysis of concrete mixes of each tier, it is seen that the GWP value of the concrete goes on increasing with the increase in PET substitution levels. Therefore, it is obvious that G_i increases with the increase in PET content in the mix. It can be seen that considering all the tiers of mixes in both grades, there is an overall increase in GWP intensity by almost 50-65% when N-Sand is replaced

for 25% of volume by PET. Although the G_i value is higher for the M30 mix in comparison to the M50 mix, the trend of variations in values with PET replacement levels is consistent for both mixes.

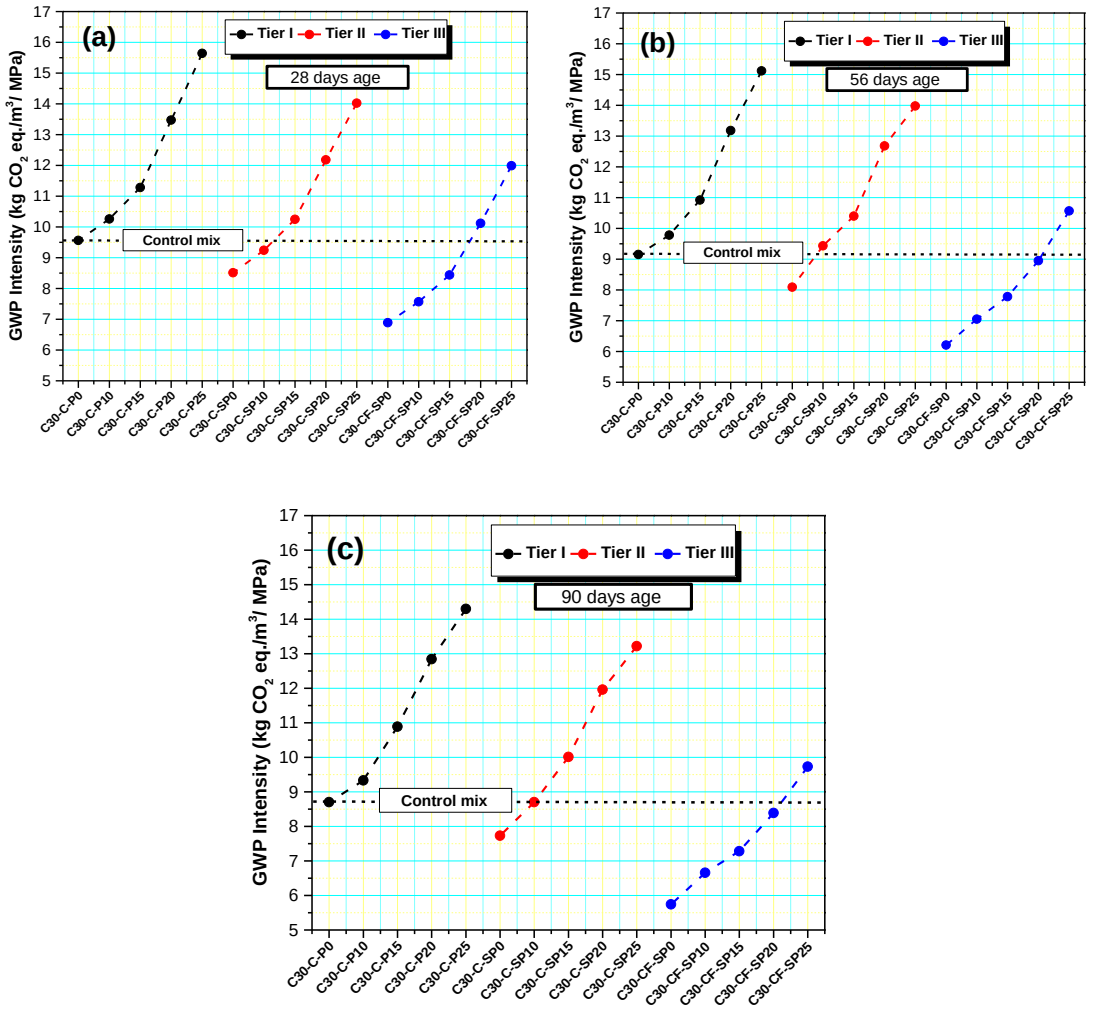

Fig. 7.12 GWP intensity of M30 concrete mixes with respect to compressive strength (a) 28 days (b) 56 days (c) 90 days

It can be seen that in the case of Tier I mixes, the GWP intensity increases by almost 65% for PET inclusion of 25% of the volume of N-Sand. Tier I mixes shows the highest G_i values for a given replacement ratio of PET compared to the other two tiers. In the case of Tier II mixes, a decrease in GWP intensity values to the order of 10-17% is reported in comparison to Tier I mixes for all ages. The lower values of G_i in the case of Tier II mixes are attributed to the increase in compressive strength of the mixes due to the inclusion of SFS-Sand due to the various reasons already discussed in Chapter 4. Tier III

mixes show a significant reduction in GWP over Tier I mixes. The reduction rate varies from 30-50% depending on the mix grade and the age of testing. These Tier III concrete specimens with FLA as supplementary binder exhibits the lowest G_i values for a given PET replacement ratio. This is attributed to the reduction in the GWP impact of the mixes due to the lower CO_2 emissions by the FLA which occupies 30% of the weight of OPC in the mixes. The latter is the giant contributor to GWP emissions as already discussed in the previous sections.

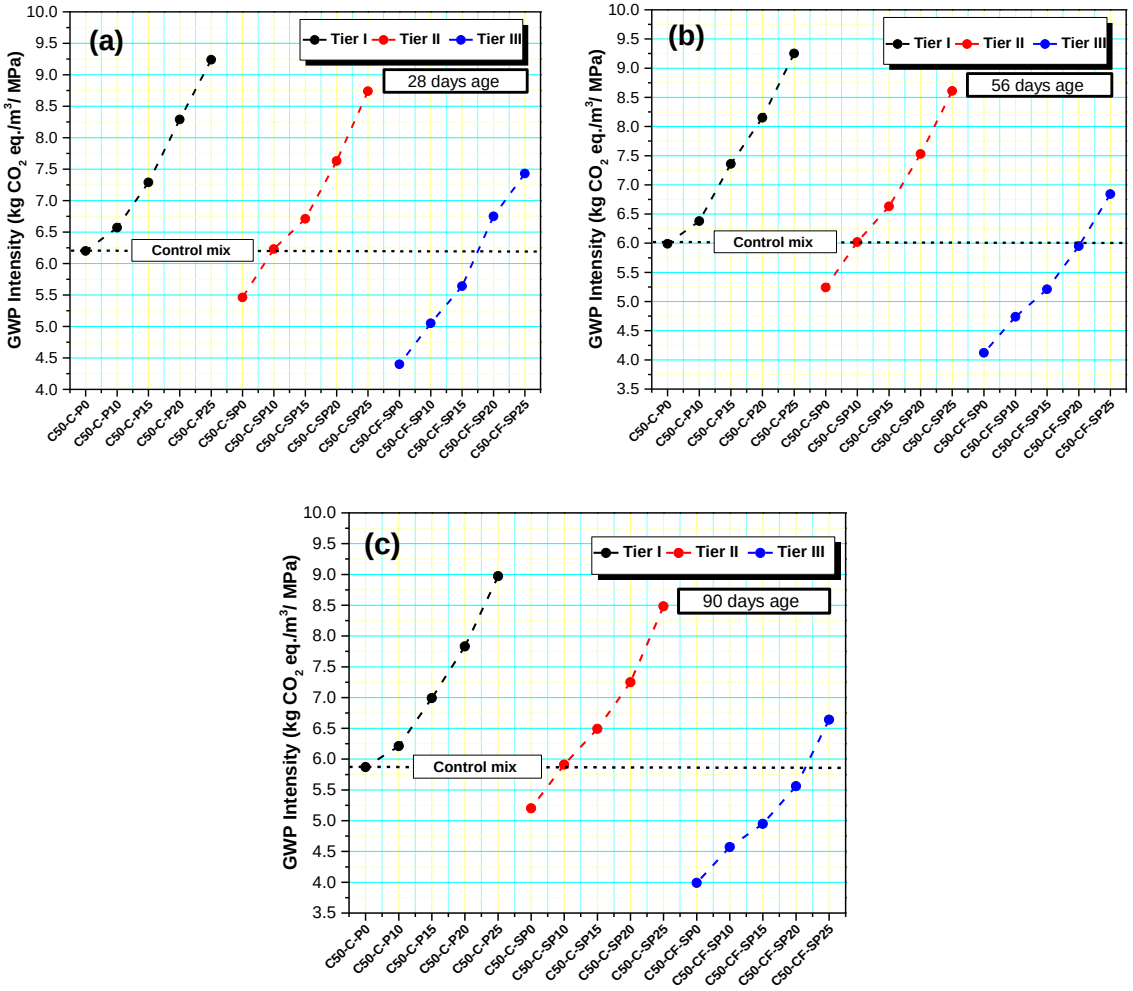

Fig. 7.13 GWP intensity of M50 concrete mixes with respect to compressive strength (a) 28 days (b) 56 days (c) 90 days

Fig. 7.12 and 7.13 also show the G_i of all the tiers of mixes relative to the G_i of the control mix. This comparative analysis enables tracing of the mixes having G_i values lower than the G_i of the control mix. From the consistency in results for M30 and M50 grade concretes, it can be confirmed that Tier II mixes with 10% PET-Sand shows G_i

values in close range with the G_i values of the control mix. In the case of Tier III mixes, at 28 days of aging, the specimens with 15% PET-Sand exhibited G_i values much lower than that of the control mix. At the same age, specimens with 20% PET-Sand showed higher G_i values compared to the control mix. On the other hand, at prolonged curing spans of 56 days and 90 days, the Tier III specimens with 20% PET showed G_i values lower than that of the control mix. This is attributed to the strength enhancement in the case of FLA blended mixes at prolonged ages due to the delayed hydration reaction of FLA.

7.2.3.3 Impact analysis for the functional unit of 1m^3 volume and specified strength

The third version of the LCIA of the concrete mixes in the current research considered the quality aspect of concrete in the selection of FU of the assessment. Along with the volumetric function of 1m^3 of concrete, compressive strength was also included as an additional parameter in FU. Two different compressive strength values (40 N/mm^2 and 60 N/mm^2 at 90 days of age) were selected to evaluate the consistency of the results of the assessment. Accordingly, two FUs were designated as "FU40" mix and "FU60" mix i.e., 1m^3 concrete having 40 N/mm^2 compressive strength at 90 days and 1m^3 concrete having 60 N/mm^2 compressive strength at 90 days respectively. The analysis with these two FUs is performed in the following steps:

1) The compressive strength values obtained from the laboratory results for M30 and M50 grade concrete (see table 5.6 in Chapter 5) are used to determine the percentage of PET in the mix for three different tiers that can deliver the specified compressive strength as per the FU selected for the analysis. These values are plotted against the respective volumes of PET in the mix as shown in Fig. 7.14 and 7.15. A best-fitting curve is plotted to obtain a mathematical relation that facilitates the evaluation of the percentage of PET-Sand that corresponds to the strength values of 40N/mm^2 and 60N/mm^2 as per FU. Mathematical correlations with high correlation coefficients are obtained for both the mixes as evident from Fig. 7.14 and 7.15. The percentage volume of PET-Sand that delivers the FU40 mix and FU60 mix is determined from the best-fitting curve. These percentage volumes of PET are presented in Table 7.16.

Table 7.16 PET proportion for concrete of with specified compressive strength

Compressive strength at 90 days	Tier I Concrete	Tier II Concrete	Tier III concrete
40 N/mm2	15.66%	18.71%	21.81%
60 N/mm2	18.32%	20.86%	21.23%

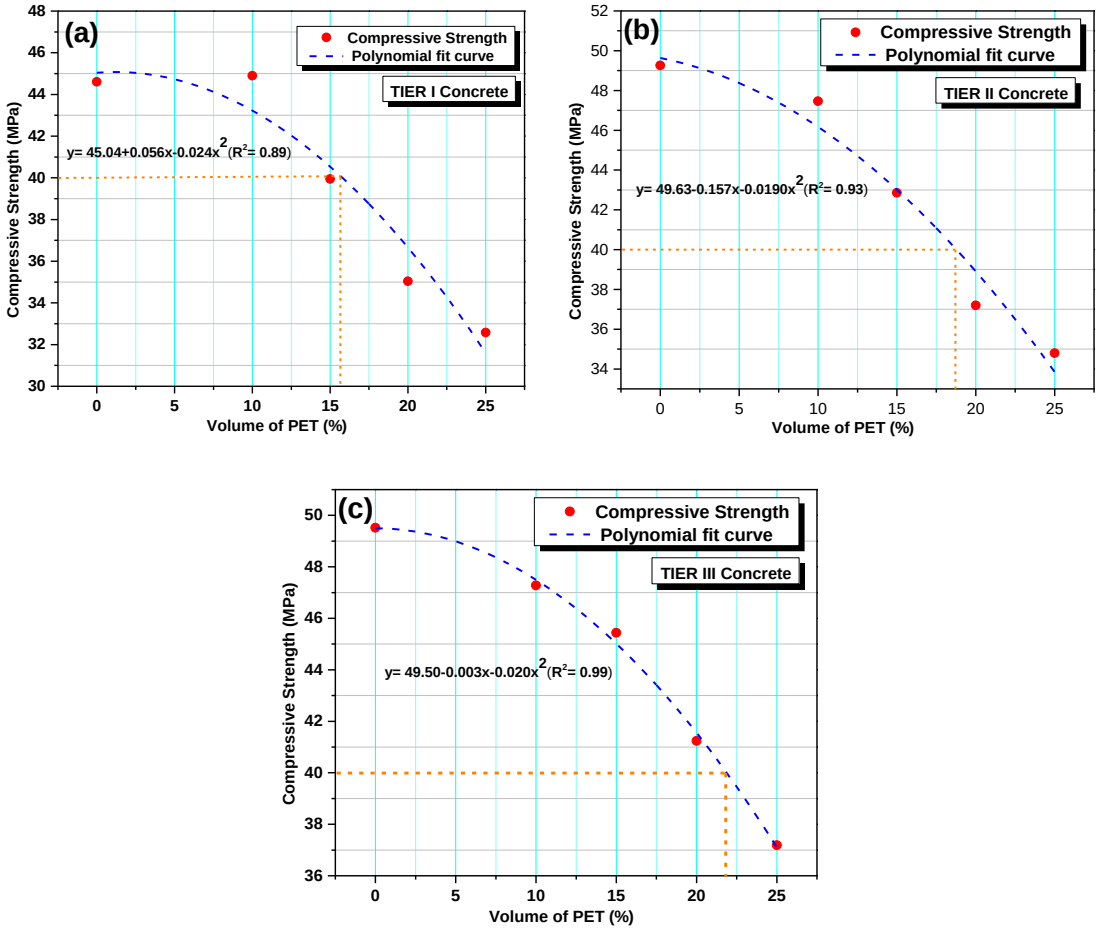

Fig. 7.14 Optimum PET content in the FU40 mix (a) Tier I (b) Tier II (c) Tier III

2) In the next step, the cement content of reference concrete mix with conventional ingredients that can deliver compressive strengths of 40 N/mm^2 and 60 N/mm^2 at 90 days of age are determined. This analysis is performed with laboratory test data obtained from compressive strength tests of control mixes with different cement contents as listed in Table 7.17. These values of compressive strength are plotted against the cement content of the mix as shown in Fig. 7.16 to obtain the cement content required to attain the compressive strength of 40 N/mm^2 and 60 N/mm^2 for the reference mix at 90 days of age.

From the plot of cement content versus compressive strength, it was found that a cement content of 354 kg/m^3 and 420 kg/m^3 was required to attain compressive strength of 40 N/mm^2 and 60 N/mm^2 respectively, for the control mix.

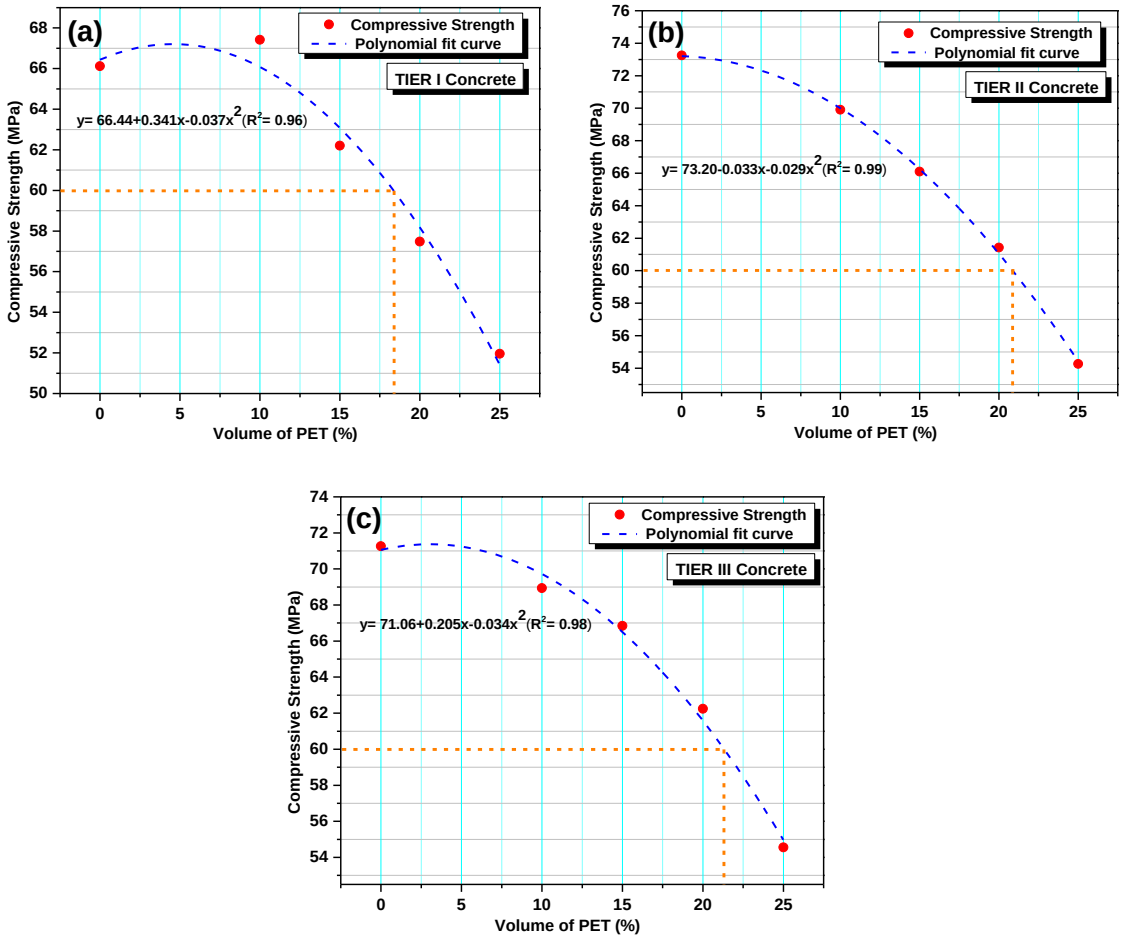

Fig. 7.15 Optimum PET content in the FU60 mix (a) Tier I (b) Tier II (c) Tier III

Table 7.17 Compressive strength at 90 days for reference concrete with different cement contents

Cement content, kg	300	350	380	430	450
Compressive strength at 90 days, N/mm^2	36.10	40.20	44.60	66.12	70.48

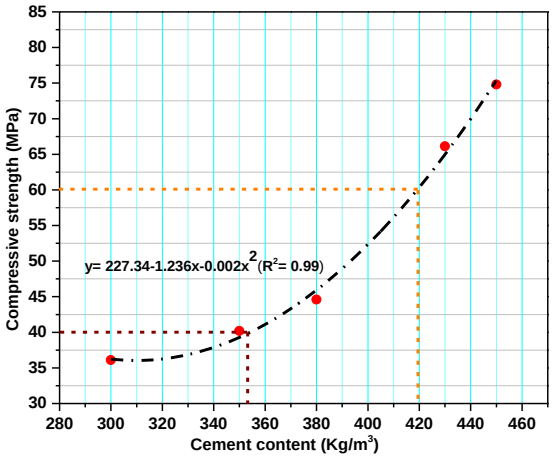

Fig. 7.16 Cement content of control mixes having a compressive strength of 40 N/mm^2 and 60 N/mm^2 at 90 days age

3) After the determination of the PET content corresponding to the specified strength of the concrete for respective tiers, the mix composition for each tier is calculated with the percentage of PET as listed in Table 7.15.

   The mix design is conducted based on the particle-matrix model, which is a common approach for concrete proportioning and is in alignment with the existing data for the selected experimental work. (Sample calculations for Tier II mix for FU40 mix are presented in **Appendix E**).

4) The mix proportions for reference concretes are determined to correspond to the cement content values obtained in step 2 above. The material proportions for reference concrete and the three tiers of mixes are listed in Table 7.18.

Table 7.18 Mix proportions for concrete for FU40 mix and FU60 mix

Materials (kg/m^3)	FU40 mix				FU60 mix			
	Control	Tier I	Tier II	Tier III	Control	Tier I	Tier II	Tier III
OPC	354	380	380	266	420	430	430	301
FLA	0	0	0	114	0	0	0	129
N-Sand	761	625	361	341	735	593	345	336
SFS Sand	0	0	280	264	0	0	268	261
PET Sand	0	54.31	64.89	74.11	0	62.30	71.06	70.65
NCA	1305	1270	1270	1208	1261	1248	1248	1220
Water	155.8	167.2	167.2	167.2	159.6	163.4	163.4	163.4
Admixture	2.48	2.66	2.66	2.66	2.52	2.58	2.58	2.58

5) Using the characterization factors for CML baseline impacts and energy demand in Table 7.11, the environmental impacts of concretes in three different tiers with PET-Sand content corresponding to the selected FU are calculated. The impact values are also calculated for the reference mixes obtained for the respective FUs. The results of the environmental impacts are presented in Table 7.19. These environmental impacts and cumulative energy demand are illustrated in Fig. 7.17 and 7.18 respectively.

Table 7.19 Results of environmental impacts and cumulative energy demand of concrete for selected FU

Impact	ADP x 10^{-1}	GWP x 10^{2}	ODP x 10^{-6}	POCP x 10^{-2}	AP x 10^{-1}	EP x 10^{-1}	PE- Nre x 10^{3}
FU40 mix							
Control	5.63	3.67	8.77	3.63	7.85	1.41	3.25
Tier I	6.04	4.37	9.54	5.96	12.77	2.08	3.35
Tier II	6.04	4.40	9.63	6.22	13.35	2.13	3.25
Tier III	4.62	3.52	7.68	6.09	12.80	2.03	2.58
FU60 mix							
Control	6.68	4.21	10.26	3.85	8.50	1.50	3.65
Tier I	6.84	4.85	10.70	6.47	13.97	2.25	3.65
Tier II	6.84	4.87	10.78	6.66	14.42	2.28	3.55
Tier III	5.22	3.78	8.54	6.10	12.91	2.05	2.82

The evaluation of the variation in impact values for different tiers of concrete having an equal volume and strength at 90 days of testing shows the effect of seeding of PET-Sand, SFS-Sand, and FLA in the mixes. This analysis may provide input to the stakeholders in the decision-making process about the optimum plastic substitution in the mix such that the mechanical performance of concrete is not sacrificed.

It can be seen that the magnitude of impacts for FU60 mixes was higher than the impacts caused by FU40 mixes. This is attributed to the relatively higher OPC content in the FU60 mixes which is a giant contributor to all CML baseline impacts and energy demands for any mix.

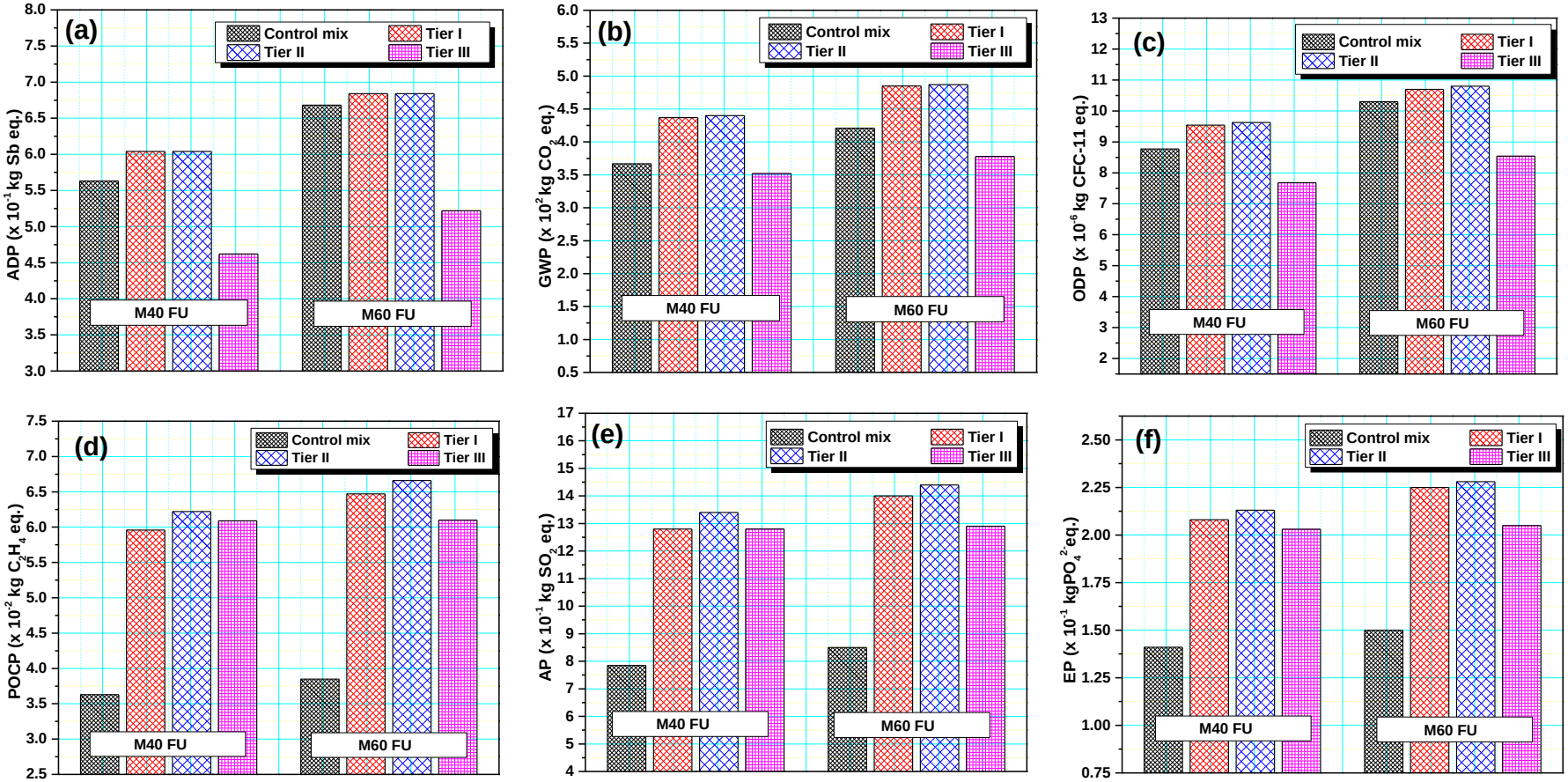

Fig. 7.17 Environmental impacts for FU40 mix and FU60 mix (a) ADP (b) GWP (c) ODP (d) POCP (e) AP (f) EP

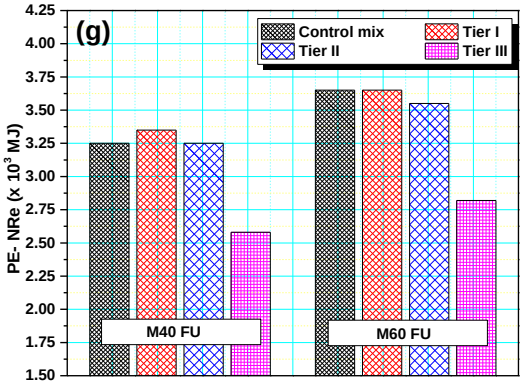

Fig. 7.18 Cumulative energy demand (PE-NRe) for FU40 mix and FU60 mix

In the case of FU40 mixes Tier I and Tier II mixes showed higher impact values relative to the control mix. A relative increase of 7% in ADP, 19-20% in GWP, 9-10% in ODP, 64-71% in POCP, 63-70% in AP, and 48-51% in EP is reported compared to the control mix. This is attributed to the higher OPC content that was required in Tier I (380 kg/m^3) and Tier II mixes (380 kg/m^3) to raise the mechanical strength of the respective mixes equivalent to the control mix. Comparatively, it is seen that an OPC content of 354 kg/m^3 is required for a conventional concrete mix to achieve the specified strength. Tier II mix showed energy demand value compared to the control mix. This was due to the significant replacement of low embodied energy materials in concrete as fine aggregates in the form of SFS and PET. Tier III mix showed environmentally friendly output compared to the control mix. There was a decrease of 18% in ADP, 4% in GWP, 12% in ODP, 32% in POCP, 37% in AP, 56% in EP, and 21% in energy demand compared to the control mix. This was attributed to the use of FLA, an SCM having significantly lower impact values than OPC that is substituted by 30% of the weight. Although the total binder content is higher in the Tier III mix i.e., 380 kg/m^3, the OPC content was 266 kg/m^3 compared to 354 kg/m^3 in the control mix. This triggers the difference in impact values.

A similar trend was noted in the case of FU60 mixes for all the tiers. The relative increase in impact values for Tier I and Tier II mixes was lower than the FU40 mixes for ADP, GWP, and ODP impacts. However, POCP, AP, and EP exhibited an increase in relative values than FU40 mixes. Furthermore, there was a decrease in cumulative energy demand in comparison to FU40 mixes.

7.2.4 Interpretation of Results

The results of LCIA of the concrete mixes were presented in three different strategies. The results presented for concrete with a $1m^3$ volume of concrete as the sole FU is intended to provide an understanding of the effect of substitution of the alternative materials i.e., PET-Sand, SFS-Sand, and FLA on the environmental impact of a given volume of modified green concrete and compare the results with the environmental impact of an equal volume of the control mix. The results presented for selected environmental impacts in terms of impact intensity are intended to evaluate and select the mix composition with alternate materials that show environmental impact intensity lower than the control mix. The third version of the results is intended to find out the mix compositions in three tiers of experimentation which fulfills the requirement of the FU of the study i.e., $1m^3$ of concrete of 40MPa/60MPa strength at 90 days of age. The interpretation of these three strategies of impact analysis is one of the most important steps of LCA. Elaborative discussions on the impact analysis have been presented in § 7.2.3.1, § 7.2.3.2, and § 7.2.3.3

From the three stages of impact analysis presented in the current research, the results can be summarized below:

1) The increase in the substitution levels of PET in the mix leads to an increase in the environmental impacts of the mix.
2) The more the OPC content inside a particular mix, the higher the environmental impacts of the mix.
3) The utilization of materials like SCM having lower embodied impacts to replace the OPC content in the mix leads to a drastic reduction in environmental impacts and energy demand. This SCM like FLA may provide the concrete mixes with some optimum replacement of PET aggregates in the mix, without sacrificing the mechanical performance of the mixes, especially at delayed curing periods.

Chapter 8

Summary and Conclusions

8.1 Summary

Plastic waste management is a seriously debated issue on the global agenda. The sporadic growth in plastic production to meet the demand for plastic in every walk of life has produced equivalent volumes of plastic waste after its short useful service life. As per the available statistics, the implementation of the circular economy concept in the plastic industry through recycling requires a major boost across the globe. Almost 90% of plastic wastes are either incinerated or dumped in the terrestrial environment or ocean waters to remain for over a hundred years causing irreparable damage on the social, environmental, and economic front. Waste management stakeholders are yet to find a satisfactory solution to tackle the menace caused by these non-biodegradable species. Considering the non-biodegradable nature of plastics and the ability of plastics to mold to any shape or size, research works are conducted worldwide to use plastic waste as an aggregate filler inside concrete which is the second most consumed material on earth, next to the water. A voluminous literature on the use of plastic waste as aggregate in concrete has concluded that there is substantial degradation in the strength of the concrete after the inclusion of plastic material. Although the use of plastic aggregates was beneficial in reducing the dead weight of concrete, the effect on the strength and durability-related properties of the modified concrete was discouraging in considering its suitability for structural purposes. Attempts were made to improve the quality of plastic-incorporated concrete by using various techniques like modifications in sizes and shapes of plastic particles, surface treatment of the plastic particles to improve the bond characteristics, a thermal fusion of plastic particles with the natural aggregates, use of pozzolanic admixtures and nano-materials like Nano-Silica, etc. Through these techniques, it was shown that it is possible to have concrete that qualifies for structural purposes provided the substitution volumes are limited to 10% of the conventional aggregates. The current study was an attempt to use PET waste as a fine aggregate in concrete by shredding the used PET bottles to a grain

size that confirms the gradation of the fine aggregates that are replaced. The idea of matching the gradation of PET-Sand with the N-Sand was sourced from the literature finding that substitution of 10% volume of PET with equivalent gradation can give concrete strength equivalent to conventional concrete. Furthermore, the current research also proposed the use of HDS from industrial waste as another fine aggregate for blending with N-Sand. This idea was sourced from the literature findings that HDS like CPS, EAF, SSS, FCS, and SFS can improve the strength of normal concrete by 10-15% provided these slags are used for optimum substitution levels in concrete. SFS-Sand was used as a supplementary aggregate in the current research after laboratory investigations to find its optimum substitution level that gives a maximum improvement in strength. This incorporation of SFS-Sand was executed with the hypothesis that the strength loss due to the inclusion of PET-Sand can be partially compensated by improvement in strength due to SFS-Sand. In addition to the use of plastic waste and industrial slag waste, the current study also aimed to seek the environmental advantage of using SCM to partially replace OPC inside the concrete. The current study was thus a novel and unprecedented attempt to obtain sustainable green concrete. This was an experimental investigation to obtain a novel concrete by utilization of waste materials like PET-Sand, SFS-Sand, and byproducts like FLA. Not considering resource conservation as the only aspect of sustainability, the current work emphasized the estimation of other environmental impacts involved in making this novel concrete and compared them with the impacts arising from making conventional concrete. A holistic approach of LCA of the novel concrete and conventional concrete was adopted in the current study for a quantitative assessment of environmental sustainability. The approach of LCA was widely used in the assessment of environmental sustainability of a wide variety of green concretes. However, concrete with PET-Sand and SFS-Sand being unprecedented experimentation, the LCA of these novel mixes is also breaking new ground in the sustainability sector. The laboratory investigations on the rheological, physical, mechanical, and durability characteristics of the novel composites were performed to ascertain their technical suitability. Furthermore, LCA analysis was performed for the novel mixes to assess their environmental implications.

The conclusions derived from the laboratory investigations and LCA analysis in the present study can go a long way in making policy decisions regarding the optimistic

use of plastic waste in cementitious mixes. Considering the novelty of the approach in the current work, there is a wide scope for further research to explore the possibility of the practical application of plastic waste in the concrete manufacturing industry.

8.2 Conclusions

The comprehensive study and the laboratory investigations in the present work were well-oriented to fulfill the objectives of the current study. To summarize the outcome of the study, the important conclusions that follow are drawn:

1) The comprehensive literature review on the use of plastic waste in cement composites presented a unanimous finding that there is a drastic reduction in the strength characteristics of concrete when the plastic content is increased to replace natural ingredients in conventional mixes irrespective of the type of plastics. The majority of the literature works dealt with PET waste as plastic waste and revealed that the use of PET fines having gradation similar to the natural fine aggregates allows substitution of 5-10% in volume without any noticeable effect on the strength values of the composites. Considering the literature inputs mechanically shredded PET fines obtained from PET drinking water bottles with particle gradation identical to N-Sand was used as plastic waste for the study.
2) The comprehensive literature review on the use of HDS in cement composites revealed a positive effect of replacing natural fine aggregates in conventional concrete with HDS aggregates such as CPS, FCS, SSS, and SFS aggregates. The findings in the majority of the studies postulated that the use of such HDS aggregates can improve the strength of conventional mix by 10-18% when used at optimum substitution levels. Depending on the availability of HDS, SFS aggregates were identified as industrial waste slag in the current study. The preliminary investigation showed that SFS-Sand replacement of 40% by volume yields optimum results.
3) The rheological studies on mortar and concrete samples containing PET-Sand showed that the workability of the composites decreases with the increase in PET content in the mix. This decrease was attributed to the increasing internal friction between cement paste and PET particles due to their non-uniform, angular, and mercenary shapes. The leaner mixes with a higher w/c ratio show a greater loss in

workability than richer mixes with a lower w/c ratio. The addition of SFS-Sand in Tier II mixes increased the workability of mixes due to the smooth and glassy surface texture of SFS-Sand offering a better lubricating effect inside the mix. The addition of FLA as SCM in Tier III mixes further enhanced the workability of the mixes by 4-5% over Tier II mixes. This effect was attributed to the reduced friction inside the mix due to the spherical shape of FLA particles and the ball-bearing effect induced in the mix.

4) There was a linear decrease in the bulk density of the cement composites with the increase in PET-Sand. This decrease was due to the lower specific weight of PET-Sand compared to N-Sand. Additionally, the increase in the porosity of the microstructure contributed to the density reduction. This loss in density was controlled by the incorporation of SFS-Sand in Tier II mixes, SFS-Sand being heavier than N-Sand that is replaced. There was no significant effect of blending FLA despite the lower specific weight of FLA in comparison to OPC. The expected reduction in density was compensated by better compaction of the mix due to improved workability.
5) There was a decrease in the compressive strength of the mixes with an increase in PET-Sand irrespective of the type of composite, period of curing, and w/c ratio. Tier I mixes showed a reduction of 29-36% and 22-27% was observed for 25% PET-Sand in the case of mortar and concrete mixes respectively. This was attributed to weak adhesion between the plastic fragments and cement paste, an increase in the porosity of the mix, and a honeycombing effect at higher substitution levels. Also, poor hydration of cement at the outskirts of PET particles because of the unavailability of water due to the hydrophobic nature of plastics is a prominent reason for the decline in strength. Leaner mixes showed a higher reduction in strength than the richer mixes. This strength loss was controlled by the addition of SFS-Sand in Tier II mixes. The reduction in strength was lowered by 8-12 % for mortar mixes and 5-6% for concrete mixes. This positive effect was due to the higher strength of SFS aggregates and an improved cohesion in the mix due to the angular, sharp edges of the slag aggregates, not to neglect the better compaction due to increased workability. Also, the microcavities on the surface of SFS particles assist in strength enhancement. In the case of Tier III mixes, the

use of FLA was found to be beneficial when strength values at prolonged curing periods were considered for the comparative analysis. At 90 days of age, the strength loss in Tier III mixes was reduced by 4-8% in comparison to Tier I mixes. This was attributed to the effect of better reactivity of FLA at older ages compared to OPC. Also, the pore-filling effect of FLA and better rheology of these mixes favored the strength gain. Regression analysis showed a strong polynomial relationship between compressive strength and dry density of all the tiers of mortar and concrete.

6) The behavior of the composites under flexural and tensile stresses showed effects similar to the compressive stresses for all the tiers of the composites. However, the loss in flexural and tensile strength was lower as compared to the loss in compressive strength. The better performance under flexural and tensile loading was attributed to the better tensile strength of PET particles. A strong linear relationship between compressive strength and flexural strength as well as compressive strength and tensile strength was observed. These relationships were validated with the mathematical models presented by the standards viz. ACI 318, Eurocode, and CEB-FIP, as well as historical studies in the literature.
7) There was a gradual decrease in the modulus of elasticity of concrete with an increase in PET-Sand in all tiers of the mixes. Tier I mix showed an elasticity modulus 21.5% lower than the control mix when PET-Sand was substituted for 25% volume. This decrease was attributed to the low elastic modulus of PET species and weak ITZ between PET-Sand and cement matrix. The effect of SFS-Sand in Tier II mixes and FLA binder in Tier III mixes on elasticity modulus was similar to the effect on strength parameters. The loss in elasticity modulus due to PET inclusion was partially mitigated by the use of SFS-Sand in Tier II mixes. However, this benefit was sacrificed in Tier III mixes due to slower strength gains in FLA mixes at early ages. Mathematical models for test results showing the relationship between compressive strength and modulus of elasticity were also presented and validated with the standards viz. ACI 318 and CEB-FIP along with the relationships available in the literature.
8) The degradation in the strength parameters of concrete containing PET-Sand was confirmed through the observed decrease in UPV values of the mixes with an

increase in PET content. For Tier I mixes, a decrease in UPV by 30% was observed for the 25% incorporation of PET-Sand. This decrease is attributed to the lack of compactness in PET-modified mixes, the increase in induced porosity of the mixes, and the poor elasticity of PET particles. Tier II mixes showed 2.5-4% higher UPV values compared to Tier I, indicating a better-quality mix than Tier I due to the utilization of SFS-Sand. The use of FLA in Tier III mixes showed an improvement in UPV values by 3-6% compared to Tier I mixes at prolonged curing age of 90 days. The effect was attributed to the pore-filling effect of FLA and better reactivity at older ages. A relationship between UPV and compressive strength was also obtained depicting a strong correlation. This relationship was compared with other relationships available in the literature.

9) The transfer behavior of the mortar and concrete mixes for all the tiers was investigated using the sorptivity test and permeability test. For Tier I mixes, the capillary absorption was 19-21% higher than the control mix for mortar samples and 9-13% higher for concrete mixes. This increase is directly related to the increase in the porosity of PET blended mixes and weak adhesion between PET particles and cement paste. This effect was reduced in the case of Tier II mixes, thanks to the relatively compact microstructure of the mix due to SFS-Sand. The sorptivity values of the Tier III mix at 28 days showed a slight decrease in values due to the pore-filling effect of FLA. The sorptivity coefficients for all the tiers showed a strong relationship with the density values of the composites at 28 days. Similar observations are noted for the permeability of the samples under pressure.
10) An identical decrease in chloride migration coefficient was observed for an increase in PET volumes from 10 to 20% for Tier I and Tier II mixes. This decrease was attributed to the impervious nature of PET particles which provides a shielding effect against chloride penetration. This showed that the inclusion of SFS did not influence the chloride migration process. Beyond the 20% inclusion of PET-Sand, a sharp increase in chloride migration was observed for both tiers. This increase in chloride ion transfer was attributed to the increase in the porosity of the concrete mixes. This concludes that the chloride shielding effect exists up to a threshold substitution level of PET-Sand beyond which an increase in global porosity disrupts the chloride barrier allowing a sharp increase in chloride

migration. In the case of the Tier III mix, the use of FLA is responsible for a 25-40% reduction in chloride migration for 20% PET-Sand inclusion. This was attributed to the chloride-binding ability of FLA in addition to a reduction in porosity due to the pore-filling effect.

11) The exposure of the concrete specimens to elevated temperatures revealed a drastic reduction in residual strength irrespective of the tier of concrete. The strength reduction of the specimens ranged from 18-21%, 33-38%, and 51-57% for exposure temperatures of 200ºC, 400ºC, and 600ºC respectively. In a lower temperature zone at 200ºC, this effect was related to the increase in porosity of the mixes after PET inclusion. This porousness induces an imbalanced thermal gradient inside the concrete initiating crack development. At higher temperatures i.e., 400ºC and 600ºC, the thermal degradation of PET particles occurs inside the mass. This leads to a further increase in porosity and associated thermal stresses causing the failure of concrete.
12) The microscopic investigation of the concrete samples using SEM images exhibited a weak ITZ between PET-Sand particle and cement matrix. A visible gap of 5-10µ was observed along the periphery of the PET particle which confirmed that weak adhesion between PET and cement paste is the major factor for the strength degradation in PET-incorporated cementitious mixes.
13) The sustainability assessment of the novel concrete using LCA methodology as per ISO 14040 (2006) showed a significant effect of incorporation of PET-Sand as an aggregate replacement and use of FLA as SCM in concrete. However, the use of SFS-Sand did not show any significant effect on environmental impacts and energy demand for concrete.
14) For a functional unit of $1m^3$ volume of concrete, it was found that there was no variation in ADP for Tier I and Tier II mix which shows that the addition of PET/SFS does not influence ADP impact for the mix. However, there was an increase in GWP value by 20% and ODP value by 4% for the maximum PET-Sand ratio in both tiers. For every 5% substitution of PET-Sand in Tier I and II there was an increase in POCP and AP by 17-20% and an increase in EP by 14-15%. A saving of 5-6% in POCP, AP, and EP was observed in Tier II due to SFS-Sand inclusion. The cumulative energy demand decreased with the increase in

PET substitution. The use of FLA in Tier III mixes affected substantial reduction in all the environmental impacts and cumulative energy demand. For the 25% replacement of PET-Sand in Tier III, the reduction in GWP, ODP, POCP, AP, EP, and PE-NRe was found to be 7%, 18%, 23%, 30%, 22%, and 24% respectively. This was majorly attributed to the reduction of OPC content in the mix.

15) The comparative environmental assessment of the mixes in terms of GWP intensity concerning the compressive strength showed that the average GWP intensity increases by 65%, 50%, and 40% for Tier I, Tier II, and Tier III mixes respectively when 25% of N-Sand is replaced by PET-Sand. This indicates the benefit of GWP reduction in the Tier III mix relative to the achieved strength. The analysis showed that the Tier III sample with 20% PET-Sand GWP intensity value same as the control mix when 90 days strength was considered for the analysis.
16) For a FU of $1m^3$ volume and specified strength, the LCA of the mixes showed that there is a relative increase of 7% in ADP, 19-20% in GWP, 9-10% in ODP, 64-71% in POCP, 63-70% in AP, and 48-51% in EP in Tier I and Tier II mixes in comparison to the control mix. This was attributed to the higher OPC content that was required to raise the mechanical strength of the respective mixes equivalent to the control mix. On the other hand, Tier III mixes showed a decrease of 18% in ADP, 4% in GWP, 12% in ODP, 32% in POCP, 37% in AP, 56% in EP, and 21% in energy demand compared to the control mix. This was attributed to the use of FLA, an SCM having significantly lower impact values than OPC.

8.3 Major contributions from the study

The outcomes of the voluminous research studies on the utilization of plastic waste as aggregates in concrete have shown lots of resistance to certifying plastic-modified concrete as a structural material. Such concrete has been accepted to be used for practical applications as lightweight concrete for subsidiary works. The current research will add to upgrade this opinion and will saw a seed of thought for considering such concrete for structural purposes. The novelty of this research lies in the utilization of high-density slag from industrial waste as a supplementary aggregate in control concrete to compensate for the strength degradation if any caused by plastic inclusions in concrete. The current study provides a convincing platform to obtain normal strength and normal

density concrete with plastic waste as a substitute for natural sand. Through extensive laboratory investigations, the current study has shown that it is possible to obtain concrete mix containing PET-Sand (up to 15% volume of NFA) which behaves identically to the concrete with conventional aggregates. To achieve this objective, the study executed the utilization of industrial waste in the form of SFS-Sand as a supplementary fine aggregate that replaced the NFA by 40% volume. Thus, it can be seen that the current investigation offers a saving of 55% volume of NFA in the novel concrete mix. Through such a novel approach, the current study has contributed toward sustainability in concrete production by providing an environmentally friendly alternative for the conservation of natural resources as well as the management of plastic and industrial waste. The current study has also performed laboratory investigation on novel mixes containing PET-Sand and SFS-Sand by utilization of SCM in the form of FLA as another sustainability initiative to reduce GHG emissions through OPC consumption. The outcomes of this investigation also showed that the novel mix with SFS-Sand and 15% volume of PET-Sand satisfies the technical standard of the conventional mix. In addition to these technical achievements, the environmental audit of this novel concrete mixes using LCA methodology as per ISO14040 (2006) is a major contribution to the current work. This environmental analysis showed that the novel concrete not only fulfills the technical characteristics of the conventional mix but also shows environmental impacts much lower than the conventional concrete. The current work thus advocates the possibility of obtaining technically suitable and environmentally sustainable concrete with plastic waste.

8.4 Recommendations of the Study

The current study and its findings suggest the following recommendations for the practical implementation of cement composites containing plastic waste as fine aggregates:

1. PET waste can be utilized as fine aggregates in cement composites if it is mechanically recycled to the particle gradation of the N-Sand that is replaced.
2. The use of PET as a partial substitute for natural aggregates can be used in making lightweight concrete which can be used for non-structural applications in the construction industry.

3. If N-Sand in the traditional mix is blended with an optimum volume of SFS-Sand, the partial substitution of the blended fine aggregate with PET-Sand can deliver concrete satisfying structural requirements.
4. The use of mineral admixture like FLA in concrete containing SFS-Sand and PET-Sand is beneficial in improving the mechanical performance of concrete. It also reduces environmental impact and cumulative energy demand compared to conventional concrete.
5. The concrete containing a 15% volume of PET-Sand as a substitute for a blend of N-Sand and SFS-Sand can be used for structural works.

8.5 Scope of future work

To grow confidence in utilizing novel composite with plastic waste for structural applications, the research demands further investigations on the behavior of concrete under dynamic loading. There is vast scope in extending this research to understand the mechanical behavior of the novel concrete under cyclic loading. Also, the seismic performance of the beam-column junctions cast using the novel concrete is a way ahead in ascertaining the structural feasibility of this concrete. The novel concrete in the current research may provide a sustainable breakthrough in pavement construction in the transportation sector. The studies on the coefficient of thermal expansion, surface shortwave radiation absorptivity, heat capacity, zero stress temperature, deformation responses, crack patterns, behavior under impact loading, etc. may explore the possibility of using this concrete in the transportation industry.

References

Ababio Ohemeng, E., Paakofi Yalley, P., Dadzie, J., Paa-Kofi Yalley, P. and Dzifa Djokoto, S. (2014) 'Utilization of Waste Low-Density Polyethylene in High Strengths Concrete Pavement Blocks Production', Civil and Environmental Research, 6(5), pp. 126-135.

Abed, J.M., Khaleel, B.A., Aldabagh, I.S. and Sor, N.H. (2021) 'The effect of recycled plastic waste polyethylene terephthalate (PET) on characteristics of cement mortar', IOP Publishing, IICESAT Conference, College of Material Engineering, University of Babylon, Iraq, Journal of Physics: Conference Series, 1973(1), pp. 1-9.

ACI 318-19 (2019) 'Building Code Requirements for Structural Concrete' Commentary on Building Code Requirements for Structural Concrete (ACI 318R-19): ACI Report American Concrete Institute.

Aciu, C., Ilutiu-Varvara, D.A., Manea, D.L., Orban, Y.A. and Babota, F. (2018) 'Recycling of plastic waste materials in the composition of ecological mortars', Procedia Manufacturing, 22, pp. 274–279.

Adegoloye, G., Beaucour, A.L., Ortola, S. and Noumowé, A. (2015) 'Concretes made of EAF slag and AOD slag aggregates from stainless steel process: Mechanical properties and durability', Construction and Building Materials, 76, pp. 313–321.

Aguayo, M., Das, S., Maroli, A., Kabay, N., Mertens, J.C.E., Rajan, S.D., Sant, G., Chawla, N. and Neithalath, N. (2016) 'The influence of microencapsulated phase change material (PCM) characteristics on the microstructure and strength of cementitious composites: Experiments and finite element simulations', Cement and Concrete Composites, 73, pp. 29–41.

Ahmad, J., Majdi, A., Elhag, A.B., Deifalla, A.F., Soomro, M., Isleem, H.F. and Qaidi, S. (2022a) 'A Step towards Sustainable Concrete with Substitution of Plastic Waste in Concrete: Overview on Mechanical, Durability and Microstructure Analysis', Crystals, 12(7), pp. 1-23.

Ahmad, J., Majdi, A., Deifalla, A.F., Isleem, H.F. and Rahmawati, C. (2022b) ‘Concrete Made with Partially Substitutions of Copper Slag (CPS): State of the Art Review’, Materials, 15(15), pp. 1-28.

Ahmad, S.I. and Rahman, M.S. (2018) ‘Mechanical and Durability Properties of Induction-Furnace-Slag-Incorporated Recycled Aggregate Concrete’, Advances in Civil Engineering, 2018, pp. 1-11.

Ahmed, A.I. and Mohammed, A.A. (2006) ‘Use PET Bottles Waste to Partially Substitute Sand in some Cement-based Mortar Applications’, Sudan Engineering Society Journal, 52(47), pp. 9-13.

Aïtcin, P.C. (2016) ‘Supplementary cementitious materials and blended cements’, Science and Technology of Concrete Admixtures. Elsevier Inc., pp. 53–73.

Akçaözoğlu, S. and Atiş, C.D. (2011) ‘Effect of Granulated Blast Furnace Slag and fly ash addition on the strength properties of lightweight mortars containing waste PET aggregates’, Construction and Building Materials, 25(10), pp. 4052–4058.

Akça, K.I.R., Çakir, Ö. and Ipek, M. (2015) ‘Properties of polypropylene fiber reinforced concrete using recycled aggregates’, Construction and Building Materials, 98, pp. 620–630.

Akçaözoğlu, S., Akçaözoğlu, K. and Atiş, C.D. (2013) ‘Thermal conductivity, compressive strength and ultrasonic wave velocity of cementitious composite containing waste PET lightweight aggregate (WPLA)’, Composites Part B: Engineering, 45(1), pp. 721–726.

Akçaözoğlu, S., Atiş, C.D. and Akçaözoğlu, K. (2010) ‘An investigation on the use of shredded waste PET bottles as aggregate in lightweight concrete’, Waste Management, 30(2), pp. 285–290.

Akçaözoğlu, S. and Ulu, C. (2014) ‘Recycling of waste PET granules as aggregate in alkali-activated blast furnace slag/metakaolin blends’, Construction and Building Materials, 58, pp. 31–37.

Akinyele, J.O., Salim, R.W. and Oyeti, G. (2015) 'Use of recycled polypropylene grains as partial replacement of fine aggregate in reinforced concrete beams', Engineering Structures and Technologies, 6(4), pp. 184–190.

Akinyele, J.O. and Toriola, I.O. (2018) 'The effect of crushed plastics waste on the structural properties of sandcrete blocks', African Journal of Science, Technology, Innovation and Development, 10(6), pp. 709–713.

Albano, C., Camacho, N., Hernández, M., Matheus, A. and Gutiérrez, A. (2009) 'Influence of content and particle size of waste pet bottles on concrete behavior at different w/c ratios', Waste Management, 29(10), pp. 2707–2716.

Alfahdawi, I.H., Osman, S.A., Hamid, R. and Ismail Al-hadithi, A. (2016) 'Utilizing waste plastic polypropylene and polyethylene terephthalate as alternative aggregates to produce lightweight concrete: a review', Journal of Engineering Science and Technology, 11(8), pp. 1165-1173.

Alizadeh, R., Chini, M., Ghods, P., Hoseini, M., Montazer, S. and Shekarchi, M. (2003) 'Utilization of Electric Arc Furnace Slag as Aggregates in Concrete-Environmental Issue', Proceedings of 6th CANMET/ACI International Conference on recent advances in concrete Technology, Bucharest, Romania, pp. 451-464.

Al-Jabri, K., Shoukry, H., Khalil, I.S., Nasir, S. and Hassan, H.F. (2018) 'Reuse of Waste Ferrochrome Slag in the Production of Mortar with Improved Thermal and Mechanical Performance', Journal of Materials in Civil Engineering, 30(8), pp. 1-10.

Al-Jabri, K.S. (2006) 'Copper slag as fine aggregate for high performance concrete', In: WIT Transactions on the Built Environment, 85, pp. 381–389.

Al-Jabri, K.S., Hisada, M., Al-Oraimi, S.K. and Al-Saidy, A.H. (2009a) 'Copper slag as sand replacement for high performance concrete', Cement and Concrete Composites, 31(7), pp. 483–488.

Al-Jabri, K.S., Hisada, M., Al-Saidy, A.H. and Al-Oraimi, S.K. (2009b) 'Performance of high strength concrete made with copper slag as a fine aggregate', Construction and Building Materials, 23(6), pp. 2132–2140.

Al-Jabri, K.S., Al-Saidy, A.H. and Taha, R. (2011) 'Effect of copper slag as a fine aggregate on the properties of cement mortars and concrete', Construction and Building Materials, 25(2), pp. 933–938.

Al-Maaded, M., Madi, N.K., Kahraman, R., Hodzic, A. and Ozerkan, N.G. (2012) 'An Overview of Solid Waste Management and Plastic Recycling in Qatar', Journal of Polymers and the Environment, 20(1), pp. 186–194.

Al-Qurishee, M., Qurishee, M.A., Iqbal, I.T., Islam, M.M. and Islam, M.S. (2016) 'Use of Slag as Coarse Aggregate and its Effect on Mechanical Properties of Concrete', Proceedings of 3rd International Conference on Advances in Civil Engineering 2016 (ICACE 2016), CUET, Chittagong, Bangladesh, pp. 1-6.

Al-Tayeb, M.M., M. Zeyad, A., Dawoud, O. and Tayeh, B.A. (2021) 'Experimental and numerical investigations of the influence of partial replacement of coarse aggregates by plastic waste on the impact load', International Journal of Sustainable Engineering, 14(4), pp. 735–742.

Almeshal, I., Tayeh, B.A., Alyousef, R., Alabduljabbar, H. and Mohamed, A.M. (2020a) 'Eco-friendly concrete containing recycled plastic as partial replacement for sand', Journal of Materials Research and Technology, 9(3), pp. 4631–4643.

Almeshal, I., Tayeh, B.A., Alyousef, R., Alabduljabbar, H., Mustafa Mohamed, A. and Alaskar, A. (2020b) 'Use of recycled plastic as fine aggregate in cementitious composites: A review', Construction and Building Materials, 253, pp.1-26.

Alnuaimi, A.S. (2012) 'Effects of Copper Slag as a Replacement for Fine Aggregate on the Behavior and Ultimate Strength of Reinforced Concrete Slender Columns', The Journal of Engineering Research, 9(2), pp. 90-102.

Alqahtani, F.K., Ghataora, G., Dirar, S., Khan, M.I. and Zafar, I. (2018) 'Experimental study to investigate the engineering and durability performance of concrete using synthetic aggregates', Construction and Building Materials, 173, pp. 350–358.

Alqahtani, F.K., Ghataora, G., Khan, M.I. and Dirar, S. (2017) 'Novel lightweight concrete containing manufactured plastic aggregate', Construction and Building Materials, 148, pp. 386–397.

Al-Salem, S.M., Lettieri, P. and Baeyens, J. (2009) 'Recycling and recovery routes of plastic solid waste (PSW): A review', Waste Management, 29(10), pp. 2625–2643.

Altwair, N.M. and Kabir, S. (2010) 'Green concrete structures by replacing cement with pozzolanic materials to reduce greenhouse gas emissions for sustainable environment', Proceedings of 6th International Engineering and Construction Conference (IECC'6), Cairo, Egypt, American Society of Civil Engineering, pp. 269-279.

Alwaeli, M. (2021) 'Use of granulated lead-zinc slag as replacement of fine aggregate in structural concrete: Compressive strength and radiation shielding study', Archives of Civil Engineering, 67(2), pp. 37–47.

Anastasiou, E., Georgiadis Filikas, K. and Stefanidou, M. (2014) 'Utilization of fine recycled aggregates in concrete with fly ash and steel slag', Construction and Building Materials, 50, pp. 154–161.

Anastasiou, E.K., Liapis, A. and Papachristoforou, M. (2017) 'Life Cycle Assessment of Concrete Products for Special Applications Containing EAF Slag', Procedia Environmental Sciences, 38, pp. 469–476.

Andrew, R.M. (2018) 'Global CO2 emissions from cement production', Earth System Science Data, 10(1), pp. 195–217.

Arena, U., Mastellone, M.L. and Perugini, F. (2003) 'LCA Case Studies: Life Cycle Assessment of a Plastic Packaging Recycling System', International Journal of Life Cycle Assessment, 8(2), pp. 92-98.

Arockia Allwin, A., Nagarathinam, N., Sivaranjan, I. and Ulagusundaram, S. (2017) 'Strength characteristics of M20 concrete on partial replacement of sand using steel slag', International Journal of Advanced Research in Innovative Discoveries in Engineering and Applications, 2(2), pp. 47-54.

Aryan, Y., Yadav, P. and Samadder, S.R. (2019) 'Life Cycle Assessment of the existing and proposed plastic waste management options in India: A case study', Journal of Cleaner Production, 211, pp. 1268–1283.

Aslani, F. and Ma, G. (2018) ‘Normal and High-Strength Lightweight Self-Compacting Concrete Incorporating Perlite, Scoria, and Polystyrene Aggregates at Elevated Temperatures’, Journal of Materials in Civil Engineering, 30(12), pp. 1-19.

ASTM C 1202 (2019) ‘Standard method for electrical indication of concretes ability of resist chloride ion penetration’, Annual book of ASTM standards.

ASTM C1585-13 (2020) Standard Test Method for Measurement of Rate of Absorption of Water by Hydraulic Cement Concretes, ASTM International, West Conshohocken, PA, USA.

Aswatama, W.K., Suyoso, H., Meyfa, N.U. and Tedy, P. (2018) ‘The Effect of Adding PET (Polyethylene Terephthalate) Plastic Waste on SCC (Self-Compacting Concrete) to Fresh Concrete Behavior and Mechanical Characteristics’, Journal of Physics: Conference Series, 953(1), pp. 12-23.

Atiş, C.D. (2005) ‘Strength properties of high-volume fly ash roller compacted and workable concrete, and influence of curing condition’, Cement and Concrete Research, 35(6), pp. 1112–1121.

Autade, P.B. and Saluja, H.S.J.S. (2016) ‘Effect of Steel Slag as a Replacement of Fine Aggregate in M40 Grade of Concrete’, International Journal of New Innovations in Engineering and Technology, 5(4), pp. 17-26.

Awoyera, P.O. and Adesina, A. (2020) ‘Plastic wastes to construction products: Status, limitations and future perspective’, Case Studies in Construction Materials, 12, pp.1-11.

Azhdarpour, A.M., Nikoudel, M.R. and Taheri, M. (2016) ‘The effect of using polyethylene terephthalate particles on physical and strength-related properties of concrete; A laboratory evaluation’, Construction and Building Materials, 109, pp. 55–62.

Baalamurugan, J., Ganesh Kumar, V., Chandrasekaran, S., Balasundar, S., Venkatraman, B., Padmapriya, R. and Bupesh Raja, V.K. (2019) ‘Utilization of induction furnace steel slag in concrete as coarse aggregate for gamma radiation shielding’, Journal of Hazardous Materials, 369, pp. 561–568.

Babafemi, A.J., Šavija, B., Paul, S.C. and Anggraini, V. (2018) ‘Engineering properties of concrete with waste recycled plastic: A review’, Sustainability, 10, pp. 1-26.

Babafemi, A.J., Sirba, N., Paul, S.C. and Miah, M.J. (2022) ‘Mechanical and Durability Assessment of Recycled Waste Plastic (Resin8 & PET) Eco-Aggregate Concrete’, Sustainability, 14(9), pp. 1-25.

Babu, D.S., Ganesh Babu, K. and Tiong-Huan, W. (2006) ‘Effect of polystyrene aggregate size on strength and moisture migration characteristics of lightweight concrete’, Cement and Concrete Composites, 28(6), pp. 520–527.

Babu, D.S., Ganesh Babu, K. and Wee, T.H. (2005) ‘Properties of lightweight expanded polystyrene aggregate concretes containing fly ash’, Cement and Concrete Research, 35(6), pp. 1218–1223.

Babu, K.G. and Babu, D.S. (2003) ‘Behaviour of lightweight expanded polystyrene concrete containing silica fume’, Cement and Concrete Research, 33(5), pp. 755–762.

Babu, K.G. and Babu, D.S. (2004) ‘Performance of fly ash concretes containing lightweight EPS aggregates’, Cement and Concrete Composites, 26(6), pp. 605–611.

Babu, K.M. and Reddy, K.S. (2018) ‘Effect of Copper Slag as a Fine Aggregate on the Properties of High Strength Concrete’ International Journal of Emerging Technologies and Innovative Research, 5(8), pp. 764-770.

Badache, A., Benosman, A.S., Senhadji, Y. and Mouli, M. (2018) ‘Thermo-physical and mechanical characteristics of sand-based lightweight composite mortars with recycled high-density polyethylene (HDPE)’, Construction and Building Materials, 163, pp. 40–52.

Bahij, S., Omary, S., Feugeas, F. and Faqiri, A. (2020) ‘Fresh and hardened properties of concrete containing different forms of plastic waste – A review’, Waste Management, 113, pp. 157–175.

Basavaraj, A. S., and Gettu, R. (2022) ‘Life cycle assessment as a tool in sustainability assessment of concrete systems: why and how?’, The Indian Concrete Journal, 96(4), pp. 1-20.

Bataineh, K.M. (2020) ‘Life-Cycle Assessment of Recycling Postconsumer High-Density Polyethylene and Polyethylene Terephthalate’, Advances in Civil Engineering, 2020, pp. 1-15.

Batayneh, M., Marie, I. and Asi, I. (2007) ‘Use of selected waste materials in concrete mixes’, Waste Management, 27(12), pp. 1870–1876.

Bednas, M.E., Day, M., Ho, K., Sander, R. and Wiles, D.M. (1981) ‘Combustion and Pyrolysis of Polyethylene Terephthalate. I. The Role of Flame Retardants on Products of Pyrolysis’, Journal of Applied Polymer Science, 26, pp. 277-289.

Benson, N.U., Bassey, D.E. and Palanisami, T. (2021) ‘COVID pollution: Impact of COVID-19 pandemic on global plastic waste footprint’, Heliyon, 7(2), pp. 1-9.

Bhagat, G. and Savoikar, P. (2019) ‘An Overview of Effect of Nano-Material Modifications in Non-Conventional Concretes and Mortars’, Proceedings of the International UKIERI Concrete Congress, Jalandhar, India, UCC 170, pp. 1-15.

Bhagat, G. V. and Savoikar, P.P. (2021) ‘Auditing carbon reduction potential of green concrete using life cycle assessment methodology’, IOP Conference Series: Earth and Environmental Science, 850 (2021), pp. 1-23.

Bhagat, G. V. and Savoikar, P.P. (2022) ‘Durability related properties of cement composites containing thermoplastic aggregates – A review’, Journal of Building Engineering, 53 (2022), pp. 1-33.

Biskri, Y., Achoura, D., Chelghoum, N. and Mouret, M. (2017) ‘Mechanical and durability characteristics of High-Performance Concrete containing steel slag and crystalized slag as aggregates’, Construction and Building Materials, 150, pp. 167–178.

Blankendaal, T., Schuur, P. and Voordijk, H. (2014) ‘Reducing the environmental impact of concrete and asphalt: A scenario approach’, Journal of Cleaner Production, 66, pp. 27–36.

Blengini, G.A., Garbarino, E., Šolar, S., Shields, D.J., Hámor, T., Vinai, R. and Agioutantis, Z. (2012) ‘Life Cycle Assessment guidelines for the sustainable production and recycling of aggregates: The Sustainable Aggregates Resource Management project (SARMa)’, Journal of Cleaner Production, 27, pp. 177–181.

Bodor, M., Santos, R.M., Cristea, G., Salman, M., Cizer, Ö., Iacobescu, R.I., Chiang, Y.W., Van Balen, K., Vlad, M. and Van Gerven, T. (2016) ‘Laboratory investigation of

carbonated BOF slag used as partial replacement of natural aggregate in cement mortars', Cement and Concrete Composites, 65, pp. 55–66.

Borg, R.P., Baldacchino, O. and Ferrara, L. (2016) 'Early age performance and mechanical characteristics of recycled PET fibre reinforced concrete', Construction and Building Materials, 108, pp. 29–47.

Borole, S.T., Shinde, R.V., Mhaske, R.B., Pagare, S.S., Tribhuvan, K.S., Pawar, N.M., Tiwari, V.D. and Sanehi, A.K. (2016) Replacement of Fine Aggregate By Steel Slag, Proceedings of International Conference on Emerging Trends in Engineering and Management Research (ICETEMR-16), Nashik, India, pp. 1582-1589.

Braga, A.M., Silvestre, J.D. and De Brito, J. (2017) 'Compared environmental and economic impact from cradle to gate of concrete with natural and recycled coarse aggregates', Journal of Cleaner Production, 162, pp. 529–543.

Brand, A.S. and Fanijo, E.O. (2020) 'A review of the influence of steel furnace slag type on the properties of cementitious composites', Applied Sciences, 10(2020), pp. 1–27.

Brand, A.S. and Roesler, J.R. (2015) 'Steel furnace slag aggregate expansion and hardened concrete properties', Cement and Concrete Composites, 60, pp. 1–9.

Brindha, D., Baskarn, T. and Nagan, S. (2010) 'Assessment of Corrosion and Durability Characteristics of Copper Slag Admixed Concrete', International Journal of Civil and Structural Engineering, 1(2), pp. 192-211.

BSI (2004) 'Eurocode 2: Design of concrete structures. Part 1-1: General rules and rules for buildings', British Standard Institution, EN 1992-1-1, London, Bucauresti.

Cadere, C.A., Barbuta, M., Rosca, B., Serbanoiu, A.A., Burlacu, A. and Oancea, I. (2018) 'Engineering properties of concrete with polystyrene granules', Procedia Manufacturing, 22, pp. 288–293.

CEB-FIP model code (1993) 'CEB Bulletin Information no. 213/214', Committee Eurointernational Du Beton, Thomas Telford.

Celik, K., Meral, C., Petek Gursel, A., Mehta, P.K., Horvath, A. and Monteiro, P.J.M. (2015) 'Mechanical properties, durability, and life-cycle assessment of self-consolidating

concrete mixtures made with blended portland cements containing fly ash and limestone powder', Cement and Concrete Composites, 56, pp. 59–72.

Chavan, R.R. and Kulkarni, D.B. (2013) 'Performance of Copper Slag on Strength Properties as Partial Replace of Fine Aggregate in Concrete Mix Design', International Journal of Advanced Engineering Research and Studies, 2(4), pp. 95-98.

Chen, C.C., Jaffe, N., Koppitz, M., Weimer, W. and Polocoser, A. (2015) 'Concrete Mixture with Plastic as Fine Aggregate Replacement', International Journal of Advances in Mechanical and Civil Engineering, 2(4), pp. 49-53.

Chen, C., Habert, G., Bouzidi, Y., Jullien, A. and Ventura, A. (2010) 'LCA allocation procedure used as an incitative method for waste recycling: An application to mineral additions in concrete', Resources, Conservation and Recycling, 54(12), pp. 1231–1240.

Chen, H., Xu, Y., Zhang, D., Huang, L., Zhu, Y. and Huang, Le (2019) 'The Influence of Nano-SiO2 and Recycled Polypropylene Plastic Content on Physical, Mechanical, and Shrinkage Properties of Mortar', Advances in Civil Engineering, 2019, article 6960216, pp. 1-12.

Chidiac, S.E. and Mihaljevic, S.N. (2011) 'Performance of dry cast concrete blocks containing waste glass powder or polyethylene aggregates', Cement and Concrete Composites, 33(8), pp. 855–863.

Choi, Y.W., Moon, D.J., Chung, J.S., and Cho, S.K. (2005) 'Effects of waste PET bottles aggregate on the properties of concrete', Cement and Concrete Research, 35(4), pp. 776–781.

Choi, Y.W., Moon, D.J., Kim, Y.J. and Lachemi, M. (2009) 'Characteristics of mortar and concrete containing fine aggregate manufactured from recycled waste polyethylene terephthalate bottles', Construction and Building Materials, 23(8), pp. 2829–2835.

Chunchu, B.R.K. and Putta, J. (2019a) 'Effect of recycled plastic granules as a partial substitute for natural resource sand on the durability of SCC', Resources, 8(3), pp. 1-14.

Chunchu, B.R.K. and Putta, J. (2019b) 'Rheological and strength behavior of binary blended SCC replacing partial fine aggregate with plastic E-waste as high impact polystyrene', Buildings, 9(2), pp. 1-15.

Colangelo, F., Forcina, A., Farina, I. and Petrillo, A. (2018a) ‘Life Cycle Assessment (LCA) of different kinds of concrete containing waste for sustainable construction’, Buildings, 8(5), pp. 1-12.

Colangelo, F., Petrillo, A., Cioffi, R., Borrelli, C. and Forcina, A. (2018b) ‘Life cycle assessment of recycled concretes: A case study in southern Italy’, Science of the Total Environment, 615, pp. 1506–1517.

Collins, F. (2010) ‘Inclusion of carbonation during the life cycle of built and recycled concrete: Influence on their carbon footprint’, International Journal of Life Cycle Assessment, 15(6), pp. 549–556.

Cong Kou, S., Poon, C.S. and Chan, D. (2007) ‘Influence of Fly Ash as Cement Replacement on the Properties of Recycled Aggregate Concrete’, Journal of Materials in Civil Engineering, 19, pp. 709-7017.

Coppola, B., Courard, L., Michel, F., Incarnato, L. and Di Maio, L. (2016) ‘Investigation on the use of foamed plastic waste as natural aggregates replacement in lightweight mortar’, Composites Part B: Engineering, 99, pp. 75–83.

Coppola, B., Courard, L., Michel, F., Incarnato, L., Scarfato, P. and Di Maio, L. (2018) ‘Hygro-thermal and durability properties of a lightweight mortar made with foamed plastic waste aggregates’, Construction and Building Materials, 170, pp. 200–206.

Coppola, L., Buoso, A., Coffetti, D., Kara, P. and Lorenzi, S. (2016) ‘Electric arc furnace granulated slag for sustainable concrete’, Construction and Building Materials, 123, pp. 115–119.

Coppola, L., Lorenzi, S. and Buoso, A. (2010) ‘Electric Arc Furnace Granulated Slag as a Partial Replacement of Natural Aggregates for Concrete Production’ Proceedings of Second International Conference on Sustainable Construction Materials and Technologies, Ancona, Italy, pp. 1-9.

Correa, P.M., Santana, M.C.R., Guimarães, D. and Graeff, A.G. (2020) ‘Post-consumer PP as partial substitute of sand: effect of surface treatment PP with surfactant on concrete properties’, Composite Interfaces, 27(9), pp. 815–828.

Correia, J.R., Lima, J.S. and De Brito, J. (2014) 'Post-fire mechanical performance of concrete made with selected plastic waste aggregates', Cement and Concrete Composites, 53, pp. 187–199.

CPCB Report (2019) 'Annual Report for the year 2018-19 of Plastic Waste Management Rues', Central Pollution Control Board, Government of India, New Delhi. https://cpcb.nic.in/uploads/plasticwaste/Annual_Report_2018-19_PWM.pdf (Accessed on 20/04/2023)

Crossin, E. (2015) 'The greenhouse gas implications of using ground granulated blast furnace slag as a cement substitute', Journal of Cleaner Production, 95, pp. 101–108.

Centre for Science and Environment (CSE) (2020) 'Managing plastic waste in India challenges and agenda' www.cseindia.org (Accessed on 14th March 2021).

Da Silva, T.R., de Azevedo, A.R.G., Cecchin, D., Marvila, M.T., Amran, M., Fediuk, R., Vatin, N., Karelina, M., Klyuev, S. and Szelag, M. (2021) 'Application of plastic wastes in construction materials: A review using the concept of life-cycle assessment in the context of recent research for future perspectives', Materials, 14, pp. 1-19.

Da Silva, A.M., De Brito, J. and Veiga, R. (2014) 'Incorporation of fine plastic aggregates in rendering mortars', Construction and Building Materials, 71, pp. 226–236.

Damineli, B.L., Kemeid, F.M., Aguiar, P.S. and John, V.M. (2010) 'Measuring the eco-efficiency of cement use', Cement and Concrete Composites, 32(8), pp. 555–562.

Darji, A., Patel, I. and Shah, J. (2014) 'Effects of Green Supplementary Materials on Engineering Properties of Recycled Aggregate Concrete', Journal of Civil Engineering and Environmental Technology, 1(4), pp. 1–4.

Dash, M.K. and Patro, S.K. (2018) 'Effects of water cooled ferrochrome slag as fine aggregate on the properties of concrete', Construction and Building Materials, 177, pp. 457–466.

Dash, M.K., Patro, S.K. and Rath, A.K. (2016) 'Sustainable use of industrial-waste as partial replacement of fine aggregate for preparation of concrete – A review', International Journal of Sustainable Built Environment, 5, pp. 484–516.

Dawood, A.O., AL-Khazraji, H. and Falih, R.S. (2021) 'Physical and mechanical properties of concrete containing PET wastes as a partial replacement for fine aggregates', Case Studies in Construction Materials, 14, pp. 1-13.

De Brito, J. and Saikia, N. (2013) 'Chapter 2: Industrial Waste Aggregates', Green Energy and Technology, 54, pp. 23–80.

De Schepper, M., Van den Heede, P., Van Driessche, I. and De Belie, N. (2014) 'Life Cycle Assessment of Completely Recyclable Concrete', Materials, 7(8), pp. 6010–6027.

De Schryver, A.M., Brakkee, K.W., Goedkoop, M.J. and Huijbregts, M.A.J. (2009) 'Characterization factors for global warming in life cycle assessment based on damages to humans and ecosystems', Environmental Science and Technology, 43(6), pp. 1689–1695.

Deepika, K.P. and Asha, K. (2016) 'Utilization of Copper Slag as a Partial Replacement of Fine Aggregate in Concrete', International Journal of Innovative Research in Advanced Engineering, 10 (3), pp. 8-13.

Demirboga, R. and Kan, A. (2012) 'Thermal conductivity and shrinkage properties of modified waste polystyrene aggregate concretes', Construction and Building Materials, 35, pp. 730–734.

Desai, G., Lohakare, P., Bhavsar, A., Ugale, A. and Bhavsar, N. (2018) 'Partial Replacement of Fine Aggregate Using Steel Slag',. International Journal of Engineering Development and Research, 6(2), pp. 730-732.

Dharan, D.S. and Lal, A. (2016) 'Study the Effect of Polypropylene Fiber with Steel Slag Aggregate in Concrete', International Journal of Science and Research, 5(5), pp. 1539-1543.

Ding, G.K.C. (2008) 'Sustainable construction-The role of environmental assessment tools', Journal of Environmental Management, 86(3), pp. 451–464.

Ding, T., Xiao, J. and Tam, V.W.Y. (2016) 'A closed-loop life cycle assessment of recycled aggregate concrete utilization in China', Waste Management, 56, pp. 367–375.

Dos Anjos, M.A.G., Sales, A.T.C. and Andrade, N. (2017) ‘Blasted copper slag as fine aggregate in Portland cement concrete’, Journal of Environmental Management, 196, pp. 607–613.

DTI (2013) ‘Environmental Product Declaration (EPD) Report for Fly Ash for concrete, Asphalt and Cement Production’, The Danish Technological Institute (DTI), p. 9.

Duta, A., Cazan, C. and Cosnita, M. (2011) ‘Fly Ash in Optimized Composites Based on Recycled Plastics and Rubber’, In: World of Coal Ash (WOCA) Conference, Denver, CO, USA, pp.1-7.

ECRA (2015) ‘Environmental Product Declaration (EPD) Report’, European Cement Association (CEMBUREAU), Brussels- Belgium. p. 22.

EN 1015-11 (2019) ‘Methods of test for mortar for masonry, Part 11: Determination of flexural and compressive strength of hardened mortar’ European Committee for Standardization (CEN).

EN 1015-10 (2019) ‘Methods of test for mortar for masonry, Part 6: Determination of bulk density of fresh mortar’ European Committee for Standardization (CEN).

EN 12390-8 (2019) ‘Methods of test for mortar for masonry, Part 8: Test on hardened concrete- Depth of penetration of water under pressure’ European Committee for Standardization (CEN).

EN 15804 (2012) ‘Sustainability of construction works - Environmental product declarations - 8 Core rules for the product category of construction products’ CEN, Brussels.

Ersan, Y.C., Gulcimen, S., Imis, T.N., Saygin, O. and Uzal, N. (2020) ‘Life cycle assessment of lightweight concrete containing recycled plastics and fly ash’, European Journal of Environmental and Civil Engineering, Taylor and Francis, pp. 1-15.

Estanqueiro, B., Dinis Silvestre, J., de Brito, J. and Duarte Pinheiro, M. (2018) ‘Environmental life cycle assessment of coarse natural and recycled aggregates for concrete’, European Journal of Environmental and Civil Engineering, 22(4), pp. 429–449.

Etxeberria, M., Pacheco, C., Meneses, J.M. and Berridi, I. (2010) 'Properties of concrete using metallurgical industrial by-products as aggregates', Construction and Building Materials, 24(9), pp. 1594–1600.

European Environment Agency (EEA), Report 18/2020, Plastics, the Circular Economy and Europe's Environment: a Priority for Action, 2021.

Faleschini, F., Alejandro Fernández-Ruíz, M., Zanini, M.A., Brunelli, K., Pellegrino, C. and Hernández-Montes, E. (2015) 'High-performance concrete with electric arc furnace slag as aggregate: Mechanical and durability properties', Construction and Building Materials, 101, pp. 113–121.

Faleschini, F., De Marzi, P. and Pellegrino, C. (2014) 'Recycled concrete containing EAF slag: Environmental assessment through LCA', European Journal of Environmental and Civil Engineering, 18(9), pp. 1009–1024.

Faraca, G. and Astrup, T. (2019) 'Plastic waste from recycling centres: Characterisation and evaluation of plastic recyclability', Waste Management, 95, pp. 388–398.

Faraj, R.H., Sherwani, A.F.H. and Daraei, A. (2019) 'Mechanical, fracture and durability properties of self-compacting high strength concrete containing recycled polypropylene plastic particles', Journal of Building Engineering, 25, pp. 1-12.

Fares, A.I., Sohel, K.M.A., Al-Jabri, K. and Al-Mamun, A. (2021) 'Characteristics of ferrochrome slag aggregate and its uses as a green material in concrete – A review', Construction and Building Materials, 294, pp. 1-18.

Farooq, A. (2019) 'Impact on concrete properties using e-plastic waste fine aggregates and silica fume', Gospodarka Surowcami Mineralnymi / Mineral Resources Management, 35(2), pp. 103–118.

Ferdous, W., Manalo, A., Siddique, R., Mendis, P., Zhuge, Y., Wong, H.S., Lokuge, W., Aravinthan, T. and Schubel, P. (2021) 'Recycling of landfill wastes (tyres, plastics and glass) in construction – A review on global waste generation, performance, application and future opportunities', Resources, Conservation and Recycling, 173, pp. 1-13.

Ferrándiz-Mas, V. and García-Alcocel, E. (2013) 'Durability of expanded polystyrene mortars', Construction and Building Materials, 46, pp. 175–182.

Ferreira, L., De Brito, J. and Saikia, N. (2012) ‘Influence of curing conditions on the mechanical performance of concrete containing recycled plastic aggregate’, Construction and Building Materials, 36, pp. 196–204.

Flower, D.J.M. and Sanjayan, J.G. (2017) ‘Greenhouse Gas Emissions Due to Concrete Manufacture’, Handbook of Low Carbon Concrete. Elsevier Inc., pp. 1–16.

Fraj, A. Ben and Idir, R. (2017) ‘Concrete based on recycled aggregates – Recycling and environmental analysis: A case study of paris’ region’, Construction and Building Materials, 157, pp. 952–964.

Frigione, M. (2010) ‘Recycling of PET bottles as fine aggregate in concrete’, Waste Management, 30(6), pp. 1101–1106.

Galvão, J.C.A., Portella, K.F., Joukoski, A., Mendes, R. and Ferreira, E.S. (2011) ‘Use of waste polymers in concrete for repair of dam hydraulic surfaces’, Construction and Building Materials, 25(2), pp. 1049–1055.

Gandhi, N., Farfaras, N., Wang, N.H.L. and Chen, W.T. (2021) ‘Life cycle assessment of recycling high-density polyethylene plastic waste’, Journal of Renewable Materials, 9(8), pp. 1463–1483.

García-Segura, T., Yepes, V. and Alcalá, J. (2014) ‘Life cycle greenhouse gas emissions of blended cement concrete including carbonation and durability’, International Journal of Life Cycle Assessment, 19(1), pp. 3–12.

Gavela, S., Karakosta, C., Nydriotis, C., Kaselouri -Rigopoulou, V., Kolias, S., Tarantili, P.A., Magoulas, C., Tassios, D. and Andreopoulos, A. (2004) ‘A Study of Concretes Containing Thermoplastic Wastes as Aggregates’, International RILEM Conference on the Use of Recycled Materials in Buildings and Structures, Barcelona, Spain, pp. 911-918.

Gayatri, D. and Popat, K. (2020) ‘Use of Recycled Plastic in Concrete as Replacement of Fine Aggregate’, International Research Journal of Engineering and Technology 7(12), 920-926.

Ge, Z., Sun, R., Zhang, K., Gao, Z. and Li, P. (2013) 'Physical and mechanical properties of mortar using waste Polyethylene Terephthalate bottles', Construction and Building Materials, 44, pp. 81–86.

Gencel, O., Koksal, F., Ozel, C. and Brostow, W. (2012) 'Combined effects of fly ash and waste ferrochromium on properties of concrete', Construction and Building Materials, 29, pp. 633–640.

Gettu, R., Patel, A., Rathi, V., Prakasan, S., Basavaraj, A.S. and Maity, S. (2016) 'Sustainability Assessment of Cements and Concretes in the Indian Context: Influence of Supplementary Cementitious Materials', Proceedings of Fourth International Conference on Sustainable Construction Materials and Technologies (SCMT4), Las Vegas, USA, pp.1-9.

Geyer, R., Jambeck, J.R. and Law, K.L. (2017) 'Production, use, and fate of all plastics ever made' Science Advances, 3, pp.1-5.

Ghernouti, Y., Rabehi, B., Safi, B. and Chaid, R. (2014) 'Use of Recycled Plastic Bag Waste in the Concrete', Journal of International Scientific Publications: Materials, Methods and Technologies, 8, pp. 480-487.

Górak, P., Postawa, P., Natalia Trusilewicz, L. and Łagosz, A. (2021) 'Lightweight PET based composite aggregates in Portland cement materials - Microstructure and physicochemical performance', Journal of Building Engineering, 34, pp. 1-57.

Gouasmi, M.T., Benosman, A.S. and Taïbi, H. (2019) 'Improving the properties of waste plastic lightweight aggregates-based composite mortars in an experimental saline environment', Asian Journal of Civil Engineering, 20(1), pp. 71–85.

Gouasmi, M.T., Benosman, A.S., Taïbi, H., Kazi Tani, N. and Belbachir, M. (2017) 'Destructive and non-destructive testing of an industrial screed mortar made with lightweight composite aggregates WPLA', International Journal of Engineering Research in Africa, 33, pp. 140–158.

Gu, L. and Ozbakkaloglu, T. (2016) 'Use of recycled plastics in concrete: A critical review', Waste Management, 51, pp. 19–42.

Guendouz, M., Debieb, F., Boukendakdji, O., Kadri, E.H., Bentchikou, M. and Soualhi, H. (2016) 'Use of plastic waste in sand concrete', Journal of Materials and Environmental Sciences, 7(2), pp. 382–389.

Guilherme, J., Alegre, C. and Lima, S. (2012) 'Fire behaviour of concrete produced with selected plastic waste aggregates' Extended abstract, MSc. Thesis, Tecnico Lisbao, pp. 1-19.

Guo, Y., Xie, J., Zheng, W. and Li, J. (2018) 'Effects of steel slag as fine aggregate on static and impact behaviours of concrete', Construction and Building Materials, 192, pp. 194–201.

Gupta, N. and Siddique, R. (2019) 'Strength and micro-structural properties of self-compacting concrete incorporating copper slag', Construction and Building Materials, 224, pp. 894–908.

Gupta, N. and Siddique, R. (2020) 'Durability characteristics of self-compacting concrete made with copper slag', Construction and Building Materials, 247, pp. 1-16.

Gursel, A.P., Maryman, H. and Ostertag, C. (2016) 'A life-cycle approach to environmental, mechanical, and durability properties of "green" concrete mixes with rice husk ash', Journal of Cleaner Production, 112, pp. 823–836.

Gursel, A.P. and Ostertag, C. (2019) 'Life-Cycle Assessment of High-Strength Concrete Mixtures with Copper Slag as Sand Replacement', Advances in Civil Engineering, 2019, pp.1-13.

Habib, M.Z., Alom, M.M. and Hoque, M.M. (2017) 'Concrete production using recycled waste plastic as aggregate', Journal of Civil Engineering (IEB), 45(1), pp. 11-17.

Haghighatnejad, N., Mousavi, S.Y., Khaleghi, S.J., Tabarsa, A. and Yousefi, S. (2016) 'Properties of recycled PVC aggregate concrete under different curing conditions', Construction and Building Materials, 126, pp. 943–950.

Hannawi, K., Kamali-Bernard, S. and Prince, W. (2010a) 'Physical and mechanical properties of mortars containing PET and PC waste aggregates', Waste Management, 30(11), pp. 2312–2320.

Hannawi, K., Prince, W. and Bernard, S.K. (2013) 'Strain Capacity and Cracking Resistance Improvement in Mortars by Adding Plastic Particles' Journal of Materials in Civil Engineering, 25, pp. 1602-1610.

Hannawi, K., Prince, W. and Kamali-Bernard, S. (2010b) 'Effect of thermoplastic aggregates incorporation on physical, mechanical and transfer behaviour of cementitious materials', Waste and Biomass Valorization, 1(2), pp. 251–259.

Hannawi, K. and Prince-Agbodjan, W. (2015) 'Transfer behaviour and durability of cementitious mortars containing polycarbonate plastic wastes', European Journal of Environmental and Civil Engineering, 19(4), pp. 467–481.

Harini, B. and Ramana, K.V. (2015) 'Use of Recycled Plastic Waste as Partial Replacement for Fine Aggregate in Concrete', International Journal of Innovative Research in Science, Engineering and Technology, 4(9), pp. 8596-8603.

Herki, B.A. and Khatib, J.M. (2017) 'Valorisation of waste expanded polystyrene in concrete using a novel recycling technique', European Journal of Environmental and Civil Engineering, 21(11), pp. 1384–1402.

Herki, B.A., Khatib, J.M. and Negim, E.M. (2013) 'Lightweight concrete made from waste polystyrene and fly ash', World Applied Sciences Journal, 21(9), pp. 1356–1360.

Herki, Bengin M.A. (2017a) 'Combined effects of densified polystyrene and unprocessed fly ash on concrete engineering properties', Buildings, 7(3), 77, pp. 1-16.

Herki, Bengin M. A. (2017b) 'Combined Effects of Modified Polystyrene and Unprocessed Fly Ash on Concrete Properties Produced by a Novel Technique of Densification', World Engineering and Applied Sciences Journal, 8(3), pp. 118–129.

Hernández, E. and Etxeberria, M. (2019) 'Influence of Plastic Recycled Aggregates in the Hardened Properties of Concretes', Proceedings of the Fifth international conference on sustainable construction materials and technologies, Coventry University and The University of Wisconsin Milwaukee Centre for By-products Utilization, UK, pp. 1-13.

Hilton, B., Bawden, K., Winnebeck, K., Chandrasiri, C., Ariyachandra, E. and Peethamparan, S. (2019) 'The functional and environmental performance of mixed

cathode ray tubes and recycled glass as partial replacement for cement in concrete', Resources, Conservation and Recycling, 151, pp. 1-11.

Hopewell, J., Dvorak, R. and Kosior, E. (2009) 'Plastics recycling: Challenges and opportunities', Philosophical Transactions of the Royal Society B: Biological Sciences, 364, pp. 2115–2126.

Hossain, M.B., Bhowmik, P. and Shaad, K.M. (2016a) 'Use of waste plastic aggregation in concrete as a constituent material', Progressive Agriculture, 27(3), pp. 383-391.

Hossain, M.U., Poon, C.S., Lo, I.M.C. and Cheng, J.C.P. (2016b) 'Comparative environmental evaluation of aggregate production from recycled waste materials and virgin sources by LCA', Resources, Conservation and Recycling, 109, pp. 67–77.

Hosseini, P., Booshehrian, A. and Madari, A. (2011) 'Developing concrete recycling strategies by utilization of nano-SiO 2 particles', Waste and Biomass Valorization, 2(3), pp. 347–355.

Huntzinger, D.N. and Eatmon, T.D. (2009) 'A life-cycle assessment of Portland cement manufacturing: comparing the traditional process with alternative technologies', Journal of Cleaner Production, 17(7), pp. 668–675.

ILCD. (2010). ILCD handbook, analysis of existing environmental impact assessment methodologies for use in life cycle assessment (LCA). JRC European Commission 2010, Available online: http://eplca.jrc.ec.europa.eu/uploads/ (accessed on 15th January 2020).

Ingrao, C., Lo Giudice, A., Tricase, C., Mbohwa, C. and Rana, R. (2014) 'The use of basalt aggregates in the production of concrete for the prefabrication industry: Environmental impact assessment, interpretation and improvement', Journal of Cleaner Production, 75, pp. 195–204.

Irwan, J.M., Annas, M.M.K., Aeslina, A.K., Othman, N., Koh, H.B., Asyraf, R.M. and Faisal, S.K. (2014) 'Cracking propagation of reinforced concrete using polyethylene terephtalate (PET) bottles as fine aggregate', In: Advanced Materials Research, Trans Tech Publications, 11, pp. 474–478.

IS 10262 (2019) 'Concrete mix proportioning- Guidelines', Bureau of Indian Standard, New Delhi.

IS 1199 (2018) ‘Fresh Concrete- Methods of sampling, testing and analysis’, Bureau of Indian Standard, New Delhi.

IS 516-5 (2018) ‘Hardened concrete- Methods of test, Part 5: Non-destructive testing of concrete, Section 1: Ultrasonic pulse velocity testing’ Bureau of Indian Standard, New Delhi.

IS 1727 (1967) (Reaffirmed-2018) ‘Methods of test for pozzolanic materials (First Revision)’, Bureau of Indian Standard, New Delhi.

IS 2386-3 (1963) (Reaffirmed 2021) ‘Methods of test for aggregates for concrete, Part 3: Specific gravity, density absorption, voids and bulking’, Bureau of Indian Standard, New Delhi.

IS 2386-6 (1963) (Reaffirmed 2021) ‘Methods of test for aggregates for concrete, Part 6: Measuring mortar making properties of fine aggregates’, Bureau of Indian Standard, New Delhi.

IS 269 (2015) ‘Ordinary Portland Cement-Specification (Sixth Revision)’, Bureau of Indian Standard, New Delhi.

IS 2720-3 (1980) ‘Methods of test for soils, Part 3: Determination of specific gravity, Section 1: Fine grained soils (First Revision)’, Bureau of Indian Standard. New Delhi.

IS 3812 (2013) ‘Pulverized fuel ash-Specification, Part 1: For use as pozzolana in cement, cement mortar, and concrete (Third Revision)’, Bureau of Indian Standard, New Delhi.

IS 383 (2016) ‘Coarse and fine aggregate for concrete – Specification (Third revision)’, Bureau of Indian Standard, New Delhi.

IS 4031-1 (1996) ‘Methods of physical tests for hydraulic cement, Part 1: Determination of fineness by dry sieving (Second Revision)’ Bureau of Indian Standard, New Delhi.

IS 4031-2 (1999) ‘Methods of physical tests for hydraulic cement, Part 2: Determination of fineness by Blaine air permeability method (Second Revision)’. Bureau of Indian Standard, New Delhi.

IS 4031-3 (1988) ‘Methods of physical tests for hydraulic cement, Part 3: Determination of soundness (First Revision)’, Bureau of Indian Standard, New Delhi.

IS 4031-4 (1988) ‘Methods of physical tests for hydraulic cement, Part 4: Determination of consistency of standard cement paste (First Revision)’, Bureau of Indian Standard, New Delhi.

IS 4031-5 (1988) ‘Methods of physical tests for hydraulic cement, Part 5: Determination of initial and final setting times (First Revision)’, Bureau of Indian Standard, New Delhi.

IS 4031-6 (1988) ‘Methods of physical tests for hydraulic cement, Part 6: Determination of compressive strength of hydraulic cement other than masonry cement (First Revision)’ Bureau of Indian Standard, New Delhi.

IS 4032 (1985) ‘Method of chemical analysis of hydraulic cement (First Revision)’, Bureau of Indian Standard, New Delhi.

IS 456 (2000) ‘Plain and Reinforced Concrete- Code of Practice (Fourth Revision)’, Bureau of Indian Standard, New Delhi.

IS 516 (2021) ‘Hardened Concrete- Methods of test, Part 1: Testing of Strength of Hardened Concrete’, Bureau of Indian Standard, New Delhi.

IS 9103 (1999) Concrete admixture – Specification (Third revision), Bureau of Indian Standard, New Delhi.

Islam, M.J., Meherier, M.S. and Islam, A.K.M.R. (2016) ‘Effects of waste PET as coarse aggregate on the fresh and harden properties of concrete’, Construction and Building Materials, 125, pp. 946–951.

Islam, M.Z., Sohel, K.M.A., Al-Jabri, K. and Al Harthy, A. (2021) ‘Properties of concrete with ferrochrome slag as a fine aggregate at elevated temperatures’, Case Studies in Construction Materials, 15, pp. 1-17.

Ismail Khalil, W. and Jumaa Khalaf, K. (2017) ‘Some Properties of Sustainable Concrete with Plastic Waste Aggregate’, Proceedings of the First International Conference for Engineering Researches Some Properties of Sustainable Concrete with Plastic Waste Aggregate, pp.1-12.

Ismail, Z.Z. and AL-Hashmi, E.A. (2008) ‘Use of waste plastic in concrete mixture as aggregate replacement’, Waste Management, 28(11), pp. 2041–2047.

ISO 14040 (2006) ‘Environmental management - Life Cycle Assessment: Principles and Framework. ISO 14040:2006’, In: International Organization for Standardization, Geneva, Switzerland.

ISO 14044 (2006) ‘Environmental management - Life Cycle Assessment: Requirements and Guidelines. ISO 14044:2006’, In: International Organization for Standardization, Geneva, Switzerland.

Iucolano, F., Liguori, B., Caputo, D., Colangelo, F. and Cioffi, R. (2013) ‘Recycled plastic aggregate in mortars composition: Effect on physical and mechanical properties’, Materials and Design, 52, pp. 916–922.

Jacob-Vaillancourt, C. and Sorelli, L. (2018) ‘Characterization of concrete composites with recycled plastic aggregates from postconsumer material streams’, Construction and Building Materials, 182, pp. 561–572.

Jain, A., Siddique, S., Gupta, T., Sharma, R.K. and Chaudhary, S. (2020) ‘Utilization of shredded waste plastic bags to improve impact and abrasion resistance of concrete’, Environment, Development and Sustainability, 22(1), pp. 337–362.

Janfeshan Araghi, H., Nikbin, I.M., Rahimi Reskati, S., Rahmani, E. and Allahyari, H. (2015) ‘An experimental investigation on the erosion resistance of concrete containing various PET particles percentages against sulfuric acid attack’, Construction and Building Materials, 77, pp. 461–471.

Jaskowska-Lemańska, J., Kucharska, M., Matuszak, J., Nowak, P. and Łukaszczyk, W. (2022) ‘Selected Properties of Self-Compacting Concrete with Recycled PET Aggregate’, Materials, 15(7), pp. 1-20.

Jiang, M., Chen, X., Rajabipour, F. and Hendrickson, C.T. (2014) ‘Comparative Life Cycle Assessment of Conventional, Glass Powder, and Alkali-Activated Slag Concrete and Mortar’, Journal of Infrastructure Systems, 20(4), pp. 1-9.

Jiang, Y., Ling, T.C., Shi, C. and Pan, S.Y. (2018) ‘Characteristics of steel slags and their use in cement and concrete—A review’, Resources, Conservation and Recycling, 136, pp. 187–197.

Jiménez, C., Barra, M., Josa, A. and Valls, S. (2015) 'LCA of recycled and conventional concretes designed using the Equivalent Mortar Volume and classic methods', Construction and Building Materials, 84, pp. 245–252.

Jiménez, L.F., Domínguez, J.A. and Vega-Azamar, R.E. (2018) 'Carbon footprint of recycled aggregate concrete', Advances in Civil Engineering, 2018, pp. 1-6.

Josa, A., Gettu, R. and Aguado, A. (2005) 'Environmental Assessment of Cement Based Products: Life Cycle Assessment and the Ecoconcrete Software Tool'. Achieving Sustainability in Construction, Thomas Telford Publishing, pp. 281-290.

Juenger, M., Provis, J.L., Elsen, J., Matthes, W., Hooton, R.D., Duchesne, J., Courard, L., He, H., Michel, F., Snellings, R. and De Belie, N. (2012) 'Supplementary cementitious materials for concrete: Characterization needs', Proceedings of Materials Research Society Symposium. Materials Research Society, 1488, pp. 106–120.

Juki, M.I., Awang, M., Annas, M.M.K., Boon, K.H., Othman, N., Kadir, A.A., Roslan, M.A. and Khalid, F.S. (2013) 'Relationship between compressive, splitting tensile and flexural strength of concrete containing granulated waste polyethylene terephthalate (PET) bottles as fine aggregate', Advanced Materials Research, Trans Tech Publications, 795, pp. 356–359.

Kamaruddin, M.A., Abdullah, M.M.A., Zawawi, M.H. and Zainol, M.R.R.A. (2017) 'Potential use of plastic waste as construction materials: Recent progress and future prospect', IOP Conference Series: Materials Science and Engineering. Institute of Physics Publishing, 267, pp.1-10.

Kan, A. and Demirboğa, R. (2009a) 'A new technique of processing for waste-expanded polystyrene foams as aggregates', Journal of Materials Processing Technology, 209(6), pp. 2994–3000.

Kan, A. and Demirboğa, R. (2009b) 'A novel material for lightweight concrete production', Cement and Concrete Composites, 31(7), pp. 489–495.

Khanzadi, M. and Behnood, A. (2009) 'Mechanical properties of high-strength concrete incorporating copper slag as coarse aggregate', Construction and Building Materials, 23(6), pp. 2183–2188.

Khasreen, M.M., Banfill, P.F.G. and Menzies, G.F. (2009) ‘Life-cycle assessment and the environmental impact of buildings: A review’, Sustainability, 1(3), pp. 674–701.

Kim, H., Koh, T. and Pyo, S. (2016) ‘Enhancing flowability and sustainability of ultra high-performance concrete incorporating high replacement levels of industrial slags’, Construction and Building Materials, 123, pp. 153–160.

Kim, T., Lee, S., Chae, C.U., Jang, H. and Lee, K. (2017) ‘Development of the CO_2 emission evaluation tool for the life cycle assessment of concrete’, Sustainability, 9(11), pp. 1-14.

Kim, T., Tae, S. and Roh, S. (2013) ‘Assessment of the CO_2 emission and cost reduction performance of a low-carbon-emission concrete mix design using an optimal mix design system’, Renewable and Sustainable Energy Reviews, 25, pp. 729–741.

Kleijer, A.L., Lasvaux, S., Citherlet, S. and Viviani, M. (2017) ‘Product-specific Life Cycle Assessment of ready mix concrete: Comparison between a recycled and an ordinary concrete’, Resources, Conservation and Recycling, 122, pp. 210–218.

Knoeri, C., Sanyé-Mengual, E. and Althaus, H.J. (2013) ‘Comparative LCA of recycled and conventional concrete for structural applications’, International Journal of Life Cycle Assessment, 18(5), pp. 909–918.

Koroneos, C.J. and Th Dompros, A. (2009) ‘Environmental assessment of the cement and concrete life cycle in Greece’, International Journal of Environmental Technology and Management, 10(1), pp. 71-88.

Kothai, P.S. and Malathy, R. (2007) ‘Utilization of Steel Slag in Concrete as a Partial Replacement Material for Fine Aggregates’, International Journal of Innovative Research in Science, Engineering and Technology, 3(4), pp. 11585-11592

Kou, S.C., Lee, G., Poon, C.S. and Lai, W.L. (2009) ‘Properties of lightweight aggregate concrete prepared with PVC granules derived from scraped PVC pipes’, Waste Management, 29(2), pp. 621–628.

Kumar, A., Luthra, S., Mangla, S.K. and Kazançoğlu, Y. (2020) ‘COVID-19 impact on sustainable production and operations management’, Sustainable Operations and Computers, 1, pp. 1–7.

Kumar, R. and Naik, T.R. (2011) 'Utilization of Post-Consumer Plastics in Sustainable Concrete: An Overview', Proceedings of Fourth International Conference on Sustainable Construction Materials and Technologies (SCMT4), Las Vegas, USA, pp. 1-9.

Kurad, R., Silvestre, J.D., de Brito, J. and Ahmed, H. (2017) 'Effect of incorporation of high volume of recycled concrete aggregates and fly ash on the strength and global warming potential of concrete', Journal of Cleaner Production, 166, pp. 485–502.

Kurda, R., Silvestre, José D. and de Brito, J. (2018a) 'Life cycle assessment of concrete made with high volume of recycled concrete aggregates and fly ash', Resources, Conservation and Recycling, 139, pp. 407–417.

Kurda, R., Silvestre, Jos D and de Brito, J. (2018b) 'Toxicity and environmental and economic performance of fly ash and recycled concrete aggregates use in concrete', Heliyon, 4, pp. 1-45.

Lakshmi, R. and Nagan, S. (2011) 'Investigations on Durability Characteristics of E-Plastic Waste Incorporated Concrete', Asian Journal of Civil Engineering (Building and Housing),12(6), pp. 773-787.

Lamba, P., Kaur, D.P., Raj, S. and Sorout, J. (2022) 'Recycling/reuse of plastic waste as construction material for sustainable development: a review', Environmental Science and Pollution Research, Springer Science and Business Media Deutschland GmbH, pp. 86156–86179.

Latawiec, R., Woyciechowski, P. and Kowalski, K.J. (2018) 'Sustainable concrete performance—CO_2-emission', Environments, 5(2), pp. 1–14.

Lee, Z.H., Paul, S.C., Kong, S.Y., Susilawati, S. and Yang, X. (2019) 'Modification of Waste Aggregate PET for Improving the Concrete Properties', Advances in Civil Engineering, 1371, pp. 1-11.

Li, W., Long, C., Tam, V.W.Y., Poon, C.S. and Hui Duan, W. (2017) 'Effects of nano-particles on failure process and microstructural properties of recycled aggregate concrete', Construction and Building Materials, 142, pp. 42–50.

Li, X., Ling, T.C. and Hung Mo, K. (2020) ‘Functions and impacts of plastic/rubber wastes as eco-friendly aggregate in concrete – A review’, Construction and Building Materials, 240, pp. 1-14.

Li, X., Zhu, Y. and Zhang, Z. (2010) ‘An LCA-based environmental impact assessment model for construction processes’, Building and Environment, 45(3), pp. 766–775.

Liu, F., Yan, Y., Li, L., Lan, C. and Chen, G. (2015) ‘Performance of Recycled Plastic-Based Concrete’, Journal of Materials in Civil Engineering, 27(2), pp. 1-9.

Liu, Y., Hossain, M.U. and Ling, T.C. (2018) ‘Carbon footprint of block prepared with recycled aggregate: A case study in China’, IOP Conference Series: Materials Science and Engineering. Institute of Physics Publishing, 431, pp. 1-7.

Lo Monte, F., Bamonte, P. and Gambarova, P.G. (2015) ‘Physical and mechanical properties of heat-Damaged structural concrete containing expanded polystyrene syntherized particles’, Fire and Materials, 39(1), pp. 58–71.

Lokeshwari, M., Ostwal, N., H, N.K., Saxena, P. and Pranay, P. (2019) ‘Utilization of Waste Plastic as Partial Replacement of Fine and Coarse Aggregates in Concrete Blocks’, International Research Journal of Engineering and Technology, 6(9), pp. 378-382.

Lye, C.Q., Koh, S.K., Mangabhai, R. and Dhir, R.K. (2015) ‘Use of copper slag and washed copper slag as sand in concrete: A state-of-the-art review’, Magazine of Concrete Research, Thomas Telford Services Ltd, pp. 665–679.

Madandoust, R., Ranjbar, M.M. and Yasin Mousavi, S. (2011) ‘An investigation on the fresh properties of self-compacted lightweight concrete containing expanded polystyrene’, Construction and Building Materials, 25(9), pp. 3721–3731.

Madheswaran, C.K., Ambily, P.S., Dattatreya, J.K. and Rajamane, N.P. (2014) ‘Studies on use of Copper Slag as Replacement Material for River Sand in Building Constructions’, Journal of The Institution of Engineers (India): Series A, 95(3), pp. 169–177.

Maharishi, A., Singh, S.P., Gupta, L.K., Shehnazdeep (2020) ‘Strength and durability studies on slag cement concrete made with copper slag as fine aggregates’, Materials Today: Proceedings, Elsevier Ltd, pp. 2639–2648.

Mahmood, R.A. and Kockal, N.U. (2020) ‘Cementitious materials incorporating waste plastics: a review’, SN Applied Sciences. Springer Nature, 2, 2072, pp.1-13.

Majeed, A.Z., Kurian, T., Davis, B., Alex, S.T., Fernandez, K.S. and Mathew, A. V. (2019) ‘Partial Replacement of Aggregates with Granulated Waste Plastic in Solid Concrete Blocks—An Intensive Study’, Green Buildings and Sustainable Engineering, Springer Transactions in Civil and Environmental Engineering, pp. 405–415.

Malkapur, S.M., Anand, A., Pandey, A.P., Ojha, A., Mani, N. and Mattur, N.C. (2014) ‘Effect of Mix Parameters on the Strength Performance of Waste Plastics Incorporated Concrete Mixes’, Journal of Structures, 2014, pp. 1–8.

Manjunatha, M., Reshma, T. V., Balaji, K.V.G.D., Bharath, A. and Tangadagi, R.B. (2021) ‘The sustainable use of waste copper slag in concrete: An experimental research’, Materials Today: Proceedings. Elsevier Ltd, pp. 3645–3653.

Marinković, S., Dragaš, J., Ignjatović, I. and Tošić, N. (2017) ‘Environmental assessment of green concretes for structural use’, Journal of Cleaner Production, 154, pp. 633–649.

Marinković, S., Radonjanin, V., Malešev, M. and Ignjatović, I. (2010) ‘Comparative environmental assessment of natural and recycled aggregate concrete’, Waste Management, 30(11), pp. 2255–2264.

Marinković, S. et al. (2016) ‘Life Cycle Analysis of Recycled Aggregate Concrete with Fly Ash ss Partial Cement Replacement’, Proceedings of Sustainable Built Environment (SBE) Regional Conference, Zurich, pp. 1-7.

Marinkovic, S.B. (2013) ‘Life cycle assessment (LCA) aspects of concrete’, In: Eco-Efficient Concrete. Elsevier Ltd., pp. 45–80.

Marinković, S.B., Ignjatović, I. and Radonjanin, V. (2013a) ‘Life-cycle assessment (LCA) of concrete with recycled aggregates (RAs)’, Handbook of Recycled Concrete and Demolition Waste. Elsevier Inc., pp. 569–604.

Marinković, S.B., Malešev, M. and Ignjatović, I. (2013b) ‘Life cycle assessment (LCA) of concrete made using recycled concrete or natural aggregates’, Eco-Efficient Construction and Building Materials: Life Cycle Assessment (LCA), Eco-Labelling and Case Studies. Elsevier Inc., pp. 239–266.

Martínez, E., Blanco, J., Jiménez, E., Saenz-Díez, J.C. and Sanz, F. (2015) 'Comparative evaluation of life cycle impact assessment software tools through a wind turbine case study', Renewable Energy, 74, pp. 237–246.

Martín-Gulló, I., Esperanza, M. and Font, R. (2001) 'Kinetic model for the pyrolysis and combustion of poly-(ethylene terephthalate) (PET)', Journal of Analytical and Applied Pyrolysis, 58, pp. 635-650.

Marzouk, O.Y., Dheilly, R.M. and Queneudec, M. (2007) 'Valorization of post-consumer waste plastic in cementitious concrete composites', Waste Management, 27(2), pp. 310–318.

Marzouk, O.Y., Dheilly, R.-M. and Queneudec, M. (2005) 'Reuse of Plastic Waste in Cementitious Concrete Composites', Plastic Waste Concrete Composites, Ice Publishing, pp. 817-824.

Maslehuddin, M., Sharif, A.M., Shameem, M., Ibrahim, M. and Barry, M. (2003) 'Comparison of properties of steel slag and crushed limestone aggregate concretes', Construction and Building Materials, 17, pp. 105-112.

Mavroulidou, M. (2017) 'Mechanical Properties and Durability of Concrete with Water Cooled Copper Slag Aggregate', Waste and Biomass Valorization, 8(5), pp. 1841–1854.

Mbadike, E.M. and Osadebe, N.N. (2012) 'Effect of Incorporating Expanded Polystyrene Aggregate Granules in Concrete Matrix', Nigerian Journal of Technology, 31(3), pp. 401–404.

Mcintyre, J., Spatari, S. and Maclean, H.L. (2009) 'Energy and Greenhouse Gas Emissions Trade-Offs of Recycled Concrete Aggregate Use in Nonstructural Concrete: A North American Case Study', Journal of Infrastructure Systems, 15, pp. 361-370.

McNeil, K. and Kang, T.H.K. (2013) 'Recycled Concrete Aggregates: A Review', International Journal of Concrete Structures and Materials, 7(1), pp. 61–69.

Mercante, I., Alejandrino, C., Ojeda, J.P., Chini, J., Maroto, C. and Fajardo, N. (2018) 'Mortar and concrete composites with recycled plastic: A review', Science and Technology of Materials, 30, pp. 69–79.

Miah, M.J., Hossain Patoary, M.M., Paul, S.C., Babafemi, A.J. and Panda, B. (2020) 'Enhancement of mechanical properties and porosity of concrete using steel slag coarse aggregate', Materials, 13(12), pp. 1-20.

Miller, S.A. (2018) 'Supplementary cementitious materials to mitigate greenhouse gas emissions from concrete: can there be too much of a good thing?', Journal of Cleaner Production, 178, pp. 587–598.

Miller, S.A., Horvath, A. and Monteiro, P.J.M. (2016) 'Readily implementable techniques can cut annual CO2 emissions from the production of concrete by over 20%', Environmental Research Letters, 11(7), pp. 1-8.

Mishra, B.K. and Bharosh, R. (2018) 'Evaluation strength and durability characteristic of concrete use steel slag', International Journal of Advance Research, Ideas and Innovations in Technology, 4(5), pp. 597-601.

Mohammadi, J. and South, W. (2017) 'Life cycle assessment (LCA) of benchmark concrete products in Australia', International Journal of Life Cycle Assessment, 22(10), pp. 1588–1608.

Mohammed, A.A. (2018) 'Mechanical strength of concrete with PVC aggregates', Use of Recycled Plastics in Eco-efficient Concrete, Elsevier Inc., pp. 115–135.

Mohammed, A.A., Mohammed, I.I. and Mohammed, S.A. (2019) 'Some properties of concrete with plastic aggregate derived from shredded PVC sheets', Construction and Building Materials, 201, pp. 232–245.

Mohammed, A.S., Ali, K.M., Rajab, N.A. and Hilal, N. (2020b) 'Mechanical Properties of Concrete and Mortar Containing Low Density Polyethylene Waste Particles as Fine Aggregate', Journal of Materials and Engineering Structures, 7, pp. 57-72.

Mohammed, H., Sadique, M., Shaw, A. and Bras, A. (2020a) 'The influence of incorporating plastic within concrete and the potential use of microwave curing; A review', Journal of Building Engineering, 32, pp. 1-19.

Mohammed Joarder, S., Saidur Rahman, M. and Haque, A. (2019) 'Study of Concrete Properties Using Polyethylene Terephthalate as Coarse Aggregate', International Journal of Science and Engineering Investigations, 8(84), pp. 103-107.

Morales-Pinzon, T., Angrill, S., Rieradevall, J., Gabarrell, X., Gasol, C.M. and Josa, A. (2011) 'LCM of rainwater harvesting systems in emerging neighbourhoods in Colombia', M. Finkbeiner (Ed.), Towards Life Cycle Sustainability Management, Springer Netherlands, Dordrecht, pp. 277-288.

Mukharjee, B.B. and Barai, S. V. (2014) 'Influence of incorporation of nano-silica and recycled aggregates on compressive strength and microstructure of concrete', Computers and Chemical Engineering, 71, pp. 570–578.

Müller, H.S., Haist, M. and Vogel, M. (2014) 'Assessment of the sustainability potential of concrete and concrete structures considering their environmental impact, performance and lifetime', Construction and Building Materials, 67(PART C), pp. 321–337.

Mustafa, M.A.T., Hanafi, I., Mahmoud, R. and Tayeh, B.A., (2019) 'Effect of partial replacement of sand by plastic waste on impact resistance of concrete: experiment and simulation', Structures, 20, pp. 519–526.

Nadeem, M. and Pofale, A.D. (2012) 'Replacement of Natural Fine Aggregate with Granular Slag-A Waste Industrial by-product in Cement Mortar Applications as an Alternative Construction Materials', International Journal of Engineering Research and Applications, 2(5), pp. 1258-1264.

Naganur, J. and Chethan, B.A. (2014) 'Effect of Copper Slag as a Partial Replacement of Fine Aggregate on the Properties of Cement Concrete', International Journal of Research, 1(8), pp. 882-893.

Naik, T.R., Singh, S.S., Huber, C.O. and Brodersen, B.S. (1996) 'Use of Post-Consumer Waste Plastics in Cement-Based Composites', Cement and Concrete Research, 26(10), pp. 1489-1492.

Napolano, L., Menna, C., Graziano, S.F., Asprone, D., D'Amore, M., De Gennaro, R. and Dondi, M. (2016) 'Environmental life cycle assessment of lightweight concrete to support recycled materials selection for sustainable design', Construction and Building Materials, 119, pp. 370–384.

Nath, P., Sarker, P.K. and Biswas, W.K. (2018) 'Effect of fly ash on the service life, carbon footprint and embodied energy of high strength concrete in the marine environment', Energy and Buildings, 158, pp. 1694–1702.

Newswire,P.R. (2020) 'Impact of COVID 19 on the global manufacturing industry'. https://www.prnewswire.com/news-releases/impact-of-covid-19-on-the-global-manufacturing-industry-2020-301042150.html (Accessed 25 November 2021).

Nibudey, R.N., Nagarnaik, P.B, Parbat, D.K. and Pande, A.M. (2013) 'Cube and cylinder compressive strengths of waste plastic fiber reinforced concrete', International Journal of Civil and Structural Engineering, 4(2), pp. 174-182.

Nijland, T.G. and Larbi, J.A. (2010) 'Microscopic examination of deteriorated concrete', Non-Destructive Evaluation of Reinforced Concrete Structures: Deterioration Processes and Standard Test Methods. Elsevier Inc., pp. 137–179.

Nikbin, I. M., Aliaghazadeh, M., Charkhtab, S.H. and Fathollahpour, A. (2016a) 'Environmental impacts and mechanical properties of lightweight concrete containing bauxite residue (red mud)', Journal of Cleaner Production, 172, pp. 2683–2694.

Nikbin, Iman M., Saman Rahimi, R., Allahyari, H. and Fallah, F. (2016b) 'Feasibility study of waste Poly Ethylene Terephthalate (PET) particles as aggregate replacement for acid erosion of sustainable structural normal and lightweight concrete', Journal of Cleaner Production, 126, pp. 108–117.

Nisbet, M.A., Marceau, M.L. and Vangeem, M.G. (2002) 'Environmental Life Cycle Inventory of Portland Cement Concrete', Portland Cement Association, Research and Development Information, PCA R&D Serial No. 2137a, pp.1-80.

NT Build 492 (1999) Concrete, mortar and cement-based repair materials: chloride migration coefficient from non-steady-state migration experiments. Nordtest, Finland.

O'Brien, K.R., Ménaché, J. and O'Moore, L.M. (2009) 'Impact of fly ash content and fly ash transportation distance on embodied greenhouse gas emissions and water consumption in concrete', International Journal of Life Cycle Assessment, 14(7), pp. 621–629.

Ogundairo, T.O., Olukanni, D.O., Akinwumi, I.I. and Adegoke, D.D. (2021) 'A review on plastic waste as sustainable resource in civil engineering applications', IOP Conference Series: Materials Science and Engineering, 1036(1), pp. 1-14.

Ohemeng, E.A. and Ekolu, S.O. (2019) 'Strength prediction model for cement mortar made with waste LDPE plastic as fine aggregate', Journal of Sustainable Cement-Based Materials, 8(4), pp. 228–243.

Ortiz, O., Castells, F. and Sonnemann, G. (2009) 'Sustainability in the construction industry: A review of recent developments based on LCA', Construction and Building Materials, 23, pp. 28–39.

Ouda, A.S. and Abdel-Gawwad, H.A. (2017) 'The effect of replacing sand by iron slag on physical, mechanical and radiological properties of cement mortar', HBRC Journal, 13(3), pp. 255–261.

Ozbakkaloglu, T., Gu, L. and Gholampour, A. (2017) 'Short-Term Mechanical Properties of Concrete Containing Recycled Polypropylene Coarse Aggregates under Ambient and Elevated Temperature', Journal of Materials in Civil Engineering, 29(10), pp. 1-10.

Pacheco-Torgal, F., Ding, Y. and Jalali, S. (2012) 'Properties and durability of concrete containing polymeric wastes (tyre rubber and polyethylene terephthalate bottles): An overview', Construction and Building Materials, 30, pp. 714–724.

Pan, S., Chen, D., Chen, X., Ge, G., Su, D. and Liu, C. (2020) 'Experimental study on the workability and stability of steel slag self-compacting concrete', Applied Sciences, 10(4), pp. 1-15.

Panesar, D.K., Seto, K.E. and Churchill, C.J. (2017) 'Impact of the selection of functional unit on the life cycle assessment of green concrete', International Journal of Life Cycle Assessment, 22(12), pp. 1969–1986.

Parikh, R., Chouhan, D.S., Gupta, T. and Sharma, R.K. (2018) 'Utilization of Waste Plastic as Sustainable Material in Construction: A Review', International Journal of Management, Technology and Engineering, 8(X), pp. 2311-2327.

Park, J., Tae, S. and Kim, T. (2012) ‘Life cycle CO 2 assessment of concrete by compressive strength on construction site in Korea’, Renewable and Sustainable Energy Reviews, 16, pp. 2940–2946.

Park, J.K. and Kim, M.O. (2020) ‘Mechanical properties of cement-based materials with recycled plastic: A review’, Sustainability, 12, pp. 1–21.

Pavlík, Z., Pavlíková, M. and Záleská, M. (2018) ‘Properties of concrete with plastic polypropylene aggregates’, Use of Recycled Plastics in Eco-efficient Concrete, Elsevier Inc., pp. 189–213.

Pellegrino, C. and Gaddo, V. (2009) ‘Mechanical and durability characteristics of concrete containing EAF slag as aggregate’, Cement and Concrete Composites, 31(9), pp. 663–671.

Penpolcharoen, M. (2005) ‘Utilization of secondary lead slag as construction material’, Cement and Concrete Research, 35(6), pp. 1050–1055.

Pereira De Oliveira, L.A. and Castro-Gomes, J.P. (2011) ‘Physical and mechanical behaviour of recycled PET fibre reinforced mortar’, Construction and Building Materials, 25(4), pp. 1712–1717.

Petek Gursel, A., Masanet, E., Horvath, A. and Stadel, A. (2014) ‘Life-cycle inventory analysis of concrete production: A critical review’, Cement and Concrete Composites, 51, pp. 38–48.

Petrella, A., Di Mundo, R. and Notarnicola, M. (2020) ‘Recycled expanded polystyrene as lightweight aggregate for environmentally sustainable cement conglomerates’, Materials, 13(4), pp. 1-17.

Pillai, R.G., Gettu, R., Santhanam, M., Rengaraju, S., Dhandapani, Y., Rathnarajan, S. and Basavaraj, A.S. (2019) ‘Service life and life cycle assessment of reinforced concrete systems with limestone calcined clay cement (LC3)’, Cement and Concrete Research, 118, pp. 111–119.

Plastics Europe (2018) ‘Plastics-the Facts 2018, An Analysis of European Plastics Production, Demand and Waste Data’.

Plastics Europe (2019) ‘Plastics-the Facts 2019, An Analysis of European Plastics Production, Demand and Waste Data’.

Plastics Europe (2021) ‘Plastics-the Facts 2020, An Analysis of European Plastics Production, Demand and Waste Data’.

Prasanna, K. and Kiranmayi, V. (2014) ‘Steel Slag as a Substitute for Fine Aggregate in High Strength Concrete’, International Journal of Engineering Research and Technology, 3(10), pp. 810-814.

Prince and Tiwary, A.K., (2018) ‘Effect of Copper Slag and Fly Ash on Mechanical Properties of Concrete’, International Journal of Civil Engineering and Technology, 9(7), pp. 354–362.

Prithiviraj, C., Swaminathan, P., Kumar, D.R., Murali, G. and Vatin, N.I. (2022) ‘Fresh and Hardened Properties of Self-Compacting Concrete Comprising a Copper Slag’, Buildings, 12(7), pp. 1-21.

Proske, T., Hainer, S., Rezvani, M. and Graubner, C.A. (2013) ‘Eco-friendly concretes with reduced water and cement contents - Mix design principles and laboratory tests’, Cement and Concrete Research, 51, pp. 38–46.

Prusinski, J.R., Marceau, M.L., and VanGeem, M.G. (2004) ‘Life cycle inventory of slag cement concrete’, Proceedings of 8th CANMET/ACI International Conferences Fly Ash, Silica Fume, Slag Natural Pozzolans, Concrete American Concrete Institute, pp. 1-26.

Qasrawi, H. (2014) ‘The use of steel slag aggregate to enhance the mechanical properties of recycled aggregate concrete and retain the environment’, Construction and Building Materials, 54, pp. 298–304.

Qasrawi, H., Shalabi, F. and Asi, I. (2009) ‘Use of low CaO unprocessed steel slag in concrete as fine aggregate’, Construction and Building Materials, 23(2), pp. 1118–1125.

Rahman, M.M., Islam, A., Ahmed, M. and Salam, M.A. (2012) ‘Recycled Polymer Materials as Aggregates for Concrete and Blocks’, Journal of Chemical Engineering, 27(1), pp. 53-57.

Rahmani, E., Dehestani, M., Beygi, M.H.A., Allahyari, H. and Nikbin, I.M. (2013) 'On the mechanical properties of concrete containing waste PET particles', Construction and Building Materials, 47, pp. 1302–1308.

Rama, B. and Jagadeesh P. (2017) 'Influence of Admixtures On Plastic Wastes In An Eco-Friendly Concrete', International Journal of Civil Engineering and Technology, 8(6), pp. 388–397.

Ramesan, A., Babu, S.S. and Lal, A. (2015) 'Performance of Light-Weight Concrete with Plastic Aggregate', Journal of Engineering Research and Applications, 5(8), pp. 105-110.

Ranjbar, M.M. and Mousavi, S.Y. (2015) 'Strength and durability assessment of self-compacted lightweight concrete containing expanded polystyrene', Materials and Structures/Materiaux et Constructions, 48(4), pp. 1001–1011.

Reap, J., Roman, F., Duncan, S. and Bras, B. (2008) 'A survey of unresolved problems in life cycle assessment. Part 2: Impact assessment and interpretation', International Journal of Life Cycle Assessment, 13, pp. 374–388.

Rezaul, R.M., Atahar, R., Tasnim, T. Bin, Kurny, A., Momtaz, R. and Gulshan, F. (2017) 'Comparison of Mechanical Properties of Induction Furnace Steel Slag and Electric Arc Furnace Steel Slag as a Replacement of Coarse Aggregate in Construction Materials', Proceedings of International Conference on Mechanical, Industrial and Materials Engineering (ICMIME2017), RUET, Bangladesh, pp. 1-6.

Rooholamini, H., Sedghi, R., Ghobadipour, B. and Adresi, M. (2019) 'Effect of electric arc furnace steel slag on the mechanical and fracture properties of roller-compacted concrete', Construction and Building Materials, 211, pp. 88–98.

Rosado, L.P., Vitale, P., Penteado, C.S.G. and Arena, U. (2017) 'Life cycle assessment of natural and mixed recycled aggregate production in Brazil', Journal of Cleaner Production, 151, pp. 634–642.

Ruiz-Herrero, J.L., Velasco Nieto, D., López-Gil, A., Arranz, A., Fernández, A., Lorenzana, A., Merino, S., De Saja, J.A. and Rodríguez-Pérez, M.Á. (2016) 'Mechanical and thermal performance of concrete and mortar cellular materials containing plastic waste', Construction and Building Materials, 104, pp. 298–310.

Rybaczewska-Blażejowska, M. and Palekhov, D. (2018) ‘Life Cycle Assessment (LCA) in Environmental Impact Assessment (EIA): Principles and practical implications for industrial projects’, Management, 22(1), pp. 138–153.

Sabău, M. and Vargas, J.R. (2018) ‘Use of e-plastic waste in concrete as a partial replacement of coarse mineral aggregate’, Computers and Concrete, 21(4), pp. 377–384.

Sabir, B.B., Wild, S. and O’Farrell, M. A (1998) ‘Water sorptivity test for mortar and concrete’, Materials and Structures, 31, pp. 568–74.

Sadrmomtazi, A., Dolati-Milehsara, S., Lotfi-Omran, O. and Sadeghi-Nik, A. (2016) ‘The combined effects of waste Polyethylene Terephthalate (PET) particles and pozzolanic materials on the properties of self-compacting concrete’, Journal of Cleaner Production, 112, pp. 2363–2373.

Safi, B., Saidi, M., Aboutaleb, D. and Maallem, M. (2013) ‘The use of plastic waste as fine aggregate in the self-compacting mortars: Effect on physical and mechanical properties’, Construction and Building Materials, 43, pp. 436–442.

Saha, A.K. and Sarker, P.K. (2017) ‘Compressive Strength of Mortar Containing Ferronickel Slag as Replacement of Natural Sand’, Procedia Engineering, 171, pp. 689–694.

Saikia, N., Cornelis, G., Cizer, Ö., Vandecasteele, C., van Gemert, D., van Balen, K. and van Gerven, T. (2012) ‘Use of Pb blast furnace slag as a partial substitute for fine aggregate in cement mortar’, Journal of Material Cycles and Waste Management, 14(2), pp. 102–112.

Saikia, N. and De Brito, J. (2012) ‘Use of plastic waste as aggregate in cement mortar and concrete preparation: A review’, Construction and Building Materials, pp. 385–401.

Saikia, N. and De Brito, J. (2013) ‘Waste polyethylene terephthalate as an aggregate in concrete’, Materials Research, 16(2), pp. 341–350.

Saikia, N. and De Brito, J. (2014) ‘Mechanical properties and abrasion behaviour of concrete containing shredded PET bottle waste as a partial substitution of natural aggregate’, Construction and Building Materials, 52, pp. 236–244.

Salas, D.A., Ramirez, A.D., Rodríguez, C.R., Petroche, D.M., Boero, A.J. and Duque-Rivera, J. (2016) 'Environmental impacts, life cycle assessment and potential improvement measures for cement production: A literature review', Journal of Cleaner Production, 46, pp. 114–122.

Sambhaji, Z.K. and Autade, P.B. (2016) 'Effect of Copper Slag as a Fine Aggregate on Properties of Concrete', International Research Journal of Engineering and Technology, 3(6), pp. 410-414.

Saxena, R., Gupta, T., Sharma, R.K., Chaudhary, S. and Jain, A. (2020) 'Assessment of mechanical and durability properties of concrete containing PET waste', Scientia Iranica, 27(1), pp. 1–9.

Saxena, R., Siddique, S., Gupta, T., Sharma, R.K. and Chaudhary, S. (2018) 'Impact resistance and energy absorption capacity of concrete containing plastic waste', Construction and Building Materials, 176, pp. 415–421.

Saxena, S. and Tembhurkar, A.R. (2018) 'Impact of use of steel slag as coarse aggregate and wastewater on fresh and hardened properties of concrete', Construction and Building Materials, 165, pp. 126–137.

Sekaran, A., Palaniswamy, M. and Balaraju, S. (2015) 'A Study on Suitability of EAF Oxidizing Slag in Concrete: An Eco-Friendly and Sustainable Replacement for Natural Coarse Aggregate', Scientific World Journal, 2015, pp. 1-8.

Senhadji, Y., Escadeillas, G., Benosman, A.S., Mouli, M., Khelafi, H. and Kaci, S.O. (2015) 'Effect of incorporating PVC waste as aggregate on the physical, mechanical, and chloride ion penetration behavior of concrete', Journal of Adhesion Science and Technology, 29(7), pp. 625–640.

Senthil Kumar, K. and Baskar, K. (2015) 'Development of Ecofriendly Concrete Incorporating Recycled High-Impact Polystyrene from Hazardous Electronic Waste', Journal of Hazardous, Toxic, and Radioactive Waste, 19(3), pp. 1-11.

Serres, N., Braymand, S. and Feugeas, F. (2016) 'Environmental evaluation of concrete made from recycled concrete aggregate implementing life cycle assessment', Journal of Building Engineering, 5, pp. 24–33.

SETAC (1993) ‘Guidelines for Life-Cycle Assessment: A Code of Practice’, Society of Environmental Toxicology and Chemistry, Pensacola, Florida, USA.

Seto, K.E., Churchill, C.J. and Panesar, D.K. (2017) ‘Influence of fly ash allocation approaches on the life cycle assessment of cement-based materials’, Journal of Cleaner Production, 157, pp. 65–75.

Sezer, G.I. and Gulderen, M. (2015) ‘Usage of steel slag in concrete as fine and/or coarse aggregate’, Indian Journal of Engineering and Material Sciences, 22, pp. 339-344.

Shalaby, A., Ward, A., Refaee, A., Abd-El-Messieh, S., Abd-El-Nour, K., El-Nashar, D. and Zayed, H.A. (2013) ‘Compressive Strength and Electrical Properties of Cement Paste Utilizing Waste Polyethylene Terephthalate Bottles’, Journal of Applied Sciences Research, 9(7), pp. 4160-4173.

Shanmugapriya, M. and Santhi, H.M. (2017) ‘Strength and Chloride Permeable Properties of Concrete with High Density Polyethylene Waste’, International Journal of Chemical Sciences, 15(1), pp. 1-8.

Sharifi, Y., Afshoon, I., Asad-Abadi, S. and Aslani, F. (2020) ‘Environmental protection by using waste copper slag as a coarse aggregate in self-compacting concrete’, Journal of Environmental Management, 271, pp. 1-17.

Sharma, R. and Bansal, P.P. (2016) ‘Use of different forms of waste plastic in concrete - A review’, Journal of Cleaner Production, 112, pp. 473–482.

Sharma, R. and Khan, Rizwan A. (2017b) ‘Durability assessment of self-compacting concrete incorporating copper slag as fine aggregates’, Construction and Building Materials, 155, pp. 617–629.

Sharma, R. and Khan, Rizwan A. (2017a) ‘Fresh and mechanical properties of self-compacting concrete containing copper slag as fine aggregates’, Journal of Materials and Engineering Structures, 4 (2017), pp. 25-36.

Sheen, Y.N., Wang, H.Y. and Sun, T.H. (2014) ‘Properties of green concrete containing stainless steel oxidizing slag resource materials’, Construction and Building Materials, 50, pp. 22–27.

Siddique, R., Khatib, J. and Kaur, I. (2008) ‘Use of recycled plastic in concrete: A review’, Waste Management, 28(10), pp. 1835–1852.

Silva, D.A., Betioli, A.M., Gleize, P.J.P., Roman, H.R., Gómez, L.A. and Ribeiro, J.L.D. (2005) ‘Degradation of recycled PET fibers in Portland cement-based materials’, Cement and Concrete Research, 35(9), pp. 1741–1746.

Silva, R. V., De Brito, J. and Saikia, N. (2013) ‘Influence of curing conditions on the durability-related performance of concrete made with selected plastic waste aggregates’, Cement and Concrete Composites, 35(1), pp. 23–31.

Silvestre, J.D., De Brito, J. and Pinheiro, M.D. (2014) ‘Environmental impacts and benefits of the end-of-life of building materials - Calculation rules, results and contribution to a “cradle to cradle” life cycle’, Journal of Cleaner Production, 66, pp. 37–45.

Singh, G. and Siddique, R. (2016a) ‘Effect of iron slag as partial replacement of fine aggregates on the durability characteristics of self-compacting concrete’, Construction and Building Materials, 128, pp. 88–95.

Singh, G. and Siddique, R. (2016b) ‘Strength properties and micro-structural analysis of self-compacting concrete made with iron slag as partial replacement of fine aggregates’, Construction and Building Materials, 127, pp. 144–152.

Singh, Khushhalpreet, Singh, G. and Singh, Khushpreet (2019) ‘Utilization of iron slag as partially replacement with fine aggrgate in high strength self-compacting concrete (HSSCC)’, International Journal of Innovative Technology and Exploring Engineering, 8(11), pp. 1177–1183.

Singh, P. and Pandey, M. (2017) ‘E Waste Management by Utilization of E-Plastic as Coarse Aggregate in Concrete’, International Research Journal of Engineering and Technology, 4(6), pp. 2916-2919.

Singh, R.K. and Ruj, B. (2015) ‘Plastic waste management and disposal techniques - Indian scenario’, International Journal of Plastics Technology, Springer India, pp. 211–226.

Sivamani, J. (2022) ‘Influence of Copper Slag on the Mechanical and Durability Properties of High Strength Concrete’, Research Square, Kalasalingam Academy of Research and Education, pp. 1-20.

Skominas, R., Zvinakevičius, L., Gurskis, V. and Šadzevičius, R. (2018) ‘Evaluation of Suitability to Use Plastic Waste In Concrete Production’, Proceedings of the 8th International Scientific Conference Rural Development 2017. Aleksandras Stulginskis University, pp. 1-5.

Sojobi, A.O. and Owamah, H.I. (2014) ‘Evaluation of the suitability of low-density polyethylene (LDPE) waste as fine aggregate in concrete’, Nigerian Journal of Technology, 33(4), pp. 409–425.

Song, D., Yang, J., Chen, B., Hayat, T. and Alsaedi, A. (2016) ‘Life-cycle environmental impact analysis of a typical cement production chain’, Applied Energy, 164, pp. 916–923.

Sri Ravindrarajah, R. and Tuck, A.J. (1994) ‘Properties of Hardened Concrete Containing Treated Expanded Polystyrene Beads’, Cement and Concrete Composites, 16, pp. 273-277.

Stafford, F.N., Dias, A.C., Arroja, L., Labrincha, J.A. and Hotza, D. (2016) ‘Life cycle assessment of the production of Portland cement: A Southern Europe case study’, Journal of Cleaner Production, 126, pp. 159–165.

Subathra Devi, V. and Gnanavel, B.K. (2014) ‘Properties of concrete manufactured using steel slag’, Procedia Engineering, 97, pp. 95–104.

Suganthy, P., Chandrasekar, D. and Sathish Kumar, P.K. (2013) ‘Utilization of Pulverized Plastic in Cement Concrete as Fine Aggregate’, International Journal of Research in Engineering and Technology, 2(6), pp. 1015-1019.

Susheel, S.M., Sathwik, S. R., Vinayak, T., Darshan, S., Sanjith, J. and Ranjith, A. (2016) ‘Development of Normal Strength Concrete using Ferrochrome Slag Aggregate as Replacement to Coarse Aggregate’, International Journal of Innovative Science, Engineering and Technology, 3(6), pp. 250-253.

Tait, M.W. and Cheung, W.M. (2016) ‘A comparative cradle-to-gate life cycle assessment of three concrete mix designs’, International Journal of Life Cycle Assessment, 21(6), pp. 847–860.

Tang, W.C., Lo, Y. and Nadeem, A. (2008) ‘Mechanical and drying shrinkage properties of structural-graded polystyrene aggregate concrete’, Cement and Concrete Composites, 30(5), pp. 403–409.

Tangadagi, R., Maddikeari, M., Ashwath, B., Shailaja, P., Tangadagi, R.B., Manjunatha, M., Bharath, A. and Preethi, S. (2020) ‘Utilization of Steel Slag as an Eco-Friendly Material in Concrete for Construction’, Journal of Green Engineering, 10(5), pp. 2408-2419.

Teixeira, E.R., Mateus, R., Camões, A.F., Bragança, L. and Branco, F.G. (2016) ‘Comparative environmental life-cycle analysis of concretes using biomass and coal fly ashes as partial cement replacement material’, Journal of Cleaner Production, 112, pp. 2221–2230.

Thorneycroft, J., Orr, J., Savoikar, P. and Ball, R.J. (2018) ‘Performance of structural concrete with recycled plastic waste as a partial replacement for sand’, Construction and Building Materials, 161, pp. 63–69.

Tošić, N., Marinković, S., Dašić, T. and Stanić, M. (2015) ‘Multicriteria optimization of natural and recycled aggregate concrete for structural use’, Journal of Cleaner Production, 87(1), pp. 766–776.

Tripathi, B. and Chaudhary, S. (2016) ‘Performance based evaluation of ISF slag as a substitute of natural sand in concrete’, Journal of Cleaner Production, 112, pp. 672–683.

Tripathi, B., Misra, A. and Chaudhary, S. (2013) ‘Strength and Abrasion Characteristics of ISF Slag Concrete’, Journal of Materials in Civil Engineering, 25(11), pp. 1611-1618.

Turk, J., Cotič, Z., Mladenovič, A. and Šajna, A. (2015) ‘Environmental evaluation of green concretes versus conventional concrete by means of LCA’, Waste Management, 45, pp. 194–205.

Uddin Mohammed, T., Ahmed Noor, M., Mostafiz Apurbo, S., Ahmed, M., Mohammed, T.U., Noor, M.A., Apurbo, S.M., Elahi, A. and Mazumder, M.H. (2017) ‘Utilization of

Induction Furnace Slag in Concrete as Coarse Aggregate' 1st International Conference on Engineering Research and Practice, Dhaka, Bangladesh, pp. 1-6.

Ultratech EPD (2020), 'Environmental Product Declaration, 2020', Ultratech Cements, India.

Umasabor, R.I. and Daniel, S.C. (2020) 'The effect of using polyethylene terephthalate as an additive on the flexural and compressive strength of concrete', Heliyon, 6, pp. 1-6.

United Nations Environment Programme (2018) 'Single-use plastics, a roadmap for sustainability', UN Environment, p.6.

U. S. Environmental Protection Agency (USEPA), (2020) 'Advancing Sustainable Materials Management: 2018 Fact Sheet Assessing Trends in Materials Generation and Management in the United States.

Valipour, M., Yekkalar, M., Shekarchi, M. and Panahi, S. (2014) 'Environmental assessment of green concrete containing natural zeolite on the global warming index in marine environments', Journal of Cleaner Production, 65, pp. 418–423.

Van den Heede, P. and De Belie, N. (2017) 'Sustainability assessment of potentially "green" concrete types using life cycle assessment', Sustainable and Nonconventional Construction Materials using Inorganic Bonded Fiber Composites. Elsevier Inc., pp. 236–263.

Van Den Heede, P. and De Belie, N. (2014) 'A service life based global warming potential for high-volume fly ash concrete exposed to carbonation', Construction and Building Materials, 55, pp. 183–193.

Van Den Heede, P. and De Belie, N. (2012) 'Environmental impact and life cycle assessment (LCA) of traditional and "green" concretes: Literature review and theoretical calculations', Cement and Concrete Composites, 34(4), pp. 431–442.

Van Den Heede, P. and De Belie, N. (2010) 'Durability Related Functional Units for Life Cycle Assessment (LCA) of High-Volume Fly Ash Concrete (HVFA concrete)', Proceedings of Second International Conference on Sustainable Construction Materials and Technologies, Ancona, Italy, pp. 1-12.

Van Den Heede, P., Maes, M., Gruyaert, E. and De Belie, N. (2012) ‘Full probabilistic service life prediction and life cycle assessment of concrete with fly ash and blast-furnace slag in a submerged marine environment: a parameter study’, International Journal of Environment and Sustainable Development, 11(1), pp. 32-49.

Van Deventer, J.S.J., Provis, J.L. and Duxson, P. (2012) ‘Technical and commercial progress in the adoption of geopolymer cement’, Minerals Engineering, 29, pp. 89–104.

Velumani, M. and Nirmalkumar, K. (2014) ‘Durability and Characteristics of Copper Slag as Fine Aggregate and Fly Ash as Cement in Concrete’, Proceedings of 2nd International Conference on Current Trends in Engineering and Technology, (ICCTET’14), Coimbatore, India, pp. 222-227.

Verdolotti, L., Iucolano, F., Capasso, I., Lavorgna, M., Lannace, S. and Ligouri, B. (2014) ‘Recycling and Recovery of PE-PP-PET-based Fiber Polymeric Wastes as Aggregate Replacement in Lightweight Mortar: Evaluation of Environmental Friendly Application’, Environmental Progress and Sustainable Energy, 33(4), pp. 1445-1451.

Vieira, D.R., Calmon, J.L. and Coelho, F.Z. (2016) ‘Life cycle assessment (LCA) applied to the manufacturing of common and ecological concrete: A review’, Construction and Building Materials, 124, pp. 656–666.

Wang, B., Yan, L., Fu, Q. and Kasal, B. (2021a) ‘A Comprehensive Review on Recycled Aggregate and Recycled Aggregate Concrete’, Resources, Conservation and Recycling, 292, pp. 1-21.

Wang, R. and Meyer, C. (2012) ‘Performance of cement mortar made with recycled high impact polystyrene’, Cement and Concrete Composites, 34(9), pp. 975–981.

Wang, R., Shi, Q., Li, Y., Cao, Z. and Si, Z. (2021b) ‘A critical review on the use of copper slag (CS) as a substitute constituent in concrete’, Construction and Building Materials, 292, pp. 1-21.

Wang, W., Lu, C., Li, Y. and Li, Q. (2017) ‘An investigation on thermal conductivity of fly ash concrete after elevated temperature exposure’, Construction and Building Materials, 148, pp. 148–154.

Wicaksono, S.T., Ardhyananta, H. and Rasyida, A. (2018) 'Study on mechanical and physical properties of composite materials with recycled PET as fillers for paving block application', Proceedings of the 3rd International Conference on Materials and Metallurgical Engineering and Technology (ICOMMET 2017), American Institute of Physics Inc., pp. 1-6.

Wimpenny, D. (2009) 'Low Carbon Concrete-Options for the Next Generation of Infrastructure', Concrete Solutions, 09, pp. 1-6.

Wu, W., Zhang, W. and Ma, G. (2010) 'Optimum content of copper slag as a fine aggregate in high strength concrete', Materials and Design, 31(6), pp. 2878–2883.

Yang, S., Yue, X., Liu, X. and Tong, Y. (2015) 'Properties of self-compacting lightweight concrete containing recycled plastic particles', Construction and Building Materials, 84, pp. 444–453.

Yazdanbakhsh, A., Bank, L.C., Baez, T. and Wernick, I. (2018) 'Comparative LCA of concrete with natural and recycled coarse aggregate in the New York City area', International Journal of Life Cycle Assessment, 23(6), pp. 1163–1173.

Zabalza Bribián, I., Valero Capilla, A. and Aranda Usón, A. (2011) 'Life cycle assessment of building materials: Comparative analysis of energy and environmental impacts and evaluation of the eco-efficiency improvement potential', Building and Environment, 46(5), pp. 1133–1140.

Záleská, M., Pavlíková, M., Pokorný, J., Jankovský, O., Pavlík, Z. and Černý, R. (2018) 'Structural, mechanical and hygrothermal properties of lightweight concrete based on the application of waste plastics', Construction and Building Materials, 180, pp. 1–11.

Zulcão, R., Luiz Calmon, J., Zulcão Mello, R. and Zanellato Coelho, F. (2016) 'LCA of waste PET particles as a partial replacement for sand in self-compacting concrete', Sustainable Urban Communities toward a Zero Impact Built Environment, SBE Series, pp. 139-148.

Bibliography

Mehta, P.K. and Monteiro, P.J.M. (2017) ‘Concrete- Microstructure, Properties and Materials’, McGraw Hill Education (India) Private Limited, New Delhi, p. 675.

Nayak, N.V., Guptha, K.G. and Savoikar, P.P. (2021) ‘Text Book of Concrete Technology’, Creative Books, New Delhi, p. 677.

Seto, K.E. (2015) ‘Life Cycle Assessment and Environmental Efficiency of Concrete Materials’, Thesis of Master of Science, University of Torento.

Shetty, M.S. (2008) ‘Concrete Technology Theory and Practice’ S.Chand and Company Limited, New Delhi, p. 623.

Neville, A.M. and Brooks, J.J. (1995) ‘Concrete Technology’ Pearson Education Limited, Harlow, England. p. 460.

Javadabadi, M.T. (2019) ‘Comparative Life Cycle Assessment of Incorporating Recycled PET Aggregates into Concrete’ Master Thesis in Sustainable Manufacturing, Norwegian University of Science and Technology. p. 75.

Sjunnesson, J. (2005) ‘Life Cycle Assessment of Concrete’ Master Thesis, Lund University, p. 61.

Yadav, I. S. (2008) ‘Laboratory investigation of concrete containing recycled plastic aggregates’, Master of Engineering thesis, Thapar University, Patiala, India.

Appendix A

A.1 Laboratory investigation to determine the optimum content of SFS-Sand in mortar mix of the current study

To determine the optimum content of SFS-Sand in the mortar mix, the compressive strength test of the mortar cubes was performed for cement: sand mix proportion of 1:3 and 1:5. SFS-Sand was substituted for N-Sand in the ratio of 10% to 70% with an incremental ratio of 10% and mortar cubes of 70.7x70.7x70.7 mm size were cast. The cubes were cured by immersion curing and tested for compressive strength at 3, 7, and 28 days of age.

The results of the compressive strength test are summarized in Table A.1 and illustrated graphically in Fig. A.1.

Table A.1 Compressive strength of mortar with SFS-Sand

Identification	Compressive Strength, N/mm^2					
	1:3 mix			1:5 mix		
	3 days	7 days	28 days	3 days	7 days	28 days
M_x-C-S0	31.87	36.70	44.79	26.80	33.84	40.93
M_x-C-S10	31.60	36.80	45.35	25.75	33.17	40.06
M_x-C-S20	32.74	38.30	47.55	25.47	36.17	41.46
M_x-C-S30	32.65	41.70	49.84	26.27	37.32	42.47
M_x-C-S40	32.50	41.75	50.20	26.94	37.45	43.68
M_x-C-S50	32.80	41.80	51.06	28.64	37.84	45.92
M_x-C-S60	32.20	40.52	48.63	24.53	35.62	42.56
M_x-C-S70	30.24	38.60	46.52	23.84	34.62	40.58

(x=3 for 1:3 mix and x=5 for 1:5 mix)

From the results of the compressive strength at 28 days age it can be seen that the compressive strength values go on increasing with the increase in replacement of N-Sand by SFS-Sand up to 50% replacement ratio and the value decreases beyond 50%. The results are consistent for both the mix proportions of i.e., 1:3 and 1:5 mix. It can be

concluded that a replacement of N-Sand for optimum value of 50% by volume gives optimum compressive strength value to the mortar.

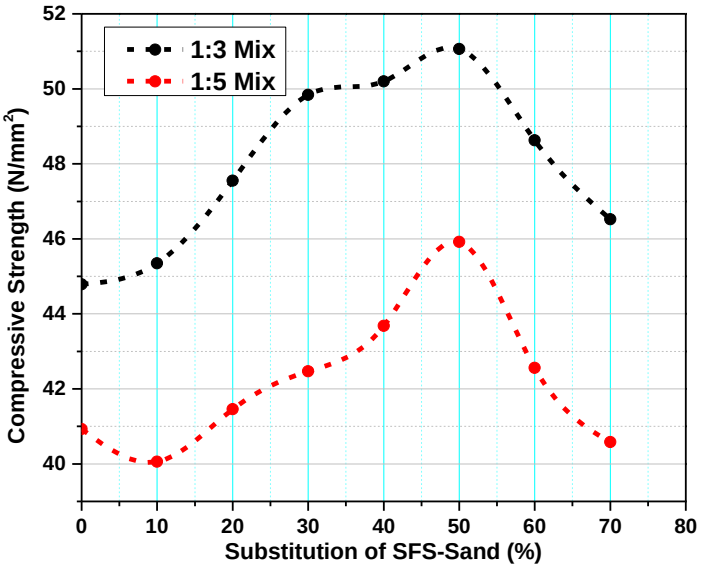

Fig. A.1 Compressive strength of mortar mixes with varying proportion of SFS-Sand

Appendix B

B.1 Laboratory investigation to determine the optimum content of SFS-Sand in concrete mix of the current study

To determine the optimum content of SFS-Sand in the concrete mix, the compressive strength test of the concrete cubes was performed for M30 and M50 mix of concrete. SFS-Sand was substituted for N-Sand in the ratio of 10% to 70% with an incremental ratio of 10% and mortar cubes of 150x150x150 mm size were cast. The cubes were cured by immersion curing and tested for compressive strength at 3, 7, and 28 days of age.

The results of the compressive strength test are summarized in Table B.1 and illustrated graphically in Fig. B.1.

Table B.1 Compressive strength of concrete with SFS-Sand

Identification	Compressive Strength, N/mm^2					
	M30 mix			M50 mix		
	3 days	7 days	28 days	3 days	7 days	28 days
C_Y-C-S0	25.30	31.40	40.22	39.28	48.31	62.60
C_Y-C-S10	24.90	31.10	40.62	40.25	50.20	62.90
C_Y-C-S20	25.62	30.80	41.50	42.60	51.26	64.20
C_Y-C-S30	26.50	31.56	42.60	43.20	52.72	66.30
C_Y-C-S40	26.80	32.82	44.82	44.10	54.62	69.68
C_Y-C-S50	26.94	30.20	42.56	42.64	53.12	66.20
C_Y-C-S60	22.10	26.20	37.50	41.30	50.10	64.10
C_Y-C-S70	20.80	25.14	34.40	39.92	48.30	60.30

($_Y$=30 for M30 mix and $_Y$=50 for M50 mix)

From the results of the compressive strength at 28 days age it can be seen that the compressive strength values go on increasing with the increase in replacement of N-Sand by SFS-Sand up to 40% replacement ratio and the value decreases beyond 40%. The results are consistent for both the mix proportions of i.e., M30 and M50 mix. It can be concluded that a replacement of N-Sand for optimum value of 40% by volume gives optimum compressive strength value to the concrete.

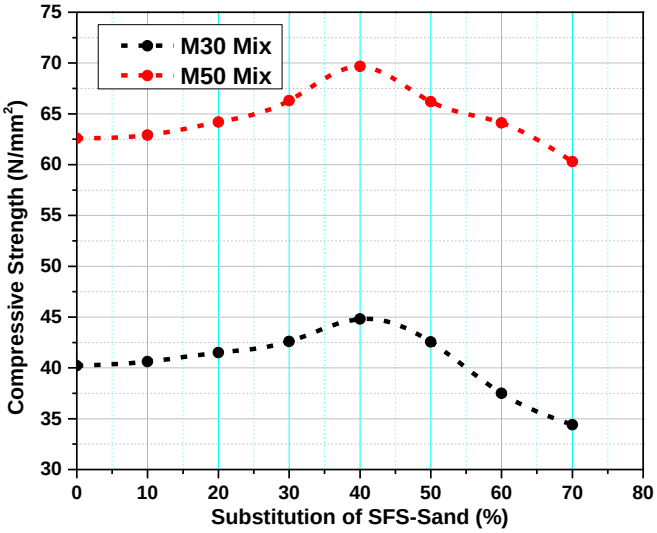

Fig. B.1 Compressive strength of concrete mixes with varying proportion of SFS-Sand

Appendix C

C.1 Actual quantities of materials for mortar mixes in the current study

The actual quantities of materials for each batch of mortar mixes proposed for the current research are presented in Table C.1, C.2, C.3 and C.4 for control mix, Tier I, Tier II and Tier III mixes respectively for 1:3 mix.

Table C.1 Material quantities for control mortar (1:3 mix)

Mix Identity	Binder (g)		Fine aggregate (g)			Water (g)	Admixture (g)
	OPC	FLA	PET-Sand	N-Sand	SFS-Sand		
M_3-C-P0	2500	0	0	7500	0	1125	15

Table C.2 Material quantities for Tier I mortar (1:3 mix)

Mix Identity	Binder (g)		Fine aggregate (g)			Water (g)	Admixture (g)
	OPC	FLA	PET-Sand	N-Sand	SFS-Sand		
M_3-C-P10	2500	0	351	6750	0	1125	15
M_3-C-P15	2500	0	527	6375	0	1125	15
M_3-C-P20	2500	0	702	6000	0	1125	15
M_3-C-P25	2500	0	878	5625	0	1125	15

Table C.3 Material quantities for Tier II mortar (1:3 mix)

Mix Identity	Binder (g)		Fine aggregate (g)			Water (g)	Admixture (g)
	OPC	FLA	PET-Sand	N-Sand	SFS-Sand		
M_3-C-SP0	2500	0	0	3750	4362	1125	15
M_3-C-SP10	2500	0	351	3375	3926	1125	15
M_3-C-SP15	2500	0	527	3188	3707	1125	15
M_3-C-SP20	2500	0	702	3000	3489	1125	15
M_3-C-SP25	2500	0	878	2813	3271	1125	15

Table C.4 Material quantities for Tier III mortar (1:3 mix)

Mix Identity	Binder (g)		Fine aggregate (g)			Water (g)	Admixture (g)
	OPC	FLA	PET-Sand	N-Sand	SFS-Sand		
M_3-CF-SP0	1750	750	0	3750	4362	1125	15
M_3-CF-SP10	1750	750	351	3375	3926	1125	15
M_3-CF-SP15	1750	750	527	3188	3707	1125	15
M_3-CF-SP20	1750	750	702	3000	3489	1125	15
M_3-CF-SP25	1750	750	878	2813	3271	1125	15

Similarly, the actual quantities of materials for each batch of mortar mixes proposed for the current research are presented in Table C.5, C.6, C.7 and C.8 for control mix, Tier I, Tier II and Tier III mixes respectively for 1:5 mix.

Table C.5 Material quantities for control mortar (1:5 mix)

Mix Identity	Binder (g)		Fine aggregate (g)			Water (g)	Admixture (g)
	OPC	FLA	PET-Sand	N-Sand	SFS-Sand		
M_5-C-P0	2000	0	0	10000	0	900	12

Table C.6 Material quantities for Tier I mortar (1:5 mix)

Mix Identity	Binder (g)		Fine aggregate (g)			Water (g)	Admixture (g)
	OPC	FLA	PET-Sand	N-Sand	SFS-Sand		
M_5-C-P10	2000	0	468	9000	0	900	12
M_5-C-P15	2000	0	702	8500	0	900	12
M_5-C-P20	2000	0	936	8000	0	900	12
M_5-C-P25	2000	0	1170	7500	0	900	12

Table C.7 Material quantities for Tier II mortar (1:5 mix)

Mix Identity	Binder (g)		Fine aggregate (g)			Water (g)	Admixture (g)
	OPC	FLA	PET-Sand	N-Sand	SFS-Sand		
M_5-C-SP0	2000	0	0	5000	5816	900	12
M_5-C-SP10	2000	0	468	4500	5234	900	12
M_5-C-SP15	2000	0	702	4250	4943	900	12
M_5-C-SP20	2000	0	936	4000	4652	900	12
M_5-C-SP25	2000	0	1170	3750	4362	900	12

Table C.8 Material quantities for Tier III mortar (1:5 mix)

Mix Identity	Binder (g)		Fine aggregate (g)			Water (g)	Admixture (g)
	OPC	FLA	PET-Sand	N-Sand	SFS-Sand		
M_5-CF-SP0	1400	600	0	5000	5816	900	12
M_5-CF-SP10	1400	600	468	4500	5234	900	12
M_5-CF-SP15	1400	600	702	4250	4943	900	12
M_5-CF-SP20	1400	600	936	4000	4652	900	12
M_5-CF-SP25	1400	600	1170	3750	4362	900	12

Appendix D

D.1 Actual quantities of materials for concrete mixes in the current study

The actual quantities of materials for each batch of mortar mixes proposed for the current research are presented in Table D.1, D.2, D.3 and D.4 for control mix, Tier I, Tier II and Tier III mixes respectively for M30 mix.

Table D.1 Material quantities for control concrete (M30 mix)

Mix Identity	Binder (kg)		Fine aggregate (kg)			Coarse aggregate (kg)	Water (kg)	Admixture (kg)
	OPC	FLA	PET-Sand	N-Sand	SFS-Sand	NCA		
C_{30}-C-P0	380	0	0	741	0	1270	167.2	2.66

Table D.2 Material quantities for Tier I concrete (M30 mix)

Mix Identity	Binder (kg)		Fine aggregate (kg)			Coarse aggregate (kg)	Water (kg)	Admixture (kg)
	OPC	FLA	PET-Sand	N-Sand	SFS-Sand	NCA		
C_{30}-C-P10	380	0	34.68	667	0	1270	167.2	2.66
C_{30}-C-P15	380	0	52.02	630	0	1270	167.2	2.66
C_{30}-C-P20	380	0	69.37	593	0	1270	167.2	2.66
C_{30}-C-P25	380	0	86.71	556	0	1270	167.2	2.66

Table D.3 Material quantities for Tier II concrete (M30 mix)

Mix Identity	Binder (kg)		Fine aggregate (kg)			Coarse aggregate (kg)	Water (kg)	Admixture (kg)
	OPC	FLA	PET-Sand	N-Sand	SFS-Sand	NCA		
C_{30}-C-SP0	380	0	0	445	345	1270	167.2	2.66
C_{30}-C-SP10	380	0	34.68	400	310	1270	167.2	2.66
C_{30}-C-SP15	380	0	52.02	378	293	1270	167.2	2.66
C_{30}-C-SP20	380	0	69.37	356	276	1270	167.2	2.66
C_{30}-C-SP25	380	0	86.71	333	259	1270	167.2	2.66

Table D.4 Material quantities for Tier III concrete (M30 mix)

Mix Identity	Binder (kg)		Fine aggregate (kg)			Coarse aggregate (kg)	Water (kg)	Admixture (kg)
	OPC	FLA	PET-Sand	N-Sand	SFS-Sand	NCA		
C_{30}-CF-SP0	266	114	0	436	338	1208	167.2	2.66
C_{30}-CF-SP10	266	114	33.98	392	304	1208	167.2	2.66
C_{30}-CF-SP15	266	114	50.97	370	287	1208	167.2	2.66
C_{30}-CF-SP20	266	114	67.96	348	270	1208	167.2	2.66
C_{30}-CF-SP25	266	114	84.95	327	253	1208	167.2	2.66

Similarly, the actual quantities of materials for each batch of concrete mixes proposed for the current research are presented in Table D.5, D.6, D.7 and D.8 for control mix, Tier I, Tier II and Tier III mixes respectively for M50 mix.

Table D.5 Material quantities for control concrete (M50 mix)

Mix Identity	Binder (kg)		Fine aggregate (kg)			Coarse aggregate (kg)	Water (kg)	Admixture (kg)
	OPC	FLA	PET-Sand	N-Sand	SFS-Sand	NCA		
C_{50}-C-P0	430	0	0	728	0	1248	163.4	2.58

Table D.6 Material quantities for Tier I concrete (M50 mix)

Mix Identity	Binder (kg)		Fine aggregate (kg)			Coarse aggregate (kg)	Water (kg)	Admixture (kg)
	OPC	FLA	PET-Sand	N-Sand	SFS-Sand	NCA		
C_{50}-C-P10	430	0	34.08	655	0	1248	163.4	2.58
C_{50}-C-P15	430	0	51.11	619	0	1248	163.4	2.58
C_{50}-C-P20	430	0	68.15	582	0	1248	163.4	2.58
C_{50}-C-P25	430	0	85.19	546	0	1248	163.4	2.58

Table D.7 Material quantities for Tier II concrete (M50 mix)

Mix Identity	Binder (kg)		Fine aggregate (kg)			Coarse aggregate (kg)	Water (kg)	Admixture (kg)
	OPC	FLA	PET-Sand	N-Sand	SFS-Sand	NCA		
C_{50}-C-SP0	430	0	0	437	339	1248	163.4	2.58
C_{50}-C-SP10	430	0	34.08	393	305	1248	163.4	2.58
C_{50}-C-SP15	430	0	51.11	371	288	1248	163.4	2.58
C_{50}-C-SP20	430	0	68.15	349	271	1248	163.4	2.58
C_{50}-C-SP25	430	0	85.19	328	254	1248	163.4	2.58

Table D.8 Material quantities for Tier III concrete (M50 mix)

Mix Identity	Binder (kg)		Fine aggregate (kg)			Coarse aggregate (kg)	Water (kg)	Admixture (kg)
	OPC	FLA	PET-Sand	N-Sand	SFS-Sand	NCA		
C_{50}-CF-SP0	301	129	0	427	331	1220	163.4	2.58
C_{50}-CF-SP10	301	129	33.29	384	298	1220	163.4	2.58
C_{50}-CF-SP15	301	129	49.92	363	281	1220	163.4	2.58
C_{50}-CF-SP20	301	129	66.56	341	265	1220	163.4	2.58
C_{50}-CF-SP25	301	129	83.20	320	248	1220	163.4	2.58

Appendix E

E.1 Sample calculation for determination of mix proportion for FU40 mix of Tier II composition using particle matrix model

Step 1: From Table 7.16, for Tier II mix with cement content of 380 kg/m^3, the amount of PET that can be substitute N-Sand to deliver 40 N/mm^2 compressive strength at 90 days = 18.71%

Step 2: With 18.71% volume of PET substituting N-Sand, it is required to determine the quantity of N-Sand and SFS-Sand in the mix.

Step 3: To determine these quantities, the calculations are as follows:

The total volume of fine and coarse aggregate in the mix can be calculated by

$$Total\ Volume\ of\ fine\ and\ coarse\ aggregate = \frac{Mass\ of\ N-Sand}{Absolute\ density\ of\ N-Sand} + \frac{Mass\ of\ PET-Sand}{Absolute\ density\ of\ PET} + \frac{Mass\ of\ SFS-Sand}{Absolute\ density\ of\ SFS-Sand} + \frac{Mass\ of\ NCA}{Absolute\ density\ of\ NCA}$$

For any mix amongst Tier II composition, e.g., C_{30}-C-SP15

$$Total\ Volume\ of\ fine\ and\ coarse\ aggregate = \frac{378}{2840} + \frac{52.02}{1280} + \frac{293}{3280} + \frac{1270}{2820}$$

$$=0.713$$

The quantity of NCA in the mix = 1270 kg/m^3

The corresponding volume of the NCA in the mix= 1270/2820= 0.450 m^3

The volume of total fine aggregates in the mix = 0.713-0.450= 0.263

The volume of PET is found to be 18.71% of volume of fine aggregates i.e., 0.04916 m^3

The mass of PET-Sand= 0.04916 x 1320 = 64.89 kg

Now, the volume of N-Sand+SFS-Sand= 0.263-0.04916= 0.2138 m^3

The Volume of SFS-Sand is 40% of the volume of N-Sand+ SFS-Sand i.e., 0.08552 m^3

Therefore, mass of SFS-Sand = 0.08552 x 3280 = 280 kg

Therefore, the volume of N-Sand in the mix= 0.2138-0.08552= 0.128 m^3

Thus, mass of N-Sand in the mix = 0.128x 2840= 361 kg

Therefore, the mix proportion for Tier II composition that can deliver 40 MPa strength with PET content of 18.71% is as given below in Table E.1

Table E.1 Mix proportion for Tier II composition for FU40 mix

Tier	PET%	OPC	FLA	N-Sand	SFS-Sand	PET-Sand	NCA	Water	Admixture
II	18.71%	380	0	361	280	64.89	1270	167.2	2.66

PUBLICATIONS

Title of paper	Authors	Publisher details	Remarks
Durability related properties of cement composites containing thermoplastic aggregates	Bhagat G. V. and Savoikar P. P.	Journal of Building Engineering, Elsevier Publication SCIE Indexed Scopus Indexed (Impact factor: 7.144)	Accepted and published
Enhancement of properties of Recycled Aggregate Concrete with Nano Materials - A Review	Bhagat G. V. and Savoikar P. P.	International Conference on Sustainable Construction and Building Materials, National Institute of Technology Karnataka, Surathkal, Mangalore, India, June 18 – 22, 2018	Published
An overview of effect of nano-material modifications in non-conventional concretes and mortars	Bhagat G. V. and Savoikar P. P.	UKIERI Concrete Congress Concrete: The Global Builder Working together for durable and sustainable infrastructure, 5 - 8 March 2019 Jalandhar, Punjab, India	Published
Auditing carbon reduction potential of green concrete using life cycle assessment methodology	Bhagat G. V. and Savoikar P. P.	IOP Conference Series, Earth and Environmental Sciences (Indexed in Scopus)	Published
On the possibility of improvement of mechanical performance of concrete containing plastic waste using high density slag	Bhagat G. V. and Savoikar P. P.	Journal of Building Engineering, Elsevier (Impact factor 6.4)	Under review